

# **Perturbation analysis and numerical discretisation of hyperbolic partial differential algebraic equations describing flow networks**

Dissertation

zur Erlangung des akademischen Grades

doctor rerum naturalium

(Dr. rer. nat.)

im Fach Mathematik

eingereicht an der

Mathematisch-Naturwissenschaftlichen Fakultät

der Humboldt-Universität zu Berlin

von

Christoph Huck, M.Sc.

Präsidentin der Humboldt-Universität zu Berlin:

Prof. Dr.-Ing. Dr. Sabine Kunst

Dekan der Mathematisch-Naturwissenschaftlichen Fakultät:

Prof. Dr. Elmar Kulke

-----  
Gutachter/innen:

1. Prof. Dr. Caren Tischendorf
2. Prof. Dr. Volker Mehrmann
3. Prof. Dr. Stephen L. Campbell

Tag der mündlichen Prüfung:

16.11.2018



# Kurzzusammenfassung

Diese Arbeit beschäftigt sich mit verschiedenen mathematischen Fragestellungen hinsichtlich der Modellierung, Analysis und numerischen Simulation von Gasnetzen. Hierbei liegt unser Fokus auf der mathematischen Handhabung von (partiellen) differential-algebraischen Gleichungen, also auf partiellen und gewöhnlichen Differentialgleichungen, die mit algebraischen Gleichungen gekoppelt sind. Diese bieten einen einfachen Zugang hinsichtlich der Modellierung von dynamischen Strukturen auf Netzen. Somit sind sie insbesondere für Gasnetze geeignet, denen im Zuge der steigenden Bedeutung von erneuerbaren Energien ein gestiegenes Interesse seitens der Öffentlichkeit, Politik und Wissenschaft entgegen gebracht wird.

Während sich die Wissenschaft dem Feld der differential-algebraische Gleichungen (DAEs) seit mehr als 30 Jahren ausgiebig widmet, ist das Interesse hinsichtlich der Analysis von gekoppelten Systemen partieller Differentialgleichungen erst in den letzten Jahren gestiegen. So gibt es über die Eigenschaften partieller differential-algebraischer Gleichungssysteme (PDAE), und ob diese Eigenschaften in der numerischen Lösung der DAE erhalten bleiben, bisher wenig Erkenntnisse.

In dieser Arbeit führen wir zunächst die gängigsten Elemente, die in Gasnetzen benötigt werden, ein und formulieren zwei PDAE-Klassen für solche Netze: Eine für reine Rohrnetze, und eine, die zusätzliche Elemente wie Verdichter und Widerstände beinhaltet. Des Weiteren untersuchen wir die Sensitivität der Lösung der Rohrnetz-PDAE hinsichtlich Störungen. Dabei berücksichtigen wir Störungen, die nicht nur den dynamischen Teil der PDAE beeinflussen, sondern auch Störungen in den algebraischen Gleichungen und weisen Stabilitätseigenschaften für die Lösung der PDAE nach.

Darüber hinaus beschäftigen wir uns mit einer neu entwickelten, an die Netztopologie angepassten Ortsdiskretisierung, welche die Stabilitätseigenschaften der PDAE auf DAE Systeme überträgt. Des Weiteren zeigen wir, wie sich die Gasnetz-DAE zu einer gewöhnlichen Differentialgleichung, welche die inhärente Dynamik der DAE widerspiegelt, entkoppeln lässt. Dieses entkoppelte System kann darüber hinaus direkt aus den Topologie- und Elementinformationen des Netzes aufgestellt werden. Abschließend demonstrieren wir die Ergebnisse an Benchmark-Gasnetzen. Dabei vergleichen wir sowohl die entkoppelte Differentialgleichung mit dem ursprünglichen DAE System, zeigen aber auch, welche Vorteile die an die Netztopologie angepasste Ortsdiskretisierung gegenüber existierenden Verfahren besitzt.





# Abstract

This thesis addresses several aspects regarding modelling, analysis and numerical simulation of gas networks. Hereby, our focus lies on (partial) differential-algebraic equations, thus systems of partial and ordinary differential equations which are coupled by algebraic equations. These coupled systems allow an easy approach towards the modelling of dynamic structures on networks. Therefore, they are well suited for gas networks, which have gained a rise of attention in society, politics and science due to the focus towards renewable energies.

While a profound theory for differential-algebraic equations (DAEs) exists, such a complete theory is missing for coupled systems of partial differential equations (PDEs) and only gained scientific interest in recent years. Regarding the analysis of partial differential-algebraic equations (PDAEs), a system of PDEs that is coupled by algebraic equations, little is known about their properties, particularly if the numerical solution of the DAE reflects the properties of the space continuous PDAE system.

We give an introduction towards gas network modelling that includes the most common elements that also appear in real gas networks and present two PDAE systems: One for pipe networks and one that includes additional elements like resistors and compressors. Furthermore, we investigate the impact of perturbations onto the pipe network PDAE, where we explicitly allow perturbations to affect the system in the differential as well as in the algebraic components. We conclude that the solution of the PDAE possesses stability properties.

In addition, this thesis introduces a new spatial discretisation that is adapted to the network topology. This topology-adapted semi-discretisation results in a DAE which possesses the same perturbation behaviour as the space continuous PDAE. Furthermore, we present a topology based decoupling procedure that allows to reformulate the DAE as an ordinary differential equation (ODE), which represents the inherent dynamics of the DAE system. This ODE, together with a decoupled set of algebraic equations, can be derived from the topology and element information directly. We conclude by demonstrating the established results for several benchmark networks. This includes a comparison of numerical solutions for the decoupled ODE and the DAE system. In addition we present the advantages of the topology-adapted spatial discretisation over existing well established methods.



# Acknowledgement

First of all, I owe gratitude to Prof. Dr. Caren Tischendorf for supervising this thesis and for taking me into her working group at the very beginning. Furthermore, for the fruitful discussions and encouragements in the last years and the opportunity to work within the SFB/TRR 154. I benefited greatly from this project.

Furthermore I would like to thank Prof. Dr. Volker Mehrmann and Prof. Dr. Stephen Campbell to serve as referees, Prof. Dr. Alexander Mielke to serve as chairperson of my doctoral committee and Prof. Dr. Helga Baum and Prof. Dr. Serhiy Yanchuk to act as committee members.

I want to thank all my colleagues, former and present, within the working group, for their company and for patiently enduring and answering my questions. Additionally, I want to thank my colleagues within the SFB/TRR 154 for their collaboration and making the project meetings something to look forward to. I enjoyed working with you tremendously even though I may not always have shown it properly. I am indebted to Dr. Benjamin Hiller for serving as my Mentor within the SFB. In particular, I want to thank Tom Walther for his companionship at project meetings, becoming a dear friend and for reading this thesis. Moreover, I am deeply indebted to Sarah Geiß for the work she did as a student employee within the TRR 154 and for being a pleasant office mate.

Furthermore, I want to thank my friends in Berlin and Cologne for their encouragement and welcome distractions. In particular Daniel and Dennis for reading this thesis and being the friends that they are.

I want to thank my family for their support throughout the years. Especially my aunt Gisela, my sister Maren and of course my parents, who have always been there with love and motivation. I am aware of the privilege I have been granted, studying free from worries. Additionally, I want to thank the Kowalczyk family for their love and encouragement, which often also came in the form of cake.

Finally, I thank Karin for her loving support and motivation, for shoving me when I needed to be shoved and for holding me back when I started to get lost. I call myself lucky to have this marvellous woman beside me.

Christoph Huck

Berlin, 12 June 2018.



# Contents

<b>Kurzzusammenfassung</b>	<b>i</b>
<b>Abstract</b>	<b>iii</b>
<b>Acknowledgement</b>	<b>v</b>
<b>List of Figures</b>	<b>ix</b>
<b>List of Tables</b>	<b>xi</b>
<b>1 Introduction</b>	<b>1</b>
<b>2 Gas network modelling</b>	<b>5</b>
2.1 Gas networks as graphs . . . . .	5
2.2 Elements of gas transport . . . . .	6
2.2.1 Pipe model . . . . .	6
2.2.2 Resistor model . . . . .	9
2.2.3 Compressor model . . . . .	10
2.2.4 Other elements . . . . .	15
2.2.4.1 Valve model . . . . .	15
2.2.4.2 Short pipes . . . . .	15
2.2.4.3 Control valves model . . . . .	15
2.2.5 Node modelling . . . . .	16
2.3 Coupled model . . . . .	16
2.4 Function spaces and norms . . . . .	18
2.5 ADAE Model . . . . .	20
2.6 Conclusion . . . . .	22
<b>3 Perturbation analysis of hyperbolic PDAEs</b>	<b>23</b>
3.1 Pipe network topology . . . . .	24
3.2 Homogenisation . . . . .	27
3.2.1 Properties of the homogenisation functions . . . . .	31
3.3 A priori estimates . . . . .	35
3.4 Perturbation analysis . . . . .	39
3.5 Uniqueness of solutions . . . . .	42
3.6 Conclusion . . . . .	43
<b>4 Topology-adaptive discretisation and DAE analysis</b>	<b>45</b>
4.1 Topology-adaptive discretisation . . . . .	49
4.2 Gas network DAE analysis . . . . .	61
4.3 Decoupling process for DAEs . . . . .	64
4.4 Extension to general networks . . . . .	68

4.5	Consistent initialisation . . . . .	83
4.6	Conclusion . . . . .	84
<b>5</b>	<b>Numerical examples</b>	<b>87</b>
5.1	Implicit box scheme . . . . .	87
5.2	Galerkin discretisation . . . . .	88
5.3	Comparison of different spatial discretisations . . . . .	89
5.4	Networks from the GasLib . . . . .	97
5.4.1	GasLib-11 . . . . .	97
5.4.2	GasLib-40 . . . . .	105
5.4.3	GasLib-135 . . . . .	109
5.5	Conclusion . . . . .	114
<b>6</b>	<b>Conclusion and outlook</b>	<b>115</b>
<b>A</b>	<b>Graph theory</b>	<b>117</b>
<b>B</b>	<b>DAE theory</b>	<b>119</b>
<b>C</b>	<b>Functionanal analysis</b>	<b>121</b>
	<b>Notation</b>	<b>123</b>
	<b>Bibliography</b>	<b>127</b>
	<b>Index</b>	<b>133</b>

## List of Figures

2.1	Model hierarchy of gas transport. . . . .	9
2.2	Compressor machine with bypass. . . . .	11
2.3	Compressor configurations. . . . .	12
3.1	Example network for the homogenisation. . . . .	29
4.1	Pipe orientation and resulting DAE index. . . . .	54
4.2	Network that does not fulfil Assumptions 4.11. . . . .	58
4.3	Compressor machine with resistors. . . . .	69
4.4	Active subgraph. . . . .	71
4.5	Network that contains an active subgraph. . . . .	77
4.6	Impact of valves on the graph topology. . . . .	79
4.7	Impact of valves on the DAE index. . . . .	80
4.8	Spatial refinement and pipe orientation for pipes connecting nodes in $V_p \cup V_A$ . . . . .	82
4.9	Spatial refinement and pipe orientation. . . . .	82
4.10	Two active elements directed at the same node. . . . .	82
4.11	Valve behind a compressor. . . . .	83
4.12	Network from Figure 4.2 that fulfils Assumptions 4.32. . . . .	83
4.13	Graph orientation and decoupling process. . . . .	85
5.1	Pipe network with two sources and one sink. . . . .	89
5.2	Boundary data for the network 5.1 Example 5.2. . . . .	91
5.3	Solution to Network 5.1 with $\Delta x = 1000$ m. . . . .	92
5.4	Solution to Network 5.1 with $\Delta x = 500$ m. . . . .	92
5.5	Solution to Network 5.1 with $\Delta x = 250$ m. . . . .	93
5.6	Solution to Network 5.1 with $\Delta x = 100$ m. . . . .	93
5.7	Boundary data for network 5.1 Example 5.3. . . . .	94
5.8	Solution to Network 5.1 with $\Delta x = 1000$ m. . . . .	95
5.9	Solution to Network 5.1 with $\Delta x = 250$ m. . . . .	95
5.10	Solution to Network 5.1 with $\Delta x = 125$ m. . . . .	96
5.11	Solution to Network 5.1 with $\Delta x = 100$ m. . . . .	96
5.12	GasLib-11 network topology. . . . .	97
5.13	GasLib-11 without a valve. . . . .	98
5.14	Scenario for the GasLib-11 (Figure 5.13). . . . .	98
5.15	Pressure solutions for the GasLib-11 (Figure 5.13). . . . .	99
5.16	Right mass flow solutions for the GasLib-11 (Figure 5.13). . . . .	100
5.17	GasLib-11 with a valve. . . . .	101
5.18	Scenario for the GasLib-11 (Figure 5.17). . . . .	101
5.19	Pressure solution for the GasLib-11 (Figure 5.17). . . . .	102
5.20	Right mass flow solution for the GasLib-11 (Figure 5.17). . . . .	103
5.21	Scenario for the GasLib-11. . . . .	104

5.22 Pressure distribution over time for the GasLib-11. . . . . 105

5.23 GasLib-40 network topology. . . . . 106

5.24 Boundary data for the GasLib-40. . . . . 107

5.25 Compressor control for the GasLib-40. . . . . 107

5.26 Pressure distribution over time for the GasLib-40. . . . . 108

5.27 States of the compressors for the GasLib-135. . . . . 109

5.28 GasLib-135 network topology. . . . . 110

5.29 Pressure distribution over time for the GasLib-135 at  $t = 0$  h. . . . . 111

5.30 Pressure distribution over time for the GasLib-135 at  $t = 12$  h. . . . . 112



# List of Tables

2.1	Pipe parameters and constants. . . . .	9
2.2	Compressor constants. . . . .	12
2.3	Symbols of gas network elements. . . . .	16
4.1	DAE variables. . . . .	55
4.2	DAE notation. . . . .	55
4.3	Element sets. . . . .	55
5.1	Pipe lengths and diameters of the GasLib-11 (Figure 5.13). . . . .	98
5.2	Pipe lengths and diameters of the GasLib 11 (Figure 5.17). . . . .	101
5.3	Compressor machines of the GasLib-40. . . . .	107
5.4	Active compressor machines of the GasLib-135. . . . .	109
5.5	Comparison of numerical effort. . . . .	113
5.6	Computational times for the GasLib examples. . . . .	113



# 1 Introduction

A theory for differential-algebraic equations (DAEs) started developing in the 1980s [GHP81; Pet82; GP83], when linear systems of partial differential equations (PDEs) were investigated and the method of lines (MOL) was applied. This semi-discretisation in space leads to a time depending system in form of an ordinary differential equation (ODE) or DAE. Another reason why DAEs gained the attention in mathematical research was that they allow a very easy and intuitive modelling of coupled systems or differential systems that appear on a network structure, e.g., electrical circuits. Other common fields of application include multibody dynamics, where ODEs are subject to certain restraints, exempli gratia (e.g.) the pendulum. Therefore, DAEs are sometimes called restrained ODEs or descriptor systems. The simplicity regarding the modelling of many fields of application comes at the cost that DAEs can be ill-posed in the sense of Hadamard [LRS86]. Lately, there have been advances to investigate DAEs in a functional analytic framework by considering them as operator equations [Mär15].

Due to the process of applying MOL to PDEs that lead to DAEs, the term PDAE was sometimes used when these semi-discretised systems were investigated. We use the term partial differential-algebraic equation (PDAE) to refer to systems where PDEs are coupled with algebraic equations, possibly even with DAEs or ODEs, hence systems that still rely on space and time variables. When we formulate these systems as operator equations, we call them abstract differential-algebraic equation (ADAE).

A profound theory for DAEs exists in the literature, e.g. in the textbooks [GM86; HLR89; BCP95; KM06; Ria08; LMT13], independent of whether these DAEs result from semi-discretised PDAEs or PDEs, or are directly modelled from applications. Such a theory for PDAEs or ADAEs has only gained scientific interest in recent years and is not as extensive as for DAEs, especially in the non-linear case. There have been first works by [CM99] and [LSE99] to extend the index concept, which is an essential tool in the analysis of DAEs, to the infinite dimensional linear case. Other works on linear ADAEs include [LMT05; Rei06]. In [Mat12], an approach originally introduced in [Tis04] for the linear case, is extended to non-linear ADAEs. In addition, a new approach to treat two specific classes of ADAEs, one of an elliptic and one of a parabolic nature, is introduced. A Galerkin approach and the theory of monotone operators are used to prove existence and uniqueness of solutions of these types of non-linear ADAEs. In [Hei14], an ADAE is addressed deriving from the incompressible Navier-Stokes equations and necessary conditions for the existence of solutions were established. A regularisation technique for ADAEs is presented in [Alt15].

This thesis addresses hyperbolic PDAEs that arise in the modelling of gas networks. Most of the research was done while working in the project *SFB/Transregio 154 - Mathematical Modelling, Simulation and Optimization using the Example of Gas Networks*, more precisely in the subproject *C02 - Hierarchical PDAE-Surrogate-Modelling and Stable PDAE-Network-Discretization for Simulating Large Non-stationary Gas Networks*.

One of the questions we asked ourselves at the beginning of the project was:

*What is a good way to handle gas networks from a (P)DAE point of view?*

This question leads to the investigation of different aspects in the analysis of PDAEs and DAEs that have their origin in the modelling of gas networks.

1. What properties does the solution of the PDAE possess?
2. How can these properties be conserved for the DAE?

It is known that spatial discretisation may act as a regularisation [CM96; Arn98] but also as a deregularisation [Gün00], thus making the solution of the DAE more robust or more vulnerable to perturbations (de- or increasing the perturbation index). From a numerical point of view, a regularisation might be something to strive for, but does not necessarily need to be the best choice. A regularisation might cut information, e.g. certain peaks the solution possesses, whereas a deregularisation might add information to the solution that is not there in the continuous case. Both scenarios can be problematic, e.g. when a numerical approximation is used to validate an optimised output that was derived by piecewise stationary optimisation.

However, to determine this, one needs to know the perturbation behaviour of the PDAE. This is addressed by the first question. The second question focuses on a suitable discretisation technique, one that does neither act as a regularisation or deregularisation but contains the behaviour of the solution on the PDAE level and transports it onto the DAE solution.

In Chapter 2, we introduce the basic background that is needed to understand gas networks as oriented graphs. We also introduce the mathematical models of elements in gas transport that are needed for this thesis. Additionally, we discuss the coupling conditions at the different types of nodes and formulate two classes of PDAEs describing gas networks: One that is valid for pipe networks only and one that also includes additional elements like resistors or compressor machines that are essential for long distance gas transport. After introducing the needed functional analytic background, we formulate these two classes of gas networks as ADAEs.

Following the modelling, we start Chapter 3 by discussing some basic properties regarding the graph topology and how we can use a specific branch orientation for a more convenient notation. Furthermore, we introduce a homogenisation technique and derive a priori bounds for the solution of the pipe network PDAE, which are used to derive perturbation results that are closely linked to the perturbation index.

Chapter 4 focuses on the DAE system which is derived from the PDAE by applying a topology-adapted spatial discretisation and demonstrate that the DAE reflects certain stability properties of the PDAE. Additionally, we present an efficient decoupling process that allows to formulate a lower dimensional ODE directly from the network topology data, which can be solved independently from a remaining algebraic system instead of solving the higher dimensional DAE system.

---

Finally, we give some numerical examples for several benchmark networks in Chapter 5 and compare the numerical solutions of the DAE and decoupled ODE. Furthermore, we compare the topology-adapted discretisation from Chapter 4 with existing methods. We conclude by summarising the results in Chapter 6.

The appendix covers additional content needed in this thesis from graph theory, DAE theory and functional analysis.



## 2 Gas network modelling

In recent years, there has been a huge shift in attention towards renewable energy in society, politics, industry and science and with it a shift in attention towards gas as an efficient and eco-friendly energy source. Gas is available for the foreseeable future, it is available fast (in contrast to coal, where the start-up of a coal power plant needs a long time compared to a gas power plant), it is already being traded and it can be stored. It can even be used to store electrical power, even though there is still a lot of room for improvement concerning the efficiency of this power-to-gas conversion.

In this chapter, we provide the needed background in gas network modelling. We discuss several branch elements such as pipes, resistors and compressor machines, that we will focus on throughout this thesis. Furthermore, we introduce additional elements like short pipes, valves and control valves we will refer to in Chapter 4. Also, we discuss node modelling which functions as coupling conditions for the branch elements.

In Section 2.3, we present two PDAE systems that describe gas networks: One for gas networks that only has pipes as branch elements and one more general system that also contains other elements such as compressors.

Section 2.4 introduces a basic functional analytic background to formulate gas networks as ADAEs in Section 2.5, which we will rely on in the perturbation analysis in Chapter 3.

For a more detailed information about gas network modelling, we refer to [Dom<sup>+</sup>17] or [Koc<sup>+</sup>15], where the latter provides a broad overview of gas network elements with a focus on stationary models. We also refer to [BGH11], where different aspects of gas pipe modelling are discussed and to [Her07; HT17] for gas networks with pipes and compressors.

### 2.1 Gas networks as graphs

It is a common approach to model gas networks as an oriented graph  $\mathcal{G} = (V, \mathcal{E})$  with a set of nodes  $V$  and a set of edges  $\mathcal{E}$ . This section provides the basic notation that we need to formulate and understand gas networks as graphs.

Concerning the edge elements, we focus on gas networks with pipes ( $\mathcal{E}_P$ ), resistors ( $\mathcal{E}_R$ ) and compressors ( $\mathcal{E}_C$ ), but we also tackle other elements like valves and control valves. Compressors, valves and control valves are often called *active elements* [Koc<sup>+</sup>15], since they can be switched. Valves can be open and close, compressors can be operated in a bypass or a compression mode, where the latter allows an actual control of the network by controlling the compression behaviour of compressor machines. We also include resistors

in the group of active elements, even though they do not allow an active handling, to make a clear distinction between pipe- ( $\mathcal{E}_P$ ) and non-pipe-elements ( $\mathcal{E}_A$ ). Regarding the vertices, we distinguish between nodes with respect to (w.r.t.) their modelling. Nodes in ( $V_p$ ) are modelled by a boundary condition for the pressure  $p_u$  for  $u \in V_p$  whereas nodes in  $V_q$  are modelled by a Kirchhoff-type balance equation for the mass flow which allows gas to enter or exit the network. This distinction of branch and node elements allows the following splitting of the respective element sets

$$V = V_p \cup V_q \quad \mathcal{E} = \mathcal{E}_P \cup \mathcal{E}_A \quad \mathcal{E}_A = \mathcal{E}_R \cup \mathcal{E}_C \cup \mathcal{E}_S,$$

with  $V_p \cap V_q = \emptyset$ . We call nodes in  $V_p$  sources and nodes in  $V_q$  sinks. In general, the set of nodes ( $V$ ) is split in sources ( $V_p$ ), sinks ( $V_q$ ) and interior nodes ( $V_0$ ) [Koc<sup>+</sup>15; Dom<sup>+</sup>17] where a possible in- or outflow of gas is not allowed at nodes contained in the latter set. The modelling of this type of nodes is the same as for nodes in  $V_q$  and they only differ in so far that for interior nodes the flow balance equation has a zero right-hand side. Therefore, we have combined these two node sets.

In addition, we define the following subsets of  $\mathcal{E}$

$$\begin{aligned} \delta^+(u) &:= \{e \in \mathcal{E} : e = (v, u), v \in V\} \\ \delta^-(u) &:= \{e \in \mathcal{E} : e = (u, v), v \in V\}, \end{aligned}$$

the sets of in- and outgoing edges of node  $u \in V$  and the subsets of  $V$

$$V_A = \{u \in V_q : \delta^+(u) \cap (\mathcal{E}_R \cup \mathcal{E}_C) \neq \emptyset\} \quad V_P = V_q \setminus V_A.$$

$V_A$  is the set of nodes that have a resistor or a compressor directed towards them. We will rely on these sets in Chapter 4. Note that we have excluded valves in the definition of  $V_A$  due to their impact on the network topology. This will be addressed in Chapter 4, too.

## 2.2 Elements of gas transport

In this section, we present the element models that appear in gas networks and are needed in later sections of this chapter as well as throughout this thesis.

### 2.2.1 Pipe model

Gas transport along a pipe can be modelled by the one dimensional Euler equations for incompressible fluids (see [Fei93])

$$\partial_t \rho + \partial_x(\rho \nu) = 0 \quad (2.1a)$$

$$\partial_t(\rho \nu) + \partial_x(p + \rho \nu^2) = -\frac{\lambda}{2D} \rho \nu |\nu| - gh' \rho \quad (2.1b)$$

$$\partial_t \left( \rho \left( \frac{1}{2} \nu^2 + e \right) \right) + \partial_x \left( \rho \nu \left( \frac{1}{2} \nu^2 + e \right) + p \nu \right) = -\frac{k_\omega}{D} (T - T_\omega), \quad (2.1c)$$



a hyperbolic system of non-linear PDEs describing conservation of mass (2.1a), momentum (2.1b) and energy (2.1c). The appearing variables  $\rho = \rho(x, t)$ ,  $\nu = \nu(x, t)$ ,  $p = p(x, t)$ ,  $T = T(x, t)$  and  $e = e(x, t)$  are density, velocity, pressure, temperature and internal energy of the gas, depending on location  $x$  and time  $t$  in the pipe for  $(x, t) \in [0, \ell] \times \mathcal{I}$ .  $\mathcal{I} = [t_0, T] \subset \mathbb{R}_+$  being a compact set and  $\ell \in \mathbb{R}_+$  the length of the pipe. The internal energy,  $e = c_v T + gh$ , is the sum of the thermo-energy and potential energy. The variable  $h = h(x)$  is the height at location  $x$  and  $h' = h'(x)$  the elevation at location  $x$ . Throughout this thesis, we assume  $h'$  to be constant. In addition, we have parameters  $g$ ,  $D$  and  $k_\omega$ , the gravitational acceleration, diameter of the pipe and thermal conductivity, as well as  $T_\omega = T_\omega(x)$  the surface temperature and  $c_v$  the heat capacity.

**Equation of state** There is of course a natural link between density  $\rho$  and pressure  $p$ . This connection can be expressed by the equation of state [Koc<sup>+</sup>15, Chapter 2.2]

$$p = R_s T z(p, T) \rho \quad (2.2)$$

where  $R_s$  is the specific gas constant and  $z$  is the compressibility factor. For the modelling of the compressibility factor  $z$  that appears in equation (2.2), there exist two models that are used very commonly. One is the formula provided by the American Gas Association (AGA), see equation (2.3), the second is the formula of Papay in equation (2.4)

$$z(p, T) = 1 + 0.257 p_r - 0.533 \frac{p_r}{T_r} \quad (2.3)$$

$$z(p, T) = 1 - 3.52 p_r e^{-2.26 T_r} + 0.274 p_r^2 e^{-1.878 T_r}. \quad (2.4)$$

The used quantities  $p_r$  and  $T_r$  are given by

$$p_r = \frac{p}{p_c} \quad T_r = \frac{T}{T_c}$$

with  $p_c$  and  $T_c$  being the critical pressure and critical temperature, respectively. While the AGA model is accurate up to a maximum pressure of 70 bar, the model of Papay gives accurate results for pressures up to 150 bar [SSW15, Chapter 3]. Apart from these two widely used models, there exist others, such as the AGA8-DC92 [SS92] or the SGERG-88 model [Kas05], which provide a higher accuracy at the cost of a higher complexity. For the purpose of this thesis, the AGA and Papay model are sufficient.

**Remark 2.1.** *Since both, the AGA and the Papay model, are polynomials w.r.t.  $p$  of degree 1 and 2, respectively,  $z$  is continuously differentiable w.r.t.  $p$ .*

**Friction factor** As for the equation of state, there exist many different approaches towards the modelling of the friction factor  $\lambda$ . The respective models depend on the *Reynolds number* [Lur08; FF09]

$$Re(q) = \frac{D}{a\eta} |q|, \quad (2.5)$$

which determines whether a flow along a pipe is *turbulent* or *laminar*. In equation (2.5),  $\eta$  stands for the *dynamic viscosity* of the gas and  $D$  and  $a$  are the diameter and the cross sectional area of the pipe. A flow is categorized as *turbulent* if  $Re(q) \geq Re_u$  where

$Re_u = 2300$  [Lur08], and *laminar* for  $Re(q) < Re_u$ . For a *laminar* flow, the friction factor can be computed by the formula of *Hagen-Poiseuille* [FF09]

$$\lambda(q) = \frac{64}{Re(q)}. \quad (2.6)$$

In the case of a *turbulent* flow, the formula of *Prandtl and Colebrook* yields the most accurate approximation of reality [Sal02]

$$\frac{1}{\sqrt{\lambda}} = -2 \log_{10} \left( \frac{2.51}{Re(q)\sqrt{\lambda}} + \frac{k}{3.71D} \right). \quad (2.7)$$

By going to the limit  $Re \rightarrow \infty$ , one can derive the formula of *Nikuradse* from equation (2.7)

$$\lambda = \left( -2 \log_{10} \left( \frac{k}{3.71D} \right) \right)^{-2}, \quad (2.8)$$

which gives an explicit expression for  $\lambda$  and does only depend on the *roughness*  $k$  and the diameter  $D$  of the pipe. Throughout this thesis, we will use the formula of *Nikuradse*.

**Isothermal modelling** Many simplifications of the Euler equations (2.1) exist, varying from a non-linear model that includes temperature, down to an isothermal algebraic model. For an overview of the various models, we refer to [Dom<sup>+</sup>17]. We consider assumptions on the gas physics that result in an isothermal, quasi-linear model (see Figure 2.1). By assuming a constant temperature  $T = T_m$ , equation (2.1c) is dropped and equations (2.1a) and (2.1b) form the isothermal Euler equations ISO1. Even though this might seem to be unrealistic, it is in fact a reasonable assumption for onshore networks [Osi96; MFH16]. By additionally assuming that  $\partial_x(\rho\nu^2)$  is small, we can neglect that term in equation (2.1b) and formulate the ISO2 model

$$\partial_t \frac{p(x,t)}{z(p(x,t))} + \frac{R_s T_m}{a} \partial_x q(x,t) = 0 \quad (2.9a)$$

$$\partial_t q(x,t) + a \partial_x p(x,t) = - \frac{\lambda R_s T_m z(p(x,t))}{2Da} \frac{q(x,t)|q(x,t)|}{p(x,t)} - \frac{gah'}{R_s T_m} \frac{p(x,t)}{z(p(x,t))} \quad (2.9b)$$

for  $(x,t) \in [0, \ell] \times \mathcal{I}$ .

**Remark 2.2.** For an isothermal model, the equation for the compressibility factor  $z$  reduces to

$$z(p) = \begin{cases} 1 + \alpha p & \text{AGA} \\ 1 + \beta_1 p + \beta_2 p^2 & \text{Papay} \end{cases} \quad (2.10)$$

with constants

$$\alpha = \frac{0.257}{p_c} - \frac{0.533}{p_c} \frac{T_m}{T_c} \quad \beta_1 = \frac{-3.52}{p_c} e^{-2.26 \frac{T_m}{T_c}} \quad \beta_2 = \frac{0.274}{p_c^2} e^{-1.878 \frac{T_m}{T_c}}.$$

The constants  $p_c$ ,  $T_c$  and  $T_m$  are the critical pressure, critical temperature and the constant temperature of the gas, respectively. Furthermore, there exists another model for the

compressibility factor, where  $z$  is assumed to be constant, given by

$$z = \frac{c^2}{R_s T_m}. \quad (2.11)$$

In the case that  $z$  is modelled as constant, the ISO2 model further simplifies to

$$\partial_t p(x, t) + \frac{c^2}{a} \partial_x q(x, t) = 0 \quad (2.12a)$$

$$\partial_t q(x, t) + a \partial_x p(x, t) = -\frac{\lambda c^2}{2Da} \frac{q(x, t)|q(x, t)|}{p(x, t)} - \frac{gh'a}{c^2} p(x, t) \quad (2.12b)$$

for  $(x, t) \in [0, \ell] \times \mathcal{I}$ . We call this the ISO2' model.

Constant	Description	SI-Unit	Constant	Description	SI-Unit
$a$	Cross sectional area	$[\text{m}^2]$	$k$	Roughness of the pipe	$[\text{m}]$
$D$	Diameter	$[\text{m}]$	$R_s$	Specific gas constant	$[\frac{\text{m}^2}{\text{s}^2 \text{K}}]$
$\lambda$	Friction coefficient	$[1]$	$T_m$	Mean temperature	$[\text{K}]$
$h'$	Elevation	$[1]$	$c$	Speed of sound	$[\frac{\text{m}}{\text{s}}]$
$\ell$	Length of the pipe	$[\text{m}]$	$g$	Gravity constant	$[\frac{\text{m}}{\text{s}^2}]$

**Table 2.1:** Parameters and constants needed for pipe modelling.

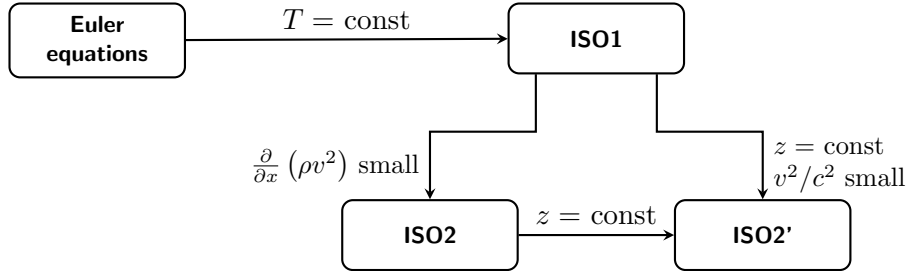


**Figure 2.1:** Model hierarchy of gas transport.

**Remark 2.3.** In the case of a constant compressibility factor  $z \equiv \frac{c^2}{R_s T_m}$ , the assumption needed to derive the ISO2' model from the ISO1 model can be understood as an assumption on the velocity. Namely, that the velocity of the gas in the network is much smaller compared to the speed of sound  $c$ .

Regarding the non-isothermal modelling of gas networks, we refer to [Her08; BGH11; LM18].

### 2.2.2 Resistor model

As in the context of circuit simulation, a resistor in a gas network context reduces pressure in the direction of the flow. For  $e^{\mathcal{R}} = (u, v) \in \mathcal{E}_{\mathcal{R}}$ , connecting nodes  $u$  and  $v$ , we can model

this behaviour by

$$p_u(t) - p_v(t) = g_{e\mathcal{R}}(p_u(t), q_{e\mathcal{R}}(t)) \quad g_{e\mathcal{R}}: \mathbb{R}^2 \rightarrow \mathbb{R} \quad (2.13)$$

with  $g_{e\mathcal{R}}$  being a non-linear function that describes the loss in pressure, depending on the left pressure of the arc  $p_u$  and the mass flow along the arc  $q_{e\mathcal{R}}$ . The function  $g_{e\mathcal{R}}$  is stated as

$$g_{e\mathcal{R}}(p, q) = R_s T_m z(p) \frac{\xi_{e\mathcal{R}}}{2} \frac{q|q|}{p}, \quad (2.14)$$

so that equation (2.13) is based on the *Darcy-Weisbach* model [Lur08; FF09]. The factor  $\xi_{e\mathcal{R}}$  is the drag factor of the resistor. Unlike in circuit simulation, the resistor element in gas networks is described by a non-linear equation and does not behave the same way in either direction of the flow, since only  $p_u$  appears in the non-linear function. Since they do not appear as natural elements in gas networks but are merely used to model accumulated pressure loss due to elements like filters or internal piping [SSW15], mostly in front of or behind a compressor machine, the direction of the flow is often fixed.

### 2.2.3 Compressor model

Compressors are needed in gas networks to guarantee gas transport over long distances. Similar to pumps in water networks, they increase the pressure at a node to enable transportation of the gas. We want to investigate the two most common types of compressors in gas networks.

**Turbo compressors** The most common type of compressor machines that are used in practice are turbo compressors [Koc<sup>+</sup>15; Dom<sup>+</sup>17], which can be modelled by a set of non-linear equations given by

$$H_{ec}(t) - R_s T_m z(p_u(t)) \frac{\kappa}{\kappa - 1} \left[ \left( \frac{p_v(t)}{p_u(t)} \right)^{\frac{\kappa-1}{\kappa}} - 1 \right] = 0 \quad (2.15a)$$

$$Q_{ec}(t) - R_s T_m z(p_u(t)) \frac{q_{ec}(t)}{p_u(t)} = 0 \quad (2.15b)$$

$$H_{ec}(t) - s_{ec}(t) \Phi(Q_{ec}(t), n_{ec}(t); A_{ec}^H) - (1 - s_{ec}(t))(n_{ec}(t) - n_{ec}^-) = 0 \quad (2.15c)$$

$$\eta_{ec}(t) - s_{ec}(t) \Phi(Q_{ec}(t), n_{ec}(t); A_{ec}^\eta) = 0 \quad (2.15d)$$

$$s_{ec}(t)(p_v(t) - p_{ec}^c(t)) + (1 - s_{ec}(t))(p_v(t) - p_u(t)) = 0 \quad (2.15e)$$

for  $e^c = (u, v)$ . The variables  $H_{ec}$ ,  $Q_{ec}$ ,  $q_{ec}$ ,  $n_{ec}$  and  $\eta_{ec}^c$  are the adiabatic enthalpy, volumetric flow rate, mass flow, speed and the efficiency of the compressor machine. The function  $p_{ec}^c \in \mathcal{C}(\mathcal{I}, \mathbb{R})$  in equation (2.15e) denotes the control function and  $\kappa$  is the isentropic exponent. The matrices  $A_{ec}^H, A_{ec}^\eta \in \mathbb{R}^{3 \times 3}$  describe the characteristic diagram that models the relation between volumetric flow rate, enthalpy, speed and efficiency of a turbo compressor. The function  $\Phi: \mathbb{R} \times \mathbb{R} \rightarrow \mathbb{R}$  is defined by

$$\Phi(Q, n; A) = \begin{pmatrix} 1 & Q & Q^2 \end{pmatrix} A \begin{pmatrix} 1 & n & n^2 \end{pmatrix}^\top$$

for a given matrix  $A \in \mathbb{R}^{3 \times 3}$ . The function  $s_{ec} \in \mathcal{C}(\mathcal{I}, [0, 1])$  allows to operate each compressor machine either in the operating-mode ( $s_{ec}(t) = 1$ ), or in bypass-mode ( $s_{ec}(t) = 0$ ) with an interpolation in between, to model the transition phase. The operating-mode gives rise to an active control of the network by increasing the outgoing pressure  $p_v$  at node  $v$ . The bypass-mode sets in- and outgoing pressures  $p_v$  and  $p_u$  as equal (see (2.15e)), as well as  $H_{ec} = 0$ ,  $\eta_{ec} = 0$  and computes the volumetric flow rate  $Q_{ec}$  through the bypass. The speed  $n_{ec}$  is set to the compressor specific lower bound for the speed  $n_{ec}^-$ . Thus, making the compressor behave like an open valve.

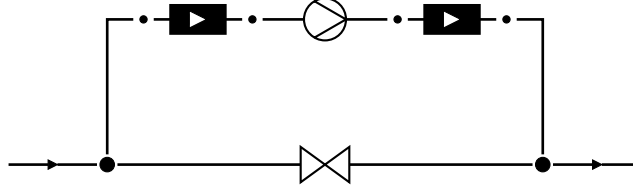


**Figure 2.2:** Diagram of a single compressor machine with bypass and resistors.

Figure 2.2 shows a prototype of a compressor with a bypass and resistors that are used to model the internal piping and additional elements like a preheater and cooler in front of and behind the compressor machine. Data for this kind of substitute model can also be found in the GasLib<sup>1</sup> [Hum<sup>+</sup>17] in form of the drag factors for the resistors in front of and behind the compressor machines.

**Piston compressor** In comparison to turbo compressors, piston compressors allow larger compression ratios than turbo compressors, but at a lower throughput [SSW15]. Their behaviour is described by characteristic diagrams in the variables volumetric flow rate  $Q$  and torque shaft  $M$  instead of enthalpy as in the case of a turbo compressor.

$$H_{ec}(t) - R_s T_m z(p_u(t)) \frac{\kappa}{\kappa - 1} \left[ \left( \frac{p_v(t)}{p_u(t)} \right)^{\frac{\kappa-1}{\kappa}} - 1 \right] = 0 \quad (2.16a)$$

$$Q_{ec}(t) - R_s T_m z(p_u) \frac{q_{ec}(t)}{p_u(t)} = 0 \quad (2.16b)$$

$$M_{ec}(t) - \frac{\bar{V}_{ec} H_{ec}(t)}{2\pi \bar{\eta}_{ec}} \frac{p_u(t)}{R_s T_m z(p_u(t))} = 0 \quad (2.16c)$$

$$s_{ec}(t) Q_{ec}(t) - \frac{\bar{V}_{ec} n_{ec}(t)}{60} + (1 - s_{ec}(t)) \frac{\bar{V}_{ec} n_{ec}^-}{60} = 0 \quad (2.16d)$$

$$s_{ec}(t)(p_v(t) - p_{ec}^c(t)) + (1 - s_{ec}(t))(p_v(t) - p_u(t)) = 0. \quad (2.16e)$$

Note that piston compressors operate at a fixed efficiency  $\bar{\eta}_{ec} \in [0, 1]$  and operating volume  $\bar{V}_{ec} > 0$ . When the piston compressors operates in bypass mode  $s_{ec}(t) = 0$ , the variables fulfil  $p_u = p_v$ ,  $H_{ec} = 0$ ,  $M_{ec} = 0$  and  $n_{ec} = n_{ec}^-$ . The volumetric flow rate along the bypass is computed as stated in equation (2.16b).

In practice, compressor machines appear in groups within compressor stations, so that they can be operated in different modifications depending on the current state of the network.

<sup>1</sup>gaslib.zib.de

Constant	Description	SI-Unit
$\kappa$	Isentropic exponent	[1]
$\bar{V}$	Operating volume of a piston compressor	[m <sup>3</sup> ]
$\bar{\eta}$	Efficiency of a piston compressor	[1]

**Table 2.2:** Constants needed for compressor modelling.

For instance, a parallel configuration of two compressors allows a higher throughput of gas, whereas a sequential configuration allows a higher compression ratio at the outgoing node (see Figure 2.3). Their main goal is to increase pressure to enable gas transport over long distances. In addition, at compressor stations, the gas routes can be changed, so that gas arriving from the east can be rerouted, e.g. to the south and not just to the west.

We focus on single compressor machines that might appear in combination with several other compressor machines. For more details about the analysis and treatment of compressor stations, we refer to [HSW16; HW17]. A polyhedral three-dimensional model for compressor machines is discussed in [WHS18].



**Figure 2.3:** Two compressors operated in a parallel (left) and a sequential configuration (right).

In general, we can describe the behaviour of a compressor machine, turbo or piston compressor by a non-linear function

$$g_{ec}(p_u, p_v, q_{ec}, y_{ec}, t) = 0$$

with

$$g_{ec} : \mathbb{R} \times \mathbb{R} \times \mathbb{R} \times \mathbb{R}^4 \times \mathcal{I} \rightarrow \mathbb{R}^5$$

where  $g_{ec}$  is given either by equation (2.15) or (2.16), depending on the compressor type. The internal compressor variables are

$$y_{ec} = \begin{cases} \begin{pmatrix} H_{ec} & Q_{ec} & n_{ec} & \eta_{ec} \end{pmatrix}^\top & e^c \text{ is a turbo compressor} \\ \begin{pmatrix} H_{ec} & Q_{ec} & n_{ec} & M_{ec} \end{pmatrix}^\top & e^c \text{ is a piston compressor.} \end{cases}$$

Concerning the compressor machines in a network, we assume that they are operated *reasonably*. This reasonable behaviour will be explained in the following assumptions.

**Assumption 2.4** (Compressor control). *For  $e^c \in \mathcal{E}_C$  we assume that in systems (2.15) and (2.16), depending on the type of compressor,*

- (1) *the control function  $p_{ec}^c$  is suitable for the network, meaning that the internal vari-*

ables fulfil

$$\begin{aligned} H_{ec}(t) &\in [H_{ec}^-, H_{ec}^+] \subset \mathbb{R}_+ & Q_{ec}(t) &\in [Q_{ec}^-, Q_{ec}^+] \subset \mathbb{R}_+ \\ n_{ec}(t) &\in [n_{ec}^-, n_{ec}^+] \subset \mathbb{R}_+ & \eta_{ec}(t) &\in [0, 1], \end{aligned}$$

for a turbo compressor and

$$\begin{aligned} H_{ec}(t) &\in [H_{ec}^-, H_{ec}^+] \subset \mathbb{R}_+ & Q_{ec}(t) &\in [Q_{ec}^-, Q_{ec}^+] \subset \mathbb{R}_+ \\ n_{ec}(t) &\in [n_{ec}^-, n_{ec}^+] \subset \mathbb{R}_+ & M_{ec}(t) &\in [M_{ec}^-, M_{ec}^+] \subset \mathbb{R}_+ \end{aligned}$$

for a piston compressor,  $\forall t \in \mathcal{I}$ .  $H_{ec}^\pm$ ,  $Q_{ec}^\pm$ ,  $n_{ec}^\pm$  and  $M_{ec}^\pm$  are compressor specific bounds.

(2) The partial derivative of  $\Phi(Q_{ec}, n_{ec}; A_{ec}^\eta)$  w.r.t.  $n_{ec}$  for  $e^c$  being a turbo compressor fulfils

$$\partial_{n_{ec}} \Phi(Q_{ec}, n_{ec}; A_{ec}^\eta) > 0 \quad \text{for } n_{ec} \in [n_{ec}^-, n_{ec}^+], Q_{ec} \in [Q_{ec}^-, Q_{ec}^+]$$

**Remark 2.5.** The assumptions regarding the compressor machines in Assumption 2.4 are usually fulfilled in practice, since compressor machines must be operated within their specific operating range which can be characterized by the introduced bounds in (1).

The second assumption (2) is fulfilled for the compressor data provided in the GasLib at least locally within the bounds given in (1). It is essential for the analysis in Chapter 4 and needed to derive the results of the following Theorem.

**Theorem 2.6** (Properties of  $g_{ec}$ ). Let  $e^c \in \mathcal{E}_C$  be a compressor that fulfils Assumptions 2.4. Then it holds that

$$(i) \ker \partial_{y_{ec}} g_{ec} = \{0\}.$$

(ii) The Jacobian of  $g_{ec}$  w.r.t.  $p_v$  is given by

$$\partial_{p_v} g_C(p_u, p_v, q_{ec}, y_{ec}, t) = \begin{pmatrix} -R_s T_m \frac{z(p_u)}{p_u^{\frac{\kappa-1}{\kappa}}} p_v^{\frac{-1}{\kappa}} \\ 0 \\ 0 \\ 0 \\ 1 \end{pmatrix}.$$

*Proof.* We start with the proof of (i).

For  $e^c = (u, v) \in \mathcal{E}_C$  being a turbo compressor, the Jacobian of  $g_{ec}$  w.r.t. the internal variables  $y_{ec} = (H_{ec} \quad Q_{ec} \quad n_{ec} \quad \eta_{ec})^\top$  is

$$\partial_{y_{ec}} g_{ec}(p_u, p_v, q_{ec}, y_{ec}, t) = \begin{pmatrix} 1 & 0 & 0 & 0 \\ 0 & 1 & 0 & 0 \\ 1 & -s_{ec}(t) \partial_{Q_{ec}} \Phi^n & -s_{ec}(t) \partial_{n_{ec}} \Phi^n - (1 - s_{ec}(t)) & 0 \\ 0 & -s_{ec}(t) \partial_{Q_{ec}} \Phi^\eta & -s_{ec}(t) \partial_{n_{ec}} \Phi^\eta & 1 \\ 0 & 0 & 0 & 0 \end{pmatrix}.$$

For a more convenient notation, we used

$$\Phi^n = \Phi(Q_{ec}, n_{ec}; A_{ec}^H) \quad \Phi^\eta = \Phi(Q_{ec}, n_{ec}; A_{ec}^\eta).$$

For  $w = (w_H \ w_Q \ w_n \ w_\eta)^\top \in \ker(\partial_{y_{ec}} g_{ec})$ , it follows from the structure of the Jacobian that  $w_H = w_Q = w_\eta = 0$ . Concerning  $w_n$  it holds that

$$s_{ec}(t) \partial_{n_{ec}} \Phi^n + (1 - s_{ec}(t)) w_n = 0 \Leftrightarrow 0 = \begin{cases} \left( \partial_{n_{ec}} \Phi^n + \frac{(1-s_{ec}(t))}{s_{ec}(t)} \right) w_n & s_{ec}(t) > 0 \\ w_n & s_{ec}(t) = 0. \end{cases}$$

Since  $\partial_{n_{ec}} \Phi^n > 0$  due to Assumption 2.4, it follows that  $w_n = 0$ .

For  $e^c = (u, v) \in \mathcal{E}_c$  being a piston compressor, the Jacobian of  $g_{ec}$  w.r.t. the internal variables  $y_{ec} = (H_{ec} \ Q_{ec} \ n_{ec} \ M_{ec})^\top$  is

$$\partial_{y_{ec}} g_{ec}(p_u, p_v, q_{ec}, y_{ec}, t) = \begin{pmatrix} 1 & 0 & 0 & 0 \\ 0 & 1 & 0 & 0 \\ -\frac{\bar{V}_{ec}}{2\pi\bar{\eta}_{ec}} \frac{p_u(t)}{R_s T_m z(p_u(t))} & 0 & 0 & 1 \\ 0 & -s_{ec}(t) & -\frac{\bar{V}_{ec}}{60} & 0 \\ 0 & 0 & 0 & 0 \end{pmatrix}.$$

Let  $w = (w_H \ w_Q \ w_n \ w_M)^\top \in \ker(\partial_{y_{ec}} g_{ec})$ . It follows directly from the structure of the Jacobian that  $w = 0$  since  $\bar{V}_{ec} > 0$ .

Assertion (ii) follows from straight forward computation.  $\square$

**Remark 2.7.** Equations (2.15c) and (2.16d) can be reformulated as

$$\begin{aligned} n_{ec} &= \Psi_{ec}(Q_{ec}, H_{ec}, t) \\ n_{ec} &= s_{ec}(t) \frac{Q_{ec} 60}{\bar{V}_{ec}} + (1 - s_{ec}(t)) n_{ec}^-. \end{aligned}$$

The function  $\Psi_{ec}$  is defined as

$$\begin{aligned} \Psi_{ec}(Q, H, t) &:= -\frac{1}{2} \frac{s_{ec}(t) A_2(Q) + 1 - s_{ec}(t)}{s_{ec}(t) A_3(Q)} \\ &+ \left| \sqrt{\left( \frac{s_{ec}(t) A_2(Q) + 1 - s_{ec}(t)}{2 s_{ec}(t) A_3(Q)} \right)^2 - \frac{s_{ec}(t) A_1(Q) - (1 - s_{ec}(t)) n_{ec}^- - H}{s_{ec}(t) A_3(Q)}} \right|. \end{aligned}$$

with terms

$$A_j(Q) := (1 \ Q \ Q^2) A_{*j}.$$

Here  $A_{*j}$  denotes the  $j^{\text{th}}$  column of  $A_{ec}^H$ .



### 2.2.4 Other elements

Let us now introduce various other elements that appear in gas networks.

#### 2.2.4.1 Valve model

Valves are also *active elements* since they change their behaviour depending on the state they are operated in [Koc<sup>+</sup>15; Dom<sup>+</sup>17]. In case that a valve  $e^S = (u, v) \in \mathcal{E}_S$  is *open*, it directly connects the nodes  $u$  and  $v$ , which can be modelled by

$$p_u(t) = p_v(t) \quad t \in \mathcal{I}.$$

For the *closed* state, this connection is cut and we can describe this behaviour by

$$q_{e^S}(t) = 0 \quad t \in \mathcal{I}.$$

Let  $s_{e^S} \in \mathcal{C}(\mathcal{I}, [0, 1])$  be a time depending function describing the state of the valve, we can model valves in a single equation by

$$s_{e^S}(t)(p_u(t) - p_v(t)) + (1 - s_{e^S}(t))q_{e^S}(t) = 0 \quad (2.17)$$

where  $s_{e^S}(t) = 1$  models the open valve and  $s_{e^S}(t) = 0$  the closed state of the valve with a (linear) interpolation in between.

#### 2.2.4.2 Short pipes

Like resistors, short pipes (also called short cuts) are artificial elements to model pipes with a length of a few metres. Due to their very short length, we can neglect the pressure loss resulting from friction with the pipe wall and it is assumed that  $\partial_t q$  and  $\partial_x q$  are small or equal to zero. Hence, for  $e = (u, v) \in \mathcal{E}_{SP}$ ,  $\mathcal{E}_{SP}$  being the set of short pipes,

$$p_u(t) = p_v(t), \quad t \in \mathcal{I}, \quad (2.18)$$

which basically makes them behave like constantly open valves.

#### 2.2.4.3 Control valves model

Control valves can be modelled as an idealised compressor, but instead of compressing the gas which leads to a gain in pressure, the pressure is being reduced. This behaviour can be modelled by

$$p_u(t) - p_v(t) = p_e^c(t) \quad t \in \mathcal{I}, e = (u, v) \in \mathcal{E}_{CS}, \quad (2.19)$$

where  $p_e^c \in \mathcal{C}(\mathcal{I}, \mathbb{R}_+)$  with  $p_e^c(t) \in [\underline{\Delta}, \bar{\Delta}]$ .  $\mathcal{E}_{CS}$  denotes the set of control valves. Further modelling approaches for control valves can be found in [Koc<sup>+</sup>15; Ben<sup>+</sup>18].

### 2.2.5 Node modelling

Depending on the type of the node, they are modelled by a different kind of equation. Nodes  $u \in V_p$  are modelled by a boundary condition for the pressure





$$p_u(t) = p_u^\Gamma(t) \quad t \in \mathcal{I}, u \in V_p \quad (2.20)$$

where  $p_u^\Gamma: \mathcal{I} \rightarrow \mathbb{R}_+$  is a given, time-dependent function, describing the pressure that is applied at node  $u$  over the complete time horizon  $\mathcal{I}$ . At the nodes  $u \in V_q$ , we model the mass flow of gas that exits the network by a Kirchhoff-type balance equation

$$\sum_{\substack{e \in \delta^+(u) \\ e \in \mathcal{E}_P}} q_e(\ell_e, t) - \sum_{\substack{e \in \delta^-(u) \\ e \in \mathcal{E}_P}} q_e(0, t) + \sum_{\substack{e \in \delta^+(u) \\ e \in \mathcal{E}_A}} q_e(t) - \sum_{\substack{e \in \delta^-(u) \\ e \in \mathcal{E}_A}} q_e(t) = q_u^\Gamma(t) \quad (2.21)$$

where  $q_u^\Gamma: \mathcal{I} \rightarrow \mathbb{R}$  is a time-dependent function that models the outflow of gas at node  $u \in V_q$ . For  $e = (u, v) \in \mathcal{E}_P$  with length  $\ell_e$ , the variable  $q_e(\ell_e, t)$  is the (possibly negative) mass flow that enters node  $v$  through pipe  $e$  and  $q_e(0, t)$  is the mass flow that enters (or leaves) node  $u$  through pipe  $e$ . Here, we explicitly allow  $q_u^\Gamma$  to be negative and thereby allow that gas can also be inserted into the network at the respective node.

Note that equation (2.21) particularly defines the coupling of branch elements w.r.t. the mass flow. Since the non-dynamical elements are naturally coupled w.r.t. the pressures by their respective equations (e.g. equation (2.13)), it remains to define the coupling of the pipe pressure variables to the adjacent node pressures.

Element	Notation	Symbol
Pipe	$e^P \in \mathcal{E}_P$	
Resistor	$e^R \in \mathcal{E}_R$	
Compressor	$e^C \in \mathcal{E}_C$	
Valve	$e^S \in \mathcal{E}_S$	

**Table 2.3:** Symbols of gas network elements.

## 2.3 Coupled model

In this section, we define two PDAE systems we will later refer to: One that describes networks that only have pipes as branch elements and one more general system that also includes the active elements we have introduced in previous sections of this chapter.

The coupling conditions for the mass flow and the boundary condition for the pressure are given by equations (2.21) and (2.20), respectively. It remains to define a coupling of the pressure variables of the pipes to the node pressures  $p_u(t)$  for  $u \in V$ .

**Pipe network model** First, we will formulate the PDAE for networks that only have pipes as branch elements. In addition, we use the constant model for the compressibility factor  $z$  as stated in equation (2.11).

$$\partial_t p_e(x, t) + \frac{c^2}{a_e} \partial_x q_e(x, t) = 0 \quad (2.22a)$$

$$\partial_t q_e(x, t) + a_e \partial_x p_e(x, t) = -\frac{\lambda_e c^2}{2D_e a_e} \frac{q_e(x, t) |q_e(x, t)|}{p_e(x, t)} - \frac{g a_e h'_e}{c^2} p_e(x, t) \quad (2.22b)$$

for  $(x, t) \in [0, \ell_e] \times \mathcal{I}$  and  $e \in \mathcal{E}_P$ ,

$$\sum_{\substack{e \in \delta^+(u) \\ e \in \mathcal{E}_P}} q_e(\ell_e, t) - \sum_{\substack{e \in \delta^-(u) \\ e \in \mathcal{E}_P}} q_e(0, t) = q_u^\Gamma(t) \quad u \in V_q \quad t \in \mathcal{I} \quad (2.22c)$$

$$p_u(t) - p_e(\ell_e, t) = 0 \quad e \in \delta^+(u), u \in V \quad t \in \mathcal{I} \quad (2.22d)$$

$$p_u(t) - p_e(0, t) = 0 \quad e \in \delta^-(u), u \in V \quad t \in \mathcal{I} \quad (2.22e)$$

$$p_u(t) = p_u^\Gamma(t) \quad u \in V_p \quad t \in \mathcal{I} \quad (2.22f)$$

$$p_e(x, 0) = p_e^0(x) \quad e \in \mathcal{E}_P \quad x \in [0, \ell_e] \quad (2.22g)$$

$$q_e(x, 0) = q_e^0(x) \quad e \in \mathcal{E}_P \quad x \in [0, \ell_e] \quad (2.22h)$$

$$p_u(0) = p_u^0 \quad u \in V. \quad (2.22i)$$

For  $e = (u, v) \in \mathcal{E}$ , the notation  $q_e(0, t)$  is the (possibly negative) mass flow that flows into the pipe at node  $u$  and  $q_e(\ell_e, t)$  is the (also possibly negative) mass flow that flows out of the pipe at  $v$ . Accordingly,  $p_e(\ell_e, t)$  is the pressure at  $x = \ell_e$  and should be equal to the pressure at node  $v$  and  $p_e(0, t)$  is the pressure at  $x = 0$  in the pipe and should be equal to the pressure at node  $u$  (see equations (2.22d) and (2.22e)).

**Gas network model** The PDAE system for general gas networks with compressors and resistors is given by

$$\partial_t \frac{p_e(x, t)}{z(p_e)} + \frac{R_s T_m}{a_e} \partial_x q_e(x, t) = 0 \quad (2.23a)$$

$$\partial_t q_e(x, t) + a_e \partial_x p_e(x, t) = -\frac{\lambda_e R_s T_m z(p_e)}{2D_e a_e} \frac{q_e(x, t) |q_e(x, t)|}{p_e(x, t)} - \frac{g a_e h'_e}{R_s T_m} \frac{p_e(x, t)}{z(p_e)} \quad (2.23b)$$

for  $(x, t) \in [0, \ell_e] \times \mathcal{I}$  and  $e \in \mathcal{E}_P$ ,

$$\sum_{\substack{e \in \delta^+(u) \\ e \in \mathcal{E}_P}} q_e(\ell_e, t) - \sum_{\substack{e \in \delta^-(u) \\ e \in \mathcal{E}_P}} q_e(0, t) + \sum_{\substack{e \in \delta^+(u) \\ e \in \mathcal{E}_A}} q_e(t) - \sum_{\substack{e \in \delta^-(u) \\ e \in \mathcal{E}_A}} q_e(t) = q_u^\Gamma(t) \quad (2.23c)$$

for  $u \in V_q, t \in \mathcal{I}$ .

$$p_u(t) - p_v(t) - g_{eR}(p_u, q_{eR}) = 0 \quad e = (u, v) \in \mathcal{E}_R, \quad t \in \mathcal{I} \quad (2.23d)$$

$$g_{eC}(p_u, p_v, q_{eC}, y_{eC}, t) = 0 \quad e = (u, v) \in \mathcal{E}_C, \quad t \in \mathcal{I} \quad (2.23e)$$

$$p_u(t) - p_e(\ell_e, t) = 0 \quad e \in \delta^+(u), u \in V, \quad t \in \mathcal{I} \quad (2.23f)$$

$$p_u(t) - p_e(0, t) = 0 \quad e \in \delta^-(u), u \in V, \quad t \in \mathcal{I} \quad (2.23g)$$

$$p_u(t) = p_u^\Gamma(t) \quad u \in V_p, \quad t \in \mathcal{I} \quad (2.23h)$$

$$p_e(x, 0) = p_e^0(x) \quad e \in \mathcal{E}_p, \quad x \in [0, \ell_e] \quad (2.23i)$$

$$q_e(x, 0) = q_e^0(x) \quad e \in \mathcal{E}_p, \quad x \in [0, \ell_e] \quad (2.23j)$$

$$p_u(0) = p_u^0 \quad u \in V \quad (2.23k)$$

$$q_e(0) = q_e^0 \quad e \in \mathcal{E}_A \quad (2.23l)$$

$$y_{ec}(0) = y_{ec}^0 \quad e^c \in \mathcal{E}_C, \quad (2.23m)$$

where we consider a general gas factor  $z$ . Note that as in the context of DAEs, the initial values of Systems (2.22) and (2.23) have to be *consistent*, meaning that they have to fulfil equations (2.22c) to (2.22f) and (2.23c) to (2.23h), respectively at  $t = 0$ .

Concerning the physical behaviour of a solution to the PDAE (2.23), we make the following assumptions.

**Assumption 2.8** (Gas physics). *We make the following assumptions on the gas physics with  $p_e = R_s T_m z(p_e) \rho_e$  and  $q_e = a_e \rho_e \nu_e$  for  $e \in \mathcal{E}_p$ .*

(i)  $\rho_e \geq \underline{\rho} > 0$  for  $e \in \mathcal{E}$  and  $\underline{\rho}$  a lower bound for the density.

(ii)  $\nu_e \leq \bar{\nu} \ll c$ , for  $e \in \mathcal{E}$  and  $\bar{\nu}$  an upper bound for the velocity of the gas inside a pipe.

**Remark 2.9.** *Assumptions 2.8 are motivated from a physical and practical point of view and they make sense in the way that a negative density and therefore a negative pressure are just not physically possible. Additionally, in a properly managed gas network there will always be a minimum amount of gas in each pipe. Concerning (2), we can assume that gas inside a network travels at a speed of approximately 20 km/h if the network is properly managed [OGE15]. Assumption 2.8 is crucial for the PDAE analysis in Chapter 3.*

**Remark 2.10.** *For a more convenient notation, we will often use  $a_i$ ,  $D_i$ ,  $\ell_i$  instead of  $a_{e_i}$ ,  $D_{e_i}$ ,  $\ell_{e_i}$  for  $e_i \in \mathcal{E}_p$ .*

## 2.4 Function spaces and norms

In this section, we introduce the basic mathematical notation and functional analytic background needed for the analysis of gas networks in a function space setting. For a more detailed overview of function spaces in connection to graphs, we refer to [Mug14] or to [Eva10] in a more general setting.

A *real Banach space*  $V$  is a complete, normed vector space on  $\mathbb{R}$ . The norm is denoted by  $\|\cdot\|_V$ . If in addition a real Banach space  $V$  is equipped with a scalar product  $(\cdot|\cdot)_V$ ,  $V$  is

a *Hilbert space*. The space of integrable functions is such a Banach space. For  $1 \leq p < \infty$  and  $\Omega \subset \mathbb{R}^n$  an open subset we define

$$L_p(\Omega) := \{f: \Omega \rightarrow \mathbb{R} \text{ measurable} \mid \|f\|_{L_p(\Omega)} < \infty\} \quad \|f\|_{L_p(\Omega)} := \left( \int_{\Omega} |f|^p dx \right)^{\frac{1}{p}}.$$

In the special case of  $p = 2$ ,  $L_2(\Omega)$  with the inner product

$$(f|g)_2 := \int_{\Omega} f(x)g(x)dx$$

is a Hilbert space.

Before we continue, we want to make clear that elements in  $L_p(\Omega)$  are not functions but equivalence classes, meaning that for  $f, g \in L_p(\Omega)$  it holds that  $f \equiv g$  if they only differ pointwise on zero-sets. We also say that  $f \equiv g$  if they are equal almost everywhere (a.e.).

The so-called *Sobolev spaces* provide a proper setting in the analysis of PDEs [Eva10], where it is often useful to have a more general definition of differentiability. For  $f, g \in L_{1,\text{loc}}(\Omega) = \{v: \Omega \rightarrow \mathbb{R}: v \in L_1(U) \text{ for each } U \subset\subset \Omega\}$ , we say that  $f$  has a *weak partial derivative* w.r.t.  $x_i$  for  $x = (x_1 \dots x_n)^{\top} \in \mathbb{R}^n$ , if there exists  $g \in L_{1,\text{loc}}(\Omega)$  so that

$$\int_{\Omega} f \partial_{x_i} \phi dx = - \int_{\Omega} g \phi dx \quad \forall \phi \in C_0^{\infty}(\Omega).$$

With this concept of weak differentiability, we can now introduce the space

$$H^1(\Omega) = \{f \in L_2(\Omega): \partial_{x_i} f \in L_2(\Omega), 1 \leq i \leq n\}.$$

The space  $H^1(\Omega)$  with

$$\begin{aligned} \|f\|_{H^1(\Omega)} &= \left( \|f\|_{L_2(\Omega)}^2 + \sum_{i=1}^n \|\partial_{x_i} f\|_{L_2(\Omega)}^2 \right)^{\frac{1}{2}} \\ (f|g)_{H^1(\Omega)} &= (f|g)_{L_2(\Omega)} + \sum_{i=1}^n (\partial_{x_i} f | \partial_{x_i} g)_{L_2(\Omega)} \end{aligned}$$

is a Hilbert space. For the case of  $\Omega \subset \mathbb{R}$ , the norm and scalar product reduce to

$$\begin{aligned} \|f\|_{H^1(\Omega)} &= \left( \|f\|_{L_2(\Omega)}^2 + \|\partial_x f\|_{L_2(\Omega)}^2 \right)^{\frac{1}{2}} \\ (f|g)_{H^1(\Omega)} &= (f|g)_{L_2(\Omega)} + (\partial_x f | \partial_x g)_{L_2(\Omega)}. \end{aligned}$$

So far, we only defined Lebesgue and Sobolev spaces on the open set  $\Omega \subset \mathbb{R}^n$ . We will now define those function spaces on Graphs. Let  $\mathfrak{G} = (V, \mathcal{E}, \ell)$  be a directed, weighted graph. Then we can define the function space

$$L_2(\mathfrak{G}) := \{f = (f_1, \dots, f_{n_{\mathcal{E}}}) \mid f_i(t) \in L_2((0, \ell_{e_i})) \text{ for } t \in \mathcal{I}\}$$

and the norm

$$\|f\|_{L_2(\mathfrak{G})} = \left( \sum_{e \in \mathcal{E}} \|f_e\|_{L_2(0, \ell_e)}^2 \right)^{\frac{1}{2}}$$

that makes  $L_2(\mathfrak{G})$  into a Banach space. Equipped with the inner product

$$(f | g)_{L_2(\mathfrak{G})} = \sum_{e \in \mathcal{E}} (f_e | g_e)_{L_2(0, \ell_e)}$$

$L_2(\mathfrak{G})$  is a Hilbert space.

For a more convenient notation, we use

$$\|\cdot\|_{\mathfrak{G}} = \|\cdot\|_{L_2(\mathfrak{G})} \quad (\cdot | \cdot)_{\mathfrak{G}} = (\cdot | \cdot)_{L_2(\mathfrak{G})}.$$

Until now, we only considered functions depending on a space variable  $x$ . The introduced Lebesgue and Sobolev spaces can be extended to functions also depending on time  $t$ , the so-called *Bochner spaces*. Let  $X$  denote a real Banach space with norm  $\|\cdot\|_X$ . The space  $\mathcal{C}(\mathcal{I}, X)$  comprises all continuous functions

$$u: \mathcal{I} \rightarrow X$$

with

$$\|u\|_{\mathcal{C}(\mathcal{I}, X)} := \max_t \|u(t)\|_X.$$

Similarly, the space  $\mathcal{C}^2(\mathcal{I}, L_2(\mathfrak{G}))$  comprises all functions

$$u: \mathcal{I} \rightarrow L_2(\mathfrak{G})$$

that are twice continuously differentiable. One can of course define the spaces  $C(\mathcal{I}, H^1(\mathfrak{G}))$  and  $C^2(\mathcal{I}, H^1(\mathfrak{G}))$  in the same way.

## 2.5 ADAE Model

This section introduces the formulation of the gas network PDAEs we formulated in Section 2.3 as ADAEs. Therefore, we define the function space

$$\mathcal{U} := H^1(\mathfrak{G}) \times H^1(\mathfrak{G})$$

and denote the dual space of  $\mathcal{U}$  by  $\mathcal{U}^*$ .

**Pipe network ADAE** We start by formulating the ADAE for a pipe network  $\mathcal{G} = (V, \mathcal{E})$ . The corresponding PDAE is given by System (2.22). For operators

$$\mathcal{A}: \mathcal{U} \rightarrow \mathcal{U}^* \quad \mathcal{B}(\cdot, t): \mathcal{U} \rightarrow \mathcal{U}^* \quad \mathcal{C}(\cdot, \cdot, t): \mathcal{U} \times \mathbb{R}^{|V|} \rightarrow \mathbb{R}^{2|\mathcal{E}|+|V|},$$

the ADAE is given by

$$\mathcal{A}u'(t) + \mathcal{B}(u(t), t) = 0 \quad \text{f.a.a. } t \in \mathcal{I} \quad (2.24a)$$

$$\mathcal{C}(u(t), z(t), t) = 0 \quad t \in \mathcal{I} \quad (2.24b)$$

for  $u = (p \ q)^\top$  being the pressures and mass flows of the pipes and  $z(t) = p_V(t) \in \mathbb{R}^{|V|}$  being pressure variables at the nodes  $u \in V = \{u_1, \dots, u_{|V|}\}$ . The pressures  $p_V$  are given by

$$p_V = (p_{u_1} \ \dots \ p_{u_{|V|}})^\top.$$

The operators for equation (2.24a) are defined as

$$\begin{aligned} \mathcal{A}(u'(t))(v) &= \sum_{e \in \mathcal{E}} ((p'_e, v_{e,1})_{L_2(0, \ell_e)} + (q'_e, v_{e,2})_{L_2(0, \ell_e)}) \\ \mathcal{B}(u(t), t)(v) &= \sum_{e \in \mathcal{E}} (\alpha_e(\partial_x p_e, v_{e,1})_{L_2(0, \ell_e)} + \beta_e(\partial_x q_e, v_{e,2})_{L_2(0, \ell_e)} - (g_e(p_e, q_e), v_{e,2})_{L_2(0, \ell_e)}), \end{aligned}$$

where  $g_e(p_e, q_e)$  is given by the right-hand side of equation (2.22b). The operator in (2.24b) defines the coupling and boundary conditions given by equations (2.22c) to (2.22f).

**Gas network ADAE** For the ADAE describing a general gas network that is given in PDAE (2.23), we define operators

$$\mathcal{A}: \mathcal{U} \rightarrow \mathcal{U}^* \quad \mathcal{B}(\cdot, t): \mathcal{U} \rightarrow \mathcal{U}^* \quad \mathcal{C}(\cdot, \cdot, t): \mathcal{U} \times \mathbb{R}^{n_z} \rightarrow \mathbb{R}^{2|\mathcal{E}_P| + n_z}.$$

The ADAE is given by

$$\mathcal{A}u'(t) + \mathcal{B}(u(t), t) = 0 \quad \text{f.a.a. } t \in \mathcal{I} \quad (2.25a)$$

$$\mathcal{C}(u(t), z(t), t) = 0 \quad t \in \mathcal{I} \quad (2.25b)$$

for  $u = (p \ q)^\top$  being the pressures and mass flows of the pipes. The remaining variable  $z(t) = (p_V(t) \ q_{\mathcal{R}}(t) \ q_{\mathcal{C}}(t) \ y_{\mathcal{C}}(t))^\top \in \mathbb{R}^{n_z}$  with  $n_z = |V| + |\mathcal{E}_{\mathcal{R}}| + 5|\mathcal{E}_{\mathcal{C}}|$ , contains the pressure at the nodes, the active element mass flows and internal variables of the compressors. The operators in equation (2.25a) are defined as

$$\begin{aligned} \mathcal{A}(u'(t))(v) &= \sum_{e \in \mathcal{E}} ((p'_e, v_{e,1})_{L_2(0, \ell_e)} + (q'_e, v_{e,2})_{L_2(0, \ell_e)}) \\ \mathcal{B}(u(t), t)(v) &= \sum_{e \in \mathcal{E}} (\alpha_e(\partial_x p_e, v_{e,1})_{L_2(0, \ell_e)} + \beta_e(\partial_x q_e, v_{e,2})_{L_2(0, \ell_e)} - (g_e(p_e, q_e), v_{e,2})_{L_2(0, \ell_e)}), \end{aligned}$$

where  $g_e(p_e, q_e)$  is given by the right-hand side of equation (2.23b). The operator  $\mathcal{C}$  defines the active element equations (2.23d) and (2.23e), as well as the coupling and boundary conditions given by equations (2.23c) to (2.23g).

### 2.6 Conclusion

In this chapter, we have introduced the basic element models for gas transport that will be needed throughout this thesis.

We briefly discussed the pipe model hierarchy, that can be derived by simplifications from the Euler equations (see equation (2.1)) with a focus on two quasi-linear hyperbolic PDE models: One with general gas factor  $z$ , the ISO2 model (see equation (2.9)), and one with constant gas factor  $z$  we call the ISO2' model (see equation (2.12)). In addition, we introduced a formula to model resistors (2.13) as well as the two most common types of compressor machines in gas networks (see equations (2.15) and (2.16)), and derived properties of the compressor equations that will be needed for the analysis in Chapter 4. For more detailed introduction to gas network modelling, we refer to [Her07; BGH11; Koc<sup>+</sup>15; Dom<sup>+</sup>17].

In Section 2.3, we defined two classes of PDAE systems, one for pipe networks and one for more general networks with active elements, we will refer to in Chapters 3 and 4. In addition, we introduced the respective ADAE formulation for the two PDAE classes in Section 2.5.



### 3 Perturbation analysis of hyperbolic PDAEs

Just as for DAEs, which allow an easy modelling of many fields of application, e.g., electrical circuits or multibody dynamics, the same is true for PDEs and PDAEs [Sim98; Sim00; Tis04], especially when it comes to physical applications such as gas and water distribution networks. Unlike the theory of DAEs, which has been developed in the last thirty years [GM86; HLR89; KM06; Ria08; LMT13], such a complete theory is missing when it comes to PDAEs or ADAEs. Nevertheless, they have attracted more interest in recent years, when index concepts, which are an essential tool in the analysis for DAEs, were defined for linear ADAEs [CM96; LSE99]. A complete theory regarding existence and uniqueness of these systems is still missing. For PDEs, a more complete theory exists. However, its approaches are either specific for the respective category of PDE, whether they are elliptic, parabolic or hyperbolic, or they are even tailored for the specific problem and are only valid for one special type of equation. By introducing additional restrictions in terms of coupling conditions, or coupling PDEs with DAEs, ODEs or algebraic equations, which is the case for PDAEs/ADAEs, one further increases the complexity.

Lately, these problems were addressed in [Tis04; LMT05] for electrical circuits or in [Mat12]. The latter established a theory to derive existence and uniqueness results for certain elliptic and parabolic PDEs that are coupled with DAEs arising from circuit simulation, leading to a non-linear ADAE system, by using the concept of monotone operators. In [Hei14] necessary conditions for the existence of solutions to ADAEs were derived for problems arising from the incompressible Navier-Stokes equations and in [Alt15] regularisation techniques for PDAEs were addressed.

In this chapter, we investigate the behaviour of solutions of the hyperbolic PDAE describing gas pipe networks. Such a system was introduced in Section 2.3 (see equation (2.22)). We are interested in the sensitivity of solutions of the PDAE w.r.t. perturbations that may appear in the PDE part, but also in the boundary and coupling conditions, as well as in the initial data.

As for the analysis of DAEs, the idea of an index concept does also exist for PDAEs. Many of these index concepts were originally defined for DAEs and have been extended to PDAEs, such as the tractability index [LMT13] or the differentiation index [MB00]. For our analysis, the approach of the perturbation index is more convenient. The concept of the perturbation index, originally defined for DAEs in [HLR89] in 1989, was extended to the infinite dimensional case, too. We want to present the definition from [Bod07] for ADAEs.

**Definition 3.1** (Perturbation index for ADAEs [Bod07, Definition 2.33]). *Let  $u_* \in S \subset X$  be a unique solution of*

$$\mathcal{A} \frac{d}{dt} \mathcal{D}(u(t), t) + \mathcal{B}(u(t), t) = 0 \quad t \in \mathcal{I} \quad (3.1)$$

in an appropriate solution space  $S$  with initial value  $u(t_0) = u_0$  and operators

$$\mathcal{A}: Z \rightarrow W \quad \mathcal{D}(\cdot, t): V \rightarrow Z \quad \mathcal{B}(\cdot, t): V \rightarrow W$$

with  $V, W, Z$  being Banach spaces where no time derivatives are measured. We also consider the perturbed system

$$\mathcal{A} \frac{d}{dt} \mathcal{D}(u^\delta(t), t) + \mathcal{B}(u^\delta(t), t) = \delta(t) \quad t \in \mathcal{I} \quad (3.2a)$$

$$u^\delta(t_0) = u_0^\delta \quad (3.2b)$$

and assume that  $\delta \in \mathcal{C}^{k-1}(\mathcal{I}, W)$  and  $u_0 - u_0^\delta = \delta_0 \in V$  are sufficiently small. If  $u_*^\delta \in S$  is a unique solution to (3.2) and  $k$  the smallest number for which an estimate of the form

$$\|u_* - u_*^\delta\|_V \leq c \left( \|\delta_0\|_V + \sum_{i=0}^{k-1} \|\delta^{(i)}\|_W \right) \quad (3.3)$$

with a constant  $c > 0$  holds. Then we say that the ADAE (3.1) has perturbation index  $k$ .

Other definitions can be found in [CM99; AR07].

The main purpose of this chapter is to derive an estimate of the form of equation (3.3) for the ADAE (2.24) describing pipe networks. To derive this result, we first discuss the properties concerning the network topology. In Section 3.2, we introduce a homogenisation technique for pipe networks that allows us to derive a priori bounds for the solution of the PDAE, but also for its first time derivative in Section 3.3. These bounds are used in Section 3.4 to derive a perturbation result similar to the concept of the perturbation index.

## 3.1 Pipe network topology

In this section, we establish the basic assumptions on the graph topology that are needed for the perturbation analysis of PDAEs describing pipe networks as formulated as in equation (2.22).

**Theorem 3.2.** *Let  $\mathcal{G} = (V, \mathcal{E})$  be a connected, oriented graph of a pipe network, hence  $\mathcal{E} = \mathcal{E}_\mathcal{P}$ . If  $V_p \neq \emptyset$ , it is possible to change the orientation of the branches in  $\mathcal{E}$  so that*

$$\delta^+(u) \neq \emptyset \quad \forall u \in V_q.$$

*If  $V_p = \emptyset$ , we choose a node  $u_0 \in V_q$  and can orientate the branches in  $\mathcal{E}$  so that*

$$\begin{aligned} \delta^+(u) &\neq \emptyset & \forall u \in V_q \setminus \{u_0\} \\ \delta^+(u_0) &= \emptyset. \end{aligned}$$

*Proof.* Let  $\mathcal{G}^0 = (V, \mathcal{E}^{(0)})$  be an arbitrary tree of  $\mathcal{G}$  and the degree of a node  $u \in V$  with

respect to a given branch set  $\mathcal{E}^{(i)}$  be defined as

$$\deg_{\mathcal{E}^{(i)}}(u) := |(\delta^+(u) \cup \delta^-(u)) \cap \mathcal{E}^{(i)}|, \quad (3.4)$$

the number of branches  $e \in \mathcal{E}^{(i)}$  that are connected to the node  $u$ . Let  $V_p \neq \emptyset$ . We orientate the pipes in  $\mathcal{G}^0$  as follows:

- (1)  $i = 0$ , set  $V^{(0)} = V$ .
- (2) If there exists a node  $u \in V_q \cap V^{(i)}$  so that  $\deg_{\mathcal{E}^{(i)}}(u) = 1$ , we change the orientation of the branch if  $e \in \delta^-(u)$  so that  $e = (v, u) \in \delta^+(u)$  and go to (4).
- (3) If there exists no such node, then there is a node  $u \in V_p \cap V^{(i)}$  with  $\deg_{\mathcal{E}^{(i)}}(u) = 1$ . If the pipe  $e = (v, u) \in \delta^+(u)$  we set  $e = (u, v)$ .
- (4) Set  $V^{(i+1)} = V^{(i)} \setminus \{u\}$ ,  $\mathcal{E}^{(i+1)} = \mathcal{E}^{(i)} \setminus \{e\}$ ,  $\mathcal{G}^{(i+1)} = (V^{(i+1)}, \mathcal{E}^{(i+1)})$ ,  $i = i + 1$ .
- (5) If  $V^{(i)} \neq \emptyset$  go to (2).
- (6) If  $\delta^+(u) \cap \mathcal{E} \setminus \mathcal{E}^{(0)} \neq \emptyset \forall u \in V_q$  change the orientation of all branches  $e \in \delta^+(u)$ ,  $u \in V_p$ .

Since each of the steps (2) to (3) operates on a tree, there always exists either a node that fulfils (2) or (3). Eventually we get to (6) and the algorithm terminates, because in step  $j$ ,  $\mathcal{G}^{(j)}$  gets reduced by one node and one arc and  $\mathcal{G}^{(j+1)}$  also is a tree.

In the case that  $V_p = \emptyset$ , we choose a node  $u_0 \in V_q$  and perform the steps above with  $\bar{V}_p = \{u_0\}$  and  $\bar{V}_q = V_q \setminus \{u_0\}$ . If  $\mathcal{G}$  is not connected, perform the steps for each connected component.  $\square$

As a consequence of this theorem, we can choose a *reference arc*  $e_u \in \mathcal{E}$  for each  $u \in V_q$ , so that  $e_u \in \delta^+(u)$  if  $u \neq u_0$  and  $e_{u_0} \in \delta^-(u_0)$  to reformulate the coupling and boundary conditions (2.23f) to (2.23h) and derive the following PDAE system for pipe networks

$$\partial_t p_e(x, t) + \alpha_e \partial_x q_e(x, t) = 0 \quad e \in \mathcal{E} \quad (3.5a)$$

$$\partial_t q_e(x, t) + \beta_e \partial_x p_e(x, t) = -g_e(p_e(x, t), q_e(x, t)) \quad e \in \mathcal{E} \quad (3.5b)$$

on  $[0, \ell_e] \times \mathcal{I}$ ,

$$\sum_{e \in \delta^+(u)} q_{e,r}(t) - \sum_{e \in \delta^-(u)} q_{e,l}(t) = q_u^\Gamma(t) \quad u \in V_q \quad t \in \mathcal{I} \quad (3.5c)$$

$$p_{e,r}(t) - p_{e_u,r}(t) = 0 \quad e \in \delta^+(u), u \in V_q \setminus \{u_0\} \quad t \in \mathcal{I} \quad (3.5d)$$

$$p_{e,l}(t) - p_{e_u,r}(t) = 0 \quad e \in \delta^-(u), u \in V_q \setminus \{u_0\} \quad t \in \mathcal{I} \quad (3.5e)$$

$$p_{e,l}(t) - p_{e_{u_0},l}(t) = 0 \quad e \in \delta^-(u_0) \quad t \in \mathcal{I} \quad (3.5f)$$

$$p_{e,l}(t) = p_u^\Gamma(t) \quad e \in \delta^-(u), u \in V_p \quad t \in \mathcal{I} \quad (3.5g)$$

$$p_{e,r}(t) = p_u^\Gamma(t) \quad e \in \delta^+(u), u \in V_q \quad t \in \mathcal{I}. \quad (3.5h)$$

$$p_e(x, t_0) = p_e^0(x) \quad e \in \mathcal{E} \quad x \in [0, \ell_e] \quad (3.5i)$$

$$q_e(x, t_0) = q_e^0(x) \quad e \in \mathcal{E} \quad x \in [0, \ell_e], \quad (3.5j)$$

with coefficients  $\alpha_e = \frac{c^2}{a_e}$ ,  $\beta_e = a_e$  and the function  $g_e$  on the right-hand side of equation (3.5b) is defined as

$$g_e(p, q) := \gamma_e \frac{q|q|}{p} + \sigma_e p \quad (3.6)$$

with constants  $\gamma_e = \frac{\lambda_e c^2}{2D_e a_e}$  and  $\sigma_e = \frac{g a_e h'_e}{c^2}$ .

In order to investigate the impact of perturbations on the solution to System (3.5), we consider the perturbed problem for pipe networks, with perturbations that appear on the right-hand side of all equations:

$$\partial_t p_e^\delta(x, t) + \alpha_e \partial_x q_e^\delta(x, t) = \delta_{p,e}^\Omega(x, t) \quad e \in \mathcal{E} \quad (3.7a)$$

$$\partial_t q_e^\delta(x, t) + \beta_e \partial_x p_e^\delta(x, t) = -g_e(p_e^\delta(x, t), q_e^\delta(x, t)) + \delta_{q,e}^\Omega(x, t) \quad e \in \mathcal{E} \quad (3.7b)$$

on  $[0, \ell_e] \times \mathcal{I}$ ,

$$\sum_{e \in \delta^+(u)} q_{e,r}^\delta(t) - \sum_{e \in \delta^-(u)} q_{e,l}^\delta(t) = q_u^\Gamma(t) + \delta_u^q(t) \quad u \in V_q \quad t \in \mathcal{I} \quad (3.7c)$$

$$p_{e,r}^\delta(t) - p_{e_u,r}^\delta(t) = \delta_{e,u}^p(t) \quad e \in \delta^+(u), u \in V_q \quad t \in \mathcal{I} \quad (3.7d)$$

$$p_{e,l}^\delta(t) - p_{e_u,r}^\delta(t) = \delta_{e,u}^p(t) \quad e \in \delta^-(u), u \in V_q \quad t \in \mathcal{I} \quad (3.7e)$$

$$p_{e,l}^\delta(t) - p_{e_{u_0},l}^\delta(t) = \delta_{e,u_0}^p(t) \quad e \in \delta^-(u_0) \quad t \in \mathcal{I} \quad (3.7f)$$

$$p_{e,r}^\delta(t) = p_u^\Gamma(t) + \delta_{e,u}^p(t) \quad e \in \delta^+(u), u \in V_p \quad t \in \mathcal{I} \quad (3.7g)$$

$$p_{e,l}^\delta(t) = p_u^\Gamma(t) + \delta_{e,u}^p(t) \quad e \in \delta^-(u), u \in V_p \quad t \in \mathcal{I} \quad (3.7h)$$

$$p_e^\delta(x, t_0) = p_e^0(x) + \delta_{p,e}^0(x) \quad e \in \mathcal{E} \quad x \in [0, \ell_e] \quad (3.7i)$$

$$q_e^\delta(x, t_0) = q_e^0(x) + \delta_{q,e}^0(x) \quad e \in \mathcal{E} \quad x \in [0, \ell_e], \quad (3.7j)$$

where we neglected parts of the arguments and used

$$\begin{aligned} p_{e,r}^\delta &= p_e^\delta(\ell_e, t) & p_{e,l}^\delta(t) &= p_e^\delta(0, t) \\ q_{e,r}^\delta &= q_e^\delta(\ell_e, t) & q_{e,l}^\delta(t) &= q_e^\delta(0, t) \end{aligned}$$

for a more convenient notation.

## 3.2 Homogenisation

This section introduces the specific homogenisation functions we need to reformulate the PDAEs (3.5) and (3.7), so that the boundary and coupling conditions are satisfied with zero right-hand side.

**Definition 3.3** (Homogenisation functions). For the perturbed PDAE (3.7), we define the homogenisation functions  $\bar{p}^\delta$  and  $\bar{q}^\delta$  component-wise for  $e = (u, v) \in \mathcal{E}$  by

$$\bar{q}_e^\delta(x, t) = \begin{cases} 0 & e \neq e_u, e \neq e_v \\ \frac{x}{\ell_e}(q_v^\Gamma(t) + \delta_v^q(t)) & e \neq e_u, e = e_v \\ -\frac{\ell_e - x}{\ell_e}(q_u^\Gamma(t) + \delta_u^q(t)) & e = e_u, e \neq e_v \\ \frac{x}{\ell_e}(q_v^\Gamma(t) + \delta_v^q(t)) - \frac{\ell_e - x}{\ell_e}(q_u^\Gamma(t) + \delta_u^q(t)) & e = e_u, e = e_v \end{cases} \quad (3.8a)$$

$$\bar{p}_e^\delta(x, t) = \begin{cases} \frac{\ell_e - x}{\ell_e}(p_u^\Gamma(t) + \delta_{e,u}^p(t)) + \frac{x}{\ell_e}(p_v^\Gamma(t) + \delta_{e,v}^p(t)) & e \neq e_u, e \neq e_v \\ \frac{\ell_e - x}{\ell_e}(p_u^\Gamma(t) + \delta_{e,u}^p(t)) & e \neq e_u, e = e_v \\ \frac{x}{\ell_e}(p_v^\Gamma(t) + \delta_{e,v}^p(t)) & e = e_u, e \neq e_v \\ 0 & e = e_u, e = e_v. \end{cases} \quad (3.8b)$$

**Remark 3.4.** We want to emphasise the following remarks concerning the homogenisation functions.

1. The homogenisation functions  $\bar{p}_e$  and  $\bar{q}_e$ ,  $e \in \mathcal{E}$  for the unperturbed PDAE (3.5) are defined by setting the perturbations  $\delta_u^q, \delta_v^q$ ,  $\delta_{e,u}^p$  and  $\delta_{e,v}^p$  in (3.8) to zero.
2. The functions  $p_u^\Gamma$  are given by

$$p_u^\Gamma(t) = \begin{cases} p_v^\Gamma(t) & u = v \in V_p \\ 0 & \text{else.} \end{cases}$$

3. Due to Theorem 3.2, the cases where  $e = e_u$  are only needed if  $V_p = \emptyset$  and  $u = u_0$ .

**Corollary 3.5.** At the boundary of pipe  $e = (u, v) \in \mathcal{E}$  the homogenisation functions are given by

$$\begin{aligned} \bar{p}_e^\delta(0, t) &= \begin{cases} p_u^\Gamma(t) + \delta_{e,u}^p(t) & e \neq e_u \\ 0 & e = e_u \end{cases} & \bar{p}_e^\delta(\ell_e, t) &= \begin{cases} p_v^\Gamma(t) + \delta_{e,v}^p(t) & e \neq e_v \\ 0 & e = e_v \end{cases} \\ \bar{q}_e^\delta(0, t) &= \begin{cases} 0 & e \neq e_u \\ -(q_u^\Gamma(t) + \delta_u^q(t)) & e = e_u \end{cases} & \bar{q}_e^\delta(\ell_e, t) &= \begin{cases} 0 & e \neq e_v \\ q_v^\Gamma(t) + \delta_v^q(t) & e = e_v. \end{cases} \end{aligned}$$

**Theorem 3.6.** Let  $p^\delta, q^\delta$  be a solution to the perturbed PDAE (3.7) and let  $\bar{p}^\delta$  and  $\bar{q}^\delta$  be defined as in Definition 3.3. Then  $\tilde{p}^\delta = p^\delta - \bar{p}^\delta$ ,  $\tilde{q}^\delta = q^\delta - \bar{q}^\delta$  solves

$$\partial_t \tilde{p}_e^\delta + \alpha_e \partial_x \tilde{q}_e^\delta = \delta_{p,e}^\Omega - \partial_t \bar{p}_e^\delta - \alpha_e \partial_x \bar{q}_e^\delta \quad e \in \mathcal{E} \quad (3.9a)$$

$$\partial_t \tilde{q}_e^\delta + \beta_e \partial_x \tilde{p}_e^\delta = \delta_{q,e}^\Omega - \partial_t \bar{q}_e^\delta - \beta_e \partial_x \bar{p}_e^\delta - g_e(\tilde{p}_e^\delta + \bar{p}_e^\delta, \tilde{q}_e^\delta + \bar{q}_e^\delta) \quad e \in \mathcal{E} \quad (3.9b)$$

on  $[0, \ell_e] \times \mathcal{I}$ ,

$$\sum_{e \in \delta^+(u)} \tilde{q}_{e,r}^\delta(t) - \sum_{e \in \delta^-(u)} \tilde{q}_{e,l}^\delta(t) = 0 \quad u \in V_q \quad t \in \mathcal{I} \quad (3.9c)$$

$$\tilde{p}_{e,r}^\delta(t) - \tilde{p}_{e_u,r}^\delta(t) = 0 \quad e \in \delta^+(u), u \in V_q \quad t \in \mathcal{I} \quad (3.9d)$$

$$\tilde{p}_{e,l}^\delta(t) - \tilde{p}_{e_u,r}^\delta(t) = 0 \quad e \in \delta^-(u), u \in V_q \quad t \in \mathcal{I} \quad (3.9e)$$

$$\tilde{p}_{e,l}^\delta(t) - \tilde{p}_{e_{u_0},l}^\delta(t) = 0 \quad e \in \delta^+(u_0) \quad t \in \mathcal{I} \quad (3.9f)$$

$$\tilde{p}_{e,r}^\delta(t) = 0 \quad e \in \delta^+(u), u \in V_p \quad t \in \mathcal{I} \quad (3.9g)$$

$$\tilde{p}_{e,l}^\delta(t) = 0 \quad e \in \delta^-(u), u \in V_p \quad t \in \mathcal{I} \quad (3.9h)$$

$$\tilde{p}_e^\delta(x, t_0) = p_e^0(x) + \delta_{p,e}^0(x) \tilde{p}_e^\delta(x, t_0) \quad e \in \mathcal{E} \quad x \in [0, \ell_e] \quad (3.9i)$$

$$\tilde{q}_e^\delta(x, t_0) = q_e^0(x) + \delta_{q,e}^0(x) - \tilde{p}_e^\delta(x, t_0) \quad e \in \mathcal{E} \quad x \in [0, \ell_e]. \quad (3.9j)$$

*Proof.* We first show the statement for equation (3.9a):

$$\begin{aligned} \partial_t \tilde{p}_e^\delta + \alpha_e \partial_x \tilde{q}_e^\delta &= \partial_t p_e^\delta + \alpha \partial_x q^\delta - \left( \partial_t \tilde{p}_e^\delta + \alpha_e \partial_x \tilde{q}_e^\delta \right) \\ &= \delta_{p,e}^\Omega - \partial_t \tilde{p}_e^\delta - \alpha_e \partial_x \tilde{q}_e^\delta. \end{aligned}$$

The statement for equation (3.9b) follows by similar calculations. Concerning the balance equation (3.9c) it holds that

$$\begin{aligned} \sum_{e \in \delta^+(u)} \tilde{q}_{e,r}^\delta(t) - \sum_{e \in \delta^-(u)} \tilde{q}_{e,l}^\delta(t) &= q_u^\Gamma(t) + \delta_{q,u}^\Gamma(t) - \tilde{q}_{e_u,r}^\delta(t) \\ &= q_u^\Gamma(t) + \delta_{q,u}^\Gamma(t) - (q_u^\Gamma(t) + \delta_{e,u}^q(t)) = 0 \end{aligned}$$

for  $u \in V_q \setminus \{u_0\}$ . For  $u = u_0$  we get

$$\begin{aligned} \sum_{e \in \delta^+(u_0)} \tilde{q}_{e,r}^\delta(t) - \sum_{e \in \delta^-(u_0)} \tilde{q}_{e,l}^\delta(t) &= q_{u_0}^\Gamma(t) + \delta_{u_0}^q(t) + \tilde{q}_{e_{u_0},l}^\delta(t) \\ &= q_{u_0}^\Gamma(t) + \delta_{u_0}^q(t) - (q_{u_0}^\Gamma(t) + \delta_{u_0}^q(t)) = 0. \end{aligned}$$

The pressure coupling at nodes  $u \in V_q \setminus \{u_0\}$  yields

$$\tilde{p}_{e,r}^\delta(t) - \tilde{p}_{e_u,r}^\delta(t) = \delta_{e,u}^p(t) - \tilde{p}_{e,r}^\delta(t) + \tilde{p}_{e_u,r}^\delta(t) = \delta_{e,u}^p(t) - \tilde{p}_{e,r}^\delta(t) = 0,$$

since  $\tilde{p}_{e_u,r}^\delta(t) = 0$  and  $\tilde{p}_{e,r}^\delta(t) = p_u^\Gamma(t) + \delta_{e,u}^p(t)$  with  $p_u^\Gamma = 0$ , since  $e \neq e_u$  and  $u \in V_q$ . The assertion for equation (3.9e) follows by similar argumentation. For the coupling at  $u_0$  it holds that

$$\tilde{p}_{e,l}^\delta(t) - \tilde{p}_{e_{u_0},l}^\delta(t) = \delta_{e,u_0}^p(t) - \tilde{p}_{e,l}^\delta(t) + \tilde{p}_{e_{u_0},l}^\delta(t) = \delta_{e,u_0}^p(t) - \tilde{p}_{e,l}^\delta(t) = 0,$$

since  $\tilde{p}_{e_{u_0},l}^\delta(t) = 0$  and  $\tilde{p}_{e,l}^\delta(t) = \delta_{e,u_0}^p(t)$ . For  $e \in \delta^+(u)$ ,  $u \in V_p$  we get

$$\tilde{p}_{e,r}^\delta(t) = p_u^\Gamma(t) + \delta_{e,u}^p(t) - \tilde{p}_{e,r}^\delta(t) = p_u^\Gamma(t) + \delta_{e,u}^p(t) - p_u^\Gamma(t) + \delta_{e,u}^p(t) = 0,$$

since  $e \neq e_u$ , because for  $u \in V_p$  no such reference node has been defined. The assertion for (3.9h) follows by similar considerations. Equations (3.9i) and (3.9j) follow by straight forward calculation.  $\square$

**Suitable homogenisation functions for an example network** For the network given by Figure 3.1, we consider two scenarios for the node and branch sets and derive homogenisation functions according to Definition 3.3.

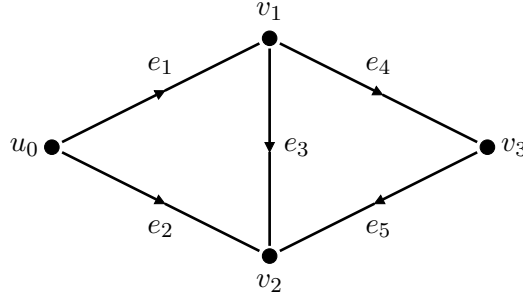


**Figure 3.1:** Example network for the homogenisation consisting of four nodes and five pipes.

**Example 3.7.** Let the node and branch sets given by

$$\begin{aligned} V_p &= \{u_0\} & V_q &= \{v_1, v_2, v_3\} \\ \delta^+(v_1) &= \{e_1\} & \delta^+(v_2) &= \{e_2, e_3, e_5\} & \delta^+(v_3) &= \{e_4\}. \end{aligned}$$

To define the coupling at the nodes in  $V_q$ , we chose the reference arcs

$$e_{v_1} = e_1 \quad e_{v_2} = e_2 \quad e_{v_3} = e_4.$$

The coupling and boundary conditions for the network are defined by

$$\begin{aligned} q_{e_1,r}^\delta(t) - q_{e_3,l}^\delta(t) - q_{e_4,l}^\delta(t) &= q_{v_1}^\Gamma(t) + \delta_{v_1}^q(t) \\ q_{e_2,r}^\delta(t) + q_{e_3,r}^\delta(t) + q_{e_5,r}^\delta(t) &= q_{v_2}^\Gamma(t) + \delta_{v_2}^q(t) \\ q_{e_4,r}^\delta(t) - q_{e_5,l}^\delta(t) &= q_{v_3}^\Gamma(t) + \delta_{v_3}^q(t) \end{aligned}$$

for the mass flow coupling,

$$\begin{aligned} p_{e_3,l}^\delta(t) - p_{e_{v_1},r}^\delta(t) &= \delta_{e_3,v_1}^p(t) & p_{e_4,l}^\delta(t) - p_{e_{v_1},r}^\delta(t) &= \delta_{e_4,v_1}^p(t) \\ p_{e_3,r}^\delta(t) - p_{e_{v_2},r}^\delta(t) &= \delta_{e_3,v_2}^p(t) & p_{e_5,r}^\delta(t) - p_{e_{v_2},r}^\delta(t) &= \delta_{e_5,v_2}^p(t) \\ p_{e_5,l}^\delta(t) - p_{e_{v_3},r}^\delta(t) &= \delta_{e_5,v_3}^p(t) \end{aligned}$$

for the pressure coupling at the sinks and

$$p_{e_1,l}^\delta(t) = p_{u_0}^\Gamma(t) + \delta_{e_1,u_0}^p(t) \quad p_{e_2,l}^\delta(t) = p_{u_0}^\Gamma(t) + \delta_{e_2,u_0}^p(t)$$

for the pressure boundary at  $u_0$ . By Definition 3.3, the homogenisation functions are

$$\begin{aligned}\bar{q}_{e_1}^\delta(x, t) &= \frac{x}{\ell_{e_1}}(q_{v_1}^\Gamma(t) + \delta_{v_1}^q(t)) & \bar{q}_{e_2}^\delta(x, t) &= \frac{x}{\ell_{e_2}}(q_{v_2}^\Gamma(t) + \delta_{v_2}^q(t)) \\ \bar{q}_{e_4}^\delta(x, t) &= \frac{x}{\ell_{e_4}}(q_{v_3}^\Gamma(t) + \delta_{v_3}^q(t)) & \bar{q}_e^\delta(x, t) &= 0 \quad e \in \{e_3, e_5\}\end{aligned}$$

for the mass flows and

$$\begin{aligned}\bar{p}_{e_1}^\delta(x, t) &= \frac{\ell_{e_1} - x}{\ell_{e_1}}(p_{u_0}^\Gamma(t) + \delta_{e_1, u_0}^p(t)) & \bar{p}_{e_2}^\delta(x, t) &= \frac{\ell_{e_2} - x}{\ell_{e_2}}(p_{u_0}^\Gamma(t) + \delta_{e_2, u_0}^p(t)) \\ \bar{p}_{e_3}^\delta(x, t) &= \frac{\ell_{e_3} - x}{\ell_{e_3}}\delta_{e_2, v_1}^p(t) + \frac{x}{\ell_{e_3}}\delta_{e_3, v_2}^p(t) & \bar{p}_{e_4}^\delta(x, t) &= \frac{\ell_{e_4} - x}{\ell_{e_4}}\delta_{e_4, v_1}^p(t) \\ \bar{p}_{e_5}^\delta(x, t) &= \frac{\ell_{e_5} - x}{\ell_{e_5}}\delta_{e_5, v_2}^p(t) + \frac{x}{\ell_{e_5}}\delta_{e_5, v_3}^p(t)\end{aligned}$$

for the pressures.

**Example 3.8.** As a second example, we consider the network topology given by Figure 3.1 with different node sets

$$V_p = \emptyset \quad V_q = \{u_0, v_1, v_2, v_3\},$$

where we choose  $u_0$  as the reference node we introduced in Theorem 3.2. To define the pressure coupling we choose

$$e_{u_0} = e_1 \quad e_{v_1} = e_1 \quad e_{v_2} = e_2 \quad e_{v_3} = e_4$$

as before. The coupling and boundary data is given by

$$\begin{aligned}-q_{e_1, l}^\delta(t) - q_{e_2, l}^\delta(t) &= q_{u_0}^\Gamma(t) + \delta_{u_0}^q(t) \\ q_{e_1, r}^\delta(t) - q_{e_3, l}^\delta(t) - q_{e_4, l}^\delta(t) &= q_{v_1}^\Gamma(t) + \delta_{v_1}^q(t) \\ q_{e_2, r}^\delta(t) + q_{e_3, r}^\delta(t) + q_{e_5, r}^\delta(t) &= q_{v_2}^\Gamma(t) + \delta_{v_2}^q(t) \\ q_{e_4, r}^\delta(t) - q_{e_5, l}^\delta(t) &= q_{v_3}^\Gamma(t) + \delta_{v_3}^q(t)\end{aligned}$$

for the mass flow coupling and

$$\begin{aligned}p_{e_3, l}^\delta(t) - p_{e_{v_1}, r}^\delta(t) &= \delta_{e_3, v_1}^p(t) & p_{e_4, l}^\delta(t) - p_{e_{v_1}, r}^\delta(t) &= \delta_{e_4, v_1}^p(t) \\ p_{e_3, r}^\delta(t) - p_{e_{v_2}, r}^\delta(t) &= \delta_{e_3, v_2}^p(t) & p_{e_5, r}^\delta(t) - p_{e_{v_2}, r}^\delta(t) &= \delta_{e_5, v_2}^p(t) \\ p_{e_5, l}^\delta(t) - p_{e_{v_3}, r}^\delta(t) &= \delta_{e_5, v_3}^p(t) & p_{e_2, l}^\delta(t) - p_{e_{u_0}, l}^\delta(t) &= \delta_{e_2, u_0}^p(t)\end{aligned}$$

for the pressure coupling at the nodes in  $V_q$ . The homogenisation functions are now given by

$$\begin{aligned}\bar{q}_{e_1}^\delta(x, t) &= \frac{\ell_{e_1} - x}{\ell_{e_1}}(q_{u_0}^\Gamma(t) + \delta_{u_0}^q(t)) + \frac{x}{\ell_{e_1}}(q_{v_1}^\Gamma(t) + \delta_{v_1}^q(t)) \\ \bar{q}_{e_2}^\delta(x, t) &= \frac{x}{\ell_{e_2}}(q_{v_2}^\Gamma(t) + \delta_{v_2}^q(t)) \\ \bar{q}_{e_4}^\delta(x, t) &= \frac{x}{\ell_{e_4}}(q_{v_3}^\Gamma(t) + \delta_{v_3}^q(t)) \\ \bar{q}_e^\delta(x, t) &= 0 \quad e \in \{e_3, e_5\}\end{aligned}$$



for the mass flows and

$$\begin{aligned}\bar{p}_{e_1}^\delta(x, t) &= 0 & \bar{p}_{e_2}^\delta(x, t) &= \frac{\ell_{e_2} - x}{\ell_{e_1}} \delta_{e_2, u_0}^p(t) \\ \bar{p}_{e_3}^\delta(x, t) &= \frac{\ell_{e_3} - x}{\ell_e} \delta_{e_3, v_1}^p(t) + \frac{x}{\ell_{e_3}} \delta_{e_3, v_2}^p(t) & \bar{p}_{e_4}^\delta(x, t) &= \frac{\ell_{e_5} - x}{\ell_{e_4}} \delta_{e_4, v_1}^p(t) \\ \bar{p}_{e_5}^\delta(x, t) &= \frac{\ell_{e_5} - x}{\ell_{e_5}} \delta_{e_5, v_3}^p(t) + \frac{x}{\ell_{e_5}} \delta_{e_5, v_2}^p(t)\end{aligned}$$

regarding the pressures.

### 3.2.1 Properties of the homogenisation functions

Concerning the boundary and coupling data, the initial values and the perturbations, we make the following assumptions:

**Assumption 3.9** (Properties of the boundary and initial data).

We assume that  $p_u^\Gamma, q_v^\Gamma \in \mathcal{C}^2(\mathcal{I}, \mathbb{R}) \forall u \in V_p, v \in V_q$  fulfil

$$(i) \max_t |p_u^\Gamma(t)| \leq C^\Gamma, \max_t |q_v^\Gamma(t)| \leq C^\Gamma, \forall u \in V_p, \forall v \in V_q,$$

$$(ii) \max_t |p_u^{\Gamma'}(t)| \leq C_t^\Gamma, \max_t |q_v^{\Gamma'}(t)| \leq C_t^\Gamma, \forall u \in V_p, \forall v \in V_q,$$

$$(iii) \max_t |p_u^{\Gamma''}(t)| \leq C_{tt}^\Gamma, \max_t |q_v^{\Gamma''}(t)| \leq C_{tt}^\Gamma, \forall u \in V_p, \forall v \in V_q,$$

for constants  $C^\Gamma, C_t^\Gamma, C_{tt}^\Gamma > 0$  and let  $p^0, q^0 \in L_2(\mathfrak{G})$  so that they fulfil equations (3.5c) to (3.5h) for  $t = 0$  and

$$(iv) \|p^0\|_{\mathfrak{G}} \leq c_0, \|q^0\|_{\mathfrak{G}} \leq c_0$$

for a constant  $c_0 > 0$ .

**Assumption 3.10** (Properties of the perturbations).

Let  $\delta_p^\Omega, \delta_q^\Omega \in \mathcal{C}^2(\mathcal{I}, L_2(\mathfrak{G}))$ ,  $\delta_{e,u}^p, \delta_v^q \in \mathcal{C}^2(\mathcal{I}, \mathbb{R})$  for  $u \in V, v \in V_q, e \in \mathcal{E}$  and we set  $\delta^\Gamma$  as the vector that contains all perturbations  $\delta_{e,u}^p$  and  $\delta_u^q$ . Let  $\delta_p^0, \delta_q^0 \in L_2(\mathfrak{G})$  so that

$$(i) \max_t \|\delta_p^\Omega(t)\|_{\mathfrak{G}} \leq c^\Omega, \max_t \|\delta_q^\Omega(t)\|_{\mathfrak{G}} \leq c^\Omega,$$

$$(ii) \max_t \|\partial_t \delta_p^\Omega(t)\|_{\mathfrak{G}} \leq c_t^\Omega, \max_t \|\partial_t \delta_q^\Omega(t)\|_{\mathfrak{G}} \leq c_t^\Omega,$$

$$(iii) \max_t \|\delta^\Gamma(t)\|_\infty \leq c^\Gamma,$$

$$(iv) \max_t \|\delta^{\Gamma'}(t)\|_\infty \leq c_t^\Gamma,$$

$$(v) \max_t \|\delta^{\Gamma''}(t)\|_\infty \leq c_{tt}^\Gamma,$$

for constants  $c^\Omega, c^\Gamma, c_t^\Omega, c_t^\Gamma, c_{tt}^\Gamma > 0$ .

**Theorem 3.11.** *If the perturbations and boundary data are bounded in the sense of Assumptions 3.9 and 3.10, the following assertions hold for the homogenisation functions given by Definition 3.3:*

$$\begin{aligned} \max_t \|\bar{q}^\delta(t)\|_{\mathfrak{G}}^2 &\leq \bar{c}, & \max_t \|\bar{p}^\delta(t)\|_{\mathfrak{G}}^2 &\leq \bar{c}, \\ \max_t \|\partial_t \bar{q}^\delta(t)\|_{\mathfrak{G}}^2 &\leq \bar{c}_t, & \max_t \|\partial_t \bar{p}^\delta(t)\|_{\mathfrak{G}}^2 &\leq \bar{c}_t, \\ \max_t \|\partial_x \bar{q}^\delta(t)\|_{\mathfrak{G}}^2 &\leq \bar{c}_x, & \max_t \|\partial_x \bar{p}^\delta(t)\|_{\mathfrak{G}}^2 &\leq \bar{c}_x, \\ \max_t \|\partial_{tx} \bar{q}^\delta(t)\|_{\mathfrak{G}}^2 &\leq \bar{c}_{tx}, & \max_t \|\partial_{tx} \bar{p}^\delta(t)\|_{\mathfrak{G}}^2 &\leq \bar{c}_{tx}, \\ \max_t \|\partial_{tt} \bar{q}^\delta(t)\|_{\mathfrak{G}}^2 &\leq \bar{c}_{tt}, & \max_t \|\partial_{tt} \bar{p}^\delta(t)\|_{\mathfrak{G}}^2 &\leq \bar{c}_{tt}, \end{aligned}$$

for constants  $\bar{c}, \bar{c}_t, \bar{c}_x, \bar{c}_{tx}, \bar{c}_{tt} > 0$  that are given by

$$\begin{aligned} \bar{c} &= (C^\Gamma + c^\Gamma)^2 \sum_{e \in \mathcal{E}} \ell_e, & \bar{c}_t &= (C_t^\Gamma + c_t^\Gamma)^2 \sum_{e \in \mathcal{E}} \ell_e, \\ \bar{c}_x &= 4 (C^\Gamma + c^\Gamma)^2 \sum_{e \in \mathcal{E}} \frac{1}{\ell_e}, & \bar{c}_{tt} &= (C_{tt}^\Gamma + c_{tt}^\Gamma)^2 \sum_{e \in \mathcal{E}} \frac{1}{\ell_e}, \\ \bar{c}_{tx} &= 4 (C_t^\Gamma + c_t^\Gamma)^2 \sum_{e \in \mathcal{E}} \frac{1}{\ell_e}. \end{aligned}$$

*Proof.* We prove the assertion for  $\bar{q}^\delta$ . Since the structure of the homogenisation is basically the same, the result for  $\bar{p}^\delta$  follows by similar considerations. Let  $e = (v, u) \in \mathcal{E}$ , with  $e = e_u, e = e_v$ .

$$\begin{aligned} \|\bar{q}_e^\delta\|_{L_2(0, \ell_e)}^2 &= \int_0^{\ell_e} \left( \frac{x}{\ell_e} (q_v^\Gamma + \delta_v^q) - \frac{\ell_e - x}{\ell_e} (q_u^\Gamma + \delta_u^q) \right)^2 dx \\ &\leq \frac{\ell_e}{3} ((q_{e,u}^\Gamma + \delta_{e,u}^q)^2 + |q_{e,u}^\Gamma + \delta_{e,u}^q| |q_u^\Gamma + \delta_{u,e}^q| + (q_u^\Gamma + \delta_{u,e}^q)^2) \\ &\leq \ell_e (C^\Gamma + c^\Gamma)^2, \end{aligned}$$

where we have used Cauchy's inequality (see Theorem C.2) to derive the last inequality. For  $e = (v, u) \in \mathcal{E}$  with  $e \neq e_u, e = e_v$  we get the estimate

$$\|q_e^\delta\|_{L_2(0, \ell_e)}^2 = \int_0^{\ell_e} \left( \frac{x}{\ell_e} (q_v^\Gamma + \delta_v^q) \right)^2 dx = \frac{\ell_e}{3} (q_u^\Gamma + \delta_{u,e}^q)^2 \leq \frac{\ell_e}{3} (C^\Gamma + c^\Gamma)^2,$$

which is the same for the remaining cases. Overall, we get

$$\|\bar{q}^\delta(t)\|_{\mathfrak{G}}^2 \leq (C^\Gamma + c^\Gamma)^2 \sum_{e \in \mathcal{E}} \ell_e.$$

Analogous calculations yield the result for  $\partial_t \bar{q}^\delta$  and  $\partial_{tt} \bar{q}^\delta$

$$\|\partial_t \bar{q}^\delta(t)\|_{\mathfrak{G}}^2 \leq (C_t^\Gamma + c_t^\Gamma)^2 \sum_{e \in \mathcal{E}} \ell_e \quad \|\partial_{tt} \bar{q}^\delta(t)\|_{\mathfrak{G}}^2 \leq (C_{tt}^\Gamma + c_{tt}^\Gamma)^2 \sum_{e \in \mathcal{E}} \ell_e.$$

The spatial derivative of  $\bar{q}_e^\delta$  is given by

$$\partial_x \bar{q}_e^\delta(x, t) = \begin{cases} 0 & e \neq e_u, e \neq e_v \\ \frac{1}{\ell_e} (q_v^\Gamma(t) + \delta_v^q(t)) & e \neq e_u, e = e_v \\ \frac{1}{\ell_e} (q_u^\Gamma(t) + \delta_u^q(t)) & e = e_u, e \neq e_v \\ \frac{1}{\ell_e} (q_v^\Gamma(t) + \delta_v^q(t) + q_u^\Gamma(t) + \delta_u^q(t)) & e = e_u, e = e_v. \end{cases}$$

Note that  $\partial_x \bar{q}_e^\delta$  does not depend on  $x$ . This allows to directly compute

$$\|\partial_x \bar{q}_e^\delta(t)\|_{L_2(0, \ell_e)}^2 \leq \frac{4}{\ell_e} (C^\Gamma + c^\Gamma)^2,$$

yielding

$$\|\partial_x \bar{q}^\delta(t)\|_{\mathfrak{G}}^2 \leq 4(C^\Gamma + c^\Gamma)^2 \sum_{e \in \mathcal{E}} \frac{1}{\ell_e}.$$

By the same approach we can show that

$$\|\partial_{tx} \bar{q}^\delta(t)\|_{\mathfrak{G}}^2 \leq 4(C_t^\Gamma + c_t^\Gamma)^2 \sum_{e \in \mathcal{E}} \frac{1}{\ell_e}$$

and complete the proof.  $\square$

**Corollary 3.12.** *If the perturbations and boundary data are bounded in the sense of Assumption 3.9, the following assertions hold:*

$$\begin{aligned} \max_t \|\bar{q}(t)\|_{\mathfrak{G}}^2 &\leq \bar{c}, & \max_t \|\bar{p}(t)\|_{\mathfrak{G}}^2 &\leq \bar{c}, \\ \max_t \|\partial_t \bar{q}(t)\|_{\mathfrak{G}}^2 &\leq \bar{c}_t, & \max_t \|\partial_t \bar{p}(t)\|_{\mathfrak{G}}^2 &\leq \bar{c}_t, \\ \max_t \|\partial_x \bar{q}(t)\|_{\mathfrak{G}}^2 &\leq \bar{c}_x, & \max_t \|\partial_x \bar{p}(t)\|_{\mathfrak{G}}^2 &\leq \bar{c}_x, \\ \max_t \|\partial_{tx} \bar{q}(t)\|_{\mathfrak{G}}^2 &\leq \bar{c}_{tx}, & \max_t \|\partial_{tx} \bar{p}(t)\|_{\mathfrak{G}}^2 &\leq \bar{c}_{tx}, \\ \max_t \|\partial_{tt} \bar{q}(t)\|_{\mathfrak{G}}^2 &\leq \bar{c}_{tt}, & \max_t \|\partial_{tt} \bar{p}(t)\|_{\mathfrak{G}}^2 &\leq \bar{c}_{tt}, \end{aligned}$$

for constants  $\bar{c}, \bar{c}_t, \bar{c}_x, \bar{c}_{tx}, \bar{c}_{tt} > 0$ .

*Proof.* The assertions follow directly as a consequence of Theorem 3.11, by setting the perturbations  $\delta_u^q, \delta_v^q, \delta_{e,u}^p$  and  $\delta_{e,v}^p$  in Definition 3.3 to zero.  $\square$

**Theorem 3.13.** *Let  $\Delta \bar{p} = \bar{p} - \bar{p}^\delta$  and  $\Delta \bar{q} = \bar{q} - \bar{q}^\delta$ , then*

$$\begin{aligned} \max_t \|\Delta \bar{p}(t)\|_{\mathfrak{G}}^2 &\leq \bar{\kappa} \max_t \|\delta^p(t)\|_{\infty}^2, & \max_t \|\Delta \bar{q}(t)\|_{\mathfrak{G}}^2 &\leq \bar{\kappa} \max_t \|\delta^q(t)\|_{\infty}^2, \\ \max_t \|\partial_x \Delta \bar{p}(t)\|_{\mathfrak{G}}^2 &\leq \bar{\kappa}_x \max_t \|\delta^p(t)\|_{\infty}^2, & \max_t \|\partial_x \Delta \bar{q}(t)\|_{\mathfrak{G}}^2 &\leq \bar{\kappa}_x \max_t \|\delta^q(t)\|_{\infty}^2, \end{aligned}$$

for constants  $\bar{\kappa}, \bar{\kappa}_x > 0$ .

*Proof.* Since the boundary data and perturbations appear linearly in the homogenisation functions, we get

$$\Delta \bar{q}_e^\delta(x, t) = \begin{cases} 0 & e \neq e_u, e \neq e_v \\ -\frac{x}{\ell_e} \delta_v^q(t) & e \neq e_u, e = e_v \\ \frac{\ell_e - x}{\ell_e} \delta_u^q(t) & e = e_u, e \neq e_v \\ -\frac{x}{\ell_e} \delta_v^q(t) + \frac{\ell_e - x}{\ell_e} \delta_u^q(t) & e = e_u, e = e_v \end{cases}$$

$$\Delta \bar{p}_e^\delta(x, t) = \begin{cases} -\frac{\ell_e - x}{\ell_e} \delta_{e,u}^p(t) - \frac{x}{\ell_e} \delta_{e,v}^p(t) & e \neq e_u, e \neq e_v \\ -\frac{\ell_e - x}{\ell_e} \delta_{e,u}^p(t) & e \neq e_u, e = e_v \\ -\frac{x}{\ell_e} \delta_{e,v}^p(t) & e = e_u, e \neq e_v \\ 0 & e = e_u, e = e_v \end{cases}$$

and

$$\partial_x \Delta \bar{q}_e^\delta(x, t) = \begin{cases} 0 & e \neq e_u, e \neq e_v \\ -\frac{1}{\ell_e} \delta_v^q(t) & e \neq e_u, e = e_v \\ -\frac{1}{\ell_e} \delta_u^q(t) & e = e_u, e \neq e_v \\ -\frac{1}{\ell_e} \delta_v^q(t) - \frac{1}{\ell_e} \delta_u^q(t) & e = e_u, e = e_v \end{cases}$$

$$\partial_x \Delta \bar{p}_e^\delta(x, t) = \begin{cases} \frac{1}{\ell_e} \delta_{e,u}^p(t) - \frac{1}{\ell_e} \delta_{e,v}^p(t) & e \neq e_u, e \neq e_v \\ \frac{1}{\ell_e} \delta_{e,u}^p(t) & e \neq e_u, e = e_v \\ -\frac{1}{\ell_e} \delta_{e,v}^p(t) & e = e_u, e \neq e_v \\ 0 & e = e_u, e = e_v \end{cases}$$

for the partial derivatives of  $\Delta \bar{p}$  and  $\Delta \bar{q}$  w.r.t.  $x$ . Similar as in the proof of Theorem 3.11, we get the following estimates

$$\|\Delta \bar{q}_e(t)\|_{L_2(0, \ell_e)}^2 \leq \frac{\ell_e}{2} (\delta_u^{q^2}(t) + \delta_v^{q^2}(t))$$

for  $e = (u, v) \in \mathcal{E}$  with  $e = e_u, e = e_v$  and

$$\|\Delta \bar{q}_e(t)\|_{L_2(0, \ell_e)}^2 \leq \frac{\ell_e}{3} \delta_u^{q^2}(t)$$

else, which proves the statement for  $\Delta \bar{q}$ . The assertion for  $\Delta \bar{p}$  and the derivatives w.r.t.  $x$  follow by similar argumentation.  $\square$

### 3.3 A priori estimates

In this section, we establish a priori estimates for solutions of the perturbed and the unperturbed PDAE (3.5) and (3.7), respectively. We want to define the spaces

$$\mathcal{P} = \{p \in \mathcal{C}^2(\mathcal{I}, H^1(\mathfrak{G})) : \text{equations (3.9d) to (3.9h) hold}\}$$

$$\mathcal{Q} = \{q \in \mathcal{C}^2(\mathcal{I}, H^1(\mathfrak{G})) : \text{equation (3.9c) holds}\}$$

so that we can reformulate the homogenised PDAE systems as

$$\partial_t p_e(x, t) + \alpha_e \partial_x q_e(x, t) = -\partial_t \bar{p}_e(x, t) - \alpha_e \partial_x \bar{q}_e(x, t) \quad (3.10a)$$

$$\partial_t q_e(x, t) + \beta_e \partial_x p_e(x, t) = -\partial_t \bar{q}_e(x, t) - \beta_e \partial_x \bar{p}_e(x, t) - g_e(p_e + \bar{p}_e, q_e + \bar{q}_e) \quad (3.10b)$$

$$p_e(x, t_0) = p_e^0(x) - \bar{p}_e(x, t_0) \quad (3.10c)$$

$$q_e(x, t_0) = q_e^0(x) - \bar{q}_e(x, t_0) \quad (3.10d)$$

for  $e \in \mathcal{E}$  on  $[0, \ell_e] \times \mathcal{I}$  with  $(p, q) \in \mathcal{P} \times \mathcal{Q}$  and

$$\partial_t p_e^\delta(x, t) + \alpha_e \partial_x q_e^\delta(x, t) = \delta_{p,e}^\Omega(x, t) - \partial_t \bar{p}_e^\delta(x, t) - \alpha_e \partial_x \bar{q}_e^\delta(x, t) \quad (3.11a)$$

$$\partial_t q_e^\delta(x, t) + \beta_e \partial_x p_e^\delta(x, t) = \delta_{q,e}^\Omega(x, t) - \partial_t \bar{q}_e^\delta(x, t) - \beta_e \partial_x \bar{p}_e^\delta(x, t) \quad (3.11b)$$

$$- g_e(p_e^\delta(x, t) + \bar{p}_e^\delta(x, t), q_e^\delta(x, t) + \bar{q}_e^\delta(x, t))$$

$$p_e^\delta(x, t_0) = p_e^0(x) + \delta_{p,e}^0(x) - \bar{p}_e^\delta(x, t_0) \quad (3.11c)$$

$$q_e^\delta(x, t_0) = q_e^0(x) + \delta_{q,e}^0(x) - \bar{q}_e^\delta(x, t_0), \quad (3.11d)$$

for  $e \in \mathcal{E}$  on  $[0, \ell_e] \times \mathcal{I}$  with  $(p^\delta, q^\delta) \in \mathcal{P} \times \mathcal{Q}$ , respectively.

We want to emphasise that  $\mathcal{P}$  and  $\mathcal{Q}$  are *Bochner spaces* (see Section 2.4), which means that for  $(p, q) \in \mathcal{P} \times \mathcal{Q}$ ,  $p(t)$  and  $q(t)$  are functions in  $H^1(\mathfrak{G})$ . For a more convenient notation, we often use  $p(t)$  and  $q(t)$  instead of  $p(x, t)$  and  $q(x, t)$ , or even neglect all arguments in more extensive equations.

**Theorem 3.14** (A priori estimates). *Let  $(p^\delta, q^\delta) \in \mathcal{P} \times \mathcal{Q}$  be a solution to the perturbed system (3.11) that fulfils Assumptions 2.8, and let the boundary, coupling and initial data and perturbations fulfil Assumptions 3.9 and 3.10. Then it holds that*

$$\begin{aligned} \max_t \|p^\delta(t)\|_{\mathfrak{G}}^2 &\leq c^a, & \max_t \|q^\delta(t)\|_{\mathfrak{G}}^2 &\leq c^a, \\ \max_t \|\partial_t p^\delta(t)\|_{\mathfrak{G}}^2 &\leq c_t^a, & \max_t \|\partial_t q^\delta(t)\|_{\mathfrak{G}}^2 &\leq c_t^a, \end{aligned}$$

for constants  $c^a, c_t^a > 0$ .

*Proof.* We start by proving the statement for  $(p^\delta, q^\delta)$ :

(i) We choose test functions  $\varphi = \left(\frac{1}{\alpha} p^\delta, \frac{1}{\beta} q^\delta\right)$ . Note that the multiplication of the reciprocal of  $\alpha = (\alpha_{e_1} \ \dots \ \alpha_{|\mathcal{E}|})^\top$  with  $p^\delta$  is to be understood component-wise (and analogue for

$\frac{1}{\beta}$  with  $q^\delta$ ). In a variational form, system (3.11) is given by

$$\begin{aligned} \frac{d}{dt} \sum_{e \in \mathcal{E}} \int_0^{\ell_e} \left( \frac{p_e^{\delta^2}}{2\alpha_e} + \frac{q_e^{\delta^2}}{2\beta_e} \right) dx &= -(\partial_x p^\delta | q^\delta)_{\mathfrak{G}} - (p^\delta | \partial_x q^\delta)_{\mathfrak{G}} - (g_e(p_e^\delta + \bar{p}_e^\delta, q_e^\delta + \bar{q}_e^\delta) | \frac{1}{\beta_e} q^\delta)_{\mathfrak{G}} \\ &\quad + (\delta_p^\Omega - \partial_t \bar{p}^\delta - \alpha_e \partial_x \bar{q}^\delta | \frac{1}{\alpha_e} p^\delta)_{\mathfrak{G}} \\ &\quad + (\delta_q^\Omega - \partial_t q^\delta - \beta_e \partial_x \bar{p}^\delta | \frac{1}{\beta_e} q^\delta)_{\mathfrak{G}} \end{aligned} \quad (3.12)$$

where  $g(p, q) = (g_{e_1}(p_{e_1}, q_{e_1}) \ \dots \ g_{e_{n_{\mathcal{E}}}}(p_{e_{n_{\mathcal{E}}}}, q_{e_{n_{\mathcal{E}}}}))^\top$ . Due to the homogenisation, it holds that

$$\begin{aligned} &(\partial_x p^\delta | q^\delta)_{\mathfrak{G}} + (p^\delta | \partial_x q^\delta)_{\mathfrak{G}} \\ &= \sum_{e \in \mathcal{E}} \int_0^{\ell_e} \partial_x (p_e^\delta(x, t) q_e^\delta(x, t)) dx = \sum_{e \in \mathcal{E}} (p_e^\delta(\ell_e, t) q_e^\delta(\ell_e, t) - p_e^\delta(0, t) q_e^\delta(0, t)) \\ &= \sum_{u \in V} p_u^\delta(t) \left( \sum_{e \in \delta^+(u)} q_e^\delta(\ell_e, t) - \sum_{e \in \delta^-(u)} q_e^\delta(0, t) \right) = 0 \end{aligned} \quad (3.13)$$

since either  $p_u^\delta(t) = 0$  for  $u \in V_p$  or the balance equation for the mass flows is equal to zero for  $v \in V_q$ . For a more convenient notation we used

$$p_u^\delta(t) = \begin{cases} p_{e_u, r}^\delta(t) & u \in V_q \setminus \{u_0\} \\ p_{e_u, l}^\delta(t) & u = u_0 \\ p_{e, r}^\delta(t) & u \in V_q, e \in \delta^+(u) \text{ arbitrary, for } \delta^+(u) \neq \emptyset \\ p_{e, l}^\delta(t) & u \in V_q, e \in \delta^-(u) \text{ arbitrary, for } \delta^-(u) \neq \emptyset. \end{cases}$$

In addition, it holds that

$$\begin{aligned} \frac{1}{\beta_e} (g_e(p_e^\delta + \bar{p}_e^\delta, q_e^\delta + \bar{q}_e^\delta) | q_e^\delta)_{L_2(0, \ell_e)} &= \int_0^{\ell_e} \left( \frac{\gamma_e}{\beta_e} \frac{(q_e^\delta + \bar{q}_e^\delta) | q_e^\delta + \bar{q}_e^\delta}{p_e^\delta + \bar{p}_e^\delta} q_e^\delta + \frac{|\sigma_e|}{\beta_e} (p_e^\delta + \bar{p}_e^\delta) q_e^\delta \right) dx \\ &= \int_0^{\ell_e} \left( \frac{\gamma_e |\nu_e|}{\beta_e c^2} (q_e^\delta + \bar{q}_e^\delta) q_e^\delta + \frac{|\sigma_e|}{\beta_e} (p_e^\delta + \bar{p}_e^\delta) q_e^\delta \right) dx \end{aligned}$$

where we used that  $q_e = \nu_e \rho_e$  and  $p_e = c^2 \rho_e$ . Making use of the bounded velocity and density in Assumption 2.8 and applying Cauchy's inequality, we get

$$\begin{aligned} \frac{1}{\beta_e} (g_e(p_e^\delta + \bar{p}_e^\delta, q_e^\delta + \bar{q}_e^\delta) | q_e^\delta)_{L_2(0, \ell_e)} &\leq \frac{\gamma_e \bar{\nu}}{\beta_e c^2} \left( \frac{3}{2} \|q_e^\delta\|_{L_2(0, \ell_e)}^2 + \frac{1}{2} \|\bar{q}_e^\delta\|_{L_2(0, \ell_e)}^2 \right) \\ &\quad + \frac{|\sigma_e|}{\beta_e} \left( \frac{1}{2} \|p_e^\delta\|_{L_2(0, \ell_e)}^2 + \frac{1}{2} \|\bar{p}_e^\delta\|_{L_2(0, \ell_e)}^2 + \|q_e^\delta\|_{L_2(0, \ell_e)}^2 \right) \\ &\leq \frac{|\sigma_e|}{2\beta_e} \|\bar{p}_e^\delta\|_{L_2(0, \ell_e)}^2 + \frac{\gamma_e \bar{\nu}}{2\beta_e c^2} \|\bar{q}_e^\delta\|_{L_2(0, \ell_e)}^2 + \frac{|\sigma_e|}{2\beta_e} \|p_e^\delta\|_{L_2(0, \ell_e)}^2 + \left( \frac{3}{2} \frac{\gamma_e \bar{\nu}}{\beta_e c^2} + \frac{|\sigma_e|}{\beta_e} \right) \|q_e^\delta\|_{L_2(0, \ell_e)}^2. \end{aligned}$$

With this estimate, we get the following estimate for the inner product

$$\begin{aligned}
 & (g(p^\delta + \bar{p}^\delta, q^\delta + \bar{q}^\delta) | \frac{1}{\beta} q^\delta)_{\mathfrak{G}} \\
 & \leq \left( \max_{e \in \mathcal{E}} \frac{\gamma_e \bar{\nu}}{2\beta_e c^2} + \max_{e \in \mathcal{E}} \frac{|\sigma_e|}{2\beta_e} \right) \bar{c} + \max_{e \in \mathcal{E}} \left( \frac{3}{2} \frac{\gamma_e \bar{\nu}}{\beta_e c^2} + \frac{|\sigma_e|}{\beta_e} \right) \left( \|p^\delta(t)\|_{\mathfrak{G}}^2 + \|q^\delta(t)\|_{\mathfrak{G}}^2 \right) \\
 & \leq \bar{c}^g + c^g \left( \|p^\delta(t)\|_{\mathfrak{G}}^2 + \|q^\delta(t)\|_{\mathfrak{G}}^2 \right), \tag{3.14}
 \end{aligned}$$

by using the bounds for the homogenisation functions  $\bar{p}^\delta$  and  $\bar{q}^\delta$  we established in Theorem 3.11. For the inner product containing perturbations, we derive the following estimate

$$\begin{aligned}
 & (\delta_{p,e}^\Omega - \partial_t \bar{p}_e^\delta - \alpha_e \partial_x \bar{q}_e^\delta | \frac{1}{\alpha_e} p_e^\delta)_{L_2(0,\ell_e)} \\
 & = \frac{1}{\alpha_e} \left( (\delta_{p,e}^\Omega | p_e^\delta)_{L_2(0,\ell_e)} - (\partial_t \bar{p}_e^\delta | p_e^\delta)_{L_2(0,\ell_e)} \right) - (\partial_x \bar{q}_e^\delta | p_e^\delta)_{L_2(0,\ell_e)} \\
 & \leq \frac{\|\alpha^{-1}\|_\infty}{2} \left( \|\delta_{p,e}^\Omega\|_{L_2(0,\ell_e)}^2 + \|\partial_t \bar{p}_e^\delta\|_{L_2(0,\ell_e)}^2 \right) + \frac{1}{2} \|\partial_x \bar{q}_e^\delta\|_{L_2(0,\ell_e)}^2 + \frac{2\|\alpha^{-1}\|_\infty + 1}{2} \|p_e^\delta\|_{L_2(0,\ell_e)}^2,
 \end{aligned}$$

where we used Cauchy's inequality. We now make use of Assumptions 3.9 and 3.10 and the estimates we derived in Theorem 3.11 and get

$$(\delta_p^\Omega - \partial_t \bar{p}^\delta - \alpha \partial_x \bar{q}^\delta | \frac{1}{\alpha} p^\delta)_{\mathfrak{G}} \leq \frac{2\|\alpha^{-1}\|_\infty + 1}{2} \left( c^{\Omega^2} + \bar{c}_t^2 + \bar{c}_x^2 + \|p^\delta(t)\|_{\mathfrak{G}}^2 \right).$$

With similar considerations we derive an analogue result for

$$(\delta_q^\Omega - \partial_t \bar{q}^\delta - \beta \partial_x \bar{p}^\delta | \frac{1}{\beta} q^\delta)_{\mathfrak{G}} \leq \frac{2\|\beta^{-1}\|_\infty + 1}{2} \left( c^{\Omega^2} + \bar{c}_t^2 + \bar{c}_x^2 + \|q^\delta(t)\|_{\mathfrak{G}}^2 \right).$$

By using Assumptions 3.9 and the bounds from Theorem 3.11, we can show that the initial values fulfil the following estimates

$$\begin{aligned}
 \|p^\delta(t_0)\|_{\mathfrak{G}}^2 & \leq \|p^0\|_{\mathfrak{G}}^2 + \|\delta_p^0\|_{\mathfrak{G}}^2 + \bar{c}^2 \leq \|\delta_p^0\|_{\mathfrak{G}}^2 + c_0^2 + \bar{c}^2 \\
 \|q^\delta(t_0)\|_{\mathfrak{G}}^2 & \leq \|q^0\|_{\mathfrak{G}}^2 + \|\delta_q^0\|_{\mathfrak{G}}^2 + \bar{c}^2 \leq \|\delta_q^0\|_{\mathfrak{G}}^2 + c_0^2 + \bar{c}^2.
 \end{aligned}$$

Integrating the variational form (3.12) in time and making use of the derived estimates in equations (3.13) and (3.14) yields

$$\begin{aligned}
 \frac{K}{2} \left( \|p^\delta(t)\|_{\mathfrak{G}}^2 + \|q^\delta(t)\|_{\mathfrak{G}}^2 \right) & \leq \frac{K}{2} \left( \|\delta_p^0\|_{\mathfrak{G}}^2 + \|\delta_q^0\|_{\mathfrak{G}}^2 \right) + K \left( c_0^2 + \bar{c}^2 \right) \\
 & \quad + \left( \bar{c}^g + (\bar{K} + 1) \left( c^{\Omega^2} + \bar{c}_t^2 + \bar{c}_x^2 \right) \right) (T - t_0) \\
 & \quad + \left( c^g + \frac{\bar{K} + 1}{2} \right) \int_{t_0}^t \left( \|p^\delta(\tau)\|_{\mathfrak{G}}^2 + \|q^\delta(\tau)\|_{\mathfrak{G}}^2 \right) d\tau. \tag{3.15}
 \end{aligned}$$

with constants

$$\bar{K} := \max\{\|\alpha^{-1}\|_\infty, \|\beta^{-1}\|_\infty\} \quad K := \min\{\|\alpha^{-1}\|_\infty, \|\beta^{-1}\|_\infty\}.$$

Dividing inequality (3.15) by  $\frac{K}{2}$  and applying Gronwall's inequality (see Theorem C.1) proves the statement for  $(p^\delta, q^\delta)$ .

(ii) For the proof concerning the partial derivatives w.r.t.  $t$ , we consider the system

$$\begin{aligned}\partial_{tt}p_e^\delta + \alpha_e \partial_{tx}q_e^\delta &= \partial_t \delta_{p,e}^\Omega - \partial_{tt}\bar{p}_e^\delta - \alpha_e \partial_{tx}\bar{q}_e^\delta \\ \partial_{tt}q_e^\delta + \beta_e \partial_{tx}p_e^\delta &= -\nabla g_e \cdot (\partial_t(p_e^\delta + \bar{p}_e^\delta), \partial_t(q_e^\delta + \bar{q}_e^\delta))^\top + \partial_t \delta_{q,e}^\Omega - \partial_{tt}\bar{q}_e^\delta - \beta_e \partial_{tx}\bar{p}_e^\delta\end{aligned}$$

for  $e \in \mathcal{E}$  on  $[0, \ell_e] \times \mathcal{I}$  and  $(p^\delta, q^\delta) \in \mathcal{P} \times \mathcal{Q}$ . It is derived from equation (3.11) by differentiation w.r.t.  $t$ . The gradient of  $g_e$  is given by

$$\nabla g_e = \nabla g_e(p_e^\delta + \bar{p}_e^\delta, q_e^\delta + \bar{q}_e^\delta) = (\partial_p g_e(p_e^\delta + \bar{p}_e^\delta, q_e^\delta + \bar{q}_e^\delta) \quad \partial_q g_e(p_e^\delta + \bar{p}_e^\delta, q_e^\delta + \bar{q}_e^\delta))$$

with partial derivatives  $\partial_p g_e$  and  $\partial_q g_e$  of  $g_e$  w.r.t. its first and second argument, respectively

$$\partial_p g_e(p_e^\delta + \bar{p}_e^\delta, q_e^\delta + \bar{q}_e^\delta) = -\frac{\lambda_e c^2}{2D_e a_e} \frac{(q_e^\delta + \bar{q}_e^\delta)|q_e^\delta + \bar{q}_e^\delta|}{(p_e^\delta + \bar{p}_e^\delta)^2} + \frac{g_a e h'_e}{c^2} \quad (3.16a)$$

$$\partial_q g_e(p_e^\delta + \bar{p}_e^\delta, q_e^\delta + \bar{q}_e^\delta) = \frac{\lambda_e c^2}{D_e a_e} \frac{|q_e^\delta + \bar{q}_e^\delta|}{p_e^\delta + \bar{p}_e^\delta} \quad (3.16b)$$

for  $e \in \mathcal{E}$ . Choosing test functions  $\varphi = (\partial_t \frac{1}{\alpha} p^\delta, \partial_t \frac{1}{\beta} q^\delta)$  and using the variational form, we get that

$$(\partial_{tx} p^\delta | \partial_t q^\delta)_\mathfrak{G} + (\partial_t p^\delta | \partial_{tx} q^\delta)_\mathfrak{G} = 0,$$

where we followed the same steps as in equation (3.13). The estimates

$$\begin{aligned}(\partial_t \delta_p^\Omega - \partial_{tt}\bar{p}^\delta - \alpha \partial_{tx}\bar{q}^\delta | \frac{1}{\alpha} \partial_t p^\delta)_\mathfrak{G} &\leq \frac{2\|\alpha^{-1}\|_\infty + 1}{2} \left( c_t^{\Omega^2} + \bar{c}_{tt}^2 + \bar{c}_{tx}^2 + \|\partial_t p^\delta(t)\|_\mathfrak{G}^2 \right) \\ (\partial_t \delta_q^\Omega - \partial_{tt}\bar{q}^\delta - \beta \partial_{tx}\bar{p}^\delta | \frac{1}{\beta} \partial_t q^\delta)_\mathfrak{G} &\leq \frac{2\|\beta^{-1}\|_\infty + 1}{2} \left( c_t^{\Omega^2} + \bar{c}_{tt}^2 + \bar{c}_{tx}^2 + \|\partial_t q^\delta(t)\|_\mathfrak{G}^2 \right)\end{aligned}$$

are derived by similar considerations as in the proof of (i) by using Assumptions 3.9 and 3.10 as well as Theorem 3.11. For the inner products containing partial derivatives of the non-linearity  $g_e$ , we have

$$\begin{aligned}(\partial_p g_e \partial_t(p_e^\delta + \bar{p}_e^\delta) | \partial_t q_e^\delta)_{L_2(0, \ell_e)} &= \int_0^{\ell_e} \left( \gamma_e \frac{\partial_t(q_e^\delta + \bar{q}_e^\delta)|q_e^\delta + \bar{q}_e^\delta|}{(p_e^\delta + \bar{p}_e^\delta)^2} + \sigma_e \right) \partial_t(p_e^\delta + \bar{p}_e^\delta) \partial_t q_e^\delta dx \\ &\leq \left( \frac{\gamma_e + a_e^2 \bar{\nu}^2}{c^4} + |\sigma_e| \right) \int_0^{\ell_e} |\partial_t(p_e^\delta + \bar{p}_e^\delta) \partial_t q_e^\delta| dx \\ &\leq \left( \frac{\gamma_e + a_e^2 \bar{\nu}^2}{2c^4} + \frac{|\sigma_e|}{2} \right) \left( \bar{c}_t^2 + \|\partial_t p_e^\delta\|_{L_2(0, \ell_e)}^2 + 3\|q_e^\delta\|_{L_2(0, \ell_e)}^2 \right) \\ (\partial_q g_e \partial_t(q_e^\delta + \bar{q}_e^\delta) | \partial_t q_e^\delta)_{L_2(0, \ell_e)} &= \int_0^{\ell_e} 2\gamma_e \frac{|q_e^\delta + \bar{q}_e^\delta|}{p_e^\delta + \bar{p}_e^\delta} \partial_t(q_e^\delta + \bar{q}_e^\delta) \partial_t q_e^\delta dx \\ &\leq \frac{2\gamma_e a_e \bar{\nu}}{2c^2} \left( \bar{c}_t^2 + 3\|q_e^\delta\|_{L_2(0, \ell_e)}^2 \right)\end{aligned}$$

due to Assumptions 2.8 and Theorem 3.11. Hence, it follows that

$$\left( \frac{d}{dt} g | \frac{1}{\beta} \partial_t q^\delta \right)_\mathfrak{G} \leq \bar{c}_t^g + c_t^g \left( \|\partial_t p^\delta(t)\|_\mathfrak{G}^2 + \|\partial_t q^\delta(t)\|_\mathfrak{G}^2 \right)$$



for constants  $\bar{c}_t^g, c_t^g > 0$ . Combining the estimates above, we derive the following inequality

$$\begin{aligned} \frac{K}{2} \left( \|\partial_t p^\delta(t)\|_{\mathfrak{G}}^2 + \|\partial_t q^\delta(t)\|_{\mathfrak{G}}^2 \right) &\leq \left( \bar{c}_t^g + (\bar{K} + 1)(c_t^{\Omega^2} + \bar{c}_{tt}^2 + \bar{c}_{tx}^2) \right) (T - t_0) \\ &\quad + \left( c_t^g + \frac{\bar{K} + 1}{2} \right) \int_{t_0}^t \left( \|\partial_t p^\delta(\tau)\|_{\mathfrak{G}}^2 + \|\partial_t q^\delta(\tau)\|_{\mathfrak{G}}^2 \right) d\tau. \end{aligned}$$

Division by  $K$  and applying Gronwall's inequality completes the proof.  $\square$

**Corollary 3.15.** *Let  $(p, q) \in \mathcal{P} \times \mathcal{Q}$  be a solution to the unperturbed system (3.10) and let the boundary data fulfil Assumptions 3.9. Then it holds that*

$$\begin{aligned} \max_t \|p^\delta(t)\|_{\mathfrak{G}}^2 &\leq c^a, & \max_t \|q^\delta(t)\|_{\mathfrak{G}}^2 &\leq c^a, \\ \max_t \|\partial_t p^\delta(t)\|_{\mathfrak{G}}^2 &\leq c_t^a, & \max_t \|\partial_t q^\delta(t)\|_{\mathfrak{G}}^2 &\leq c_t^a, \end{aligned}$$

for constants  $c^a, c_t^a > 0$ .

*Proof.* This follows directly from Theorem 3.14 by setting the perturbations  $\delta^\Omega, \delta^0$  that appear in (3.11) and the perturbations  $\delta^q$  and  $\delta^p$  that appear in the homogenisation functions  $\bar{p}^\delta$  and  $\bar{q}^\delta$  to zero.  $\square$

### 3.4 Perturbation analysis

We investigate the ADAE given by the difference of the unperturbed, homogenised PDAE (3.10) and the perturbed, homogenised PDAE (3.11) to derive estimates for  $p - p^\delta$  and  $q - q^\delta$ . Here, we use the a priori estimates for the solutions and their first derivatives w.r.t. time, which we established in Section 3.3.

For a solution  $(p, q) \in \mathcal{P} \times \mathcal{Q}$  of System (3.10) and a solution  $(p^\delta, q^\delta) \in \mathcal{P} \times \mathcal{Q}$  of System (3.11) we set

$$\Delta p(x, t) = p(x, t) - p^\delta(x, t) \quad \Delta q(x, t) = q(x, t) - q^\delta(x, t)$$

and formulate the following system

$$\partial_t \Delta p_e + \alpha_e \partial_x \Delta q_e = -\delta_{p,e}^\Omega - \partial_t \Delta \bar{p}_e - \alpha_e \partial_x \Delta \bar{q}_e \quad e \in \mathcal{E} \quad (3.17a)$$

$$\partial_t \Delta q_e + \beta_e \partial_x \Delta p_e = -\Delta g_e - \delta_{q,e}^\Omega - \partial_t \Delta \bar{q}_e - \beta_e \partial_x \Delta \bar{p}_e \quad e \in \mathcal{E} \quad (3.17b)$$

for  $(x, t) \in [0, \ell_e] \times \mathcal{I}$ ,

$$\Delta p(x, t_0) = -\delta_p^0(x) - \Delta \bar{p}(x, t_0) \quad (3.17c)$$

$$\Delta q(x, t_0) = -\delta_q^0(x) - \Delta \bar{q}(x, t_0), \quad (3.17d)$$

that is derived by subtracting equations (3.10) and (3.11). The term  $\Delta g_e$  is given by

$$\Delta g_e = g_e(p_e + \bar{p}_e, q_e + \bar{q}_e) - g_e(p_e^\delta + \bar{p}_e^\delta, q_e^\delta + \bar{q}_e^\delta) \quad (3.18)$$

for a more convenient notation.

**Corollary 3.16.** *Let  $(p, q), (p^\delta, q^\delta) \in \mathcal{P} \times \mathcal{Q}$  be solutions to Systems (3.10) and (3.11), respectively, that fulfil the requirements of Theorem 3.14. Then  $\partial_t \Delta p$  and  $\partial_t \Delta q$  are bounded by*

$$\max_t \|\partial_t \Delta p(t)\|_{\mathfrak{G}}^2 \leq 2c^a, \quad \max_t \|\partial_t \Delta q(t)\|_{\mathfrak{G}}^2 \leq 2c_t^a.$$

*Proof.* This is a direct consequence of Theorem 3.14 □

**Theorem 3.17** (Perturbation analysis). *Let  $(p, q), (p^\delta, q^\delta) \in \mathcal{P} \times \mathcal{Q}$  be solutions to the unperturbed and perturbed problem (3.10) and (3.11) respectively that fulfil Assumptions 2.8. Let the perturbed and unperturbed problem fulfil Assumptions 3.9 and 3.10. Then it holds that*

$$\begin{aligned} \max_t \|p(t) - p^\delta(t)\|_{\mathfrak{G}}^2 + \max_t \|q(t) - q^\delta(t)\|_{\mathfrak{G}}^2 \\ \leq C \left( \|\delta^0\|_{\mathfrak{G}}^2 + \max_t \|\delta^\Omega(t)\|_{\mathfrak{G}}^2 + \max_t \|\delta^\Gamma(t)\|_\infty + \max_t \|\delta^\Gamma(t)\|_\infty^2 \right) \end{aligned}$$

for a constant  $C > 0$ .

*Proof.* Choosing the test function  $\varphi = (\frac{1}{\alpha} \Delta p, \frac{1}{\beta} \Delta q)$ , we can formulate the System (3.17) in the variational form as

$$\begin{aligned} \frac{1}{2} \frac{d}{dt} \left( \left\| \frac{1}{\alpha} \Delta p(t) \right\|_{\mathfrak{G}}^2 + \left\| \frac{1}{\beta} \Delta q(t) \right\|_{\mathfrak{G}}^2 \right) &= -(\partial_x \Delta p | \Delta q)_{\mathfrak{G}} - (\Delta p | \partial_x \Delta q)_{\mathfrak{G}} \\ &\quad - (\Delta g | \frac{1}{\beta} \Delta q)_{\mathfrak{G}} - (\delta_p^\Omega + \partial_t \Delta \bar{p} + \alpha \partial_x \Delta \bar{q} | \frac{1}{\alpha} \Delta p)_{\mathfrak{G}} \\ &\quad - (\delta_q^\Omega + \partial_t \Delta \bar{q} + \beta \partial_x \Delta \bar{p} | \frac{1}{\beta} \Delta q)_{\mathfrak{G}}. \end{aligned} \quad (3.19)$$

Since  $(\Delta p, \Delta q) \in \mathcal{P} \times \mathcal{Q}$ , we can make use of the fact that

$$(\partial_x \Delta p | \Delta q)_{\mathfrak{G}} + (\Delta p | \partial_x \Delta q)_{\mathfrak{G}} = 0,$$

following the same arguments as we did for equation (3.13). After integrating equation (3.19) in time, we get

$$\begin{aligned} \frac{K}{2} (\|\Delta p(t)\|_{\mathfrak{G}}^2 + \|\Delta q\|_{\mathfrak{G}}^2(t)) &\leq \frac{K}{2} (\|\delta_p^0 + \Delta \bar{p}(t_0)\|_{\mathfrak{G}}^2 + \|\delta_q^0 + \Delta \bar{q}(t_0)\|_{\mathfrak{G}}^2) \\ &\quad - \int_{t_0}^t (\Delta g | \frac{1}{\beta} \Delta q(\tau))_{\mathfrak{G}} d\tau - \int_{t_0}^t (\partial_t \Delta \bar{p}(\tau) | \frac{1}{\alpha} \Delta p(\tau))_{\mathfrak{G}} + (\partial_t \Delta \bar{q}(\tau) | \frac{1}{\beta} \Delta q(\tau))_{\mathfrak{G}} d\tau \\ &\quad - \int_{t_0}^t (\delta_p^\Omega(\tau) + \alpha \partial_x \Delta \bar{q}(\tau) | \frac{1}{\alpha} \Delta p(\tau))_{\mathfrak{G}} + (\delta_q^\Omega(\tau) + \beta \partial_x \Delta \bar{p}(\tau) | \frac{1}{\beta} \Delta q(\tau))_{\mathfrak{G}} d\tau \\ &= \frac{K}{2} (\|\delta_p^0 + \Delta \bar{p}(t_0)\|_{\mathfrak{G}}^2 + \|\delta_q^0 + \Delta \bar{q}(t_0)\|_{\mathfrak{G}}^2) - \int_{t_0}^t (\Delta g | \frac{1}{\beta} \Delta q(\tau))_{\mathfrak{G}} d\tau \\ &\quad - \int_{t_0}^t (\delta_p^\Omega(\tau) + \alpha \partial_x \Delta \bar{q}(\tau) | \frac{1}{\alpha} \Delta p(\tau))_{\mathfrak{G}} + (\delta_q^\Omega(\tau) + \beta \partial_x \Delta \bar{p}(\tau) | \frac{1}{\beta} \Delta q(\tau))_{\mathfrak{G}} d\tau \\ &\quad + \int_{t_0}^t (\Delta \bar{p}(\tau) | \frac{1}{\alpha} \partial_t \Delta p(\tau))_{\mathfrak{G}} + (\Delta \bar{q}(\tau) | \frac{1}{\beta} \partial_t \Delta q(\tau))_{\mathfrak{G}} d\tau - (\Delta \bar{p} | \frac{1}{\alpha} \Delta p)_{\mathfrak{G}} - (\Delta \bar{q} | \frac{1}{\beta} \Delta q)_{\mathfrak{G}}. \end{aligned}$$

For the inner product of  $\Delta q$  with  $\Delta g$ , we derive that

$$\begin{aligned} (\Delta g_e | \Delta q_e)_{L_2(0, \ell_e)} &= \int_0^{\ell_e} \left( g_e(p_e + \bar{p}_e, q_e + \bar{q}_e) - g_e(p_e^\delta + \bar{p}_e^\delta, q_e^\delta + \bar{q}_e^\delta) \right) \Delta q_e \, dx \\ &= \int_0^{\ell_e} \left( \int_0^1 \nabla g_e(\mathbf{p}(s), \mathbf{q}(s)) \cdot (\Delta p_e + \Delta \bar{p}_e, \Delta q_e + \Delta \bar{q}_e)^\top \, ds \, \Delta q_e \right) \, dx \end{aligned}$$

where the gradient of  $g_e$  is given by equation (3.16) and

$$\begin{aligned} \mathbf{p}(s) &= s(p_e + \bar{p}_e) + (1-s)(p_e^\delta + \bar{p}_e^\delta) \\ \mathbf{q}(s) &= s(q_e + \bar{q}_e) + (1-s)(q_e^\delta + \bar{q}_e^\delta). \end{aligned}$$

Due to Assumptions 2.8, it holds that

$$\begin{aligned} \nabla g_e(\mathbf{p}(s), \mathbf{q}(s)) \cdot (\Delta p_e + \Delta \bar{p}_e, \Delta q_e + \Delta \bar{q}_e)^\top \\ \leq \left( \frac{\gamma_e a_e^2 \bar{v}^2}{c^4} + |\sigma_e| \right) |\Delta p_e + \Delta \bar{p}_e| + \frac{2\gamma_e a_e \bar{v}}{c^2} |\Delta q_e + \Delta \bar{q}_e|, \end{aligned}$$

which we can use to conclude that

$$\begin{aligned} (\Delta g_e | \frac{1}{\beta_e} \Delta q_e)_{L_2(0, \ell_e)} &\leq \left( \frac{2\gamma_e a_e^2 \bar{v}^2}{\beta_e c^4} + \frac{|\sigma_e|}{\beta_e} \right) \int_0^{\ell_e} (|\Delta p_e + \Delta \bar{p}_e| |\Delta q_e| + |\Delta q_e + \Delta \bar{q}_e| |\Delta q_e|) \, dx \\ &\leq \left( \frac{2\gamma_e a_e^2 \bar{v}^2}{\beta_e c^4} + \frac{|\sigma_e|}{\beta_e} \right) \int_0^{\ell_e} \left( \frac{1}{2} (\Delta p_e)^2 + \frac{3}{2} (\Delta q_e)^2 + |\Delta \bar{p}_e \Delta q_e| + |\Delta \bar{q}_e \Delta q_e| \right) \, dx \\ &\leq c^g \left( \|\Delta p_e\|_{L_2(0, \ell_e)}^2 + \|\Delta q_e\|_{L_2(0, \ell_e)}^2 + \int_0^{\ell_e} (|\Delta \bar{p}_e \Delta q_e| + |\Delta \bar{q}_e \Delta q_e|) \, dx \right). \end{aligned} \quad (3.20)$$

With this estimate, we have

$$\begin{aligned} (\Delta g | \frac{1}{\beta} \Delta q)_{\mathfrak{G}} &\leq c^g \left( \|\Delta p(t)\|_{\mathfrak{G}}^2 + \|\Delta q(t)\|_{\mathfrak{G}}^2 + \sum_{e \in \mathcal{E}} \int_0^{\ell_e} |\Delta \bar{p}_e \Delta q_e| + |\Delta \bar{q}_e \Delta q_e| \, dx \right) \\ &\leq c^g (\|\Delta p(t)\|_{\mathfrak{G}}^2 + \|\Delta q(t)\|_{\mathfrak{G}}^2 + \|\Delta \bar{p}\|_{\mathfrak{G}} \|\Delta q(t)\|_{\mathfrak{G}} + \|\Delta \bar{q}\|_{\mathfrak{G}} \|\Delta q(t)\|_{\mathfrak{G}}) \\ &\leq c^g (\|\Delta p(t)\|_{\mathfrak{G}}^2 + \|\Delta q(t)\|_{\mathfrak{G}}^2) + 2c^g c^a \sqrt{\bar{\kappa}} \max_t \|\delta^\Gamma(t)\|_\infty \end{aligned}$$

as well as the estimates

$$(\Delta \bar{p} | \frac{1}{\beta} \Delta p)_{\mathfrak{G}} \leq \|\beta^{-1}\|_\infty \|\Delta \bar{p}\|_{\mathfrak{G}} \|\Delta p\|_{\mathfrak{G}} \leq \bar{K} c^a \sqrt{\bar{\kappa}} \max_t \|\delta^\Gamma(t)\|_\infty \quad (3.21a)$$

$$(\Delta \bar{q} | \frac{1}{\alpha} \Delta q)_{\mathfrak{G}} \leq \|\alpha^{-1}\|_\infty \|\Delta \bar{q}\|_{\mathfrak{G}} \|\Delta q\|_{\mathfrak{G}} \leq \bar{K} c^a \sqrt{\bar{\kappa}} \max_t \|\delta^\Gamma(t)\|_\infty \quad (3.21b)$$

and

$$\begin{aligned} (\Delta \bar{p} | \frac{1}{\alpha} \partial_t \Delta p)_{\mathfrak{G}} &\leq \|\alpha^{-1}\|_\infty \|\Delta \bar{p}\|_{\mathfrak{G}} \|\partial_t \Delta p\|_{\mathfrak{G}} \leq 2\bar{K} c_t^a \sqrt{\bar{\kappa}} \max_t \|\delta^\Gamma(t)\|_\infty \\ (\Delta \bar{q} | \frac{1}{\beta} \partial_t \Delta q)_{\mathfrak{G}} &\leq \|\beta^{-1}\|_\infty \|\Delta \bar{q}\|_{\mathfrak{G}} \|\partial_t \Delta q\|_{\mathfrak{G}} \leq 2\bar{K} c_t^a \sqrt{\bar{\kappa}} \max_t \|\delta^\Gamma(t)\|_\infty. \end{aligned}$$

Making use of the estimates we established in Theorem 3.13, we derive

$$\begin{aligned}
 (\delta_p^\Omega + \alpha \partial_x \Delta \bar{q} | \frac{1}{\alpha} \Delta p)_\mathfrak{G} &= (\delta_p^\Omega | \frac{1}{\alpha} \Delta p)_\mathfrak{G} + (\partial_x \Delta \bar{q} | \Delta p)_\mathfrak{G} \\
 &\leq \frac{\bar{K}}{2} \max_t \|\delta_p^\Omega(t)\|_\mathfrak{G}^2 + \frac{\bar{\kappa}_x}{2} \max_t \|\delta^\Gamma(t)\|_\infty^2 + \frac{\bar{K} + \bar{\kappa}_x}{2} \|\Delta p(t)\|_\mathfrak{G}^2 \\
 &\leq \frac{\bar{K} + 1}{2} \left( \max_t \|\delta_p^\Omega(t)\|_\mathfrak{G}^2 + \max_t \|\delta^\Gamma(t)\|_\infty^2 + \|\Delta p(t)\|_\mathfrak{G}^2 \right) \quad (3.22a)
 \end{aligned}$$

$$\begin{aligned}
 (\delta_q^\Omega + \beta \partial_x \Delta \bar{p} | \frac{1}{\beta} \Delta q)_\mathfrak{G} &= (\delta_q^\Omega | \frac{1}{\beta} \Delta q)_\mathfrak{G} + (\partial_x \Delta \bar{p} | \Delta q)_\mathfrak{G} \\
 &\leq \frac{\bar{K} + 1}{2} \left( \max_t \|\delta_q^\Omega(t)\|_\mathfrak{G}^2 + \max_t \|\delta^\Gamma(t)\|_\infty^2 + \|\Delta q(t)\|_\mathfrak{G}^2 \right). \quad (3.22b)
 \end{aligned}$$

With the estimates stated in inequalities (3.21a) to (3.22b) and the results of Theorem 3.13, we can derive the following estimate from the variational form

$$\begin{aligned}
 \frac{K}{2} (\|\Delta p\|_\mathfrak{G}^2 + \|\Delta q\|_\mathfrak{G}^2) &\leq \frac{K}{2} (\|\delta_p^0\|_\mathfrak{G}^2 + \|\delta_q^0\|_\mathfrak{G}^2) \\
 &\quad + \frac{\bar{K} + 1}{2} (T - t_0) \left( \max_t \|\delta_p^\Omega(t)\|_\mathfrak{G}^2 + \max_t \|\delta_q^\Omega(t)\|_\mathfrak{G}^2 \right) \\
 &\quad + \left( (\bar{c}^g + 2\bar{K}c_t^a\sqrt{\bar{\kappa}})(T - t_0) + 2\bar{K}c^a\sqrt{\bar{\kappa}} \right) \max_t \|\delta^\Gamma(t)\|_\infty \\
 &\quad + (K\bar{\kappa} + (\bar{K} + 1)(T - t_0)) \max_t \|\delta^\Gamma(t)\|_\infty^2 \\
 &\quad + \left( c^g + \frac{\bar{K} + 1}{2} \right) \int_{t_0}^t (\|\Delta p(\tau)\|_\mathfrak{G}^2 + \|\Delta q(\tau)\|_\mathfrak{G}^2) d\tau.
 \end{aligned}$$

Division by  $\frac{K}{2}$  and applying Gronwall's inequality completes the proof.  $\square$

### 3.5 Uniqueness of solutions

In this section, we briefly discuss uniqueness properties of solutions of the pipe network PDAE given by equation (3.10).

**Theorem 3.18** (Uniqueness of solutions). *Let  $u, \tilde{u} \in \mathcal{P} \times \mathcal{Q}$  be two solutions to the PDAE (3.10) with  $u = (p, q)$  and  $\tilde{u} = (\tilde{p}, \tilde{q})$ . Then it holds that*

$$u(t) = \tilde{u}(t) \quad t \in \mathcal{I}$$

*Proof.* Let  $u, \tilde{u} \in \mathcal{P} \times \mathcal{Q}$  be two solutions to the PDAE (3.10). Then it holds for  $\Delta u = u - \tilde{u}$  that

$$\begin{aligned}
 \partial_t \Delta p_e + \alpha_e \partial_x \Delta q_e &= 0 \\
 \partial_t \Delta q_e + \beta_e \partial_x \Delta p_e &= -\Delta g_e
 \end{aligned}$$

with

$$\Delta g_e = g_e(p_e + \bar{p}_e, q_e + \bar{q}_e) - g_e(\tilde{p}_e + \bar{p}_e, \tilde{q}_e + \bar{q}_e).$$

By choosing the test function  $\varphi = (\frac{1}{\alpha}\Delta p, \frac{1}{\beta}\Delta q)$ , the variational form of the system above is

$$\frac{1}{2}\partial_t \left( \left\| \frac{1}{\alpha}\Delta p(t) \right\|_{\mathfrak{G}}^2 + \left\| \frac{1}{\beta}\Delta q(t) \right\|_{\mathfrak{G}}^2 \right) = -(\Delta g | \frac{1}{\beta}\Delta q)_{\mathfrak{G}},$$

where we have already made use of the fact that  $(\Delta p | \partial_x \Delta q)_{\mathfrak{G}} + (\partial_x \Delta p | \Delta q)_{\mathfrak{G}} = 0$  (see equation (3.13)). We can use the technique from Section 3.4 to derive that

$$(\Delta g | \frac{1}{\beta}\Delta q)_{\mathfrak{G}} \leq c^g (\|\Delta p(t)\|_{\mathfrak{G}}^2 + \|\Delta q(t)\|_{\mathfrak{G}}^2),$$

as we did for equation (3.20). Hence, we get the following result from the variational form

$$\frac{K}{2} (\|\Delta p(t)\|_{\mathfrak{G}}^2 + \|\Delta q(t)\|_{\mathfrak{G}}^2) \leq c^g \int_{t_0}^t (\|\Delta p(\tau)\|_{\mathfrak{G}}^2 + \|\Delta q(\tau)\|_{\mathfrak{G}}^2) d\tau.$$

Division by  $\frac{K}{2}$  and applying Gronwall's inequality yields

$$\|\Delta p(t)\|_{\mathfrak{G}}^2 + \|\Delta q(t)\|_{\mathfrak{G}}^2 = 0$$

which completes the proof.  $\square$

## 3.6 Conclusion

In this chapter, we have shown that the solution of a perturbed hyperbolic PDAE that arises in the modelling of gas pipe networks (see equation (2.22)) possesses similar stability properties w.r.t. perturbations as a solution of a PDAE of perturbation index 1. Note that we explicitly allowed perturbations in the differential part of the system and the initial values, but also in the coupling and boundary conditions.

A topology-specific homogenisation was introduced in Section 3.2. After the homogenisation, the PDAE (3.5) system is subject to the influence of derivatives of the boundary data, since they appear on the right-hand side of equation (3.10). Hence, the perturbed PDAE (3.11) is affected by derivatives of perturbations in the same way.

In Section 3.3, we established a priori estimates for the perturbed and for the unperturbed solution of the respective PDAEs as well as for their first derivatives w.r.t. time.

The main result of this chapter, Theorem 3.17 was proven in Section 3.4. It states that the solutions of the perturbed and unperturbed PDAEs do not depend on derivatives, but only on the boundary data and perturbations themselves. The perturbation result is closely linked to the concept of the perturbation index for PDAEs, and suggests a perturbation index of 1. Furthermore, it shows a continuous dependency of the solution on the input data in form of boundary and coupling data. This extends the results from [EK18], where a continuous dependency on the right-hand side was proven for a homogeneous system of damped wave equations. In our case, this would include that the solution also depends on derivatives of the boundary and coupling data. However, Theorem 3.17 proves that this is not the case here.

Additionally, we used the results from Section 3.4 to prove uniqueness of solutions in Section 3.5.

The presented perturbation result for the time and space continuous description of networks is of particular interest for the numerical simulation. Proper spatial discretisations of hyperbolic PDAEs shall lead to differential-algebraic equations with similar perturbation behaviour, hence index 1. This will be discussed in the following chapter.

We want to emphasise that the analysis in this chapter is very general w.r.t. the modelling of boundary conditions, especially the modelling of in- and outflow of gas. It is also independent from the network topology, which is no longer the case for the DAE system that is derived by semi-discretisation of the PDAE. This will be discussed in Chapter 4.

In addition, we want to emphasise that the results of this chapter can easily be extended to water networks. It only needs a minor change in the argumentation of the non-linear friction term, since it slightly differs due to the non-compressibility of water.

We expect that one can extend the perturbation results to flow networks with non-linear constraints (e.g. gas networks including compressor units we have introduced in Section 2.2.3), by formulating the system in Riemann characteristics as in [GU17] and extend the Picard iteration by introducing an additional Krawczyk-Operator as it has been done in [AC16] for DAEs. However, this needs further investigation, since it is unclear what the convergence criteria for such a Picard-Krawczyk operator are and whether this approach can be extended to the context of PDAEs.

## 4 Topology-adaptive discretisation and DAE analysis

In the analysis of DAEs, the concept of an index plays an important role. The index of a DAE measures how far away the DAE is from an ODE, to give a very basic interpretation of this concept. Hence, it provides a measure of how difficult it is to solve the respective DAE. A first approach was the *Kronecker index* [GP83; GM86], transforming regular matrix pencils into the Kronecker normalform [Gan70]. However, this approach only works for linear DAEs with constant coefficients (see Definition B.3).

To extend this concept to more general DAEs, e.g., DAEs in standard form, the *differentiation index* [Cam87; Gea88; BCP95; CG95a; CG95b] and the *perturbation index* [HLR89], among others, have been developed. We want to give a short introduction to these two specific index concepts that are widely used [KM06].

**Definition 4.1** (DAE in standard form). *Let  $\mathcal{I} \subset \mathbb{R}$  and  $D_x, D_{x'} \subset \mathbb{R}^n$  be open with  $t_0 \in \mathcal{I}$ . Let  $F \in \mathcal{C}(D_{x'} \times D_x \times \mathcal{I}, \mathbb{R}^n)$  be continuous so that the partial derivatives  $\frac{\partial}{\partial x^1} F(x^1, x, t)$  and  $\frac{\partial}{\partial x} F(x^1, x, t)$  are continuous with  $\frac{\partial}{\partial x^1} F(x^1, x, t)$  being singular for all triples  $(x^1, x, t) \in D_{x'} \times D_x \times \mathcal{I}$ . We call*

$$F(x'(t), x(t), t) = 0 \qquad x(t_0) = x^0 \qquad (4.1)$$

*a DAE in standard form with initial conditions.*

**Differentiation index** The *differentiation index* was first introduced by Petzold and Campbell [Cam87; BCP95] and is a commonly used concept since it is very intuitive and approachable. It represents the minimal number of times that the DAE (4.1) has to be differentiated in order to extract an ODE, the so called underlying ODE. For a formal definition we first need to introduce the notion of an inflated system.

**Definition 4.2** (Inflated system [KM06, p. 153]). *With respect to the DAE (4.1), we gather the original equation and its derivatives up to order  $\nu \in \mathbb{N}_0$  into an inflated system*

$$F_\nu(x^{\nu+1}(t), \dots, x^1(t), x(t), t) = 0, \qquad (4.2)$$

where  $F_\nu$  has the form

$$\begin{aligned} F_\nu(x^{\nu+1}, \dots, x^1, x, t) &= \begin{pmatrix} F(x^1, x, t) \\ \frac{d}{dt} F(x^1, x, t) \\ \vdots \\ \left(\frac{d}{dt}\right)^\nu F(x^1, x, t) \end{pmatrix} \\ &= \begin{pmatrix} F(x^1, x, t) \\ \frac{\partial}{\partial x^1} F(x^1, x, t)x^2 + \frac{\partial}{\partial x} F(x^1, x, t)x^1 + \frac{\partial}{\partial t} F(x^1, x, t) \\ \vdots \end{pmatrix}. \end{aligned}$$

**Definition 4.3** (Differentiation index, [GHM92, p. 5]). *The DAE (4.1) has differentiation index  $\mu_d$ , if and only if  $F \in C^\mu(D_{x'} \times D_x \times \mathcal{I}, \mathbb{R}^n)$  and  $\mu$  is the minimal number so that an explicit ODE of the form  $x'(t) = f(x(t), t)$  can be extracted from  $F_\mu(x^{\mu+1}, \dots, x', x, t) = 0$  by algebraic manipulations only with  $f$  being continuous.*

For the special case of a *semi-explicit DAE*

$$x'(t) = f(x, y, t) \tag{4.3a}$$

$$0 = g(x, y, t), \tag{4.3b}$$

the following result can be shown.

**Lemma 4.4.** *If  $\partial_y g(x, y, t)$  is non-singular for all triples  $(x, y, t)$ , then the DAE (4.3) has differentiation index  $\mu_d = 1$ .*

*Proof.* Differentiation of equation (4.3b) yields

$$0 = \partial_x g(x, y, t)x'(t) + \partial_y g(x, y, t)y'(t) + \partial_t g(x, y, t).$$

Since  $\partial_y g$  is non-singular, we can reformulate this equation and extract the underlying ODE

$$\begin{aligned} x'(t) &= f(x, y, t) \\ y'(t) &= -(\partial_y g(x, y, t))^{-1} (\partial_x g(x, y, t)f(x, y, t) + \partial_t g(x, y, t)) \end{aligned}$$

which completes the proof.  $\square$

**Remark 4.5.** *Lemma 4.4 illustrates that one does not necessarily need all parts of  $F$  to be in  $C^\mu(D_{x'} \times D_x \times \mathcal{I}, \mathbb{R}^n)$  as stated in Definition 4.3, but only parts of  $F$  must be sufficiently smooth.*

**Perturbation index** The *perturbation index* was first introduced by Hairer, Lubich and Roche in [HLR89], and measures the influence of perturbations that appear on the right-hand side of equation (4.1) on the solution. Therefore, we define the *perturbed DAE in standard form* as

$$F(x^{\delta'}(t), x^\delta(t), t) = \delta(t) \qquad x^\delta(t_0) = x^0 + \delta^0 \tag{4.4}$$

with perturbations  $\delta(t)$  and  $\delta^0$ , which we assume to be sufficiently small.



---

**Definition 4.6** (Perturbation index, [HLR89, Definition 1.1]). *Equation (4.1) has perturbation index  $\mu_p$  along a solution  $x$  on  $\mathcal{I}$ , if  $\mu_p$  is the smallest integer, so that, for all functions  $x^\delta$  that solve equation (4.4), there exists on  $\mathcal{I}$  an estimate*

$$\|x(t) - x^\delta(t)\| \leq C \left( \|\delta^0\| + \max_{\tau \in \mathcal{I}} \|\delta(\tau)\| + \dots + \max_{\tau \in \mathcal{I}} \|\delta^{\mu_d-1}(\tau)\| \right)$$

whenever  $\delta(t)$  and  $\delta^0$  are sufficiently small. Here,  $C$  denotes a constant which depends only on  $F$  and the length of the interval  $\mathcal{I}$ .

**Example 4.7.** *Let us consider the following DAE*

$$x'(t) - y(t) = g_1(t) \tag{4.5a}$$

$$y(t) = g_2(t) \tag{4.5b}$$

for  $t \in \mathcal{I}$  with consistent initial conditions  $x(t_0) = x^0$ ,  $y(t_0) = y^0$ ,  $g_1 \in \mathcal{C}(\mathcal{I}, \mathbb{R})$  and  $g_2 \in \mathcal{C}^1(\mathcal{I}, \mathbb{R})$ . By differentiating (4.5b) once, we can extract the ODE

$$x'(t) = y(t) + g_1(t) \qquad y'(t) = g_2'(t)$$

which gives us differentiation index  $\mu_d = 1$ . If we add perturbations to the right-hand side of equation (4.5) and to the initial values, we get the perturbed DAE

$$x^{\delta'}(t) - y^\delta(t) = g_1(t) + \delta_1(t) \tag{4.6a}$$

$$y^\delta(t) = g_2(t) + \delta_2(t) \tag{4.6b}$$

with initial conditions  $x_1^\delta(t_0) = x^0 + \delta_x^0$ ,  $y^\delta(t_0) = y^0 + \delta_y^0$ , for sufficiently small  $\delta_1$ ,  $\delta_2$  and  $\delta_x^0$ ,  $\delta_y^0$ . By integrating the difference of equations (4.5a) and (4.6a), we get an expression for  $x(t) - x^\delta(t)$  and derive an estimate of the form

$$\begin{aligned} |x(t) - x^\delta(t)| + |y(t) - y^\delta(t)| &= |\delta_x^0 + \int_{t_0}^t (\delta_1(\tau) + \delta_2(\tau)) d\tau| + |\delta_2(t)| \\ &\leq (T - t_0 + 1) \left( \|\delta^0\|_1 + \max_{\tau \in \mathcal{I}} \|\delta(\tau)\|_1 \right) \end{aligned}$$

and hence perturbation index  $\mu_p = 1$ .

Let us now consider a slight modification to the DAE (4.5)

$$x'(t) - y(t) = g_1(t) \tag{4.7a}$$

$$x(t) = g_2(t) \tag{4.7b}$$

for  $t \in \mathcal{I}$  with consistent initial conditions  $x(t_0) = x^0$  and  $y(t_0) = y^0$ ,  $g_1 \in \mathcal{C}^1(\mathcal{I}, \mathbb{R})$  and  $g_2 \in \mathcal{C}^2(\mathcal{I}, \mathbb{R})$ . Then the DAE (4.7) is of differentiation index  $\mu_d = 2$ , since we need to differentiate the system twice to extract the ODE

$$x'(t) = g_2'(t) \qquad y'(t) = g_2''(t) - g_1'(t).$$

Comparing the solution of (4.7) with the solution of the perturbed DAE

$$x^{\delta'}(t) - y^{\delta}(t) = g_1(t) + \delta_1(t) \quad (4.8a)$$

$$x^{\delta}(t) = g_2(t) + \delta_2(t), \quad (4.8b)$$

we can use the derivative of the difference of equations (4.7b) and (4.8b) to get an estimate

$$\begin{aligned} |x(t) - x^{\delta}(t)| + |y(t) - y^{\delta}(t)| &= |\delta_2(t)| + |\delta_2'(t) - \delta_1(t)| \\ &\leq \|\delta^0\|_1 + \max_{\tau \in \mathcal{I}} \|\delta(\tau)\|_1 + \max_{\tau \in \mathcal{I}} \|\delta'(\tau)\|_1 \end{aligned}$$

and therefore perturbation index  $\mu_p = 2$ .

Another concept for the analysis of DAEs is the *tractability index* [GM86; LMT13], where projector matrices are used to extract the inherent ODE together with a decoupled set of algebraic equations. This yields another index concept but also gives way to derive existence and uniqueness results for solutions of DAEs.

Of course, there exist many more index concepts for the analysis of DAEs. They include the *strangeness index*, introduced in [KM06], which also relies on the *inflated system* (4.2). Other concepts are the *geometric index* [Rhe84; Rei90; Rhe91], the *structural index* [Pan88; Pry01] or the *dissection index* [Jan15]. For more details, we refer to the respective literature. Comparisons of the different index concepts can be found in [GHM92; CG95b; Meh15].

One of the reasons why DAEs came into the focus of mathematical research is that they provide an easy approach towards modelling of many applications, like electrical circuits, multibody dynamics or chemical engineering. Moreover, they appear naturally when PDAEs are semi-discretised in space. However, this simplicity w.r.t. the modelling often results in other problems in the analysis or the numerical treatment, since DAEs may be ill-posed [LRS86] or suffer from instabilities or drift-off effects, e.g. in multibody dynamics. For instance, let us consider the DAE (4.7) in Example 4.7 for  $\mathcal{I} = [0, 2\pi]$  with functions

$$g_1(t) = 0 \quad g_2(t) = \cos(t) \quad \delta_1(t) = 0 \quad \delta_2(t) = 10^{-k} \cos(10^{2k}t),$$

with  $k \gg 1$  and initial values

$$\begin{aligned} x(0) &= 1 & x^{\delta}(0) &= 1 + 10^{-k} \\ y(0) &= 0 & y^{\delta}(0) &= 0. \end{aligned}$$

The solutions of the unperturbed and perturbed problem are given by

$$\begin{aligned} x(t) &= \cos(t) & x^{\delta}(t) &= \cos(t) + 10^{-k} \cos(10^{2k}t) \\ y(t) &= -\sin(t) & y^{\delta}(t) &= -\sin(t) - 10^k \sin(10^{2k}t). \end{aligned}$$

Even though the perturbations are small, the solution of the perturbed DAE deviates significantly in the  $y$ -component. Another major difference between ODEs and DAEs is illustrated in Example 4.7 as well. Whereas ODEs can be interpreted as integration

problems, DAEs may give rise to differentiation problems as in equation (4.7) of Example 4.7. This also illustrates the possible ill-posedness of DAEs.

Spatial and full discretisations for hyperbolic PDEs have been discussed in the recent past, e.g., in the textbooks of Kröner or LeVeque [Krö97; LeV02], but also in particular for gas and water networks applications. For instance, the midpoint rule or implicit box scheme are widely used [KLB10; DKL11; Gru<sup>+</sup>14]. Other spatial discretisations include the Crank-Nicholson discretisation [Her<sup>+</sup>09] or Galerkin discretisations [Egg16; EKW17].

In this chapter, we present a procedure to adapt the spatial discretisation to the gas network topology, with the goal to obtain a DAE of index 1. First we discuss the necessary topology assumptions for gas networks with pipes and active elements that occur as single elements in the network in Section 4.1. Afterwards, we show how it is possible to adapt the discretisation to the network topology by changing the orientation of the pipes in the network in a specific way.

The resulting DAE system is analysed in Section 4.2, where we also discuss the structure the DAE inherits from the network topology.

Section 4.3 introduces a decoupling procedure that allows a reformulation of the gas network DAE as an ODE system with a decoupled set of algebraic equations. We show that the ODE system can be formulated by just relying on topology and element information.

In Section 4.4, possible extensions of the DAE analysis and decoupling are discussed. This includes topology assumptions but also additional elements.

Furthermore, we address the computation of consistent initial values and how the decoupling process can be used to derive them in Section 4.5.

## 4.1 Topology-adaptive discretisation

In this section, we present an approach for a spatial discretisation of gas networks which we have introduced in Chapter 2 in equation (2.23). It is well-known that spatial discretisation of PDAEs may act as a regularisation [Arn98; CM96], but also as a deregularisation [Gün00]. We demonstrate this in Example 4.8 and show how this connects to the network topology.

We know from Chapter 3, that the solution of the PDAE (2.22) possesses a behaviour that is closely linked to perturbation index 1. This motivates us to present a discretisation that is adapted to the network topology and that guarantees an index 1 DAE, not only for pipe networks, but also for networks with active elements, if certain topology assumptions are fulfilled. These and other requirements regarding the network topology are discussed. In the second part of this section, we show what can be gained by making use of the network topology for the discretisation approach.

**Spatial discretisation from a PDE point of view** Spatial discretisation of hyperbolic PDEs is often closely linked to the characteristics of the PDE. Let us consider the one-dimensional advection or transport equation

$$\partial_t u(x, t) + a \partial_x u(x, t) = 0, \quad (4.9)$$

for  $(x, t) \in \mathbb{R} \times \mathcal{I}$ ,  $\mathcal{I} \subset \mathbb{R}$  compact, with initial value  $u(x, t_0) = u^0(x)$ . The solution is given by

$$u(x, t) = u^0(x - a(t - t_0))$$

and is constant along the characteristic  $(a \quad 1)^\top$ . If we move from the initial value problem (IVP) to the boundary value problem (BVP) and restrain  $(x, t) \in [0, \ell] \times \mathcal{I}$ , the sign of  $a$  determines on where the boundary condition can be imposed (either at  $x = 0$  or  $x = \ell$ ) to derive a BVP that is well-posed. For  $a > 0$ , the boundary condition must be imposed at  $x = 0$  and for  $a < 0$  at  $x = \ell$  in order to derive a well-posed BVP. For  $a > 0$ , the solution of the well-posed BVP with boundary condition  $u(0, t) = u^\Gamma(t)$  is determined by

$$u(x, t) = \begin{cases} u^\Gamma\left(t - \frac{x}{a}\right) & x < a(t - t_0) \\ u^0(x - a(t - t_0)) & a(t - t_0) < x. \end{cases}$$

Numerical methods that are used for this kind of problem are so-called *upwind methods* [LeV02] that are given by

$$\frac{d}{dt} u(x_i, t) + \frac{a}{h} (u(x_i, t) - u(x_{i-1}, t)) = 0 \quad i = 1, \dots, N$$

with  $h = \frac{\ell}{N}$ , here stated in a semi-discretised form for  $a > 0$  and

$$\frac{d}{dt} u(x_i, t) + \frac{a}{h} (u(x_{i+1}, t) - u(x_i, t)) = 0 \quad i = 0, \dots, N - 1$$

for  $a < 0$ .

Nevertheless, it is also possible to impose the boundary condition at  $x = \ell$  for  $a > 0$  and substitute  $\hat{u}(x, t) = u(\ell - x, t)$  in equation (4.9), which leads to the following BVP

$$\partial_t \hat{u}(x, t) - a \hat{u}(x, t) = 0 \quad \hat{u}(\ell, t) = u^\Gamma(t)$$

with initial condition  $\hat{u}(x, t_0) = u^0(\ell - x)$ . This is once again a well-posed problem.

**Spatial discretisation from a DAE point of view** From a DAE point of view, the question regarding well-posedness is a minor one, since DAEs can be ill-posed problems. Instead, the focus is more on the index of a DAE with special interest regarding index 1. This is not only true from an analytical perspective, but also and especially when it comes to numerics, where a higher index makes the computation of solutions much more difficult. Nevertheless, the question of well-posedness and the index 1 property are closely linked in the context of DAEs [Mär15]. For instance, applying a semi-discretisation to the

PDE (4.9), which is of the form

$$\frac{d}{dt}u(\ell, t) + \frac{a}{\ell}(u(\ell, t) - u(0, t)) = 0,$$

and considering different boundary conditions, results in DAEs of different indices:

- (i) If the boundary condition is given at  $x = 0$ ,

$$u(0, t) = u^{\Gamma}(t),$$

this yields a DAE of index 1,

- (ii) whereas imposing the boundary condition at  $x = \ell$ ,

$$u(\ell, t) = u^{\Gamma}(t),$$

results in a DAE of index 2.

A semi-discretisation of the form

$$\frac{d}{dt}u(0, t) + \frac{a}{\ell}(u(\ell, t) - u(0, t)) = 0$$

also yields DAEs of different indices depending on where the boundary condition is imposed.

- (i) Imposing the boundary condition at  $x = 0$ ,

$$u(0, t) = u^{\Gamma}(t),$$

results in a DAE of index 2,

- (ii) but if the boundary condition is given at  $x = \ell$ ,

$$u(\ell, t) = u^{\Gamma}(t),$$

the DAE is of index 2.

Note that what one considers to be an ill-posed BVP results in a DAE of higher index, which is in turn also considered as ill-posed in the DAE context [Mär15]. The DAE of differentiation index  $\mu_d = 1$  can in this case be derived by adapting the spatial discretisation to the boundary conditions.

We want to further demonstrate the impact of spatial discretisations from a DAE point of view by considering a simplified version of the one-pipe problem, given by equation (4.10) in the following example.

**Example 4.8.** *Considering a constant gas factor, setting the coefficients to 1 and by neglecting the friction and pipe-elevation terms one derives the two-dimensional advection*

equation

$$\partial_t p(x, t) + \partial_x q(x, t) = 0 \quad (x, t) \in [0, 1] \times \mathcal{I} \quad (4.10a)$$

$$\partial_t q(x, t) + \partial_x p(x, t) = 0 \quad (x, t) \in [0, 1] \times \mathcal{I}. \quad (4.10b)$$

We want to analyse the impact of the following spatial discretisation

$$\frac{d}{dt} p(1, t) + q(1, t) - q(0, t) = 0 \quad (4.11a)$$

$$\frac{d}{dt} q(0, t) + p(1, t) - p(0, t) = 0 \quad (4.11b)$$

under different sets of boundary conditions.

- (i) We first want to consider a pressure boundary condition at  $x = 0$  and a condition for the mass flow at  $x = 1$  given by

$$p(0, t) = p^\Gamma(t) \quad q(1, t) = q^\Gamma(t)$$

Differentiating the boundary conditions once leads to the DAE system

$$\frac{d}{dt} p(0, t) = \frac{d}{dt} p^\Gamma(t)$$

$$\frac{d}{dt} p(1, t) = q(0, t) - q(1, t)$$

$$\frac{d}{dt} q(0, t) = p(0, t) - p(1, t)$$

$$\frac{d}{dt} q(1, t) = \frac{d}{dt} q^\Gamma(t)$$

and hence differentiation index  $\mu_d = 1$ .

- (ii) By changing the boundary condition to

$$p(1, t) = p^\Gamma(t) \quad q(0, t) = q^\Gamma(t)$$

we need to differentiate the System (4.11) and the boundary conditions twice to extract

$$\frac{d}{dt} p(0, t) = \frac{d}{dt} p^\Gamma(t) + \frac{d^2}{dt^2} q^\Gamma(t)$$

$$\frac{d}{dt} p(1, t) = \frac{d}{dt} p^\Gamma(t)$$

$$\frac{d}{dt} q(0, t) = \frac{d}{dt} q^\Gamma(t)$$

$$\frac{d}{dt} q(1, t) = \frac{d}{dt} q^\Gamma(t) - \frac{d^2}{dt^2} p^\Gamma(t)$$

This implies differentiation index  $\mu_d = 2$ .

- (iii) Another possible set of boundary conditions could be

$$q(0, t) = q_l^\Gamma(t) \quad q(1, t) = q_r^\Gamma(t)$$

or

$$p(0, t) = p_l^\Gamma(t) \quad p(1, t) = p_r^\Gamma(t).$$

Both sets of boundary conditions lead to a DAE of differentiation index  $\mu_d = 3$ , since we need to differentiate System (4.11) and the boundary conditions three times to extract the ODE systems

$$\begin{aligned} \frac{d}{dt}p(0, t) &= \frac{d^2}{dt^2}q_l^\Gamma(t) - q(0, t) + q(1, t) \\ \frac{d}{dt}p(1, t) &= q(0, t) - q(1, t) \\ \frac{d}{dt}q(0, t) &= \frac{d}{dt}q_l^\Gamma(t) \\ \frac{d}{dt}q(1, t) &= \frac{d}{dt}q_r^\Gamma(t) \end{aligned}$$

and

$$\begin{aligned} \frac{d}{dt}p(0, t) &= \frac{d}{dt}p_l^\Gamma(t) \\ \frac{d}{dt}p(1, t) &= \frac{d}{dt}p_r^\Gamma(t) \\ \frac{d}{dt}q(0, t) &= p(0, t) - p(1, t) \\ \frac{d}{dt}q(1, t) &= p(0, t) - p(1, t) - \frac{d^2}{dt^2}p_l^\Gamma(t), \end{aligned}$$

respectively.

(iv) In the case that both variables are subject to constraints at the same node

$$p(x^\Gamma, t) = p^\Gamma(t) \quad q(x^\Gamma, t) = q^\Gamma(t) \quad x^\Gamma \in \{0, \ell\},$$

the DAE is of index 3 and leads to the underlying ODE

$$\begin{aligned} \frac{d}{dt}p(0, t) &= \frac{d}{dt}p^\Gamma(t) \\ \frac{d}{dt}p(1, t) &= \frac{d}{dt}p^\Gamma(t) - \frac{d^2}{dt^2}q^\Gamma(t) \\ \frac{d}{dt}q(0, t) &= \frac{d}{dt}q^\Gamma(t) \\ \frac{d}{dt}q(1, t) &= \frac{d}{dt}q^\Gamma(t) - \frac{d^2}{dt^2}p^\Gamma(t) + \frac{d^3}{dt^3}q^\Gamma(t), \end{aligned}$$

here stated for  $x^\Gamma = 0$ .

**Remark 4.9** (Well-posedness). In Chapter 3, we were able to prove that the solution of the PDAE depends continuously on the boundary and coupling data for the scenarios (i) and (ii) and the first set of boundary conditions in (iii).

**Remark 4.10** (Pipe-orientation). The difference between (i) and (ii) can be interpreted as a change in the orientation of the pipe as depicted in Figure 4.1.



**Figure 4.1:** Pipe orientation that leads to an index 1 DAE (left) and index 2 DAE (right).

Since the position of the nodes in a network is fixed, the position of the respective boundary condition cannot be changed. However, a change of orientation of a pipe is merely a change of the sign of the mass flow-variable and has no further consequences.

We know from Example 4.7 and Remark 4.10 that the pipe orientation is crucial for deriving a DAE of index 1. Therefore, we propose the following spatial discretisation for the pipe PDE (2.9) that, combined with a special pipe orientation, leads to a DAE of index 1.

$$\frac{d}{dt} \frac{p_v(t)}{z(p_v(t))} + \frac{R_s T_m}{a_e \ell_e} (q_{e,r}(t) - q_{e,l}(t)) = 0 \quad e = (u, v) \in \mathcal{E}_{\mathcal{P}} \quad (4.12a)$$

$$\frac{d}{dt} q_{e,l}(t) + \frac{a_e}{\ell_e} (p_v(t) - p_u(t)) = -g_e(p_v(t), q_{e,l}(t)) \quad e = (u, v) \in \mathcal{E}_{\mathcal{P}}. \quad (4.12b)$$

where  $g_{e^{\mathcal{P}}} : \mathbb{R} \times \mathbb{R} \rightarrow \mathbb{R}$  is given by

$$g_{e^{\mathcal{P}}}(p, q) = \frac{\lambda_{e^{\mathcal{P}}} R_s T_m z(p)}{2D_{e^{\mathcal{P}}} a_{e^{\mathcal{P}}}} \frac{q|q|}{p} + \frac{g a_{e^{\mathcal{P}}} h'_{e^{\mathcal{P}}}}{R_s T_m} \frac{p}{z(p)} \quad (4.13)$$

for  $e^{\mathcal{P}} \in \mathcal{E}_{\mathcal{P}}$ . For a general gas network  $\mathcal{G} = (V, \mathcal{E})$  with the elements and coupling conditions as described in Chapter 2, we can formulate the DAE system as

$$\Sigma_p^{\top} \left( \frac{p_p}{z(p_p)} \right)' + \Sigma_{\mathcal{A}}^{\top} \left( \frac{p_{\mathcal{A}}}{z(p_{\mathcal{A}})} \right)' + \Sigma_{\mathcal{P}}^{\top} \left( \frac{p_{\mathcal{P}}}{z(p_{\mathcal{P}})} \right)' + D_q(q_r - q_l) = 0 \quad (4.14a)$$

$$q_l' + D_p^{\mathcal{P}} p_p + D_{\mathcal{A}}^{\mathcal{P}} p_{\mathcal{A}} + D_{\mathcal{P}}^{\mathcal{P}} p_{\mathcal{P}} + G_{\mathcal{P}}(p_p, p_{\mathcal{A}}, p_{\mathcal{P}}, q_l) = 0 \quad (4.14b)$$

$$D_p^{\mathcal{R}} p_p + D_{\mathcal{A}}^{\mathcal{R}} p_{\mathcal{A}} + D_{\mathcal{P}}^{\mathcal{R}} p_{\mathcal{P}} + G_{\mathcal{R}}(p_p, p_{\mathcal{A}}, p_{\mathcal{P}}, q_{\mathcal{R}}) = 0 \quad (4.14c)$$

$$G_{\mathcal{C}}(p_p, p_{\mathcal{A}}, p_{\mathcal{P}}, q_{\mathcal{C}}, y_{\mathcal{C}}, t) = 0 \quad (4.14d)$$

$$A_r q_r + A_l q_l + A_{\mathcal{R}} q_{\mathcal{R}} + A_{\mathcal{C}} q_{\mathcal{C}} - q^{\Gamma}(t) = 0 \quad (4.14e)$$

$$p_p - p^{\Gamma} = 0, \quad (4.14f)$$

where  $\frac{p}{z(p)}$  is meant to be understood componentwise. Before we define the matrices and functions in equation (4.14), we want to introduce the following notation given by Tables 4.1 to 4.3.



Variable	Description
$p_p(t)$	Vector of pressures at nodes $u \in V_p$
$p_A(t)$	Vector of pressures at nodes $u \in V_A$
$p_P(t)$	Vector of pressures at nodes $u \in V_P$
$q_r(t)$	Vector of mass flows along pipes at $x = \ell$
$q_l(t)$	Vector of mass flows along pipes at $x = 0$
$q_R(t)$	Vector of mass flows along resistors
$q_C(t)$	Vector of mass flows along compressors

**Table 4.1:** Variables for gas network DAE modelling.

Variable	Description	Variable	Description
$m_V =  V $	Number of nodes $u \in V$	$n_{\mathcal{E}} =  \mathcal{E} $	Number of arcs
$m_p =  V_p $	Number of nodes $u \in V_p$	$n_P =  \mathcal{E}_P $	Number of pipes
$m_A =  V_A $	Number of nodes $u \in V_A$	$n_R =  \mathcal{E}_R $	Number of resistors
$m_P =  V_P $	Number of nodes $u \in V_P$	$n_C =  \mathcal{E}_C $	Number of compressors
$m_q = m_A + m_P$	Number of nodes $u \in V_q$	$n_A = n_R + n_C$	Number of active elements

**Table 4.2:** Notation for gas network DAE modelling.

Set	Description	Set	Description
$V = \{u_1, \dots, u_{m_V}\}$	Set of nodes	$\mathcal{E} = \{e_1, \dots, e_{n_{\mathcal{E}}}\}$	Set of arcs
$V_p = \{u_1^p, \dots, u_{m_p}^p\}$	Set of sources	$\mathcal{E}_P = \{e_1^P, \dots, e_{n_P}^P\}$	Set of pipes
$V_q = \{u_1^q, \dots, u_{m_q}^q\}$	Set of sinks	$\mathcal{E}_R = \{e_1^R, \dots, e_{n_R}^R\}$	Set of compressors
$V_P = \{u_1^P, \dots, u_{m_P}^P\}$	Set of nodes in $V_P$	$\mathcal{E}_C = \{e_1^C, \dots, e_{n_C}^C\}$	Set of resistors
$V_A = \{u_1^A, \dots, u_{m_A}^A\}$	Set of nodes in $V_A$	$\mathcal{E}_A = \{e_1^A, \dots, e_{n_A}^A\}$	Set of active elements

**Table 4.3:** Element sets for gas network DAE modelling.

Next, we will define the matrices and non-linear functions for the DAE (4.14). The matrices for the differential components are given by

$$\Sigma_p \in \mathbb{R}^{m_p \times n_P} \quad (\Sigma_p)_{ij} = \begin{cases} 1 & e_j^P \in \delta^+(u_i^p) \\ 0 & \text{else} \end{cases} \quad (4.15)$$

$$\Sigma_A \in \mathbb{R}^{m_A \times n_P} \quad (\Sigma_A)_{ij} = \begin{cases} 1 & e_j^P \in \delta^+(u_i^A) \\ 0 & \text{else} \end{cases} \quad (4.16)$$

$$\Sigma_P \in \mathbb{R}^{m_P \times n_P} \quad (\Sigma_P)_{ij} = \begin{cases} 1 & e_j^P \in \delta^+(u_i^P) \\ 0 & \text{else.} \end{cases} \quad (4.17)$$

The discretisation matrices in equations (4.14a) and (4.14b) are

$$D_q \in \mathbb{R}^{n_P \times n_P} \quad D_q = \text{diag} \left( \frac{R_s T_m}{a_1 \ell_1}, \dots, \frac{R_s T_m}{a_{n_P} \ell_{n_P}} \right) \quad (4.18)$$

$$D_p^{\mathcal{P}} \in \mathbb{R}^{n_P \times m_P} \quad (D_p^{\mathcal{P}})_{ij} = \begin{cases} \frac{a_i}{\ell_i} & e_i^{\mathcal{P}} = (u, u_j^{\mathcal{P}}) \\ -\frac{a_i}{\ell_i} & e_i^{\mathcal{P}} = (u_j^{\mathcal{P}}, u) \\ 0 & \text{else} \end{cases} \quad (4.19)$$

$$D_{\mathcal{A}}^{\mathcal{P}} \in \mathbb{R}^{n_P \times m_{\mathcal{A}}} \quad (D_{\mathcal{A}}^{\mathcal{P}})_{ij} = \begin{cases} \frac{a_i}{\ell_i} & e_i^{\mathcal{P}} = (u, u_j^{\mathcal{A}}) \\ -\frac{a_i}{\ell_i} & e_i^{\mathcal{P}} = (u_j^{\mathcal{A}}, u) \\ 0 & \text{else} \end{cases} \quad (4.20)$$

$$D_{\mathcal{P}}^{\mathcal{P}} \in \mathbb{R}^{n_P \times m_P} \quad (D_{\mathcal{P}}^{\mathcal{P}})_{ij} = \begin{cases} \frac{a_i}{\ell_i} & e_i^{\mathcal{P}} = (u, u_j^{\mathcal{P}}) \\ -\frac{a_i}{\ell_i} & e_i^{\mathcal{P}} = (u_j^{\mathcal{P}}, u) \\ 0 & \text{else.} \end{cases} \quad (4.21)$$

For the resistor equation (4.14c), the matrices computing the pressure differences are

$$D_p^{\mathcal{R}} \in \mathbb{R}^{n_{\mathcal{R}} \times m_P} \quad (D_p^{\mathcal{R}})_{ij} = \begin{cases} 1 & e_i^{\mathcal{R}} = (u, u_j^{\mathcal{P}}) \\ -1 & e_i^{\mathcal{R}} = (u_j^{\mathcal{P}}, u) \\ 0 & \text{else} \end{cases} \quad (4.22)$$

$$D_{\mathcal{A}}^{\mathcal{R}} \in \mathbb{R}^{n_{\mathcal{R}} \times m_{\mathcal{A}}} \quad (D_{\mathcal{A}}^{\mathcal{R}})_{ij} = \begin{cases} 1 & e_i^{\mathcal{R}} = (u, u_j^{\mathcal{A}}) \\ -1 & e_i^{\mathcal{R}} = (u_j^{\mathcal{A}}, u) \\ 0 & \text{else} \end{cases} \quad (4.23)$$

$$D_{\mathcal{P}}^{\mathcal{R}} \in \mathbb{R}^{n_{\mathcal{R}} \times m_P} \quad (D_{\mathcal{P}}^{\mathcal{R}})_{ij} = \begin{cases} 1 & e_i^{\mathcal{R}} = (u, u_j^{\mathcal{P}}) \\ -1 & e_i^{\mathcal{R}} = (u_j^{\mathcal{P}}, u) \\ 0 & \text{else} \end{cases} \quad (4.24)$$

and the incidence matrices are defined as

$$A_r \in \mathbb{R}^{m_q \times n_P} \quad (A_r)_{ij} = \begin{cases} 1 & e_j^{\mathcal{P}} = (u, u_i^q) \\ 0 & \text{else} \end{cases} \quad (4.25)$$

$$A_l \in \mathbb{R}^{m_q \times n_P} \quad (A_l)_{ij} = \begin{cases} -1 & e_j^{\mathcal{P}} = (u_i^q, u) \\ 0 & \text{else} \end{cases} \quad (4.26)$$

$$A_{\mathcal{R}} \in \mathbb{R}^{m_q \times n_{\mathcal{R}}} \quad (A_{\mathcal{R}})_{ij} = \begin{cases} 1 & e_j^{\mathcal{R}} = (u, u_i^q) \\ -1 & e_j^{\mathcal{R}} = (u_i^q, u) \\ 0 & \text{else} \end{cases} \quad (4.27)$$

$$A_{\mathcal{C}} \in \mathbb{R}^{m_q \times n_{\mathcal{C}}} \quad (A_{\mathcal{C}})_{ij} = \begin{cases} 1 & e_j^{\mathcal{C}} = (u, u_i^q) \\ -1 & e_j^{\mathcal{C}} = (u_i^q, u) \\ 0 & \text{else.} \end{cases} \quad (4.28)$$

The non-linear functions are

$$G_{\mathcal{P}}: \mathbb{R}^{m_p} \times \mathbb{R}^{m_A} \times \mathbb{R}^{m_{\mathcal{P}}} \times \mathbb{R}^{n_{\mathcal{P}}} \rightarrow \mathbb{R}^{n_{\mathcal{P}}}$$

with

$$G_{\mathcal{P}}(p_p, p_A, p_{\mathcal{P}}, q_l) = \begin{pmatrix} g_{e_1^{\mathcal{P}}} & \cdots & g_{e_{n_{\mathcal{P}}}^{\mathcal{P}}} \end{pmatrix}^{\top}.$$

The functions  $g_{e^{\mathcal{P}}}$  are given by equation (4.13). For the resistors and compressors we introduce

$$G_{\mathcal{R}}: \mathbb{R}^{m_p} \times \mathbb{R}^{m_A} \times \mathbb{R}^{m_{\mathcal{P}}} \times \mathbb{R}^{n_{\mathcal{R}}} \rightarrow \mathbb{R}^{n_{\mathcal{R}}}$$

$$G_C: \mathbb{R}^{m_p} \times \mathbb{R}^{m_A} \times \mathbb{R}^{m_{\mathcal{P}}} \times \mathbb{R}^{n_C} \times \mathbb{R}^{4n_C} \times \mathcal{I} \rightarrow \mathbb{R}^{5n_C}$$

that are defined componentwise by

$$G_{\mathcal{R}}(p_p, p_A, p_{\mathcal{P}}, q_{\mathcal{R}}) = \begin{pmatrix} g_{e_1^{\mathcal{R}}} & \cdots & g_{e_{n_{\mathcal{R}}}^{\mathcal{R}}} \end{pmatrix}^{\top}$$

$$G_C(p_p, p_A, p_{\mathcal{P}}, q_C, y, t) = \begin{pmatrix} g_{e_1^C} & \cdots & g_{e_{n_C}^C} \end{pmatrix}^{\top}$$

with functions  $g_{e^{\mathcal{R}}}$  and  $g_{e^C}$  given by equation (2.13) and equations (2.15) and (2.16), respectively. The functions  $q^{\Gamma}: \mathcal{I} \rightarrow \mathbb{R}^{|V_q|}$  and  $p^{\Gamma}: \mathcal{I} \rightarrow \mathbb{R}^{|V_p|}$  in equations (4.14e) and (4.14f) are given componentwise by the demand and pressure functions at the sinks and sources, respectively:

$$q^{\Gamma} = \begin{pmatrix} q_{u_1^q}^{\Gamma} & \cdots & q_{u_{m_q}^q}^{\Gamma} \end{pmatrix}^{\top} \quad p^{\Gamma} = \begin{pmatrix} p_{u_1^p}^{\Gamma} & \cdots & p_{u_{m_p}^p}^{\Gamma} \end{pmatrix}^{\top}. \quad (4.29)$$

Next, we investigate a certain class of gas networks where active elements are not connected to each other. Hence, for now we are focusing on graphs of gas networks that fulfil the following assumptions.

**Assumption 4.11.**

Let  $\mathcal{G} = (V, \mathcal{E})$  be the graph of a gas network with  $V_p, V_q \neq \emptyset$  containing pipes, resistors and compressors, so that

1.  $\nexists e^{\mathcal{P}} = (u, v) \in \mathcal{E}_{\mathcal{P}}$  with  $u, v \in V_p \cup V_A$ .
2. Each connected component of  $\mathcal{G}_{\mathcal{P}} = (V, \mathcal{E}_{\mathcal{P}})$  contains at least one node  $u \in V_p \cup V_A$ .
3.  $|\delta^+(u) \cap \mathcal{E}_A| \leq 1 \quad \forall u \in V \quad \text{and} \quad \delta^+(u) \cap \mathcal{E}_A = \emptyset \quad \forall u \in V_p$ .
4. There are no paths of active elements in  $\mathcal{G}$ , hence  $\forall e^A = (u, v) \in \mathcal{E}_A: u \in V_p \cup V_p$ .

**Remark 4.12.** The topology requirements stated in Assumption 4.11 can be translated to:

1. There should be no pipe that directly connects sources ( $V_p$ ) and nodes that have active elements directed towards them ( $V_A$ ) with each other.
2. Each connected component should contain at least one reference node regarding pressure.
3. There is at most one active element directed towards any node in the network.

4. Active elements are not connected to other active elements.

**Example 4.13.** Consider the graph in Figure 4.2 with the sets

$$\begin{array}{lll}
 V_p = \{u_1, u_2, u_3\} & V_{\mathcal{P}} = \{v_1, v_2, v_4\} & V_{\mathcal{A}} = \{v_3, v_5, v_6\} \\
 \delta^+(u_1) = \{e_1^{\mathcal{P}}\} & \delta^+(u_2) = \{e_8^{\mathcal{P}}\} & \delta^+(u_3) = \emptyset \\
 \delta^+(v_1) = \emptyset & \delta^+(v_2) = \{e_3^{\mathcal{P}}\} & \delta^+(v_3) = \{e_4^{\mathcal{P}}, e_1^{\mathcal{R}}, e_2^{\mathcal{C}}\} \\
 \delta^+(v_4) = \{e_5^{\mathcal{P}}\} & \delta^+(v_5) = \{e_2^{\mathcal{P}}, e_6^{\mathcal{P}}, e_1^{\mathcal{C}}\} & \delta^+(v_6) = \{e_7^{\mathcal{P}}, e_2^{\mathcal{R}}\}.
 \end{array}$$

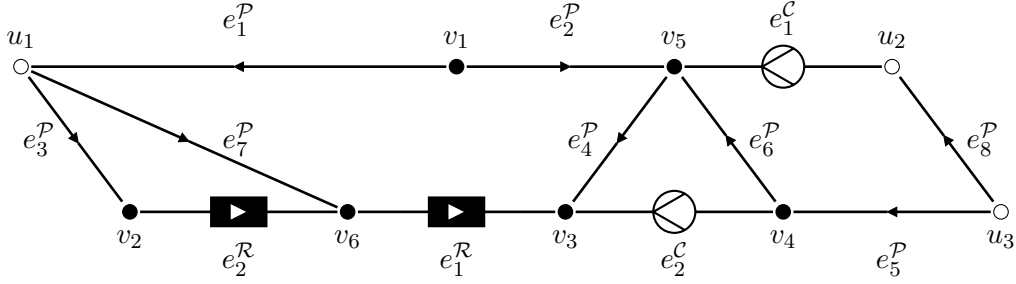


**Figure 4.2:** Network that does not fulfil Assumptions 4.11.

This graph does not fulfil Assumptions 4.11, since the first condition prohibits pipes  $e_4^{\mathcal{P}}$ ,  $e_7^{\mathcal{P}}$  and  $e_8^{\mathcal{P}}$ . In addition,

$$\delta^+(v_5) \cap \mathcal{E}_{\mathcal{A}} = \{e_1^{\mathcal{R}}, e_2^{\mathcal{C}}\}$$

contains more than one active element, which violates the third assumption. Obviously, the fourth assumption is not fulfilled due to the path containing  $e_1^{\mathcal{R}}$  and  $e_2^{\mathcal{R}}$ .

Extensions, that would allow us to handle networks as in Figure 4.2, are discussed in Section 4.4. We also address the inclusion of other active elements like valves.

**Theorem 4.14.**

Let  $\mathcal{G} = (V, \mathcal{E})$  be an oriented graph of a gas network that fulfils Assumption 4.11. Then it holds that the pipes in  $\mathcal{G}$  can be directed in a way that

- (i)  $\forall u \in V_p : \quad \delta^+(u) = \emptyset.$
- (ii)  $\forall u \in V_{\mathcal{P}} : \quad \delta^+(u) \cap \mathcal{E}_{\mathcal{P}} \neq \emptyset.$
- (iii)  $\forall u \in V_{\mathcal{A}} : \quad \delta^+(u) \cap \mathcal{E}_{\mathcal{P}} = \emptyset.$

*Proof.* We prove the statement for a connected graph  $\mathcal{G}$ . Let  $\mathcal{G}_{\mathcal{P}} = (V, \mathcal{E}_{\mathcal{P}})$  be connected and  $\mathcal{G}^{(0)} = (V, \mathcal{E}_{\mathcal{P}}^{(0)})$  be an arbitrary tree of  $\mathcal{G}_{\mathcal{P}}$ . The degree of  $u \in V$  with respect to a branch set  $\mathcal{E}^{(i)}$  is given by equation (3.4) as the number of arcs  $e \in \mathcal{E}^{(i)}$  that are connected to the node  $u$ . We orientate the pipes in the tree as follows:

- (1)  $i = 0$ ,  $V^{(0)} = V$ .
- (2) If there exists a node  $u \in V_{\mathcal{P}} \cap V^{(i)}$  so that  $\deg_{\mathcal{E}_{\mathcal{P}}^{(i)}}(u) = 1$  and the respective pipe is  $e^{\mathcal{P}} = (u, v) \in \delta^-(u)$ , then we set  $e^{\mathcal{P}} = (v, u)$ . If  $e^{\mathcal{P}} \in \delta^+(u)$ , the orientation of the pipe remains as it is.
- (3) If there exists no such node, then there is a node  $u \in (V_{\mathcal{P}} \cup V_{\mathcal{A}}) \cap V^{(i)}$ , so that  $\deg_{\mathcal{E}_{\mathcal{P}}^{(i)}}(u) = 1$ . If this pipe  $e^{\mathcal{P}} = (v, u) \in \delta^+(u)$ , we set  $e^{\mathcal{P}} = (u, v)$ .
- (4) Set  $V^{(i+1)} = V^{(i)} \setminus \{u\}$ ,  $\mathcal{E}_{\mathcal{P}}^{(i+1)} = \mathcal{E}_{\mathcal{P}}^{(i)} \setminus \{e^{\mathcal{P}}\}$ ,  $\mathcal{G}^{(i+1)} = (V^{(i+1)}, \mathcal{E}_{\mathcal{P}}^{(i+1)})$ ,  $i = i + 1$ .
- (5) If  $V^{(i)} \neq \emptyset$ , go to (2).
- (6) If  $\delta^+(V_{\mathcal{P}} \cup V_{\mathcal{A}}) \cap (\mathcal{E}_{\mathcal{P}} \setminus \mathcal{E}_{\mathcal{P}}^{(0)}) \neq \emptyset$ , change the direction of all  $e^{\mathcal{P}} \in \delta^+(V_{\mathcal{P}} \cup V_{\mathcal{A}}) \cap (\mathcal{E}_{\mathcal{P}} \setminus \mathcal{E}_{\mathcal{P}}^{(0)})$ .

As in the proof of Theorem 3.2, there always exists either a node that fulfils (2) or (3) until  $V^i = \emptyset$  in (4) and we finally get to (6). The algorithm terminates eventually because in each step  $j$ ,  $\mathcal{G}^{(j)}$  is a tree and gets reduced by one node and one arc so that  $\mathcal{G}^{(j+1)}$  is also a tree.

If  $\mathcal{G}_{\mathcal{P}}$  is not connected, perform the steps for each connected component. The same holds for the case that  $\mathcal{G}$  consists of multiple connected components.  $\square$

**Definition 4.15.** Let  $u_j^{\mathcal{P}} \in V_{\mathcal{P}}$ , for  $j \in 1, \dots, m_{\mathcal{P}}$ . Then we define  $s_j, r_j \in \mathbb{N}$  as

$$s_j := |\delta^+(u_j^{\mathcal{P}})| \qquad r_j = \sum_{k=1}^j s_k.$$

**Corollary 4.16.** For a graph  $\mathcal{G} = (V, \mathcal{E})$  that fulfils Assumptions 4.11 and that is oriented according to Theorem 4.14, the following assertions hold:

(i) Nodes and arcs can be enumerated so that

$$\begin{aligned} \delta^+(u_j^{\mathcal{P}}) &= \{e_{r_{j-1}+1}^{\mathcal{P}}, \dots, e_{r_j}^{\mathcal{P}}\} & u_j^{\mathcal{P}} &\in V_{\mathcal{P}} \\ \delta^+(u_j^{\mathcal{A}}) &= \begin{cases} \{e_j^{\mathcal{R}}\} & 1 \leq j \leq n_{\mathcal{R}} \\ \{e_{j-n_{\mathcal{R}}}^{\mathcal{C}}\} & n_{\mathcal{R}} + 1 \leq j \leq n_{\mathcal{A}} \end{cases} & u_j^{\mathcal{A}} &\in V_{\mathcal{A}} \end{aligned}$$

(ii)  $\Sigma_+ = 0$ ,  $\Sigma_{\mathcal{A}} = 0$ ,  $D_{\mathcal{A}}^{\mathcal{R}} = (-I_{\mathcal{R}} \ 0)$

(iii) The incidence matrices have a block structure given by

$$A_r = \begin{pmatrix} A_r^{\mathcal{P}} \\ 0 \\ 0 \end{pmatrix} \qquad A_{\mathcal{R}} = \begin{pmatrix} A_{\mathcal{R}}^{\mathcal{P}} \\ I_{\mathcal{R}} \\ 0 \end{pmatrix} \qquad A_{\mathcal{C}} = \begin{pmatrix} A_{\mathcal{C}}^{\mathcal{P}} \\ 0 \\ I_{\mathcal{C}} \end{pmatrix}. \quad (4.30)$$

$I_{\mathcal{R}} \in \mathbb{R}^{n_{\mathcal{R}} \times n_{\mathcal{R}}}$ ,  $I_{\mathcal{C}} \in \mathbb{R}^{n_{\mathcal{C}} \times n_{\mathcal{C}}}$  being identity matrices of the respective dimensions.

The submatrices  $A_r^{\mathcal{P}} \in \mathbb{R}^{m_{\mathcal{P}} \times n_{\mathcal{P}}}$ ,  $A_{\mathcal{R}}^{\mathcal{P}} \in \mathbb{R}^{m_{\mathcal{P}} \times n_{\mathcal{R}}}$  and  $A_{\mathcal{C}}^{\mathcal{P}} \in \mathbb{R}^{m_{\mathcal{P}} \times n_{\mathcal{C}}}$  are defined by

$$A_r^{\mathcal{P}} = \begin{pmatrix} a_r^1 & & 0 \\ & \ddots & \\ 0 & & a_r^{m_{\mathcal{P}}} \end{pmatrix} \quad \text{with} \quad a_r^j = \mathbf{1}^\top \in \mathbb{R}^{1 \times s_j}$$

and

$$(A_{\mathcal{R}}^{\mathcal{P}})_{ij} = \begin{cases} -1 & e_j^{\mathcal{R}} \in \delta^-(u_i^{\mathcal{P}}) \\ 0 & \text{else} \end{cases} \quad (A_{\mathcal{C}}^{\mathcal{P}})_{ij} = \begin{cases} -1 & e_j^{\mathcal{C}} \in \delta^-(u_i^{\mathcal{P}}) \\ 0 & \text{else.} \end{cases}$$

(iv) The non-linear functions  $G_{\mathcal{P}}$  and  $G_{\mathcal{R}}$  only depend on the arguments

$$\begin{aligned} G_{\mathcal{P}}(p_p, p_A, p_{\mathcal{P}}, q_l) &= G_{\mathcal{P}}(p_{\mathcal{P}}, q_l) \\ \text{and} \quad G_{\mathcal{R}}(p_p, p_A, p_{\mathcal{P}}, q_{\mathcal{R}}) &= G_{\mathcal{R}}(p_p, p_{\mathcal{P}}, q_{\mathcal{R}}), \end{aligned}$$

respectively.

As a consequence, we can model a gas network as a DAE with properly stated leading term (see Definition B.2) of the form

$$E \frac{d}{dt} d(u) + b(u, t) = 0 \tag{4.31}$$

with  $u = (p_p \ p_A \ p_{\mathcal{P}} \ q_r \ q_l \ q_{\mathcal{R}} \ q_{\mathcal{C}} \ y_{\mathcal{C}})^\top$ , where  $p_p$ ,  $p_A$  and  $p_{\mathcal{P}}$  corresponds to the pressures at the nodes in  $V_p$ ,  $V_A$  and  $V_{\mathcal{P}}$ , respectively. Further, let  $n_u$  be the dimension of  $u$ .  $E$  and the function  $d$  in equation (4.31) are defined by

$$d: \mathbb{R}^{n_u} \rightarrow \mathbb{R}^{m_{\mathcal{P}} + n_{\mathcal{P}}} \quad d(u) = \left( \frac{p_{\mathcal{P}}}{z(p_{\mathcal{P}})} \quad q_l \right)^\top \tag{4.32a}$$

$$E \in \mathbb{R}^{n_u \times (m_{\mathcal{P}} + n_{\mathcal{P}})} \quad E = \begin{pmatrix} \Sigma_{\mathcal{P}}^\top & 0 \\ 0 & I_{\mathcal{P}} \\ 0 & 0 \end{pmatrix} \tag{4.32b}$$

with  $I_{\mathcal{P}} \in \mathbb{R}^{n_{\mathcal{P}} \times n_{\mathcal{P}}}$  being the identity matrix of dimension  $n_{\mathcal{P}}$ . The non-linear function  $b: \mathbb{R}^{n_u} \times \mathcal{I} \rightarrow \mathbb{R}^{n_u}$  is defined as

$$b(u, t) = \begin{pmatrix} D_q(q_r - q_l) \\ D_p^{\mathcal{P}} p_p + D_{\mathcal{P}}^{\mathcal{P}} p_{\mathcal{P}} + D_A^{\mathcal{P}} p_A + G_{\mathcal{P}}(p_{\mathcal{P}}, q_l) \\ D_p^{\mathcal{R}} p_p + D_{\mathcal{P}}^{\mathcal{R}} p_{\mathcal{P}} + D_A^{\mathcal{R}} p_A + G_{\mathcal{R}}(p_p, p_{\mathcal{P}}, q_{\mathcal{R}}) \\ G_{\mathcal{C}}(p_p, p_A, p_{\mathcal{P}}, q_{\mathcal{C}}, y_{\mathcal{C}}, t) \\ A_r q_r + A_l q_l + A_{\mathcal{R}} q_{\mathcal{R}} + A_{\mathcal{C}} q_{\mathcal{C}} - q^\Gamma(t) \\ p_p - p^\Gamma(t) \end{pmatrix}. \tag{4.32c}$$

## 4.2 Gas network DAE analysis

This section provides analytical results for the DAE given by equation (4.32) regarding its index. Here, we rely on a technique similar to the approach towards the dissection index by Jansen in [Jan15] to prove the following theorem.

**Theorem 4.17.** *Let  $\mathcal{G} = (V, \mathcal{E})$  be the graph of a gas network that fulfils Assumptions 4.11 and let the pipes of  $\mathcal{G}$  be directed as proposed in Theorem 4.14. Then the DAE (4.31) describing the gas network is of index 1.*

Before we present the proof for this Theorem, we introduce the following basis functions.

**Definition 4.18** (Basis functions). Let  $M \in \mathbb{R}^{m \times n}$  with constant rank and let  $m_k = \dim \ker M^\top$ . Choose the matrix functions  $V \in \mathbb{R}^{m \times m_k}$ ,  $W \in \mathbb{R}^{m \times n - m_k}$  so that

$$\text{im } V = \text{coker } M^\top \quad \text{im } W = \ker M^\top.$$

Hence, the columns of  $W$  are a basis of  $\ker M^\top$  and  $V$  complements that basis to a basis of  $\mathbb{R}^n$ .

**Lemma 4.19.** *Let  $\mathcal{G} = (V, \mathcal{E})$  be the graph of a gas network that fulfils Assumptions 4.11 and let the pipes of  $\mathcal{G}$  be directed as proposed in Theorem 4.14. Let  $V$  and  $W$  be the associated basis functions of the matrix  $E$  in equation (4.31). It is possible to choose  $V$  and  $W$  so that  $(V)_{ij}, (W)_{ik} \in \{-1, 0, 1\}$  for  $1 \leq i \leq n_u$ ,  $1 \leq j \leq m_{\mathcal{P}}$ ,  $1 \leq k \leq m_{\mathcal{A}} + m_{\mathcal{P}}$ .*

*Proof.* Due to construction, each row of  $\Sigma_{\mathcal{P}}^\top$  contains exactly one entry that is 1 and else only entries that are 0. Let  $\sigma_j$  be the  $j^{\text{th}}$  column of  $\Sigma_{\mathcal{P}}^\top$  corresponding to node  $u_j^{\mathcal{P}} \in V_{\mathcal{P}}$ . Then  $\sigma_j$  contains only entries that are either 1 or 0 and there are exactly  $s_j$  entries in  $\sigma_j$  that are equal to 1 at the positions  $r_{j-1} + 1, \dots, r_j$ . We define the vectors

$$(v^j)_k = \begin{cases} 1 & k = r_{j-1} + 1 \\ 0 & \text{else} \end{cases} \quad j \in \{1, \dots, m_{\mathcal{P}}\}, k \in \{1, \dots, m_{\mathcal{A}} + m_{\mathcal{P}}\}$$

and for  $j \in \{1, \dots, m_{\mathcal{P}}\}$  with  $s_j > 1$

$$(w_i^j)_k = \begin{cases} 1 & k = r_{j-1} + 1 \\ -1 & k = r_{j-1} + 1 + i \\ 0 & \text{else} \end{cases} \quad i \in \{1, \dots, s_j - 1\}, k \in \{1, \dots, m_{\mathcal{A}} + m_{\mathcal{P}}\}.$$

Let  $\hat{V}$  and  $\hat{W}$  be the matrices that have  $v^j$  and  $w_i^j$  as columns. Then

$$V = \begin{pmatrix} \hat{V} & 0 \\ 0 & I_{\mathcal{P}} \\ 0 & 0 \end{pmatrix} \in \mathbb{R}^{n_u \times (m_{\mathcal{P}} + n_{\mathcal{P}})} \quad W = \begin{pmatrix} \hat{W} & 0 \\ 0 & 0 \\ 0 & I \end{pmatrix} \in \mathbb{R}^{n_u \times n_u - (m_{\mathcal{P}} + n_{\mathcal{P}})}$$

are associated basis functions of  $E$  as in Definition 4.18. It holds that

$$V^\top E = I \quad W^\top E = 0$$

□

**Corollary 4.20.** *By a proper arrangement of the columns in  $W$ , it holds that*

$$\begin{aligned} V^\top b(u, t) &= \begin{pmatrix} \bar{D}_q(q_r - q_l) \\ D_p^{\mathcal{P}} p_p + D_p^{\mathcal{P}} p_{\mathcal{P}} + D_{\mathcal{A}}^{\mathcal{P}} p_{\mathcal{A}} + G_{\mathcal{P}}(p_{\mathcal{P}}, q_l) \end{pmatrix} \\ W^\top b(u, t) &= \begin{pmatrix} D_p^{\mathcal{R}} p_p + D_p^{\mathcal{R}} p_{\mathcal{P}} + D_{\mathcal{R}}^{\mathcal{P}} p_{\mathcal{A}} + G_{\mathcal{R}}(p_p, p_{\mathcal{P}}, q_{\mathcal{R}}) \\ G_{\mathcal{C}}(p_p, p_{\mathcal{A}}, p_{\mathcal{P}}, q_{\mathcal{C}}, y_{\mathcal{C}}, t) \\ \bar{A}_r q_r + \bar{A}_l q_l + \bar{A}_{\mathcal{R}} q_{\mathcal{R}} + \bar{A}_{\mathcal{C}} q_{\mathcal{C}} - \bar{q}^\Gamma(t) \\ p_p - p^\Gamma(t) \end{pmatrix} \end{aligned}$$

where  $\bar{D}_q \in \mathbb{R}^{m_{\mathcal{P}} \times n_{\mathcal{P}}}$  contains part of the rows of  $D_q$  and is defined by

$$(\bar{D}_q)_{ij} = \begin{cases} \frac{R_s T_m}{a_j \ell_j} & j = r_{i-1} + 1 \\ 0 & \text{else.} \end{cases}$$

The vector-valued function  $\bar{q}^\Gamma: \mathcal{I} \rightarrow \mathbb{R}^{n_{\mathcal{P}}}$  is given by

$$\bar{q}_i^\Gamma = \begin{cases} q_{u_j^{\mathcal{P}}}^\Gamma & i = r_{j-1} + 1 \\ q_{u_j^{\mathcal{A}}}^\Gamma & i = r_{m_{\mathcal{P}}} + j \\ 0 & \text{else.} \end{cases}$$

The matrices  $\bar{A}_r, \bar{A}_l \in \mathbb{R}^{n_{\mathcal{P}} \times n_{\mathcal{P}}}$  contain additional rows that are linear combinations of rows of  $D_q$ , and  $\bar{A}_{\mathcal{R}} \in \mathbb{R}^{n_{\mathcal{P}} \times n_{\mathcal{R}}}$  and  $\bar{A}_{\mathcal{C}} \in \mathbb{R}^{n_{\mathcal{P}} \times n_{\mathcal{C}}}$  contain additional zero-rows due to the multiplication with  $W^\top$  from the left. In addition,  $\bar{A}_r$  has a specific block-structure

$$\bar{A}_r = \begin{pmatrix} \bar{A}_r^{\mathcal{P}} \\ 0 \end{pmatrix} = \begin{pmatrix} A_r^1 & & 0 \\ & \ddots & \\ 0 & & A_r^{m_{\mathcal{P}}} \\ 0 & \dots & 0 \end{pmatrix} \in \mathbb{R}^{n_{\mathcal{E}} \times n_{\mathcal{P}}}. \quad (4.33)$$

The zero-rows at the bottom of  $\bar{A}_r$  correspond to the nodes in  $V_{\mathcal{A}}$  that have no pipes directed towards them due to Theorem 4.14. The blocks  $A_r^j$  are defined as

$$A_r^j = \begin{pmatrix} 1 & 1 & \dots & 1 \\ \alpha_{r_{j-1}+1} & -\alpha_{r_{j-1}+2} & & \\ \vdots & & \ddots & \\ \alpha_{r_{j-1}+1} & 0 & & -\alpha_{r_j} \end{pmatrix} \in \mathbb{R}^{s_j \times s_j} \quad \alpha_i = \frac{R_s T_m}{a_i \ell_i} \quad (4.34)$$

due to the special choice of  $W$  in Lemma 4.19.

**Lemma 4.21.** *Under the Assumptions 4.11 and if the pipes of the graph  $\mathcal{G}$  are directed according to Theorem 4.14, the matrix  $(\bar{A}_r \quad \bar{A}_{\mathcal{R}} \quad \bar{A}_{\mathcal{C}}) \in \mathbb{R}^{n_{\mathcal{E}} \times n_{\mathcal{E}}}$  is non-singular.*

*Proof.*  $\bar{A}_r$  is given by equation (4.33). Due to the structure of the matrices  $A_r^j$  in equa-



tion (4.34), we get

$$\begin{aligned} \det(A_r^j) &= \det \begin{pmatrix} -\alpha_{r_{j-1}+2} & & 0 \\ & \ddots & \\ 0 & & -\alpha_{r_j} \end{pmatrix} \begin{pmatrix} 1 - \alpha_{r_{i-1}+1} \mathbf{1}^\top & & \\ & \ddots & \\ & & 1 \end{pmatrix}^{-1} \begin{pmatrix} -\alpha_{r_{j-1}+2} & & 0 \\ & \ddots & \\ 0 & & -\alpha_{r_j} \end{pmatrix} \\ &= \prod_{i=2}^{s_j} (-\alpha_{r_{j-1}+i}) \left( 1 + \alpha_{r_{j-1}+1} \sum_{i=2}^{s_j} \alpha_{r_{j-1}+i}^{-1} \right) \neq 0, \end{aligned}$$

since each of the coefficients  $\alpha_i > 0$ ,  $i \in \{1, \dots, n_{\mathcal{P}}\}$ . As a direct consequence, we get that

$$\bar{A}_r^{\mathcal{P}} = \begin{pmatrix} A_r^1 & & 0 \\ & \ddots & \\ 0 & & A_r^{m_{\mathcal{P}}} \end{pmatrix}$$

is non-singular.

We know that the ingoing arcs of the nodes  $u^{\mathcal{A}} \in V_{\mathcal{A}}$  are given by

$$\begin{aligned} \delta^+(u_j^{\mathcal{A}}) &= \{e_j^{\mathcal{R}}\} & 1 \leq j \leq n_{\mathcal{R}} \\ \delta^+(u_j^{\mathcal{A}}) &= \{e_{j-n_{\mathcal{R}}}^{\mathcal{C}}\} & n_{\mathcal{R}} + 1 \leq j \leq n_{\mathcal{R}} + n_{\mathcal{C}}. \end{aligned}$$

Due to the construction of the sets above, we get the following structure for  $\bar{A}_{\mathcal{R}}$  and  $\bar{A}_{\mathcal{C}}$ :

$$(\bar{A}_{\mathcal{R}} \quad \bar{A}_{\mathcal{C}}) = \begin{pmatrix} \bar{A}_{\mathcal{R}}^{\mathcal{P}} & \bar{A}_{\mathcal{C}}^{\mathcal{P}} \\ I_{\mathcal{R}} & 0 \\ 0 & I_{\mathcal{C}} \end{pmatrix} \quad I_{\mathcal{R}} \in \mathbb{R}^{n_{\mathcal{R}} \times n_{\mathcal{R}}}, I_{\mathcal{C}} \in \mathbb{R}^{n_{\mathcal{C}} \times n_{\mathcal{C}}}.$$

Hence,

$$(\bar{A}_r \quad \bar{A}_{\mathcal{R}} \quad \bar{A}_{\mathcal{C}}) = \begin{pmatrix} \bar{A}_r^{\mathcal{P}} & \bar{A}_{\mathcal{A}}^{\mathcal{P}} \\ 0 & I \end{pmatrix} \quad \text{with} \quad \bar{A}_{\mathcal{A}}^{\mathcal{P}} = (\bar{A}_{\mathcal{R}}^{\mathcal{P}} \quad \bar{A}_{\mathcal{C}}^{\mathcal{P}}) \quad (4.35)$$

is non-singular.  $\square$

We now want to prove Theorem 4.17.

*Proof.* We choose the associated basis functions  $V$  and  $W$  of the matrix  $A$  as in Lemma 4.19. After multiplying the DAE (4.31) from the left with  $(V^\top \quad W^\top)$ , we end up with

$$\begin{aligned} \frac{d}{dt} d(u_1) &= -V^\top b(u_1, u_2, t) \\ 0 &= W^\top b(u_1, u_2, t) \end{aligned}$$

where  $u_1 = (p_{\mathcal{P}} \quad q_l)^\top$  and  $u_2 = (p_p \quad p_{\mathcal{A}} \quad q_r \quad q_{\mathcal{A}} \quad y)^\top$  and  $d(u_1) = \left( \frac{p_{\mathcal{P}}}{z(p_{\mathcal{P}})} \quad q_l \right)^\top$ . Due to Lemma 4.4 and [LMT13, Chapter 3], it suffices to show that the Jacobian of  $W^\top b(u_1, u_2, t)$

w.r.t.  $u_2$  and the Jacobian of  $d(u_1)$  are non-singular. The former is given by

$$\partial_{u_2} W^\top b(u_1, u_2, t) = \begin{pmatrix} D_p^\mathcal{R} + \partial_{p_p} G_\mathcal{R} & D_A^\mathcal{R} & 0 & \partial_{q_\mathcal{R}} G_\mathcal{R} & 0 & 0 \\ \partial_{p_p} G_\mathcal{C} & \partial_{p_A} G_\mathcal{C} & 0 & 0 & \partial_{q_\mathcal{C}} G_\mathcal{C} & \partial_{y_\mathcal{C}} G_\mathcal{C} \\ 0 & 0 & \bar{A}_r & \bar{A}_\mathcal{R} & \bar{A}_\mathcal{C} & 0 \\ I & 0 & 0 & 0 & 0 & 0 \end{pmatrix} \quad (4.36)$$

Let  $w = (w_p \ w_\mathcal{A} \ w_r \ w_\mathcal{R} \ w_\mathcal{C} \ w_y)^\top \in \ker(\partial_{u_2} W^\top b(u_1, u_2, t))$ . It follows directly from the structure of the matrix that  $w_p = 0$ . From Lemma 4.21 we derive that  $w_r, w_\mathcal{R}, w_\mathcal{C} = 0$ . The properties of the compressor equations given by Theorem 2.6 yield  $w_y = 0$ .

From Corollary 4.16 it follows that

$$\begin{pmatrix} D_A^\mathcal{R} \\ \partial_{p_A} G_\mathcal{C} \end{pmatrix} = \begin{pmatrix} -I_\mathcal{R} & & & \\ & \beta_1 & & \\ & & \ddots & \\ & & & \beta_{n_\mathcal{C}} \end{pmatrix} \quad \beta_j = \begin{pmatrix} -\frac{R_s T_m z(p_u)}{p_u^{\frac{\kappa-1}{\kappa}}} p_{u_{n_\mathcal{R}+j}}^{\frac{-1}{\kappa}} \\ 0 \\ 0 \\ 0 \\ 1 \end{pmatrix} \in \mathbb{R}^{5 \times 1}.$$

and hence  $w_\mathcal{A} = 0$ . The Jacobian of  $d(u_1)$  is given by

$$\frac{d}{du_1} d(u_1) = \begin{pmatrix} Z(p) & 0 \\ 0 & I \end{pmatrix},$$

with  $Z(p)$  being a diagonal matrix which is defined as

$$Z(p) = \text{diag} \left( \frac{z(p_{\mathcal{P},1}) - p_{\mathcal{P},1} z'(p_{\mathcal{P},1})}{z(p_{\mathcal{P},1})^2} \quad \dots \quad \frac{z(p_{\mathcal{P},m_\mathcal{P}}) - p_{\mathcal{P},m_\mathcal{P}} z'(p_{\mathcal{P},m_\mathcal{P}})}{z(p_{\mathcal{P},m_\mathcal{P}})^2} \right). \quad (4.37)$$

Due to Remark 2.1, we know that  $z$  is continuously differentiable and

$$z(p) - z'(p)p = \begin{cases} \frac{c^2}{R_s T_m} & z \text{ constant} \\ 1 & \text{AGA} \\ 1 - \beta_2 p^2 & \text{Papay} \end{cases}$$

with constant  $\beta_2$  as stated in Remark 2.2. Since  $\beta_2$  is roughly of the order  $\mathcal{O}(10^{-6})$ , the term  $z(p) - z'(p)p \neq 0$ , for values of  $p$  as they normally appear in gas networks ( $\approx \mathcal{O}(10^6)$ ). This completes the proof.  $\square$

### 4.3 Decoupling process for DAEs

In this section, we demonstrate how we can use the results that we established in this chapter to reformulate the DAE (4.31) as an ODE with a decoupled system of algebraic equations. In addition, we show that the ODE system can be derived from the topology and element information directly.

We know from Lemma 4.21 that

$$\begin{pmatrix} q_r \\ q_{\mathcal{R}} \\ q_{\mathcal{C}} \end{pmatrix} = (\bar{A}_r \quad \bar{A}_{\mathcal{R}} \quad \bar{A}_{\mathcal{C}})^{-1} (\bar{q}^T - \bar{A}_l q_l).$$

By construction, the matrix  $(\bar{A}_r \quad \bar{A}_{\mathcal{R}} \quad \bar{A}_{\mathcal{C}})$  has a block-structure (see equation (4.35)), and hence its inverse is given by

$$(\bar{A}_r \quad \bar{A}_{\mathcal{R}} \quad \bar{A}_{\mathcal{C}})^{-1} = \begin{pmatrix} \bar{A}_r^{\mathcal{P}^{-1}} & -\bar{A}_r^{\mathcal{P}^{-1}} \bar{A}_{\mathcal{R}}^{\mathcal{P}} & -\bar{A}_r^{\mathcal{P}^{-1}} \bar{A}_{\mathcal{C}}^{\mathcal{P}} \\ 0 & I_{\mathcal{R}} & 0 \\ 0 & 0 & I_{\mathcal{C}} \end{pmatrix}$$

with

$$\bar{A}_r^{\mathcal{P}^{-1}} = \begin{pmatrix} A_r^{1^{-1}} & & 0 \\ & \ddots & \\ 0 & & A_r^{m_{\mathcal{P}}^{-1}} \end{pmatrix} \quad A_r^{j^{-1}} \in \mathbb{R}^{s_j \times s_j}. \quad (4.38)$$

The inverse of the blocks  $A_r^j$  (see equation (4.34)) is computed using the Schur complement method and is given by

$$A_r^{j^{-1}} = \frac{1}{1 + \alpha_{j_1} \sum_{i=j_2}^{j_m} \alpha_i^{-1}} \begin{pmatrix} 1 & \alpha_{j_2}^{-1} & \dots & \alpha_{j_m}^{-1} \\ \frac{\alpha_{j_1}}{\alpha_{j_2}} & & & \\ \vdots & & S_j & \\ \frac{\alpha_{j_1}}{\alpha_{j_m}} & & & \end{pmatrix}, \quad (4.39)$$

with  $j_1 = r_{j-1} + 1, \dots, j_m = r_j, m = s_j$ , and

$$S_j = (1 + \alpha_{j_1} \sum_{i=j_2}^{j_m} \alpha_i^{-1}) M_j + \alpha_{j_1} M_j \mathbf{1} \mathbf{1}^T M_j \in \mathbb{R}^{(s_j-1) \times (s_j-1)},$$

where  $M_j = \text{diag}(-\alpha_{j_2}^{-1} \quad \dots \quad -\alpha_{j_m}^{-1})$ .

**Remark 4.22.** In practice, the number of pipes that are connected to a node is rather small, what makes the computation of the inverse of  $\bar{A}_r^{\mathcal{P}}$  cheap, especially since the required matrix  $M_j$  can be built by just knowing the topology and pipe parameters.

This allows us to give explicit expressions for the mass flows  $q_r$ ,  $q_{\mathcal{R}}$  and  $q_{\mathcal{C}}$  that only depend on  $t$  and  $q_l$ :

$$q_r = h_r(q_l, t) = (\bar{A}_r^{\mathcal{P}^{-1}} \quad -\bar{A}_r^{\mathcal{P}^{-1}} \bar{A}_{\mathcal{R}}^{\mathcal{P}} \quad -\bar{A}_r^{\mathcal{P}^{-1}} \bar{A}_{\mathcal{C}}^{\mathcal{P}}) (\bar{q}^T - \bar{A}_l q_l) \quad (4.40a)$$

$$q_{\mathcal{R}} = h_{\mathcal{R}}(q_l, t) = (0 \quad I_{\mathcal{R}} \quad 0) (\bar{q}^T - \bar{A}_l q_l) \quad (4.40b)$$

$$q_{\mathcal{C}} = h_{\mathcal{C}}(q_l, t) = (0 \quad 0 \quad I_{\mathcal{C}}) (\bar{q}^T - \bar{A}_l q_l). \quad (4.40c)$$

**Theorem 4.23.** Let  $\mathcal{G} = (V, \mathcal{E})$  be the graph of a gas network consisting of pipes, resistors, compressors as well as sources and sinks, that fulfils Assumption 4.11 and is directed

according to Theorem 4.14. Then it is possible to reformulate the DAE (4.31) as an ODE

$$\mathbf{u}' = f(\mathbf{u}, t)$$

that can be solved independently of an algebraic system

$$\begin{aligned} \mathbf{v}_1 &= f_1(\mathbf{u}, t) \\ \mathbf{v}_2 &= f_2(\mathbf{u}, \mathbf{v}_1, t) \\ \mathbf{v}_3 &= f_3(\mathbf{v}_1, \mathbf{v}_2, t) \end{aligned}$$

*Proof.* We choose the associated basis functions  $V$  and  $W$  as in the proof of Theorem 4.17 and multiply the DAE (4.31) from the left with  $V^\top$  and  $W^\top$ . This leaves us with the differential system

$$\left( \frac{p_{\mathcal{P}}}{z(p_{\mathcal{P}})} \right)' = -\bar{D}_q(q_r - q_l) \quad (4.41a)$$

$$q_l' = -D_p^{\mathcal{P}} p_p - D_{\mathcal{P}}^{\mathcal{P}} p_{\mathcal{P}} - D_{\mathcal{A}}^{\mathcal{P}} p_{\mathcal{A}} - G_{\mathcal{P}}(p_{\mathcal{P}}, q_l) \quad (4.41b)$$

and the algebraic system

$$D_p^{\mathcal{R}} p_p + D_{\mathcal{P}}^{\mathcal{R}} p_{\mathcal{P}} + D_{\mathcal{A}}^{\mathcal{R}} p_{\mathcal{A}} + G_{\mathcal{R}}(p_p, p_{\mathcal{P}}, q_{\mathcal{R}}) = 0 \quad (4.42a)$$

$$G_{\mathcal{C}}(p_p, p_{\mathcal{A}}, p_{\mathcal{P}}, q_{\mathcal{C}}, y_{\mathcal{C}}, t) = 0 \quad (4.42b)$$

$$\bar{A}_r q_r + \bar{A}_l q_l + \bar{A}_{\mathcal{R}} q_{\mathcal{R}} + \bar{A}_{\mathcal{C}} q_{\mathcal{C}} = \bar{q}^\Gamma(t) \quad (4.42c)$$

We can use equations (4.40a) and (4.40b) to replace  $q_r$  and  $q_{\mathcal{R}}$  in equations (4.41a) and (4.42a), respectively. By making use of the boundary condition at the sources, we can replace  $p_p$  with the boundary data  $p^\Gamma$ . Note that  $G_{\mathcal{R}}$  in equation (4.42a) actually only depends on  $p_{\mathcal{P}}$ ,  $p_p$  and  $q_{\mathcal{R}}$ , due to the topology assumptions. Hence, we can reformulate  $G_{\mathcal{R}}$  as

$$\bar{G}_{\mathcal{R}}(p_{\mathcal{P}}, q_l, t) = G_{\mathcal{R}}(p^\Gamma(t), p_{\mathcal{P}}, h_{\mathcal{R}}(q_l, t))$$

by replacing the  $p_p$  variables with the boundary data. We now use the resistor and compressor equations to substitute  $p_{\mathcal{A}}$  as follows. The resistor equations give us an explicit expression for the first  $n_{\mathcal{R}}$  entries in  $p_{\mathcal{A}}$  in terms of  $q_l$ ,  $p_{\mathcal{P}}$  and  $t$ :

$$D_{\mathcal{A}}^{\mathcal{R}} p_{\mathcal{A}} = -D_p^{\mathcal{R}} p^\Gamma - \bar{G}_{\mathcal{R}}(p_{\mathcal{P}}, q_l, t) - D_{\mathcal{P}}^{\mathcal{R}} p_{\mathcal{P}} \quad D_{\mathcal{A}}^{\mathcal{R}} = \begin{pmatrix} -I_{\mathcal{R}} & 0 \end{pmatrix}. \quad (4.43)$$

Similar as for the boundary pressures  $p_p$ , we can replace the last  $n_{\mathcal{C}}$  components of  $p_{\mathcal{A}}$  by the control functions of the compressors (see equation (2.15e) or (2.16e)). This enables us to give the following explicit expression for  $p_{\mathcal{A}}$ :

$$p_{\mathcal{A}} = -D_{\mathcal{A}}^{\mathcal{R}\top} [D_{\mathcal{P}}^{\mathcal{R}} p_{\mathcal{P}} + \bar{G}_{\mathcal{R}}(p_{\mathcal{P}}, q_l, t) + D_p^{\mathcal{R}} p^\Gamma(t)] + D_{\mathcal{A}}^{\mathcal{C}\top} [S_{\mathcal{C}}(t)(p_{\mathcal{C}}^c(t) - D_{\mathcal{P}}^{\mathcal{C}} p_{\mathcal{P}}) + D_{\mathcal{P}}^{\mathcal{C}} p_{\mathcal{P}}]$$

with  $D_{\mathcal{A}}^{\mathcal{C}} = \begin{pmatrix} 0 & I_{\mathcal{C}} \end{pmatrix} \in \mathbb{R}^{n_{\mathcal{C}} \times m_{\mathcal{A}}}$  and

$$S_{\mathcal{C}} \in \mathcal{C}(\mathcal{I}, \mathbb{R}^{n_{\mathcal{C}} \times n_{\mathcal{C}}}) \quad S_{\mathcal{C}}(t) = \text{diag} \left( s_{e_1^{\mathcal{C}}}(t) \quad \dots \quad s_{e_{n_{\mathcal{C}}}^{\mathcal{C}}}(t) \right).$$

Substituting the expression for  $p_{\mathcal{A}}$  above into equation (4.41b) yields the following ODE

$$\left( \frac{p_{\mathcal{P}}}{z(p_{\mathcal{P}})} \right)' = B_q q_l + r_q(t) \quad (4.44a)$$

$$q_l' = B_p p_{\mathcal{P}}(t) + G_l(p_{\mathcal{P}}, q_l, t) + r_p(t). \quad (4.44b)$$

The matrices are given by

$$\begin{aligned} B_q &= \bar{D}_q [(\bar{A}_r^{\mathcal{P}-1} - \bar{A}_r^{\mathcal{P}-1} \hat{A}_{\mathcal{A}}^{\mathcal{P}}) \bar{A}_l + I] \\ B_p(t) &= D_{\mathcal{A}}^{\mathcal{P}} \left[ D_{\mathcal{A}}^{\mathcal{R}\top} D_{\mathcal{P}}^{\mathcal{R}} - D_{\mathcal{A}}^{\mathcal{C}\top} (I_{\mathcal{C}} - S_{\mathcal{C}}(t)) D_{\mathcal{P}}^{\mathcal{C}} \right] - D_{\mathcal{P}}^{\mathcal{P}}, \end{aligned}$$

the non-linear part by

$$G_l(p_{\mathcal{P}}, q_l, t) = -G_{\mathcal{P}}(p_{\mathcal{P}}, q_l) - D_{\mathcal{A}}^{\mathcal{R}} D_{\mathcal{A}}^{\mathcal{R}\top} \bar{G}_{\mathcal{R}}(p_{\mathcal{P}}, q_l, t)$$

and

$$\begin{aligned} r_q(t) &= -\bar{D}_q (\bar{A}_r^{\mathcal{P}-1} - \bar{A}_r^{\mathcal{P}-1} \bar{A}_{\mathcal{A}}^{\mathcal{P}}) \bar{q}^{\Gamma}(t) \\ r_p(t) &= \left( D_{\mathcal{A}}^{\mathcal{P}} D_{\mathcal{A}}^{\mathcal{R}\top} D_{\mathcal{P}}^{\mathcal{R}} - D_{\mathcal{P}}^{\mathcal{P}} \right) p^{\Gamma}(t) - D_{\mathcal{A}}^{\mathcal{P}} D_{\mathcal{A}}^{\mathcal{C}\top} S_{\mathcal{C}}(t) p_{\mathcal{C}}^{\mathcal{C}}(t). \end{aligned}$$

The remaining algebraic system is

$$q_r = h_r(q_l, t) \quad q_{\mathcal{R}} = h_{\mathcal{R}}(q_l, t) \quad q_{\mathcal{C}} = h_{\mathcal{C}}(q_l, t) \quad (4.45)$$

with functions  $h_r$ ,  $h_{\mathcal{R}}$  and  $h_{\mathcal{C}}$  as stated in equation (4.40),

$$\begin{aligned} p_{\mathcal{A}} &= -D_{\mathcal{A}}^{\mathcal{R}\top} \left[ D_{\mathcal{P}}^{\mathcal{R}} p_{\mathcal{P}} + \bar{G}_{\mathcal{R}}(p_{\mathcal{P}}, q_l, t) + D_{\mathcal{P}}^{\mathcal{R}} p^{\Gamma}(t) \right] \\ &\quad + D_{\mathcal{A}}^{\mathcal{C}\top} \left[ S_{\mathcal{C}}(t) (p_{\mathcal{C}}^{\mathcal{C}}(t) - D_{\mathcal{P}}^{\mathcal{C}} p_{\mathcal{P}}) + D_{\mathcal{P}}^{\mathcal{C}} p_{\mathcal{P}} \right] \end{aligned} \quad (4.46)$$

as well as

$$H_{ec} = R_s T_m z(p_u) \frac{\kappa}{\kappa - 1} \left[ \left( \frac{p_{ec}^{\mathcal{C}}(t)}{p_u} \right)^{\frac{\kappa-1}{\kappa}} - 1 \right] \quad e^{\mathcal{C}} = (u, v) \in \mathcal{E}_{\mathcal{C}} \quad (4.47a)$$

$$Q_{ec} = R_s T_m z(p_u) \frac{q_{ec}}{p_u} \quad e^{\mathcal{C}} = (u, v) \in \mathcal{E}_{\mathcal{C}} \quad (4.47b)$$

$$n_{ec} = \Psi_{ec}(Q_{ec}, H_{ec}, t) \quad e^{\mathcal{C}} \in \mathcal{E}_{\mathcal{C}}^{\text{Tu}} \quad (4.47c)$$

$$n_{ec} = s_{ec}(t) \frac{Q_{ec} 60}{\bar{V}_{ec}} + (1 - s_{ec}(t)) n_{ec}^- \quad e^{\mathcal{C}} \in \mathcal{E}_{\mathcal{C}}^{\text{Pi}} \quad (4.47d)$$

$$M_{ec} = \frac{\bar{V}_{ec} H_{ec}}{2\pi \eta_{ec}} \frac{p_u}{R_s T_m z(p_u)} \quad e^{\mathcal{C}} \in \mathcal{E}_{\mathcal{C}}^{\text{Pi}} \quad (4.47e)$$

$$\eta_{ec} = s_{ec}(t) \Phi(Q_{ec}, n_{ec}; A_{ec}^{\eta}) \quad e^{\mathcal{C}} \in \mathcal{E}_{\mathcal{C}}^{\text{Tu}} \quad (4.47f)$$

for the compressor variables. The sets  $\mathcal{E}_{\mathcal{C}}^{\text{Tu}}, \mathcal{E}_{\mathcal{C}}^{\text{Pi}} \subseteq \mathcal{E}_{\mathcal{C}}$  in equations (4.47c) to (4.47f) represent the set of turbo- and piston compressors, respectively. The right-hand side of equation (4.47c) has been defined in Remark 2.7.

Since  $z$  is continuously differentiable w.r.t.  $p$  (see Remark 2.1), we can reformulate equa-

tion (4.44a) as

$$\begin{aligned} p'_{\mathcal{P}}(t) &= Z^{-1}(p_{\mathcal{P}}(t))(B_q q_l(t) + r_q(t)) \\ q'_l(t) &= B_p(t)p_{\mathcal{P}}(t) + G_l(p_{\mathcal{P}}(t), q_l(t), t) + r_p(t) \end{aligned}$$

with  $Z^{-1}(p)$  being the inverse of  $Z(p)$  in the proof of Theorem 4.17 (see equation (4.37)) given by

$$Z^{-1}(p_{\mathcal{P}}) = \text{diag} \left( \frac{z^2(p_{\mathcal{P},1})}{z(p_{\mathcal{P},1}) - z'_p(p_{\mathcal{P},1})p_{\mathcal{P},1}} \quad \cdots \quad \frac{z^2(p_{\mathcal{P},m_{\mathcal{P}}})}{z(p_{\mathcal{P},m_{\mathcal{P}}}) - z'_p(p_{\mathcal{P},m_{\mathcal{P}}})p_{\mathcal{P},m_{\mathcal{P}}}} \right). \quad (4.48)$$

Setting  $\mathbf{u} = (p_{\mathcal{P}} \ q_l)^\top$ ,  $\mathbf{v}_1 = (q_r \ q_{\mathcal{R}} \ q_c \ p_A \ H \ Q)^\top$ ,  $\mathbf{v}_2 = (n \ M)$  and  $\mathbf{v}_3 = \eta$  completes the proof. The specific functions to compute  $\mathbf{v}_1$  to  $\mathbf{v}_3$  are given by equations (4.45) to (4.47b) for  $f_1$ , equations (4.47c) to (4.47e) for  $f_2$  and equation (4.47f) for  $f_3$ .

Note that  $M$  only is part of  $\mathbf{v}_2$  if there is a piston compressor in the network and that  $\mathbf{v}_3$  only occurs if the network contains a turbo compressor.  $\square$

**Remark 4.24.** *In the case that  $z$  is constant, the diagonal entries in the matrix  $Z^{-1}(p)$  in equation (4.48) are all equal to  $\frac{c^2}{R_s T_m}$ .*

**Remark 4.25.** *Due to Remark 2.7, all algebraic variables can be computed explicitly.*

**Remark 4.26.** *By making use of the topology and the proposed discretisation of the pipe equations, the presented decoupling procedure reduces the solving of a non-linear DAE of dimension  $n_D = |V| + 2|\mathcal{E}_{\mathcal{P}}| + |\mathcal{E}_{\mathcal{A}}| + 4|\mathcal{E}_{\mathcal{C}}|$  to solving an ODE of dimension  $n_O = |V_{\mathcal{P}}| + |\mathcal{E}_{\mathcal{P}}|$ . The remaining algebraic variables can be computed directly, without solving a non-linear system.*

### 4.4 Extension to general networks

In this section we discuss possible extensions of the decoupling procedure to more general networks. This includes an extension in the sense of weakening the requirements on the network topology in Assumption 4.11 as well as an extension to networks that contain additional elements like valves. We start with discussing the impact of allowing active elements to be coupled with each other.

**Paths of active elements** Let us first allow paths (see Definition A.3) of active elements that fulfil the following assumptions.

**Assumption 4.27.** *Let  $\mathcal{T}_{\mathcal{A}} = (V_{\mathcal{T}}, \mathcal{E}_{\mathcal{T}})$  with  $\mathcal{E}_{\mathcal{T}} \subseteq \mathcal{E}_{\mathcal{A}}$  be a directed subgraph of active elements in  $\mathcal{G} = (V, \mathcal{E})$  with root  $u_r$  and leaf  $u_\ell$ , so that*

1.  $\delta^+(u_r) \cap \mathcal{E}_{\mathcal{T}} = \emptyset$ ,
2.  $|\delta^+(u) \cap \mathcal{E}_{\mathcal{T}}| = 1$  for  $u \in V_{\mathcal{T}} \setminus \{u_r\}$ ,
3.  $(\delta^+(u) \cup \delta^-(u)) \cap (\mathcal{E} \setminus \mathcal{E}_{\mathcal{T}}) = \emptyset, \forall u \in V_{\mathcal{T}} \setminus \{u_r, u_\ell\}$ ,

4.  $q_u^\Gamma \equiv 0$  for  $u \in V_{\mathcal{T}} \setminus \{u_r, u_\ell\}$ .

**Remark 4.28.** The first two assumptions guarantee that  $\mathcal{T}_{\mathcal{A}}$  is a directed path. The third assumption states that the subgraph is only connected to the remaining network at the root and the leaf. The last assumption prohibits a demand at nodes  $u \in V_{\mathcal{T}} \setminus \{u_r, u_\ell\}$ .

**Example 4.29.** Figure 4.3 shows a path of active elements, in this case two resistors in front of and behind a compressor. As mentioned in Section 2.2.3, this coupling of resistors and a compressor is used to model internal piping, preheater and cooler.

$$\begin{aligned} V_{\mathcal{P}} &= \{u\} & V_{\mathcal{P}} &= \{v_1, v_2\} & V_{\mathcal{A}} &= \{v_3, v_4, v_5\} \\ \mathcal{E}_{\mathcal{P}} &= \{e_1^{\mathcal{P}}, e_2^{\mathcal{P}}\} & \mathcal{E}_{\mathcal{R}} &= \{e_1^{\mathcal{R}}, e_2^{\mathcal{R}}\} & \mathcal{E}_{\mathcal{C}} &= \{e^{\mathcal{C}}\} \\ V_{\mathcal{T}} &= \{v_2, \dots, v_5\} & \mathcal{E}_{\mathcal{T}} &= \{e_1^{\mathcal{R}}, e_2^{\mathcal{R}}, e^{\mathcal{C}}\}. \end{aligned}$$

The root of the active path is  $u_r = v_2$  and the leaf is  $u_\ell = v_3$ .

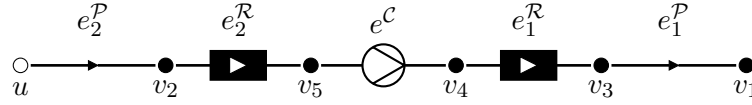


**Figure 4.3:** Diagram of a single compressor machine with resistors.

Due to the fourth assumption in Assumption 4.27, we can understand the active path as a single and more complex element  $e_{\mathcal{A}} = (v_2, v_3)$  with mass flow  $q_{\mathcal{A}}$ . The element equations for  $e_{\mathcal{A}}$  are then given by the system

$$p_{v_2} - p_{v_5} - s_{e_{\mathcal{A}}}(t)q_{e_2^{\mathcal{R}}}(p_{v_2}, q_{\mathcal{A}}) = 0 \quad (4.49a)$$

$$H_{e^c} - R_s T_m z(p_{v_3}) \frac{\kappa}{\kappa - 1} \left[ \left( \frac{p_{v_4}}{p_{v_5}} \right)^{\frac{\kappa-1}{\kappa}} - 1 \right] = 0 \quad (4.49b)$$

$$Q_{e^c} - R_s T_m z(p_{v_5}) \frac{q_{\mathcal{A}}}{p_{v_5}} = 0 \quad (4.49c)$$

$$H_{e^c} - s_{\mathcal{A}}(t)\Phi(Q_{e^c}, n_{e^c}; A_{e^c}^H) - (1 - s_{\mathcal{A}}(t))(n_{e^c} - n_{e^c}^-) = 0 \quad (4.49d)$$

$$\eta_{e^c} - s_{\mathcal{A}}(t)\Phi(Q_{e^c}, n_{e^c}; A_{e^c}^\eta) = 0 \quad (4.49e)$$

$$s_{\mathcal{A}}(t)(p_{v_4} - p^c) + (1 - s_{\mathcal{A}}(t))(p_{v_4} - p_{v_5}) = 0 \quad (4.49f)$$

$$p_{v_4} - p_{v_3} - s_{\mathcal{A}}(t)q_{e_1^{\mathcal{R}}}(p_{v_4}, q_{\mathcal{A}}) = 0. \quad (4.49g)$$

Note that we have integrated a bypass mode for the whole element  $e_{\mathcal{A}}$  as depicted in Figure 2.2. The DAE for the network depicted in Figure 4.3 is defined by system (4.49) and

$$p'_{\mathcal{P}} + \begin{pmatrix} \frac{c^2}{a_1 \ell_1} & 0 \\ 0 & \frac{c^2}{a_2 \ell_2} \end{pmatrix} (q_r - q_l) = 0 \quad (4.50a)$$

$$q'_l + \begin{pmatrix} \frac{a_1}{\ell_1} & 0 \\ 0 & \frac{a_2}{\ell_2} \end{pmatrix} p_{\mathcal{P}} + \begin{pmatrix} -\frac{a_1}{\ell_1} & 0 & 0 \\ 0 & 0 & 0 \end{pmatrix} p_{\mathcal{A}} + \begin{pmatrix} 0 \\ -\frac{a_2}{\ell_2} \end{pmatrix} p_p + G_{\mathcal{P}}(p_{\mathcal{P}}, q_l) = 0 \quad (4.50b)$$

$$\begin{pmatrix} 1 & 0 \\ 0 & 1 \\ 0 & 0 \end{pmatrix} q_r + \begin{pmatrix} 0 & 0 \\ 0 & 0 \\ -1 & 0 \end{pmatrix} q_l + \begin{pmatrix} 0 \\ -1 \\ 1 \end{pmatrix} q_{\mathcal{A}} = \begin{pmatrix} q_{v_1}^{\Gamma} \\ q_{v_2}^{\Gamma} \\ q_{v_3}^{\Gamma} \end{pmatrix} \quad (4.50c)$$

$$p_p = p_u^{\Gamma}. \quad (4.50d)$$

The respective pressure variables are

$$p_{\mathcal{P}} = (p_{v_1} \quad p_{v_2})^{\top} \quad p_{\mathcal{A}} = (p_{v_3} \quad p_{v_4} \quad p_{v_5})^{\top} \quad p_p = p_u.$$

For the decoupling, one only has to substitute parts of  $p_{\mathcal{A}}$  in equation (4.50b), namely the pressure at the leaf  $p_{v_3}$ , and  $q_r$  in equation (4.50a), both in terms of  $p_{\mathcal{P}}$ ,  $q_l$  and  $t$ . From the flow balance equation (4.50c) we derive an expression for

$$q_r = \begin{pmatrix} 1 & 0 & 0 \\ 0 & 1 & 1 \end{pmatrix} q^{\Gamma} + \begin{pmatrix} 0 & 0 \\ 1 & 0 \end{pmatrix} q_l \quad q_{\mathcal{A}} = (0 \quad 0 \quad 1) q^{\Gamma} + (1 \quad 0) q_l. \quad (4.51)$$

By substituting equation (4.49f) into (4.49g), we get the expression

$$p_{v_3} = s_{\mathcal{A}}(t)p^c + (1 - s_{\mathcal{A}}(t))p_{v_5} - s_{\mathcal{A}}(t)g_{e_1^{\mathcal{R}}}(s_{\mathcal{A}}(t)p^c + (1 - s_{\mathcal{A}}(t))p_{v_5}, q_{\mathcal{A}}) \quad (4.52)$$

where  $p_{v_5}$  can be replaced by

$$p_{v_5} = p_{v_2} - s_{e_{\mathcal{A}}}(t)g_{e_2^{\mathcal{R}}}(p_{v_2}, q_{e_{\mathcal{A}}}). \quad (4.53)$$

This yields an explicit expression for  $p_{v_3}$  in terms of  $p_{\mathcal{P}}$ ,  $q_l$  and  $t$ . By making use of equations (4.51) to (4.53), we can derive the ODE

$$p'_{\mathcal{P}} = \begin{pmatrix} \frac{c^2}{a_1 \ell_1} & 0 \\ -\frac{c^2}{a_2 \ell_2} & \frac{c^2}{a_2 \ell_2} \end{pmatrix} q_l + r_q$$

$$q'_l = \begin{pmatrix} -\frac{a_1}{\ell_1} & \frac{(1-s_{\mathcal{A}}(t))a_1}{\ell_1} \\ 0 & -\frac{a_2}{\ell_2} \end{pmatrix} p_{\mathcal{P}} + G_l(p_{\mathcal{P}}, q_l, t) + r_p$$

with

$$r_q = \begin{pmatrix} -\frac{c^2}{a_1 \ell_1} & 0 & 0 \\ 0 & -\frac{c^2}{a_2 \ell_2} & -\frac{c^2}{a_2 \ell_2} \end{pmatrix} q^{\Gamma} \quad r_p = \begin{pmatrix} 0 & \frac{a_1 s_{\mathcal{A}}(t)}{\ell_1} \\ \frac{a_2}{\ell_2} & 0 \end{pmatrix} \begin{pmatrix} p_u^{\Gamma} \\ p^c \end{pmatrix}.$$

The non-linear function  $G_l$  is a composition of  $G_{\mathcal{P}}$  and the non-linear part of equations (4.52) and (4.53)

$$G_l(p_{\mathcal{P}}, q_l, t) = \begin{pmatrix} -\frac{a_1 s_{\mathcal{A}}(t)}{\ell_1} \\ 0 \end{pmatrix} \left( g_{e_1^{\mathcal{R}}}(s_{\mathcal{A}}(t)p^c + (1 - s_{\mathcal{A}}(t))p_{v_5}, q_{\mathcal{A}}) + (1 - s_{\mathcal{A}}(t))g_{e_2^{\mathcal{R}}}(p_{v_2}, q_{\mathcal{A}}) \right) - G_{\mathcal{P}}(p_{\mathcal{P}}, q_l),$$



where  $p_{v_5}$  and  $q_A$  need to be substituted by the expressions in equations (4.53) and (4.51). The decoupled algebraic part is given by equation (4.49) and equation (4.51).

**Remark 4.30.** By considering coupled active elements that fulfil Assumption 4.27 as a single, more complex active element, results in more non-linearity in the ODE due to the coupling of elements that are modelled by non-linear equations. However, the analysis of the DAE discussed in Section 4.2 does not need to be adapted.

The next part addresses the coupling of active elements in a more general form, when they appear as a subgraph in the gas network and may be connected to the graph at more than two nodes.

**Subgraphs of active elements** In contrast to paths, we allow subgraphs to possess a tree-structure. In addition, they may be connected to the remaining gas network graph at all their nodes and not only at the root and leaf.

**Assumption 4.31** (Subgraphs of active elements). Let  $\mathcal{T}_A = (V_{\mathcal{T}}, \mathcal{E}_{\mathcal{T}})$  be a subgraph of  $\mathcal{G} = (V, \mathcal{E})$ , containing only active elements, hence  $\mathcal{E}_{\mathcal{T}} \subseteq \mathcal{E}_A$ , with root  $u_r$  so that

1.  $\delta^+(u_r) \cap \mathcal{E}_{\mathcal{T}} = \emptyset$ .
2.  $|\delta^+(u) \cap \mathcal{E}_{\mathcal{T}}| = 1$  for  $u \in V_{\mathcal{T}} \setminus \{u_r\}$ .

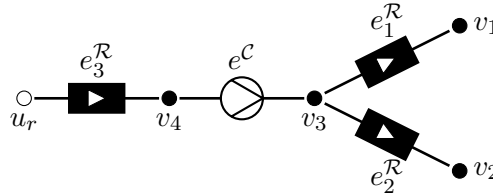


**Figure 4.4:** Example of an active subgraph that fulfils Assumptions 4.32.

**Assumption 4.32** (Graphs with subgraphs of active elements). Let  $\mathcal{G} = (V, \mathcal{E})$  consist of sources and sinks as well as pipes, resistors and compressors, so that

1.  $\nexists e^P = (u, v) \in \mathcal{E}_P$  with  $u, v \in V_p \cup V_A$ .
2. Each connected component of  $\mathcal{G}_P = (V, \mathcal{E}_P)$  contains at least one node  $u \in V_p \cup V_A$ .
3.  $|\delta^+(u) \cap \mathcal{E}_A| \leq 1 \quad \forall u \in V \quad \text{and} \quad \delta^+(u) \cap \mathcal{E}_A = \emptyset \quad \forall u \in V_p$ .
4. All subgraphs of  $\mathcal{G}$  of active elements fulfil Assumption 4.31.

**Corollary 4.33.** Let  $\mathcal{G} = (V, \mathcal{E})$  be an oriented graph of a gas network with  $V_p, V_q \neq \emptyset$  that contains pipes, resistors and compressors. Let  $\mathcal{G}$  fulfil Assumptions 4.32. Then the pipes in  $\mathcal{G}$  can be directed in a way that

- (i)  $\forall u \in V_p: \delta^+(u) = \emptyset$ .

$$(ii) \quad \forall u \in V_{\mathcal{P}}: \delta^+(u) \cap \mathcal{E}_{\mathcal{P}} \neq \emptyset.$$

$$(iii) \quad \forall u \in V_{\mathcal{A}}: \delta^+(u) \cap \mathcal{E}_{\mathcal{P}} = \emptyset.$$

*Proof.* The proof of Theorem 4.14 can be applied without restrictions. It only differs in so far that there might occur connected components in  $\mathcal{G}_{\mathcal{P}} = (V, \mathcal{E}_{\mathcal{P}})$  that only consist of one node  $u \in V_{\mathcal{A}}$ .  $\square$

We want to make the following convention for the numbering of nodes in  $V_{\mathcal{A}}$  and active elements in  $\mathcal{E}_{\mathcal{A}}$ :

**Remark 4.34.** Let  $\mathcal{G} = (V, \mathcal{E})$  be the graph of a gas network that fulfils Assumptions 4.32 and let  $\mathcal{G}$  contain  $k \in \mathbb{N}$  active subgraphs  $\mathcal{T}_i = (V_{\mathcal{T}_i}, \mathcal{E}_{\mathcal{T}_i})$ ,  $i = 1, \dots, k$ . We define numbers  $\bar{s}_i, \bar{r}_i \in \mathbb{N}$  for  $i = 1, \dots, k$  so that

$$\bar{s}_i = |\mathcal{E}_{\mathcal{T}_i}| \qquad \bar{r}_i = \sum_{j=1}^i \bar{s}_j.$$

Since the active subgraphs that we consider are in fact trees,  $\bar{s}_i$  is also the number of active nodes in  $V_{\mathcal{A}}$  that are contained in  $\mathcal{T}_i$ . We want to index the nodes in  $V_{\mathcal{A}}$  as follows: Let  $m_i$  be the number of leaves of  $\mathcal{T}_i$ . Then we denote the leaf nodes by  $u_{\bar{r}_{i-1}+1}^{\mathcal{A}}, \dots, u_{\bar{r}_{i-1}+m_i}^{\mathcal{A}}$ . The rest of the nodes are numbered backwards, so that  $u_{\bar{r}_i}^{\mathcal{A}}$  is one of the nodes that is directly connected to the root  $u_r$ . By a proper indexing of active elements in the active subgraphs, we get

$$\delta^+(u_i^{\mathcal{A}}) = \{e_i^{\mathcal{A}}\} \qquad i = 1, \dots, \bar{r}_k.$$

See Figure 4.4 for an example.

**Remark 4.35.** By allowing gas networks to contain subgraphs of active elements that fulfil Assumptions 4.32, the basic structure of the DAE is still given by

$$E \frac{d}{dt} d(u) + b(u, t) = 0 \tag{4.54}$$

with  $E$ ,  $d$  and  $b$  given as in equations (4.31) to (4.32c) stays the same. They only differ in the structure of the incidence matrices  $A_{\mathcal{R}}$ ,  $A_{\mathcal{C}}$  and the matrix  $D_{\mathcal{A}}^{\mathcal{R}}$ . Whereas all three matrices contained an identity block before (see equations (4.30) and (4.43)), this is no longer the case for active subgraphs.

**Example 4.36.** Let us consider the active subgraph in Figure 4.4. The incidence matrices  $A_{\mathcal{R}}$ ,  $A_{\mathcal{C}}$  and the matrix  $D_{\mathcal{A}}^{\mathcal{R}}$  are given by

$$A_{\mathcal{R}} = \begin{pmatrix} 0 & 0 & -1 \\ 1 & 0 & 0 \\ 0 & 1 & 0 \\ -1 & -1 & 0 \\ 0 & 0 & 1 \end{pmatrix} \qquad A_{\mathcal{C}} = \begin{pmatrix} 0 \\ 0 \\ 0 \\ 1 \\ -1 \end{pmatrix} \qquad D_{\mathcal{A}}^{\mathcal{R}} = \begin{pmatrix} -1 & 0 & 1 & 0 \\ 0 & -1 & 1 & 0 \\ 0 & 0 & 0 & 1 \end{pmatrix}.$$

Ordering the elements in  $\mathcal{E}_A$  according to Remark 4.34 yields  $q_A = \begin{pmatrix} q_{e_1^R} & q_{e_2^R} & q_{e^C} & q_{e_3^R} \end{pmatrix}^\top$  and we get the incidence matrix for the active elements by

$$A_A = \begin{pmatrix} 0 & 0 & 0 & -1 \\ 1 & 0 & 0 & 0 \\ 0 & 1 & 0 & 0 \\ -1 & -1 & 1 & 0 \\ 0 & 0 & -1 & 1 \end{pmatrix}. \quad (4.55)$$

Note that by neglecting the first row, which is incident to the root  $u_r$ , the remaining part of the matrix is a non-singular, lower triangular matrix.

**Theorem 4.37.** Let  $\mathcal{G} = (V, \mathcal{E})$  be the graph of a gas network that fulfils Assumptions 4.32 and let the pipes of  $\mathcal{G}$  be oriented as proposed in Corollary 4.33. Then the DAE (4.31) describing the gas network is of index 1.

**Remark 4.38.** The proof of this theorem follows the same ideas as the proof of Theorem 4.17. Let  $V, W$  be basis functions of the matrix  $E$  in equation (4.54) according to Lemma 4.19. By multiplying the DAE (4.54) with  $V^\top$  and  $W^\top$  from the left we derive

$$\begin{aligned} \frac{d}{dt}d(u_1) + V^\top b(u_1, u_2, t) &= 0 \\ W^\top b(u_1, u_2, t) &= 0. \end{aligned}$$

As in the proof of Theorem 4.17 it suffices to show that

$$\partial_{u_2} W^\top b(u_1, u_2, t) = \begin{pmatrix} D_p^R + \partial_{p_p} G_R & D_A^R & 0 & \partial_{q_A} G_R & 0 \\ \partial_{p_p} G_C & \partial_{p_A} G_C & 0 & \partial_{q_A} G_C & \partial_{y_C} G_C \\ 0 & 0 & \bar{A}_r & \bar{A}_A & 0 \\ I & 0 & 0 & 0 & 0 \end{pmatrix}$$

and that the Jacobian of  $d(u_1)$  are non-singular. The assertion regarding  $d(u_1)$  can be shown in the same way as in the proof of Theorem 4.17. Regarding the Jacobian of  $W^\top b(u_1, u_2, t)$ , it suffices to prove that  $(\bar{A}_r \quad \bar{A}_A)$  is non-singular and that

$$\ker \begin{pmatrix} D_A^R \\ \partial_{p_A} G_C \end{pmatrix} = \{0\},$$

due to Remark 4.35.

**Lemma 4.39.** Let  $\mathcal{G} = (V, \mathcal{E})$  with  $V_p, V_q \neq \emptyset$  fulfil Assumptions 4.32 and let the pipes in  $\mathcal{G}$  be directed according to Corollary 4.33. Then it holds, that the matrix  $(\bar{A}_r \quad \bar{A}_A) \in \mathbb{R}^{n_{\mathcal{E}} \times n_{\mathcal{E}}}$  is non-singular.

*Proof.* As in Section 4.2, the matrix  $(\bar{A}_r \quad \bar{A}_A)$  has a specific block-structure given by

$$(\bar{A}_r \quad \bar{A}_A) = \begin{pmatrix} \bar{A}_r^P & \bar{A}_A^P \\ 0 & \bar{A}_A^A \end{pmatrix}$$

with  $\bar{A}_r^P$  being the block-matrix given by equations (4.33) and (4.34). Hence,  $\bar{A}_r^P$  is non-singular and its inverse can be computed directly as in equations (4.38) and (4.39).

Furthermore, it holds that

$$\bar{A}_{\mathcal{A}}^{\mathcal{P}} \in \mathbb{R}^{n_{\mathcal{P}} \times n_{\mathcal{A}}} \quad (\bar{A}_{\mathcal{A}}^{\mathcal{P}})_{ij} = \begin{cases} -1 & e_j^{\mathcal{A}} \in \delta^-(u_i^{\mathcal{P}}) \\ 0 & \text{else} \end{cases}$$

and that  $A_{\mathcal{A}}^{\mathcal{A}}$  has the block-structure

$$A_{\mathcal{A}}^{\mathcal{A}} = \begin{pmatrix} A_{\mathcal{A}}^1 & & 0 \\ & \ddots & \\ 0 & & A_{\mathcal{A}}^k \end{pmatrix} \quad (4.56)$$

where  $A_{\mathcal{A}}^k$  is the incidence matrix for the active subgraph  $\mathcal{T}_k$  with the root node in  $V_{\mathcal{P}} \cup V_{\mathcal{P}}$  being neglected. By construction it is a lower triangular matrix with all entries on the diagonal being equal to 1. Hence, each of the blocks  $A_{\mathcal{A}}^k$  is non-singular and therefore  $A_{\mathcal{A}}^{\mathcal{A}}$  as well. This completes the proof.  $\square$

Next we prove Theorem 4.37.

*Proof.* Due to Remark 4.38 and Lemma 4.39 it remains to show that

$$\ker \begin{pmatrix} D_{\mathcal{A}}^{\mathcal{R}} \\ \partial_{p_{\mathcal{A}}} G_{\mathcal{C}} \end{pmatrix} = \{0\}.$$

As a consequence of Remark 4.34, we obtain

$$\begin{pmatrix} D_{\mathcal{A}}^{\mathcal{R}} \\ \partial_{p_{\mathcal{A}}} G_{\mathcal{C}} \end{pmatrix} = \begin{pmatrix} D_{\mathcal{A},1}^{\mathcal{R}} & & 0 \\ & \ddots & \\ 0 & & D_{\mathcal{A},k}^{\mathcal{R}} \\ (\partial_{p_{\mathcal{A}}} G_{\mathcal{C}})_1 & & 0 \\ & \ddots & \\ 0 & & (\partial_{p_{\mathcal{A}}} G_{\mathcal{C}})_k \end{pmatrix}, \quad \text{where} \quad \begin{pmatrix} D_{\mathcal{A},j}^{\mathcal{R}} \\ (\partial_{p_{\mathcal{A}}} G_{\mathcal{C}})_j \end{pmatrix}$$

corresponds to  $\mathcal{T}_j$ . Due to the specific numbering of the nodes in Remark 4.34, each of the blocks

$$\begin{pmatrix} D_{\mathcal{A},j}^{\mathcal{R}} \\ (\partial_{p_{\mathcal{A}}} G_{\mathcal{C}})_j \end{pmatrix}$$

can be transformed by permutation of its columns to a matrix with the following structure

$$\begin{pmatrix} -U_{\mathcal{A},j}^{\mathcal{R}} & * & \dots & * \\ 0 & \beta_1 & & 0 \\ & & \ddots & \\ & & & \beta_{n_{\mathcal{C},j}} \end{pmatrix} \quad \beta_i = \begin{pmatrix} -\frac{R_s T_m z(p_{v_i})}{p_{v_i}^{\frac{\kappa-1}{\kappa}}} p_{w_i}^{\frac{-1}{\kappa}} \\ 0 \\ 0 \\ 0 \\ 1 \end{pmatrix},$$

for  $e_i^{\mathcal{C}} = (v_i, w_i) \in \mathcal{E}_{\mathcal{T}_j}$  and  $n_{\mathcal{C},j}$  being the number of compressors in  $\mathcal{T}_j$ . Here,  $U_{\mathcal{A},j}^{\mathcal{R}}$  represents a quadratic, upper triangular matrix with all diagonal entries being equal to 1.

Since  $U_{\mathcal{A},j}^{\mathcal{R}}$  is a non-singular matrix and  $\beta_i$  has zero kernel, it follows that

$$\ker \left( \begin{matrix} D_{\mathcal{A}}^{\mathcal{R}} \\ \partial_{p_{\mathcal{A}}} G_C \end{matrix} \right) = \{0\}.$$

□

**Lemma 4.40.** *The inverse of  $A_{\mathcal{A}}^A$  (see equation (4.56)) can be computed explicitly by just using topology information.*

*Proof.* It suffices to prove the assertion for a block matrix  $A_{\mathcal{A}}^j$ ,  $j \in \{1, \dots, k\}$ , which is the incidence matrix for the active subgraph  $\mathcal{T}_j = (V_{\mathcal{T}_j}, \mathcal{E}_{\mathcal{T}_j})$  contained in a gas network  $\mathcal{G}$ , where the root node  $u_r$  of  $\mathcal{T}_j$  has been neglected.  $\forall v \in V_{\mathcal{T}_j}$ , let  $P(v) \setminus \{u_r\}$  be the path from the root to node  $v$ . The authors in [Jac<sup>+</sup>08, Chapter 4] show that the inverse of the incidence matrix of such a tree is given by

$$(A_{\mathcal{A}}^{j-1})_{i\ell} = \begin{cases} 1 & v_i \in V_{\mathcal{T}_j} \setminus \{u_r\} \text{ is in } (v_\ell) \text{ and } e_\ell \in \delta^+(u_i) \text{ for } e_\ell \in \mathcal{E}_{\mathcal{T}_1} \\ -1 & v_i \in V_{\mathcal{T}_j} \setminus \{u_r\} \text{ is in } P(v_\ell) \text{ and } e_\ell \in \delta^-(u_i) \text{ for } e_\ell \in \mathcal{E}_{\mathcal{T}_1} \\ 0 & v_i \in V_{\mathcal{T}_j} \setminus \{u_r\} \text{ is not in } P(v_\ell). \end{cases}$$

□

**Example 4.41** (Topological inverse of  $A_{\mathcal{A}}^A$ ). *Let us consider the submatrix  $A_{\mathcal{A}}^A$  of  $A_{\mathcal{A}}$  given by equation (4.55) with  $q_{\mathcal{A}} = \begin{pmatrix} q_{e_1^{\mathcal{R}}} & q_{e_2^{\mathcal{R}}} & q_{e^c} & q_{e_3^{\mathcal{R}}} \end{pmatrix}$ .  $A_{\mathcal{A}}^A$  and its inverse shall be given by*

$$A_{\mathcal{A}}^A = \begin{pmatrix} 1 & 0 & 0 & 0 \\ 0 & 1 & 0 & 0 \\ -1 & -1 & 1 & 0 \\ 0 & 0 & -1 & 1 \end{pmatrix} \quad A_{\mathcal{A}}^{A^{-1}} = \begin{pmatrix} 1 & 0 & 0 & 0 \\ 0 & 1 & 0 & 0 \\ 1 & 1 & 1 & 0 \\ 1 & 1 & 1 & 1 \end{pmatrix}.$$

*The inverse  $A_{\mathcal{A}}^{A^{-1}}$  is constructed in the following way: Since nodes  $v_1$  and  $v_2$  are only included in the paths that lead to themselves, whereas  $v_3$  is in the path to itself and the paths to  $v_1$  and  $v_2$ . Finally,  $v_4$  is contained in all paths.*

As in Section 4.3, we want to formulate a decoupling procedure for the DAE (4.54) which allows us to simulate gas networks that fulfil Assumptions 4.32 as an ODE of a lower dimension.

**Theorem 4.42.** *Let  $\mathcal{G} = (V, \mathcal{E})$  be the graph of a gas network consisting of pipes, resistors and compressors as well as sources and sinks. Furthermore, let  $\mathcal{G}$  fulfil Assumption 4.32 and let the pipes of  $\mathcal{G}$  be directed according to Corollary 4.33. Then it is possible to reformulate the DAE (4.31) as an ODE*

$$\mathbf{u}' = f(\mathbf{u}, t)$$

*that can be solved independent of an algebraic system*

$$g(\mathbf{u}, \mathbf{v}, t) = 0.$$

*Proof.* The proof follows the same ideas as the proof of Theorem 4.23, but needs a few more technicalities. After multiplying the DAE (4.54) from the left with the basis functions  $V^\top$  and  $W^\top$ , the transformed system consists of the differential part

$$\left(\frac{p_{\mathcal{P}}}{z(p_{\mathcal{P}})}\right)' = -\bar{D}_q(q_r - q_l) \quad (4.57a)$$

$$q_l' = -D_{\mathcal{P}}^{\mathcal{P}} p_{\mathcal{P}} - D_{\mathcal{A}}^{\mathcal{P}} p_{\mathcal{A}} - D_p^{\mathcal{P}} p_p + G_{\mathcal{P}}(p_{\mathcal{P}}, q_l) \quad (4.57b)$$

and the algebraic part

$$D_p^{\mathcal{R}} p_p + D_{\mathcal{P}}^{\mathcal{R}} p_{\mathcal{P}} + D_{\mathcal{A}}^{\mathcal{R}} p_{\mathcal{A}} + G_{\mathcal{R}}(p_p, p_{\mathcal{A}}, p_{\mathcal{P}}, q_{\mathcal{A}}) = 0 \quad (4.57c)$$

$$G_{\mathcal{C}}(p_p, p_{\mathcal{P}}, p_{\mathcal{A}}, q_{\mathcal{A}}, y_{\mathcal{C}}, t) = 0 \quad (4.57d)$$

$$\bar{A}_r q_r + \bar{A}_l q_l + \bar{A}_{\mathcal{A}} q_{\mathcal{A}} = \bar{q}^{\Gamma} \quad (4.57e)$$

$$p_p = p^{\Gamma}. \quad (4.57f)$$

By Lemmata 4.39 and 4.40, we derive

$$\begin{pmatrix} q_r \\ q_{\mathcal{A}} \end{pmatrix} = \begin{pmatrix} \bar{A}_r^{\mathcal{P}^{-1}} & -\bar{A}_r^{\mathcal{P}^{-1}} \bar{A}_{\mathcal{A}}^{\mathcal{P}} \\ 0 & \bar{A}_{\mathcal{A}}^{\mathcal{A}^{-1}} \end{pmatrix} (\bar{q}^{\Gamma} - \bar{A}_l q_l).$$

While we are able to substitute  $p_{\mathcal{A}}$  by an explicit expression in terms of  $p_{\mathcal{P}}$ ,  $q_r$  and  $t$  as in Section 4.3 (see equation (4.46)), this is no longer the case for active subgraphs due to the more complicated structure of  $D_{\mathcal{A}}^{\mathcal{R}}$ . Instead of an explicit expression, we derive

$$p_u - p_v = g_{e^{\mathcal{R}}}(p_u, q_{e^{\mathcal{R}}}) \quad (4.58)$$

for each resistor  $e^{\mathcal{R}} = (u, v) \in \mathcal{E}_{\mathcal{T}_j}$ , where  $u, v \in V_{\mathcal{T}_j}$  and  $v \neq u_r$ . For each compressor  $e^{\mathcal{C}} = (u, v) \in \mathcal{E}_{\mathcal{T}_i}$ , we can make use of the control equation and get

$$p_v = s_{e^{\mathcal{C}}}(t) p_{e^{\mathcal{C}}}^{\mathcal{C}} + (1 - s_{e^{\mathcal{C}}}(t)) p_u \quad (4.59)$$

with  $u, v \in V_{\mathcal{T}_j}$  and  $v \neq u_r$ . Combining equations (4.58) and (4.59), we derive

$$\begin{pmatrix} D_{\mathcal{A},j}^{\mathcal{R}} \\ \Sigma_{\mathcal{A},j}^{\mathcal{C}} \end{pmatrix} p_{\mathcal{A},j} = G_{\mathcal{A},j}(p_p, p_{\mathcal{P}}, p_{\mathcal{A}}, q_{\mathcal{A}}, t), \quad (4.60)$$

where  $G_{\mathcal{A},j}$  contains the right-hand sides of equations (4.58) and (4.59). The pressure  $p_{\mathcal{A},j}$  contains the pressure variables of the nodes in  $V_{\mathcal{T}_j} \setminus \{u_r\}$ . The matrix  $\Sigma_{\mathcal{A},j}^{\mathcal{C}}$  maps the pressures  $p_{\mathcal{A},j}$  to the pressures at the right side of the compressors that are contained in  $\mathcal{T}_j$ . Due to the specific numbering of the nodes and active elements in the active subgraph (see Remark 4.34), we can multiply equation (4.60) by a non-singular matrix  $T_j$  so that

$$U_{\mathcal{A},j} p_{\mathcal{A},j} = T_j \begin{pmatrix} D_{\mathcal{A},j}^{\mathcal{R}} \\ \Sigma_{\mathcal{A},j}^{\mathcal{C}} \end{pmatrix} p_{\mathcal{A},j} = T_j G_{\mathcal{A},j}(p_p, p_{\mathcal{P}}, p_{\mathcal{A}}, q_{\mathcal{A}}, t), \quad (4.61)$$

where  $U_{\mathcal{A},j}$  is an upper triangular matrix with non-zero entries on its diagonal. Even though  $p_{\mathcal{A}}$  appears on the right-hand side in  $G_{\mathcal{A},j}$ , the pressure at node  $v_i$  with  $i \in \bar{r}_{j-1} + 1, \dots, \bar{r}_j$  does only depend on pressures at nodes  $v_\ell$  with  $\ell < i$ . Hence, equation (4.61) can be solved bottom-to-top and therefore be replaced in the differential part.  $\square$

**Example 4.43.** To illustrate the decoupling process for networks with active subgraphs, we want to consider a graph that contains the active subgraph from Figure 4.4.

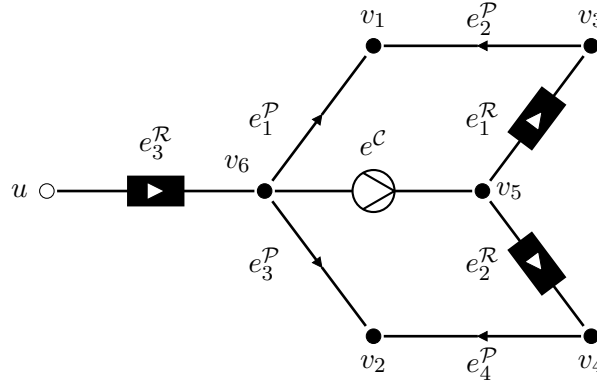


**Figure 4.5:** Network that contains an active subgraph.

The node sets for the network given by Figure 4.5 are

$$V_p = \{u\} \quad V_{\mathcal{P}} = \{v_1, v_2\} \quad V_{\mathcal{A}} = \{v_3, v_4, v_5, v_6\}.$$

For the sake of simplicity, we assume the gas factor to be constant,  $z \equiv \frac{c^2}{R_s T_m}$  and that  $q_u^\Gamma = 0$  for  $u \in V_q \setminus \{v_1, v_2\}$ . The respective variables are

$$p_{\mathcal{P}} = (p_{v_1} \quad p_{v_2})^\top \quad p_{\mathcal{A}} = (p_{v_3} \quad \dots \quad p_{v_6})^\top \quad p_p = p_u,$$

and the decoupled ODE is given by

$$p'_{\mathcal{P}}(t) = \begin{pmatrix} \frac{c^2}{a_1 \ell_1 + a_2 \ell_2} & \frac{c^2}{a_1 \ell_1 + a_2 \ell_2} & 0 & 0 \\ 0 & 0 & \frac{c^2}{a_3 \ell_3 + a_4 \ell_4} & \frac{c^2}{a_3 \ell_3 + a_4 \ell_4} \end{pmatrix} q_l + r_q(t)$$

$$q'_l(t) = \begin{pmatrix} -\frac{a_1}{\ell_1} & 0 \\ -\frac{a_2}{\ell_2} & 0 \\ 0 & -\frac{a_3}{\ell_3} \\ 0 & -\frac{a_4}{\ell_4} \end{pmatrix} p_{\mathcal{P}}(t) + G_l(p_{\mathcal{P}}, q_l, t) + r_p,$$

with

$$r_q = \begin{pmatrix} \frac{-c^2}{a_1 \ell_1 + a_2 \ell_2} & 0 \\ 0 & \frac{-c^2}{a_3 \ell_3 + a_4 \ell_4} \end{pmatrix} \begin{pmatrix} q_{v_2}^\Gamma \\ q_{v_4}^\Gamma \end{pmatrix} \quad r_p = \begin{pmatrix} \frac{a_1}{\ell_1} & 0 \\ \frac{(1-s_{e^C}(t))a_2}{\ell_2} & \frac{s_{e^C}(t)a_2}{\ell_2} \\ \frac{a_3}{\ell_3} & 0 \\ \frac{(1-s_{e^C}(t))a_4}{\ell_4} & \frac{s_{e^C}(t)a_4}{\ell_4} \end{pmatrix} \begin{pmatrix} p_u^\Gamma \\ p^c \end{pmatrix}.$$

The non-linear function  $G_l$  is stated as

$$G_l(p_{\mathcal{P}}, q_l, t) = \begin{pmatrix} 0 & 0 & -\frac{a_1}{\ell_1} \\ -\frac{a_2}{\ell_2} & 0 & -\frac{(1-s_{ec}(t))a_2}{\ell_2} \\ 0 & 0 & -\frac{a_3}{\ell_3} \\ 0 & -\frac{a_4}{\ell_4} & -\frac{(1-s_{ec}(t))a_4}{\ell_4} \end{pmatrix} \begin{pmatrix} g_{e_1^{\mathcal{R}}}(p_{v_5}, q_{e_1^{\mathcal{R}}}) \\ g_{e_2^{\mathcal{R}}}(p_{v_5}, q_{e_2^{\mathcal{R}}}) \\ g_{e_3^{\mathcal{R}}}(p_u^{\Gamma}, q_{e_3^{\mathcal{R}}}) \end{pmatrix} - G_{\mathcal{P}}(p_{\mathcal{P}}, q_l), \quad (4.62)$$

where  $p_{\mathcal{A}}$  and  $q_{\mathcal{A}}$  can be replaced in the following way by expressions only depending on  $p_{\mathcal{P}}$ ,  $q_l$  and  $t$ . The pressures at the nodes in  $V_{\mathcal{A}}$  are given by

$$p_{v_6} = p_u^{\Gamma} - g_{e_3^{\mathcal{R}}}(p_u^{\Gamma}, q_{e_3^{\mathcal{R}}}) \quad (4.63a)$$

$$p_{v_5} = s_{ec}(t)p^c(t) + (1 - s_{ec}(t)) \left( p_u^{\Gamma} - g_{e_3^{\mathcal{R}}}(p_u^{\Gamma}, q_{e_3^{\mathcal{R}}}) \right) \quad (4.63b)$$

$$p_{v_4} = s_{ec}(t)p^c(t) + (1 - s_{ec}(t))p_{v_6} - g_{e_2^{\mathcal{R}}}(p_{v_5}, q_{e_2^{\mathcal{R}}}) \quad (4.63c)$$

$$p_{v_3} = s_{ec}(t)p^c(t) + (1 - s_{ec}(t))p_{v_6} - g_{e_1^{\mathcal{R}}}(p_{v_5}, q_{e_1^{\mathcal{R}}}) \quad (4.63d)$$

and yield an explicit expression for  $p_{\mathcal{A}}$  by replacing  $p_{v_5}$  and  $p_{v_6}$  in equations (4.63c) and (4.63d) by equations (4.63a) and (4.63b) and the mass flow along the active elements by

$$q_{\mathcal{A}} = \begin{pmatrix} 0 & 1 & 0 & 0 \\ 0 & 0 & 0 & 1 \\ 0 & 1 & 0 & 1 \\ 1 & 1 & 1 & 1 \end{pmatrix} q_l. \quad (4.64)$$

The remaining algebraic system is given by equations (4.63) and (4.64) together with

$$q_r = \begin{pmatrix} \frac{a_1\ell_1}{a_1\ell_1+a_2\ell_2} & 0 \\ \frac{a_2\ell_2}{a_1\ell_1+a_2\ell_2} & 0 \\ 0 & \frac{a_3\ell_3}{a_3\ell_3+a_4\ell_4} \\ 0 & \frac{a_4\ell_4}{a_3\ell_3+a_4\ell_4} \end{pmatrix} \begin{pmatrix} q_{v_2}^{\Gamma} \\ q_{v_4}^{\Gamma} \end{pmatrix} - \begin{pmatrix} \frac{a_2\ell_2}{a_1\ell_1+a_2\ell_2} & \frac{-a_1\ell_1}{a_1\ell_1+a_2\ell_2} & 0 & 0 \\ \frac{-a_2\ell_2}{a_1\ell_1+a_2\ell_2} & \frac{a_1\ell_1}{a_1\ell_1+a_2\ell_2} & 0 & 0 \\ 0 & 0 & \frac{a_4\ell_4}{a_3\ell_3+a_4\ell_4} & \frac{-a_3\ell_3}{a_3\ell_3+a_4\ell_4} \\ 0 & 0 & \frac{-a_4\ell_4}{a_3\ell_3+a_4\ell_4} & \frac{a_3\ell_3}{a_3\ell_3+a_4\ell_4} \end{pmatrix} q_l$$

and

$$H_{ec} = c^2 \frac{\kappa}{\kappa - 1} \left[ \left( \frac{p^c}{p_{v_6}} \right)^{\frac{\kappa-1}{\kappa}} - 1 \right]$$

$$Q_{ec} = c^2 \frac{q_{ec}}{p_{v_6}}$$

$$n_{ec} = \Psi_{ec}(Q_{ec}, H_{ec}, t)$$

$$\eta_{ec} = s_{ec}(t)\Phi(Q_{ec}, n_{ec}; A_{ec}^{\eta}),$$

where  $\Psi_{ec}$  has been defined in Remark 2.7.

**Networks with valves** By considering valves in our networks, the analysis in this chapter becomes more complicated due to the fact that valves have two states: *open* and *closed*. This has a huge impact on the network topology and affects the DAE and ODE structure. It may also have an influence on the DAE index. We illustrate this in the following examples.

**Example 4.44.** Let us consider a small example network consisting of three pipes and a



valve  $e^S = (v_1, v_2)$  with node sets

$$V_p = \{u\} \quad V_q = \{v_1, v_2, v_3\}.$$

The network topology is shown in Figure 4.6 (middle), with the impact of the valve on the network topology on the left (valve open) and on the right (valve closed).

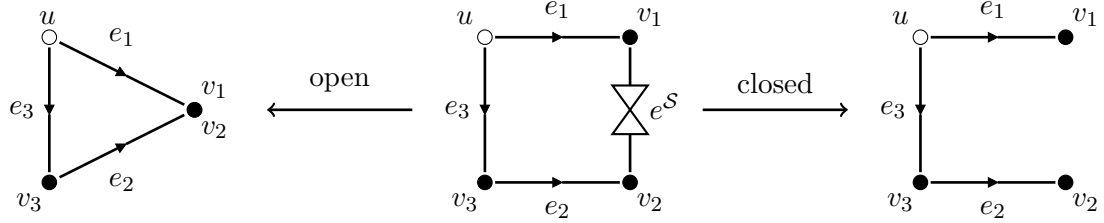


Figure 4.6: Impact of valves on the graph topology.

The DAE system for the network with a valve is given by

$$\begin{aligned} & \begin{pmatrix} \frac{p_{v_1}}{z(p_{v_1})} \\ \frac{p_{v_2}}{z(p_{v_2})} \\ \frac{p_{v_3}}{z(p_{v_3})} \end{pmatrix}' + \begin{pmatrix} \frac{R_s T_m}{a_1 \ell_1} & 0 & 0 \\ 0 & \frac{R_s T_m}{a_2 \ell_2} & 0 \\ 0 & 0 & \frac{R_s T_m}{a_3 \ell_3} \end{pmatrix} (q_r - q_l) = 0 \\ & q_l' + \begin{pmatrix} -\frac{a_1}{\ell_1} \\ 0 \\ -\frac{a_3}{\ell_3} \end{pmatrix} p_u + \begin{pmatrix} \frac{a_1}{\ell_1} & 0 & 0 \\ 0 & \frac{a_2}{\ell_2} & -\frac{a_2}{\ell_2} \\ 0 & 0 & \frac{a_3}{\ell_3} \end{pmatrix} \begin{pmatrix} p_{v_1} \\ p_{v_2} \\ p_{v_3} \end{pmatrix} + G_{\mathcal{P}}(p_q, q_l) = 0 \\ & \begin{pmatrix} 1 & 0 & 0 \\ 0 & 1 & 0 \\ 0 & 0 & 1 \end{pmatrix} q_r + \begin{pmatrix} 0 & 0 & 0 \\ 0 & 0 & 0 \\ 0 & -1 & 0 \end{pmatrix} q_l + \begin{pmatrix} -1 \\ 1 \\ 0 \end{pmatrix} q_S = \begin{pmatrix} q_{v_1}^F \\ q_{v_2}^F \\ q_{v_3}^F \end{pmatrix} \\ & s_{e^S}(t)(p_{v_1} - p_{v_2}) + (1 - s_{e^S}(t))q_S(t) = 0 \\ & p_u = p_u^F. \end{aligned}$$

If the valve is open, the decoupled ODE is stated as

$$\begin{aligned} & \begin{pmatrix} \frac{p_{v_1}}{z(p_{v_1})} \\ \frac{p_{v_3}}{z(p_{v_3})} \end{pmatrix}' = \begin{pmatrix} \frac{R_s T_m}{a_1 \ell_1 + a_2 \ell_2} & \frac{R_s T_m}{a_1 \ell_1 + a_2 \ell_2} & 0 \\ 0 & -\frac{R_s T_m}{a_3 \ell_3} & \frac{R_s T_m}{a_3 \ell_3} \end{pmatrix} q_l + r_q \\ & q_l' = \begin{pmatrix} -\frac{a_1}{\ell_1} & 0 \\ -\frac{a_2}{\ell_2} & \frac{a_2}{\ell_2} \\ 0 & -\frac{a_3}{\ell_3} \end{pmatrix} \begin{pmatrix} p_{v_1} \\ p_{v_3} \end{pmatrix} + G_{\mathcal{P}}(p_{v_1}, p_{v_2}, q_l) + r_p \end{aligned}$$

with decoupled algebraic equations

$$q_r = \begin{pmatrix} \frac{a_1 \ell_1}{a_1 \ell_1 + a_2 \ell_2} & \frac{a_1 \ell_1 a_2 \ell_2}{R_s T_m (a_1 \ell_1 + a_2 \ell_2)} & 0 \\ \frac{a_2 \ell_2}{a_1 \ell_1 + a_2 \ell_2} & -\frac{a_1 \ell_1 a_2 \ell_2}{R_s T_m (a_1 \ell_1 + a_2 \ell_2)} & 0 \\ 0 & 0 & 1 \end{pmatrix} \begin{pmatrix} q_{v_1}^F \\ 0 \\ q_{v_3}^F \end{pmatrix} - \begin{pmatrix} \frac{-a_2 \ell_2}{a_1 \ell_1 + a_2 \ell_2} & \frac{a_1 \ell_1}{a_1 \ell_1 + a_2 \ell_2} & 0 \\ \frac{a_2 \ell_2}{a_1 \ell_1 + a_2 \ell_2} & -\frac{a_1 \ell_1}{a_1 \ell_1 + a_2 \ell_2} & 0 \\ 0 & -1 & 0 \end{pmatrix} q_l.$$

The time-dependent functions  $r_q$  and  $r_p$  are given by

$$r_q = \begin{pmatrix} \frac{R_s T_m}{a_1 \ell_1 + a_2 \ell_2} & -\frac{a_2 \ell_2}{a_1 \ell_1 + a_2 \ell_2} & 0 \\ 0 & 0 & -\frac{R_s T_m}{a_3 \ell_3} \end{pmatrix} \begin{pmatrix} q_{v_1}^\Gamma + q_{v_2}^\Gamma \\ 0 \\ q_{v_3}^\Gamma \end{pmatrix} \quad r_p = \begin{pmatrix} \frac{a_1}{\ell_1} \\ 0 \\ \frac{a_3}{\ell_3} \end{pmatrix} p_u^\Gamma.$$

The mass flow along the valve  $q_S$  can be calculated by

$$q_S = q_{e_1, r} - q_{v_2}^\Gamma.$$

In the case that the valve is closed, the ODE is of dimension six instead of dimension five and is given by

$$\begin{pmatrix} \frac{p_{v_1}}{z(p_{v_1})} \\ \frac{p_{v_2}}{z(p_{v_2})} \\ \frac{p_{v_3}}{z(p_{v_3})} \end{pmatrix}' = \begin{pmatrix} \frac{R_s T_m}{a_1 \ell_1} & 0 & 0 \\ 0 & \frac{R_s T_m}{a_2 \ell_2} & 0 \\ 0 & -\frac{R_s T_m}{a_3 \ell_3} & \frac{R_s T_m}{a_3 \ell_3} \end{pmatrix} q_l + r_q$$

$$q_l' = \begin{pmatrix} -\frac{a_1}{\ell_1} & 0 & 0 \\ 0 & -\frac{a_2}{\ell_2} & \frac{a_2}{\ell_2} \\ 0 & 0 & -\frac{a_3}{\ell_3} \end{pmatrix} \begin{pmatrix} p_{v_1} \\ p_{v_2} \\ p_{v_3} \end{pmatrix} + G_P(p_{v_1}, p_{v_2}, p_{v_3}, q_l) + r_p$$

with decoupled algebraic system

$$q_r = q^\Gamma - \begin{pmatrix} \frac{-a_2 \ell_2}{a_1 \ell_1 + a_2 \ell_2} & \frac{a_1 \ell_1}{a_1 \ell_1 + a_2 \ell_2} & 0 \\ \frac{a_2 \ell_2}{a_1 \ell_1 + a_2 \ell_2} & \frac{-a_1 \ell_1}{a_1 \ell_1 + a_2 \ell_2} & 0 \\ 0 & -1 & 0 \end{pmatrix} q_l.$$

and time-dependent functions

$$r_q = \begin{pmatrix} -\frac{R_s T_m}{a_1 \ell_1} & 0 & 0 \\ 0 & -\frac{R_s T_m}{a_2 \ell_2} & 0 \\ 0 & 0 & -\frac{R_s T_m}{a_3 \ell_3} \end{pmatrix} q^\Gamma \quad r_p = \begin{pmatrix} \frac{a_1}{\ell_1} \\ 0 \\ \frac{a_3}{\ell_3} \end{pmatrix} p_u^\Gamma.$$

The mass flow along the valve is given by  $q_S = 0$ , since the valve is closed.

**Example 4.45.** To demonstrate the impact of valves on the DAE index, we want to consider the network given by Figure 4.7 with node sets

$$V_p = \{u\} \quad V_q = \{v_1, v_2, v_3\}$$

and valve  $e^S = (v_1, v_2)$ .

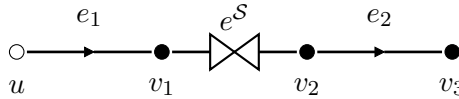


**Figure 4.7:** Impact of valves on the DAE index.

The DAE for the gas network in Figure 4.7 is

$$p'_{v_1} + \frac{c^2}{a_1 \ell_1} (q_{e_1,r} - q_{e_1,l}) = 0 \quad (4.65a)$$

$$p'_{v_3} + \frac{c^2}{a_2 \ell_2} (q_{e_2,r} - q_{e_2,l}) = 0 \quad (4.65b)$$

$$q'_{e_1,l} + \frac{a_1}{\ell_1} (p_{v_1} - p_u) = -g_{e_1}(p_{v_1}, q_{e_1,l}) \quad (4.65c)$$

$$q'_{e_2,l} + \frac{a_2}{\ell_2} (p_{v_3} - p_{v_2}) = -g_{e_2}(p_{v_3}, q_{e_2,l}) \quad (4.65d)$$

$$s_{eS}(t)(p_{v_1} - p_{v_2}) + (1 - s_{eS}(t))q_S = 0 \quad (4.65e)$$

$$q_{e_1,r} - q_S = q_{v_1}^\Gamma \quad (4.65f)$$

$$q_S - q_{e_2,l} = q_{v_2}^\Gamma \quad (4.65g)$$

$$q_{e_2,r} = q_{v_3}^\Gamma \quad (4.65h)$$

$$p_u = p_u^\Gamma. \quad (4.65i)$$

For  $s_{eS}(t) = 1$ , the system above has to be differentiated once, to extract the underlying ODE given by equations (4.65a) to (4.65d) and

$$\begin{aligned} p'_{v_2} &= -\frac{c^2}{a_2 \ell_2} (q_{e_2,r} - q_{e_2,l}) \\ q'_S &= q_{v_2}^{\Gamma'} - \frac{a_1}{\ell_1} (p_{v_1} - p_u) - g_{e_1}(p_{v_1}, q_{e_1,l}) \\ q'_{e_1,r} &= q_{v_1}^{\Gamma'} + q_{v_2}^{\Gamma'} - \frac{a_1}{\ell_1} (p_{v_1} - p_u) - g_{e_1}(p_{v_1}, q_{e_1,l}) \\ q'_{e_2,r} &= q_{v_3}^{\Gamma'} \\ p'_u &= p_u^{\Gamma'}. \end{aligned}$$

However, if the valve is closed and therefore  $s_{eS}(t) = 0$ , the index of this DAE is 2, since one has to differentiate the system twice to extract the differential equation for  $p_{v_2}$

$$\begin{aligned} p'_{v_2} &= p'_{v_3} + \frac{\ell_2}{a_2} \frac{d}{dt} (g_{e_2}(p_{v_3}, q_{e_2,l}) + q'_{e_2,l}) \\ &= \frac{-c^2}{a_2 \ell_2} \left( 1 + \frac{\ell_2}{a_2} \partial_p g_{e_2}(p_{v_3}, q_{e_2,l}) \right) (q_{e_2,r} - q_{e_2,l}) + \frac{\ell_2}{a_2} \left( \partial_q g_{e_2}(p_{v_3}, q_{e_2,l}) q_{v_2}^{\Gamma'} + q_{v_2}^{\Gamma''} \right). \end{aligned}$$

**Remark 4.46** (Adapting sets  $V_{\mathcal{P}}$  and  $V_{\mathcal{A}}$ ). *The analysis in Section 4.2 can be applied to DAEs that contain valves. For  $e^S = (u, v) \in \mathcal{E}_S$ , the right node  $v$  must be treated as a node in  $V_{\mathcal{P}}$  and not as a node in  $V_{\mathcal{A}}$  as it is the case for compressors or resistors. In addition, we require that the left node  $u \in V_{\mathcal{P}}$ , too. If  $u \notin V_{\mathcal{P}}$ , there exists a pipe  $e^{\mathcal{P}} \in \delta^+(v)$ , that would be directed towards  $u \in V_{\mathcal{A}} \cup V_{\mathcal{P}}$  for  $s_{eS}(t) = 1$ . However, the assumption that  $\delta^+(u) \cap \mathcal{E}_{\mathcal{P}} = \emptyset$  was crucial in the analysis in Section 4.2.*

**Remark 4.47** (Decoupling process for networks with valves). *The decoupling procedure from Section 4.3 can only be applied for subintervals of  $\mathcal{I}$  where all switching functions  $s_{eS}$  for  $e^S \in \mathcal{E}_S$  are constant, if the requirements of Remark 4.46 are fulfilled. This will be demonstrated in Chapter 5.*

**Short pipes** Short pipes are modelled as constantly open valves (see Section 2.2.4) and can therefore be treated as such.

**Control valves** Control valves can easily be incorporated into the framework presented in this chapter. The model equation (2.19) is very similar to the equation modelling the compressor control for  $s_{ec}(t) = 1$ . The considerations of Sections 4.2 and 4.3 can be applied without further restrictions.

**Pipes that directly connect nodes in  $V_p \cup V_A$**  The first restriction in Assumption 4.11 can be neglected in general, not only for the analysis in Sections 4.2 and 4.3, but also for the extensions mentioned in this section. If there exists a pipe  $e = (u, v) \in \mathcal{E}_P$  with  $u, v \in V_p \cup V_A$ , we can introduce an artificial node  $w$  in the middle of  $e$  at position  $x = \frac{\ell_e}{2}$ , and consider pipes  $(u, w)$  and  $(v, w)$  instead (see Figure 4.8).



**Figure 4.8:** Pipe that connects nodes in  $V_p \cup V_A$  (left) with a finer spatial discretisation and pipe orientation (right).

**Remark 4.48.** Since gas pipes usually have a length of several tens of kilometres, the application of a finer spatial discretisation as mentioned above is often inevitable, especially for the purpose of simulation. For pipes  $e = (u, v) \in \mathcal{E}_P$  with  $u, v \in V_p \cup V_A$ , one could discretise the pipe in  $k \in \mathbb{N}$  subpipes of length  $\frac{\ell_e}{k}$  and orientate all but the last subpipe in the same direction as  $e^P$ , while applying the reverse orientation to the  $k^{\text{th}}$  subpipe. Pipes that do not directly connect nodes in  $V_p \cup V_A$  can be oriented the same way as the pipe is.

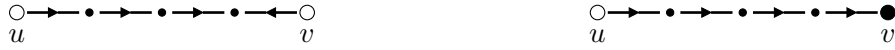


**Figure 4.9:** Finer spatial discretisation and pipe orientation for  $u, v \in V_p \cup V_A$  (left) and for  $u \in V, v \in V_P$  (right).

**Active elements directed at the same node** If there exists a node  $u \in V_A$  so that  $|\delta^+(u) \cap \mathcal{E}_A| > 1$ , one can add additional pipes with a short length that connect the active elements in  $\delta^+(u) \cap \mathcal{E}_A$  to the node  $u$  (see Figure 4.10).



**Figure 4.10:** Two active elements directed towards the same node (left) with additional short artificial pipes (right).

The same approach is also applicable to the case that a valve is connected to a compressor or resistor as depicted in Figure 4.11.



**Figure 4.11:** A valve that is directly placed behind a compressor (left) with an additional short artificial pipe (right).

The extensions discussed in this section enable us to treat the network shown in Figure 4.2, by considering

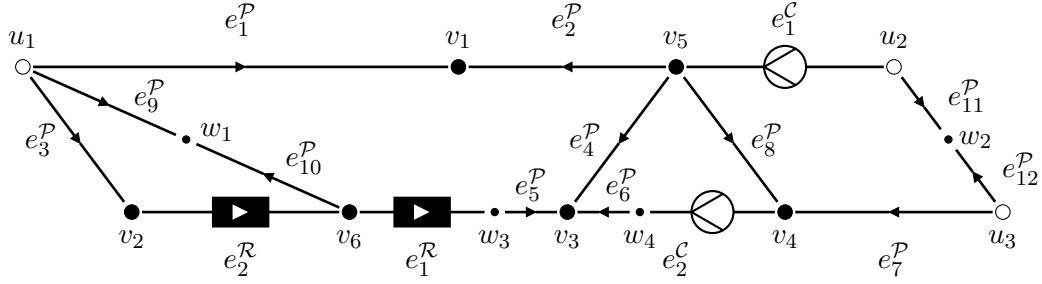


**Figure 4.12:** Network from Figure 4.2 that fulfils Assumptions 4.32.

with element sets

$$\begin{aligned} V_p &= \{u_1, u_2, u_3\} \\ V_{\mathcal{P}} &= \{v_1, v_2, v_3, v_4, w_1, w_2\} \\ V_{\mathcal{A}} &= \{v_5, w_3, v_6, w_4\} \end{aligned}$$

and  $q_{\mathcal{A}} = (q_{e_1^C} \quad q_{e_1^R} \quad q_{e_2^R} \quad q_{e_2^C})^\top$ . Note that the pipes are oriented according to Theorem 4.14 and the nodes in  $V_{\mathcal{A}}$  as well as the active elements in  $\mathcal{E}_{\mathcal{A}}$  are sorted as proposed in Remark 4.34.

## 4.5 Consistent initialisation

The presented topological decoupling procedure can also be used to calculate consistent initial values for the DAE (4.31) in a very convenient way.

The initial data for  $\mathbf{u} = (p_{\mathcal{P}} \quad q_l)^\top$  can be chosen freely and can then be used to directly compute the remaining initial values for

$$\mathbf{v}_1 = (q_r \quad q_R \quad q_C \quad p_A \quad H \quad Q)^\top \quad \mathbf{v}_2 = (n \quad M)^\top \quad \mathbf{v}_3 = \eta$$

by explicit expressions for the respective variables

$$\mathbf{v}_1 = f_1(\mathbf{u}, t) \quad \mathbf{v}_2 = f_2(\mathbf{u}, \mathbf{v}_1, t) \quad \mathbf{v}_3 = f_3(\mathbf{v}_1, \mathbf{v}_2, t)$$

as stated in Theorem 4.23. The functions  $f_1$ ,  $f_2$  and  $f_3$ , to compute  $\mathbf{v}_1$  to  $\mathbf{v}_3$  are given by equations (4.45) to (4.47b), equations (4.47c) to (4.47e) and equation (4.47f), respectively. This procedure will not require the solving of a more complex non-linear system to compute initial values for the DAE (4.31) or even the use of projection methods, e.g., for the case of other spatial discretisations that would result in a DAE of index  $\geq 2$ .

This topological computation of consistent initial values might further be of use when simulating gas networks that contain valves or when the modelling of compressors includes a mode, where the compressor is off, thus acting as a closed valve. As shown in Section 4.4, the inclusion of such elements allows the decoupling procedure only between switching points. In this case, it might be more reasonable to simulate the gas network as a DAE. However, we can still use the topological decoupling to compute consistent initial values. Since we are only interested in the behaviour of the network at a specific time point ( $t = t_0$ ), we do not need to be concerned about possible switching times and formulate the ODE system at  $t = t_0$  and compute the consistent initial values.

### 4.6 Conclusion

In this chapter, we have introduced a new spatial discretisation of gas networks under reasonable topological restrictions (see Assumptions 4.11 and 4.32). We presented a procedure to orientate the pipes in gas networks in a specific way (see Theorem 3.2) so that the spatial discretisation we proposed in Section 4.1 (see equation (4.12)) yields a DAE of index 1 (see Theorems 4.17 and 4.37 in Sections 4.2 and 4.4). This, in turn guarantees a certain stability of the solution of the DAE and also makes it less difficult to solve from a numerical point of view. In addition, this reflects the properties of the original PDAE system, at least for pipe networks, where we proved in Chapter 3 that the solution of the PDAE possesses a perturbation index 1 behaviour (see Theorem 3.17).

Furthermore, we introduced a decoupling procedure in Section 4.3 which allows the formulation of the gas network directly as an ODE that can be solved independent of a remaining system of non-linear equations. Instead of solving a DAE of dimension  $n_D$  with

$$n_D = 2|\mathcal{E}_P| + |V| + |\mathcal{E}_A| + 4|\mathcal{E}_C|,$$

the decoupling procedure allows us to solve an ODE of a lower dimension  $n_O$  with

$$n_O = |V_P| + |\mathcal{E}_P|$$

and then computing the remaining variables directly. The process to derive the decoupled ODE from the gas network DAE is depicted in Figure 4.13. Regarding the decoupling of DAEs to ODEs, this often comes at a cost in form of projector matrices [Gru<sup>+</sup>14] and it is not trivial to compute the needed projectors. However, the decoupling procedure we presented, combined with the suitable pipe orientation and the adapted spatial discretisation, does not rely on projectors at all. The ODE can be formulated directly from the topology and element information.

Another benefit of the topological decoupling is the easy computation of consistent ini-



**Figure 4.13:** Graph orientation and decoupling process to an ODE with a decoupled set of algebraic equations (AE).

tial values. This is even possible in the case of networks with valves or more complex compressor models, as we stated in Section 4.5.

In addition to a more efficient simulation, the presented approach towards the reformulation of the gas network as an ODE gives way for the application of ODE specific numerical integration methods. Furthermore, one could apply model order reduction (MOR) methods for ODEs, for instance as it is described in [Gru<sup>+</sup>14].





## 5 Numerical examples

In this chapter, we want to give some numerical examples of gas networks. Most of them can be found in the GasLib [Hum<sup>+</sup>17]. We briefly introduce two common discretisation techniques in Sections 5.1 and 5.2: The implicit box scheme [BKL09; KLB10] and a Galerkin discretisation that is proposed in [EKW17]. We compare the numerical solutions of these two discretisations with the solution of the topology-adapted semi-discretisation for a benchmark network in Section 5.3. In Section 5.4, we present numerical simulations for several GasLib networks and also compare the solutions of the topology-adapted DAE with the decoupled ODE.

### 5.1 Implicit box scheme

Strictly speaking, the implicit box scheme [BKL09; KLB10] is a full discretisation and not just a spatial discretisation. For a better comparison, we state the implicit box scheme in a semi-discretised form for the ISO2' model (2.12):

$$\frac{d}{dt} \frac{p_u(t) + p_v(t)}{2} + \frac{c^2}{a_e \ell_e} (q_{e,l}(t) - q_{e,r}(t)) = 0 \quad (5.1a)$$

$$\frac{d}{dt} \frac{q_{e,r}(t) + q_{e,l}(t)}{2} + \frac{a_e}{\ell_e} (p_v(t) - p_u(t)) = - \frac{g_e(p_u(t), q_{e,l}(t)) + g_e(p_v(t), q_{e,r}(t))}{2} \quad (5.1b)$$

for  $e = (u, v) \in \mathcal{E}_P$ .

**Theorem 5.1.** *Let  $\mathcal{G} = (V, \mathcal{E})$  be the graph of a gas pipe network,  $\mathcal{E} = \mathcal{E}_P$ . Then it holds that the DAE that results from the semi-discretisation (5.1) has an index  $\mu \leq 2$ . The DAE has index 1 if and only if  $|V_P| = 1$ .*

*Proof.* The assertion of the theorem has been proven for the midpoint rule in [Gru<sup>+</sup>14, Lemmata 4.1 and 4.2]. The midpoint rule only differs in the approximation of the non-linear right-hand side in equation (5.1b)

$$g_e(p_e(x, t), q_e(x, t)) \approx g_e \left( \frac{p_u(t) + p_v(t)}{2}, \frac{q_{e,r}(t) + q_{e,l}(t)}{2} \right).$$

Hence, the proof can be applied without restrictions.  $\square$

## 5.2 Galerkin discretisation

In this Section, we formulate the Galerkin discretisation as stated in [EKW17, Section 3.2], but restrict ourselves to pipe networks. Let  $\mathcal{G} = (V, \mathcal{E})$  be the graph of a pipe network with  $V_p, V_q \neq \emptyset$ .

Let  $T_h(e) = \{T\}$  be a uniform mesh of  $e \in \mathcal{E}$  with subintervals  $T$  of length  $h_e$ . The global mesh is then defined by  $T_h(\mathcal{E}) = \{T_h(e) : e \in \mathcal{E}\}$ . We denote the space of piecewise polynomials on  $T_h(\mathcal{E})$  by

$$P_k(T_h(\mathcal{E})) := \{f \in L_2(\mathfrak{G}) : f|_e \in P_k(T_h(e)), e \in \mathcal{E}\},$$

where  $P_k(T_h(e)) = \{f \in L_2([0, \ell_e]) : f|_T \in P_k(T), T \in T_h(e)\}$  and  $P_k(T)$  is the space of polynomials of degree  $\leq k$  on the subinterval  $T$ . Note that  $P_k(T_h(e)) \subset L_2([0, \ell_e])$ . For the approximation of mass flow and pressure, we now consider the following finite element spaces:

$$V_h = P_1(T_h(\mathcal{E})) \cap H(\text{div}; \mathfrak{G}) \quad \text{and} \quad Q_h = P_0(T_h(\mathcal{E})),$$

with  $H(\text{div}; \mathfrak{G}) = \{f \in L_2(\mathfrak{G}) : f_e \in H^1([0, \ell_e])\}$ . In general the space  $H(\text{div}; \mathfrak{G})$  includes additional restrictions on the functions it contains. However, the restrictions that are imposed in [EKW17] only concern specific types of nodes that we do not consider here. By Galerkin approximation, we then obtain the following semi-discrete system for the ISO2' model

$$(\partial_t p_h(t)|m_h)_{\mathfrak{G}} + c^2(a^{-1}\partial_x q_h(t)|m_h)_{\mathfrak{G}} = 0 \quad (5.2a)$$

$$\begin{aligned} (\partial_t q_h(t)|v_h)_{\mathfrak{G}} - (ap_h(t)|\partial_x v_h)_{\mathfrak{G}} = & -(d(p_h(t), m_h)m_h|v_h)_{\mathfrak{G}} - (ap^T(t)|v_h n)_{V_p} \\ & - (ap_{q,h}(t)|v_h n)_{V_q}, \end{aligned} \quad (5.2b)$$

that holds for all  $m_h \in Q_h, v_h \in V_h$  and for a.e.  $t \in \mathcal{I}$ . The factor  $a$  which appears within the scalar products is the cross sectional area of the respective pipe. The multiplication of  $a$  and  $a^{-1}$  is meant to be understood componentwise. The scalar product  $(\cdot|\cdot)_V$  is defined by

$$(f|g)_V = \sum_{u \in V} f(u)g(u) \quad \text{for} \quad f, g \in L_2(\mathfrak{G})$$

with

$$f_e(u) := \begin{cases} f_e(0, t) & e = (u, v) \\ f_e(\ell_e, t) & e = (v, u) \\ 0 & \text{else.} \end{cases}$$

In addition we define  $n = (n_1 \ \dots \ n_{|\mathcal{E}|})^\top$ , which appears in equation (5.2b), componentwise as

$$n_e(u) := \begin{cases} 1 & e = (v, u) \\ -1 & e = (u, v) \\ 0 & \text{else.} \end{cases}$$

The non-linear term  $d = (d_1 \dots d_{|\mathcal{E}|})^\top$  on the right-hand side of equation (5.2b) is stated componentwise as

$$d_i(p, q) := \frac{\lambda_i c^2}{2D_i a_i} \frac{|q|}{p} \quad i = 1, \dots, |\mathcal{E}|$$

and does not account for a possible elevation of the pipe. For the purpose of this chapter this is sufficient. The Galerkin approach is set on finding a solution  $(p_h, q_h, p_{q,h})$  to System (5.2) with the proper coupling conditions and initial values, with  $(p_h, q_h, p_{q,h}) \in H^1(\mathcal{I}, Q_h \times V_h \times \mathbb{R}^{|V_q|})$ . Hence, each component of  $p_h$  describes the pressure on a pipe, whereas the pressure variables in the topology-adapted and implicit box discretisation are incident to nodes. However, the pressures at the nodes in  $V_q$  are also contained in the Galerkin discretisation, namely  $p_{q,h}$ . For more details, we refer to [EKW17].

### 5.3 Comparison of different spatial discretisations

In this section, we compare numerical examples for topology-adapted discretisation we have introduced in Chapter 4, with the implicit box scheme (see Section 5.1) and the Galerkin approach (see Section 5.2). The network we consider is given in Figure 5.1 with node sets

$$V_p = \{u_1, u_2\} \quad V_q = \{v\} \quad \mathcal{E} = \{e_1, e_2\}.$$

It contains two sources,  $u_1, u_2 \in V_p$ , that are connected to a node  $v \in V_q$  by pipes  $e_1$  and  $e_2$ , respectively.

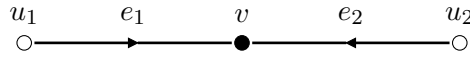


**Figure 5.1:** Pipe network with two sources and one sink.

For a more convenient notation, we choose  $z \equiv \frac{c^2}{R_s T_m}$ . The discretisation we have introduced in Chapter 4 yields the following differential system

$$p'_v + \frac{c^2}{a_1 \ell_1} (q_{e_1,r} - q_{e_1,l}) = 0 \quad (5.3a)$$

$$p'_v + \frac{c^2}{a_2 \ell_2} (q_{e_2,r} - q_{e_2,l}) = 0 \quad (5.3b)$$

$$q'_{e_1,l} + \frac{a_1}{\ell_1} (p_v - p_{u_1}) + g_{e_1}(p_v, q_{e_1,l}) = 0 \quad (5.3c)$$

$$q'_{e_2,l} + \frac{a_2}{\ell_2} (p_v - p_{u_2}) + g_{e_2}(p_v, q_{e_2,l}) = 0, \quad (5.3d)$$

whereas the implicit box scheme results in a differential system that is given by

$$\frac{(p_v + p_{u_1})'}{2} + \frac{c^2}{a_1 \ell_1} (q_{e_1,r} - q_{e_1,l}) = 0 \quad (5.4a)$$

$$\frac{(p_v + p_{u_2})'}{2} + \frac{c^2}{a_2 \ell_2} (q_{e_2,r} - q_{e_2,l}) = 0 \quad (5.4b)$$

$$\frac{(q_{e_1,r} + q_{e_1,l})'}{2} + \frac{a_1}{\ell_1} (p_v - p_{u_1}) + \frac{g_{e_1}(p_v, q_{e_1,r}) + g_{e_1}(p_{u_1}, q_{e_1,l})}{2} = 0 \quad (5.4c)$$

$$\frac{(q_{e_2,r} + q_{e_2,l})'}{2} + \frac{a_2}{\ell_2} (p_{u_2} - p_{u_1}) + \frac{g_{e_2}(p_v, q_{e_2,r}) + g_{e_2}(p_{u_2}, q_{e_2,l})}{2} = 0. \quad (5.4d)$$

The Galerkin discretisation is based on constant ansatz functions for the pressure and linear ansatz functions for the mass flow (see Section 5.2) and is stated as

$$p'_{e_1} + \frac{c^2}{a_1 \ell_1} (q_{e_1,r} - q_{e_1,l}) = 0 \quad (5.5a)$$

$$p'_{e_2} + \frac{c^2}{a_2 \ell_2} (q_{e_2,r} - q_{e_2,l}) = 0 \quad (5.5b)$$

$$q'_{e_1,l} + \frac{2a_1}{\ell_1} (p_{e_1} - p_{u_1}) + g_{e_1}(p_{e_1}, q_{e_1,l}) = 0 \quad (5.5c)$$

$$q'_{e_1,r} + \frac{2a_1}{\ell_1} (p_v - p_{e_1}) + g_{e_1}(p_{e_1}, q_{e_1,r}) = 0 \quad (5.5d)$$

$$q'_{e_2,l} + \frac{2a_2}{\ell_2} (p_{e_2} - p_{u_2}) + g_{e_2}(p_{e_2}, q_{e_2,l}) = 0 \quad (5.5e)$$

$$q'_{e_2,r} + \frac{2a_2}{\ell_2} (p_v - p_{e_2}) + g_{e_2}(p_{e_2}, q_{e_2,r}) = 0. \quad (5.5f)$$

This formulation of the variational form in equation (5.2) can be derived by choosing basis functions for the spaces  $Q_h$  and  $V_h$  and then compute the scalar products for each of the basis functions. As already stated in Section 5.2,  $p_{e_1}$  and  $p_{e_2}$  are the pressures along the respective pipes and are not incident to nodes.

The coupling and boundary condition for the network are given by

$$q_{e_1,r} + q_{e_2,r} = q_{u_2}^\Gamma \quad (5.6a)$$

$$p_{u_1} = p_{u_1}^\Gamma \quad (5.6b)$$

$$p_{u_2} = p_{u_2}^\Gamma. \quad (5.6c)$$

Since the graph of Figure 5.1 fulfils Assumptions 4.11, the DAE given by equations (5.3) and (5.6) is of index 1. However, the implicit box DAE, given by equations (5.4) and (5.6), is of index 2, since  $|V_p| > 1$  (see Theorem 5.1). The Galerkin DAE given by equations (5.5) and (5.6) has also differentiation index  $\mu_d = 2$ , since one has to differentiate the

system twice to derive the differential equation for  $p_v$ :

$$p'_v = \frac{1}{a_1\ell_2 + a_2\ell_1} \left( \ell_2 a_1 p_{u_1}^{\Gamma'} + a_1 \ell_2 p_{v_2}^{\Gamma'} + \frac{\ell_1 c^2 \partial_p g_{e_1}}{2a_1} (q_{e_1,r} - q_{e_1,l}) + \frac{\ell_2 c^2 \partial_p g_{e_2}}{2a_1} (q_{e_2,r} - q_{e_2,l}) \right) + \frac{\ell_1 \ell_2}{2(a_1 \ell_2 + a_2 \ell_1)} \left( (\partial_q g_{e_1} - \partial_q g_{e_2}) \left( \frac{2a_1}{\ell_1} (p_v - p_{u_1}) + g_1(p_1, q_{e_2}) \right) + \partial_q g_{e_2} q^{\Gamma'} - q^{\Gamma''} \right).$$

**Example 5.2.** In this first example we impose the boundary conditions given by Figure 5.2.

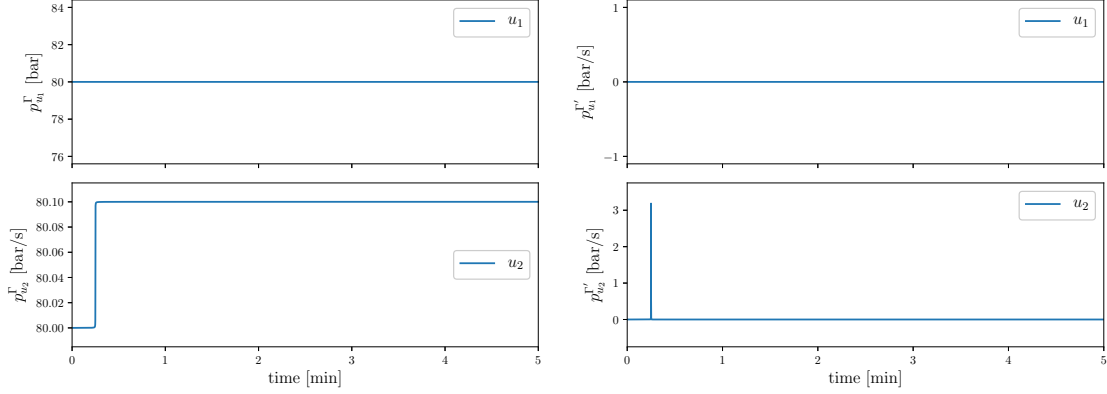


**Figure 5.2:** Pressure boundary at nodes  $u_1$  and  $u_2$  (left) and their derivatives (right).

The mass flow at  $v \in V_q$  is constant,  $q_v^\Gamma(t) = 30 \frac{\text{kg}}{\text{s}}$ , as is the pressure boundary at  $u_1 \in V_q$ ,  $p_{u_1}^\Gamma(t) = 80 \text{ bar}$ . The pressure boundary at  $u_2$  changes rapidly at  $t = 15 \text{ s}$  and is given by

$$p_{u_2}^\Gamma(t) = \frac{10^{-1}}{\arctan(-1500) - \arctan(1500)} \arctan(100(15 - t)) + 80.05 \text{ bar}.$$

Even though the pressure is raised by just 0.1 bar, the fast increase results in a significant peak at  $t = 15 \text{ s}$  in the derivative of  $p_{u_2}^\Gamma$ , given by

$$p_{u_2}^{\Gamma'}(t) = \frac{-10}{\arctan(-1500) - \arctan(1500)} \frac{1}{1 + (100(15 - t))^2}.$$

The solution to the respective DAEs (5.3) and (5.4) as well as the DAE that is derived from the Galerkin approach in equation (5.5), are shown in Figures 5.3 to 5.6. Each figure depicts the numerical solutions for different spatial refinements, from  $\Delta x = 1000 \text{ m}$  in Figure 5.3 to  $\Delta x = 100 \text{ m}$  in Figure 5.6.  $\Delta x = 1000 \text{ m}$  means that we discretised each pipe as one, whereas  $\Delta x = 100 \text{ m}$  means that we substituted each pipe by ten subpipes of length 100 m each (see Remark 4.48).

## 5 Numerical examples

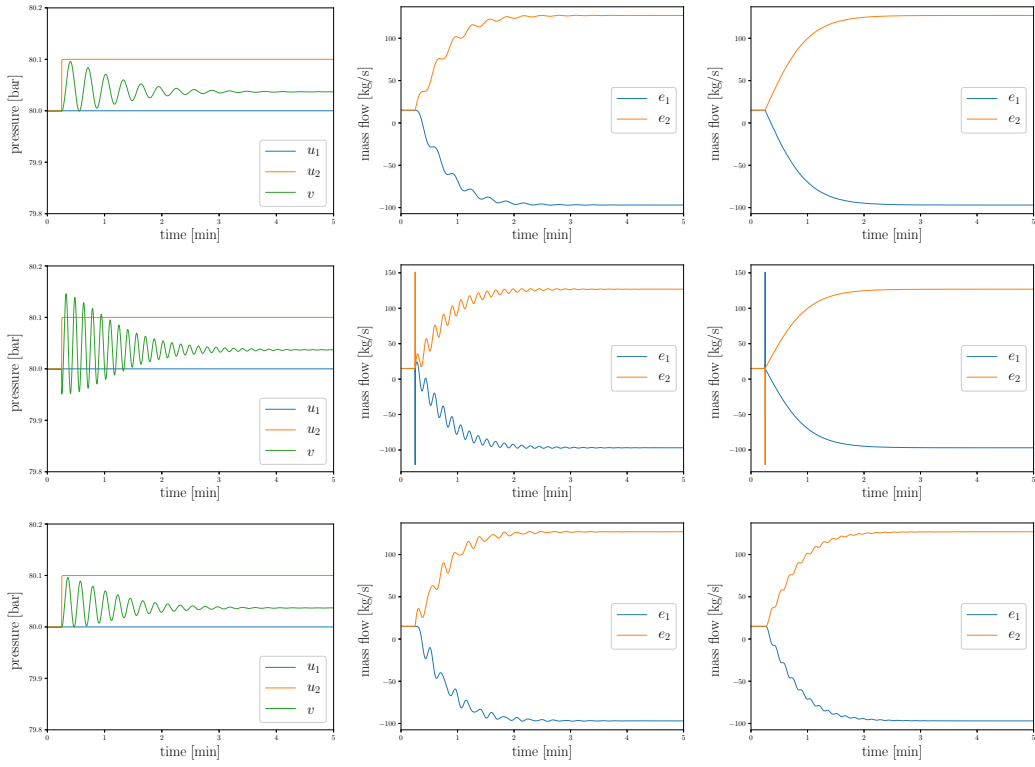


**Figure 5.3:**  $\Delta x = 1000$  m. Topology-adapted (top), implicit box (middle), Galerkin ansatz (bottom). Pressures (left), left mass flows (center), right mass flows (right).

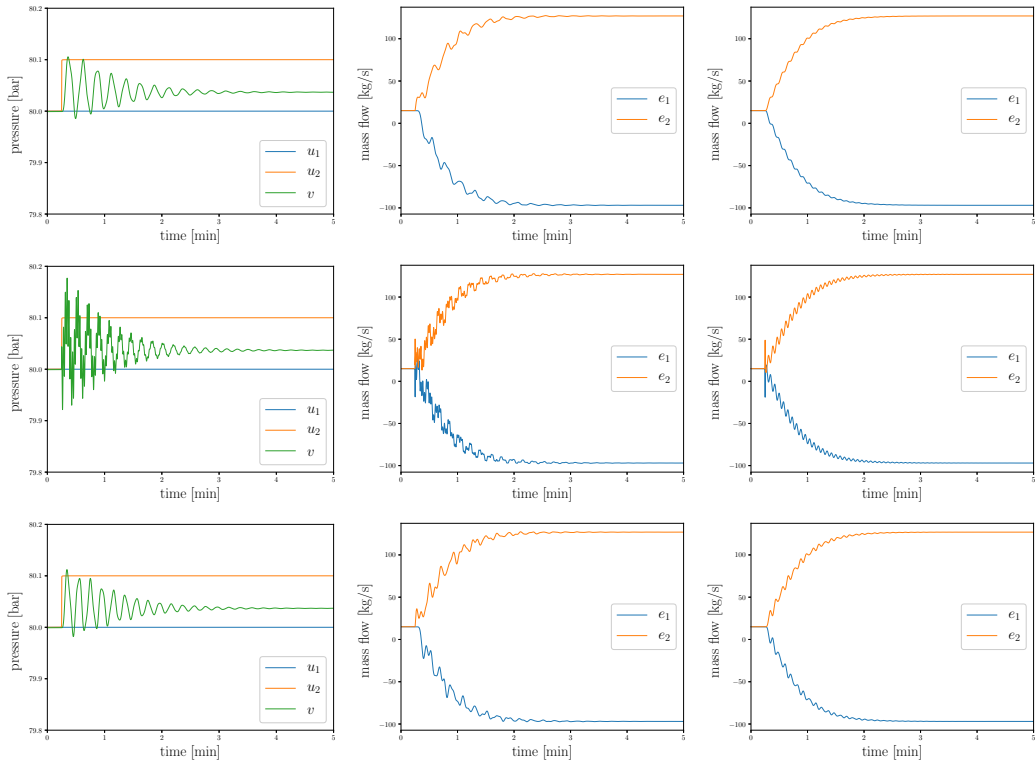


**Figure 5.4:**  $\Delta x = 500$  m. Topology-adapted (top), implicit box (middle), Galerkin ansatz (bottom). Pressures (left), left mass flows (center), right mass flows (right).

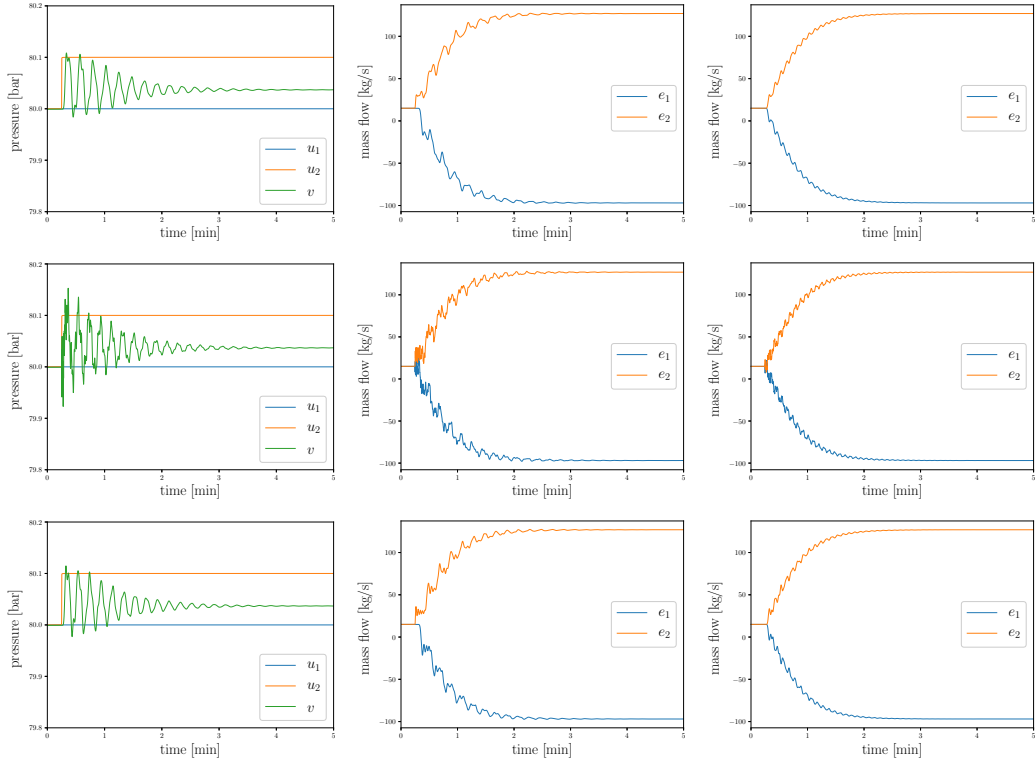


**Figure 5.5:**  $\Delta x = 250$  m. Topology-adapted (top), implicit box (middle), Galerkin ansatz (bottom). Pressures (left), left mass flows (center), right mass flows (right).

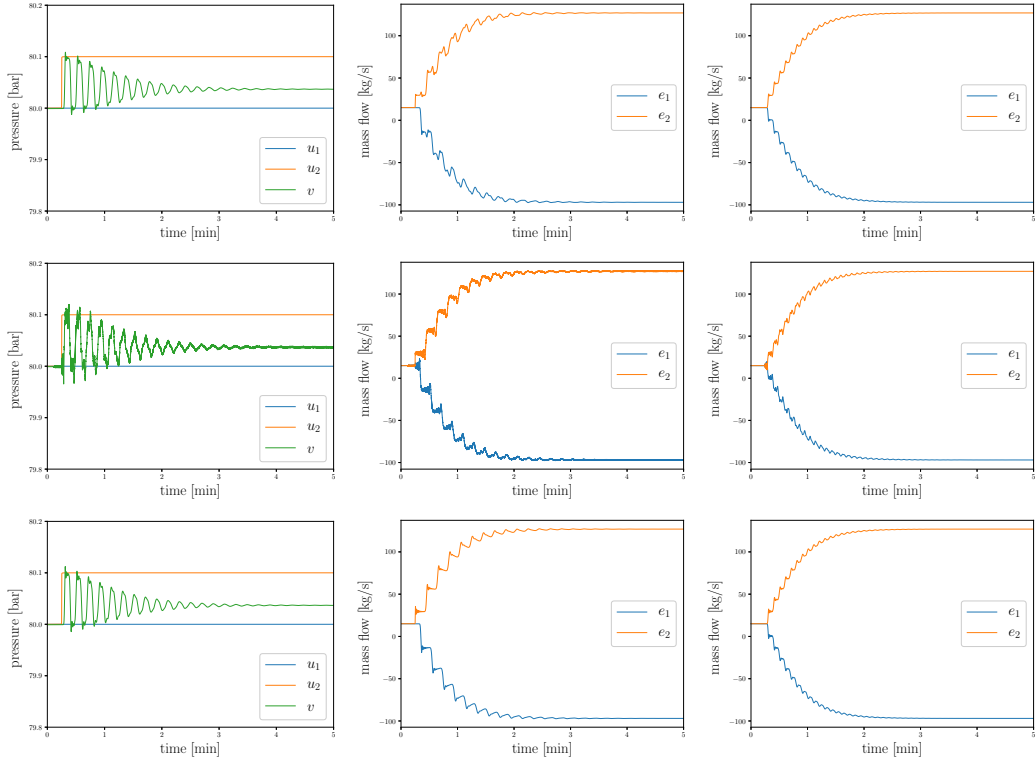


**Figure 5.6:**  $\Delta x = 100$  m. Topology-adapted (top), implicit box (middle), Galerkin ansatz (bottom). Pressures (left), left mass flows (center), right mass flows (right).

Whereas the solutions of the topology-adapted discretisation and the Galerkin approach show a very similar behaviour, the solution of the implicit box DAE deviates. One can clearly see the impact of the first derivative of the pressure boundary  $p_{u_2}^\Gamma$  (see Figure 5.2) on the mass flow solutions in Figures 5.3 and 5.4. In Figures 5.5 and 5.6, this influence is no longer visible. The topology-adapted discretisation as well as the Galerkin ansatz are not affected by the time derivative of  $p_{u_2}^\Gamma$ . In addition, the implicit box solution shows more oscillation as the solutions of the topology-adapted and the Galerkin DAE. Whereas both, the topology-adapted and the Galerkin discretisation, yield similar solutions, even for large spatial step sizes  $\Delta x$ , the former provides a smoother solution.

**Example 5.3.** As a second example, we want to compare the results for the scenario given in Figure 5.7. The pressure at  $u_1, u_2 \in V_p$  is constant at 80 bar. The mass flow at  $v \in V_q$  is given by

$$q_v^\Gamma(t) = \frac{5}{\arctan(-300) - \arctan(300)} \arctan(20(15 - t)) + 32.5 \frac{\text{kg}}{\text{s}}$$

with derivative

$$q_v^{\Gamma'}(t) = \frac{-100}{\arctan(-300) - \arctan(300)} \frac{1}{1 + (20(15 - t))^2}.$$

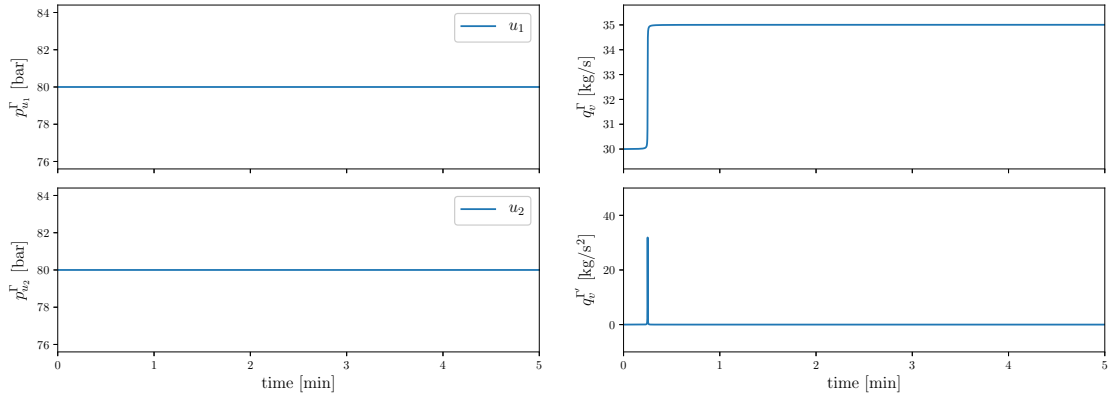


**Figure 5.7:** Pressure-boundary at nodes  $u_1$  and  $u_2$  (left). Mass flow boundary at  $v$  (upper right) and its derivatives (lower right).

Similar to Example 5.2, the mass flow boundary is increased by a small amount over a short time period. This results in a peak in the first time derivative  $q_v^{\Gamma'}$  at  $t = 15$  s. As in the previous example, we want to compare the numerical solutions for the three DAEs given by the topology-adapted discretisation we have introduced in Chapter 4, the implicit box scheme (see Section 5.1) and the Galerkin ansatz (see Section 5.2). In this example, the impact of the derivative of  $q_v^\Gamma$  (see Figure 5.7) is clearly visible in the solutions of the Galerkin approach, especially in Figures 5.8 to 5.10. Just when each pipe is discretised into 10 subpipes of length 100 m, the influence of the derivative is no longer visible in the solution (see Figure 5.11).



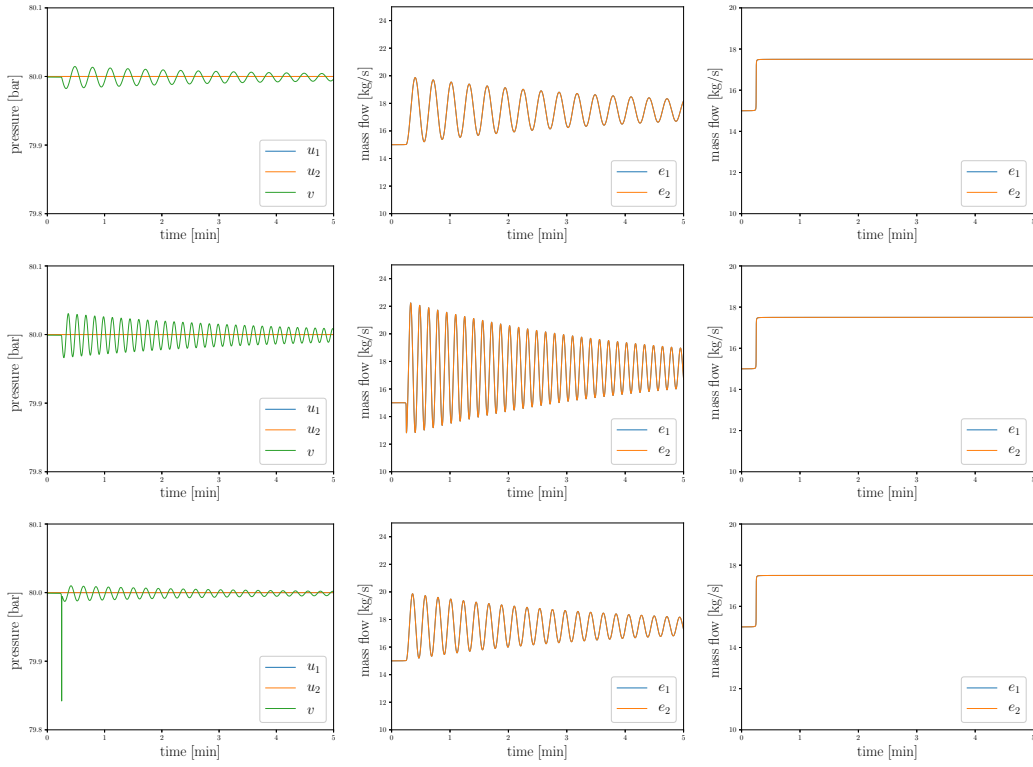


**Figure 5.8:**  $\Delta x = 1000$  m. Topology-adapted (top), implicit box (middle), Galerkin ansatz (bottom). Pressures (left), left mass flows (center), right mass flows (right).

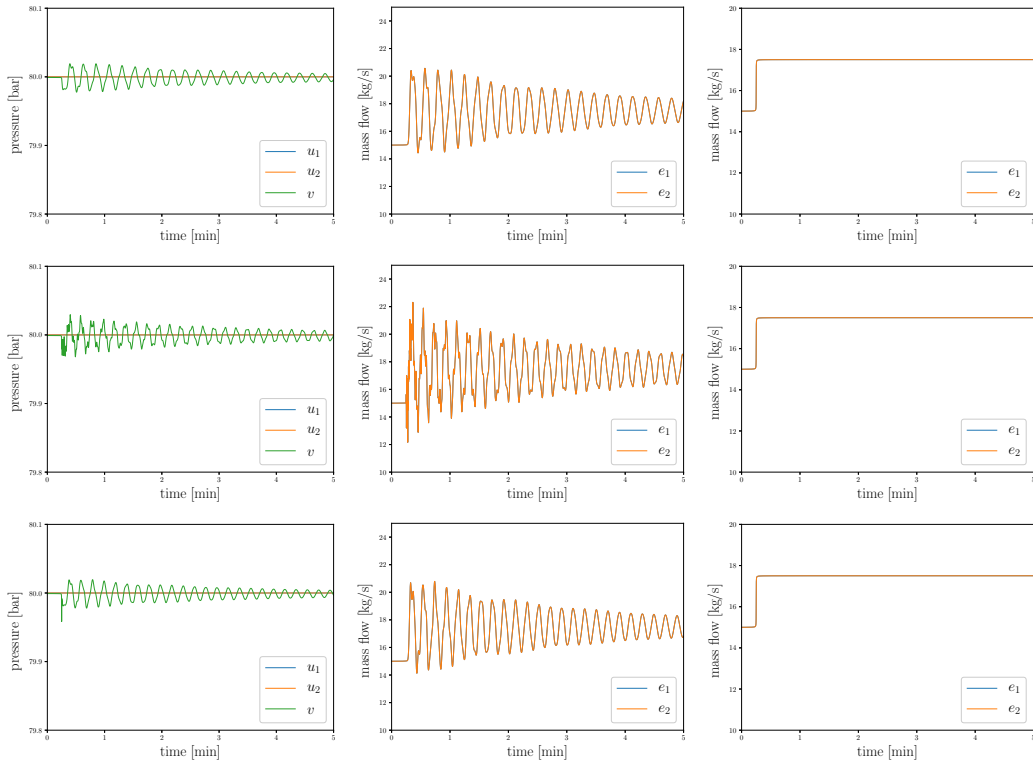


**Figure 5.9:**  $\Delta x = 250$  m. Topology-adapted (top), implicit box (middle), Galerkin ansatz (bottom). Pressures (left), left mass flows (center), right mass flows (right).

## 5 Numerical examples

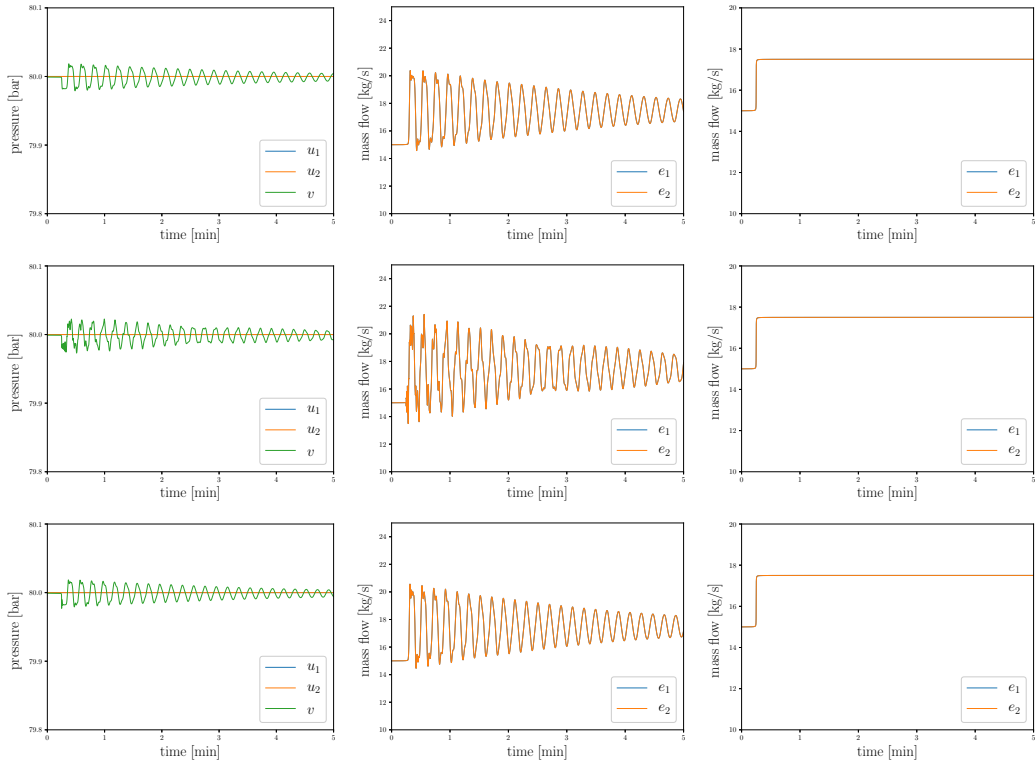


**Figure 5.10:**  $\Delta x = 125$  m. Topology-adapted (top), implicit box (middle), Galerkin ansatz (bottom). Pressures (left), left mass flows (center), right mass flows (right).

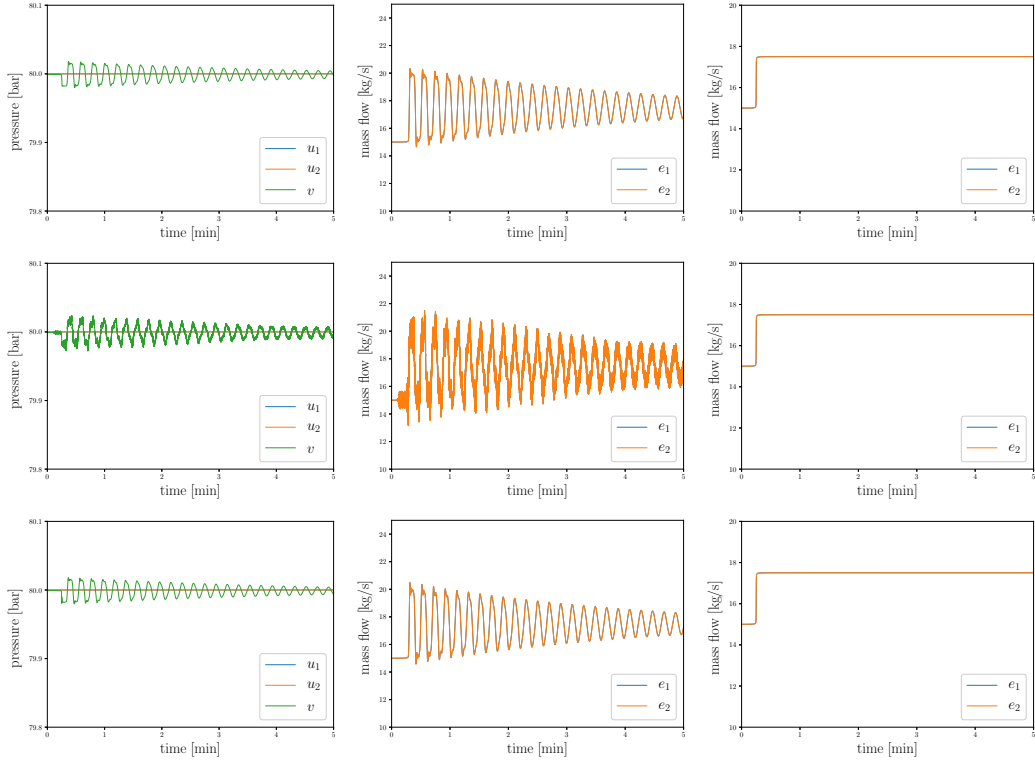


**Figure 5.11:**  $\Delta x = 100$  m. Topology-adapted (top), implicit box (middle), Galerkin ansatz (bottom). Pressures (left), left mass flows (center), right mass flows (right).

*Remark 5.4.* Even though the solution of the Galerkin approach is affected by first time derivatives of the boundary and coupling data, which suggests that this type of discretisation results in a DAE of index 2, the solution shows a similar behaviour as the solution of the topology-adapted discretisation for  $\Delta x$  becoming small. The solution of the implicit box scheme shows also the index-2 behaviour in the numerical solution (see Example 5.2). In addition, the solution possesses more oscillation in the pressure, as well as in the mass flow variables. The topology-adapted discretisation yields good approximations for both examples, even for large spatial step sizes  $\Delta x$ .

## 5.4 Networks from the GasLib

For a more detailed comparison, we investigate examples from the GasLib, namely GasLib-11, GasLib-40 and GasLib-135. We compare the solutions derived from the topology-adapted DAE with the solution of the decoupled ODE for two instances of the GasLib-11. Additionally, we calculate pressure distributions for all three networks over a long time interval and make statements regarding the numerical effort.

### 5.4.1 GasLib-11

In this section, we compare the simulation results for the GasLib-11. The topology of this network is depicted in Figure 5.12 and contains eleven nodes, eight pipes, two compressors and one valve. The node sets are

$$V_p = \{u_1, u_2, u_3\} \quad V_q = \{v_1, \dots, v_8\}.$$

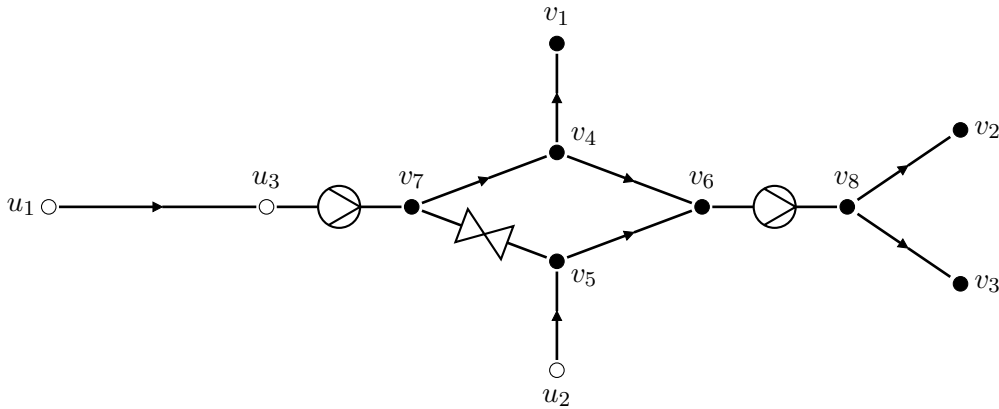


**Figure 5.12:** GasLib-11 network topology.

We start by comparing the numerical solutions of the DAE (see equation (4.31)) and the decoupled ODE (see equation 4.44).

**Comparison of DAE and ODE solution** We will consider two different versions of the GasLib-11 in Figure 5.12 to compare the numerical solutions of the DAE and ODE.

**Example 5.5.** We consider a version of the GasLib-11 that only contains pipes and compressors. Therefore, we substituted the valve by a pipe and introduced the artificial node  $w_1$  between sources  $u_1$  and  $u_2$ , to comply with Assumptions 4.11. The new network is given by Figure 5.13 and contains twelve nodes, ten pipes and two compressors. The node sets are given by

$$V_p = \{u_1, u_2, u_3\} \quad V_P = \{v_1, \dots, v_6, w_1\} \quad V_A = \{v_7, v_8\}.$$

The respective lengths and diameters of the pipes can be found in Table 5.1. The boundary conditions and the state of the compressors are shown in Figure 5.14.

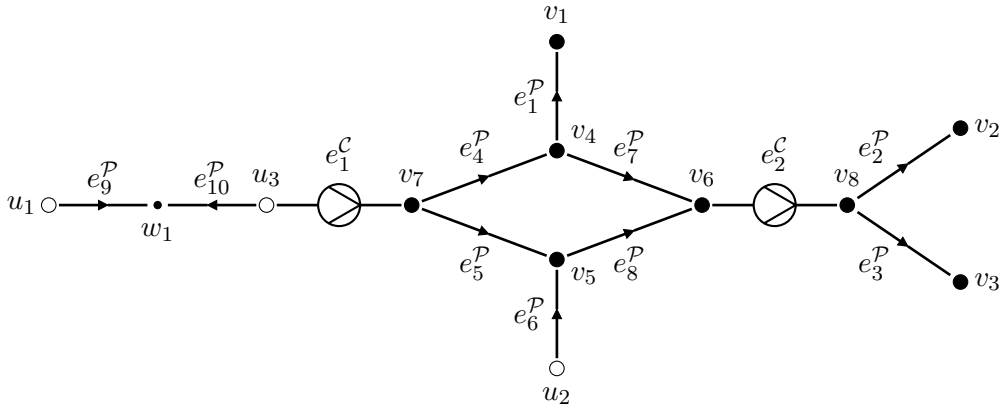


**Figure 5.13:** GasLib-11, where the valve is replaced by a pipe.

Pipe	Length	Diameter	Pipe	Length	Diameter
$e_1^P$	55000 [m]	0.5 [m]	$e_6^P$	55000 [m]	0.5 [m]
$e_2^P$	55000 [m]	0.5 [m]	$e_7^P$	55000 [m]	0.5 [m]
$e_3^P$	55000 [m]	0.5 [m]	$e_8^P$	55000 [m]	0.5 [m]
$e_4^P$	55000 [m]	0.5 [m]	$e_9^P$	27500 [m]	0.5 [m]
$e_5^P$	55000 [m]	0.5 [m]	$e_{10}^P$	27500 [m]	0.5 [m]

**Table 5.1:** Pipe lengths and diameters of the GasLib-11 (Figure 5.13).

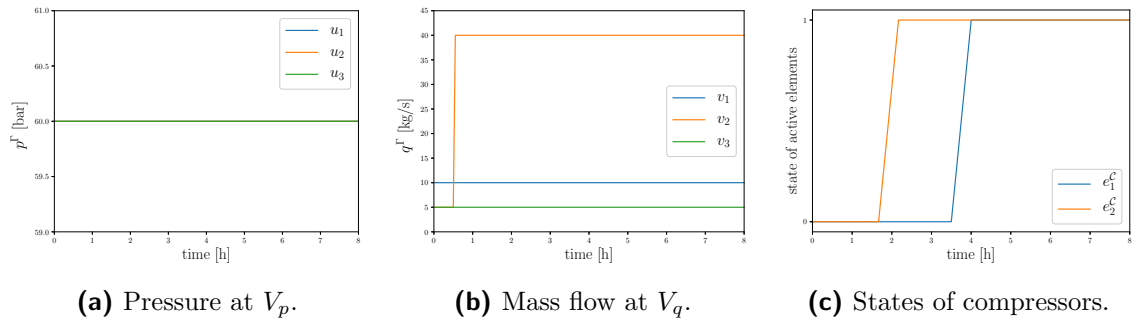


**Figure 5.14:** Scenario for the GasLib-11 (Figure 5.13).

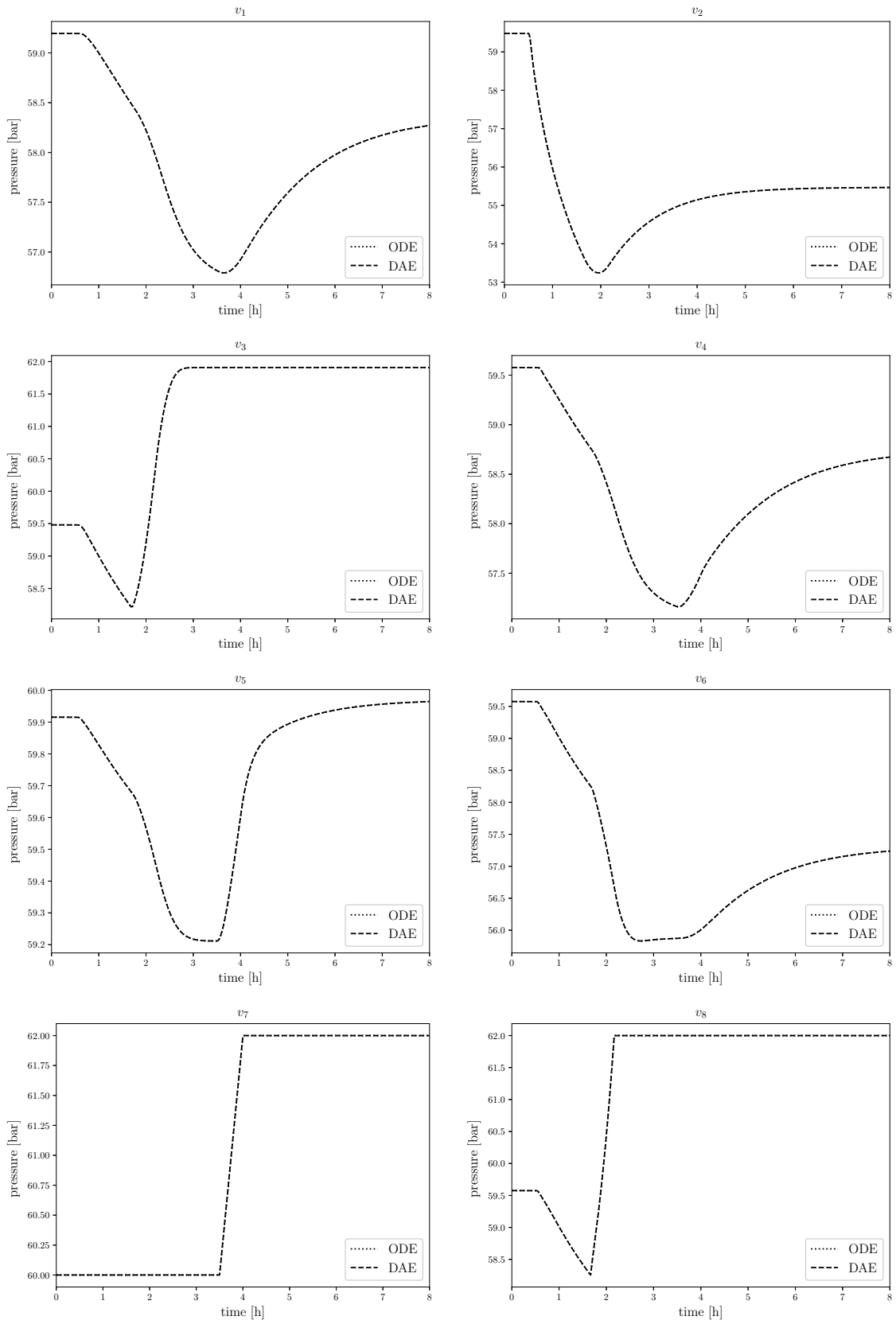


**Figure 5.15:** Pressure solutions for the GasLib-11 (Figure 5.13).

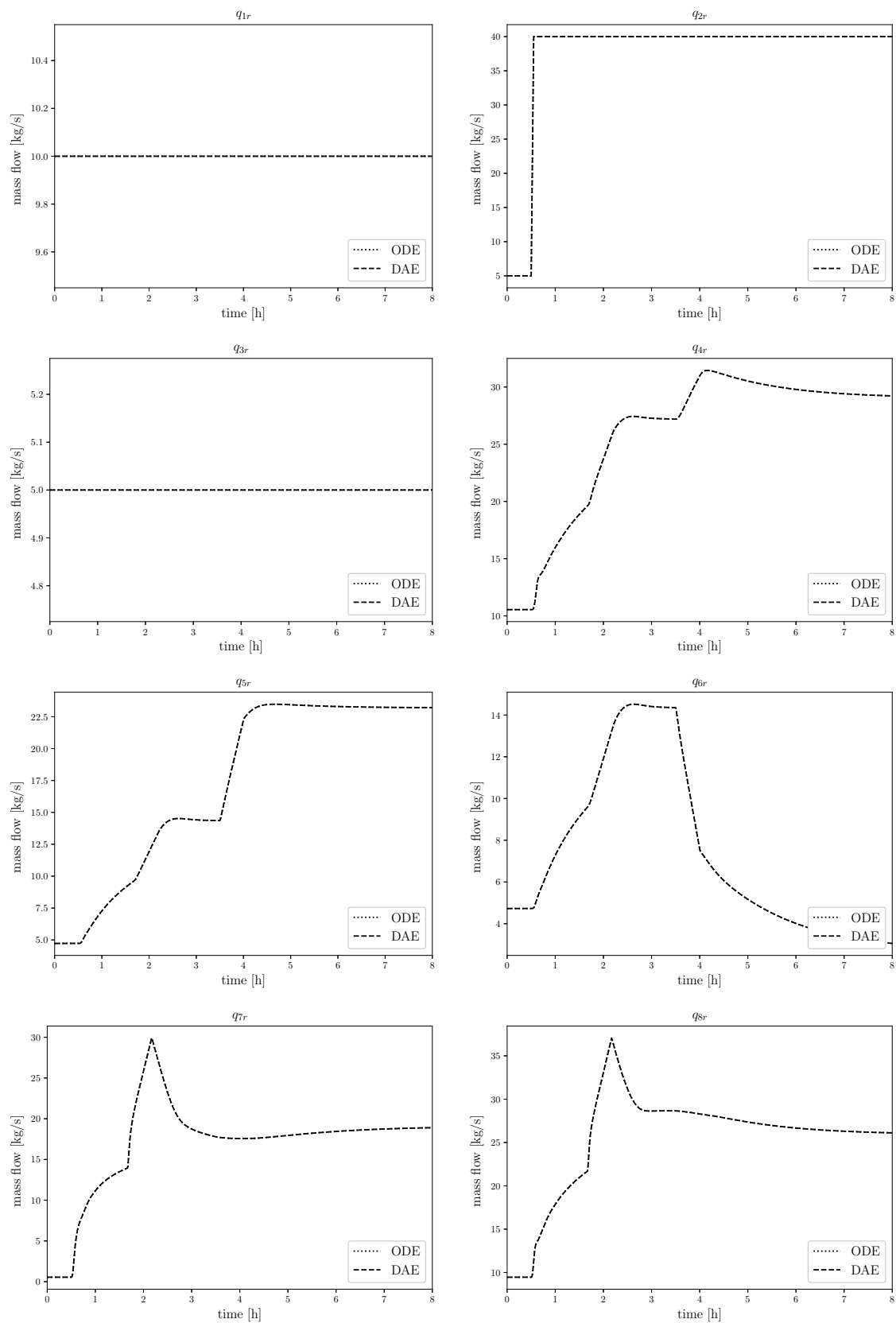


Figure 5.16: Right mass flow solutions for the GasLib-11 (Figure 5.13).

Figures 5.15 and 5.16 depict the solutions of the ODE and DAE regarding the pressures at the sinks and the right mass flows of the pipes. They show that the DAE and ODE solution coincide.

**Example 5.6.** As a second example, we consider the GasLib-11 that contains a valve (see Figure 5.17), which is opened at  $t = 1$  h. Note that we have added a pipe with a length of 10 m between the compressor  $e_1^C$  and the node  $v_7$ , so that we do not need to apply a finer discretisation and a change of orientation of pipe  $e_5^P$  when the valve switches. In addition we added an artificial node between  $u_1$  and  $u_3$  to comply with Assumption 4.11.

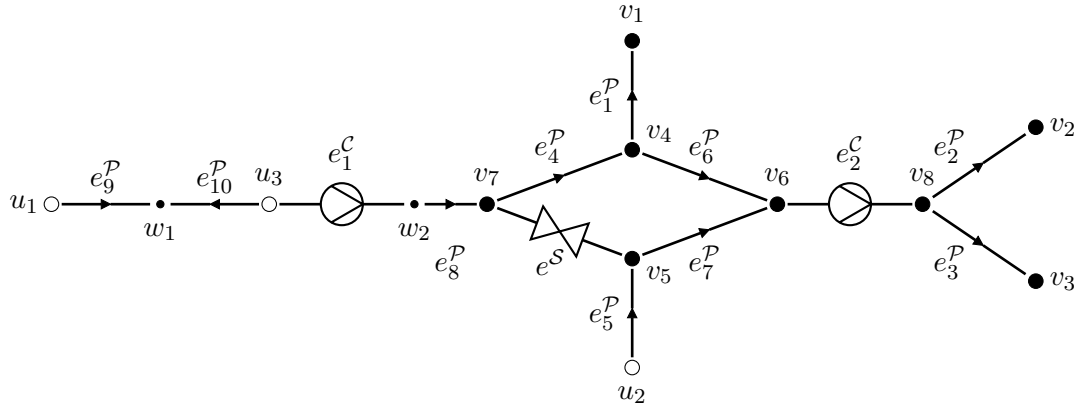


Figure 5.17: GasLib-11 with a valve.

The respective pipe lengths and diameters are given in Table 5.2. The boundary conditions and the state of the active elements are depicted in Figure 5.18.

Pipe	Length	Diameter	Pipe	Length	Diameter
$e_1^P$	55000 [m]	0.5 [m]	$e_6^P$	55000 [m]	0.5 [m]
$e_2^P$	55000 [m]	0.5 [m]	$e_7^P$	55000 [m]	0.5 [m]
$e_3^P$	55000 [m]	0.5 [m]	$e_8^P$	10 [m]	0.5 [m]
$e_4^P$	55000 [m]	0.5 [m]	$e_9^P$	27500 [m]	0.5 [m]
$e_5^P$	55000 [m]	0.5 [m]	$e_{10}^P$	27500 [m]	0.5 [m]

Table 5.2: Pipe lengths and diameters of the GasLib 11 (Figure 5.17).

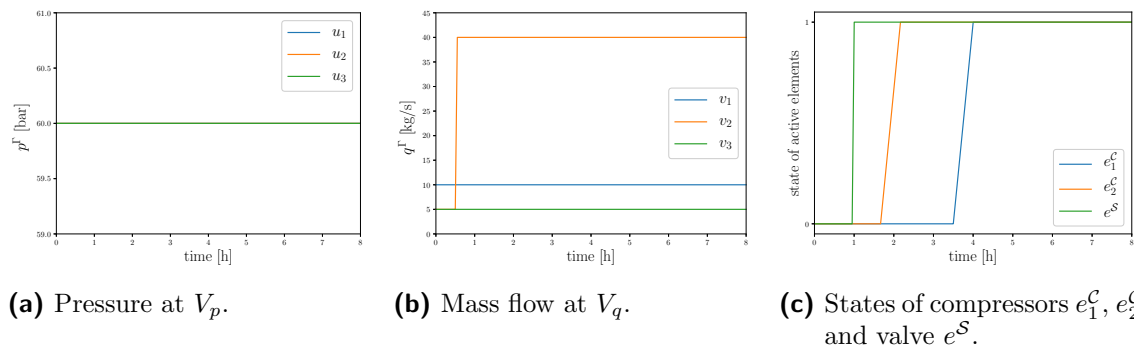


Figure 5.18: Scenario for the GasLib-11 (Figure 5.17). The valve is opened at  $t = 1$  h.

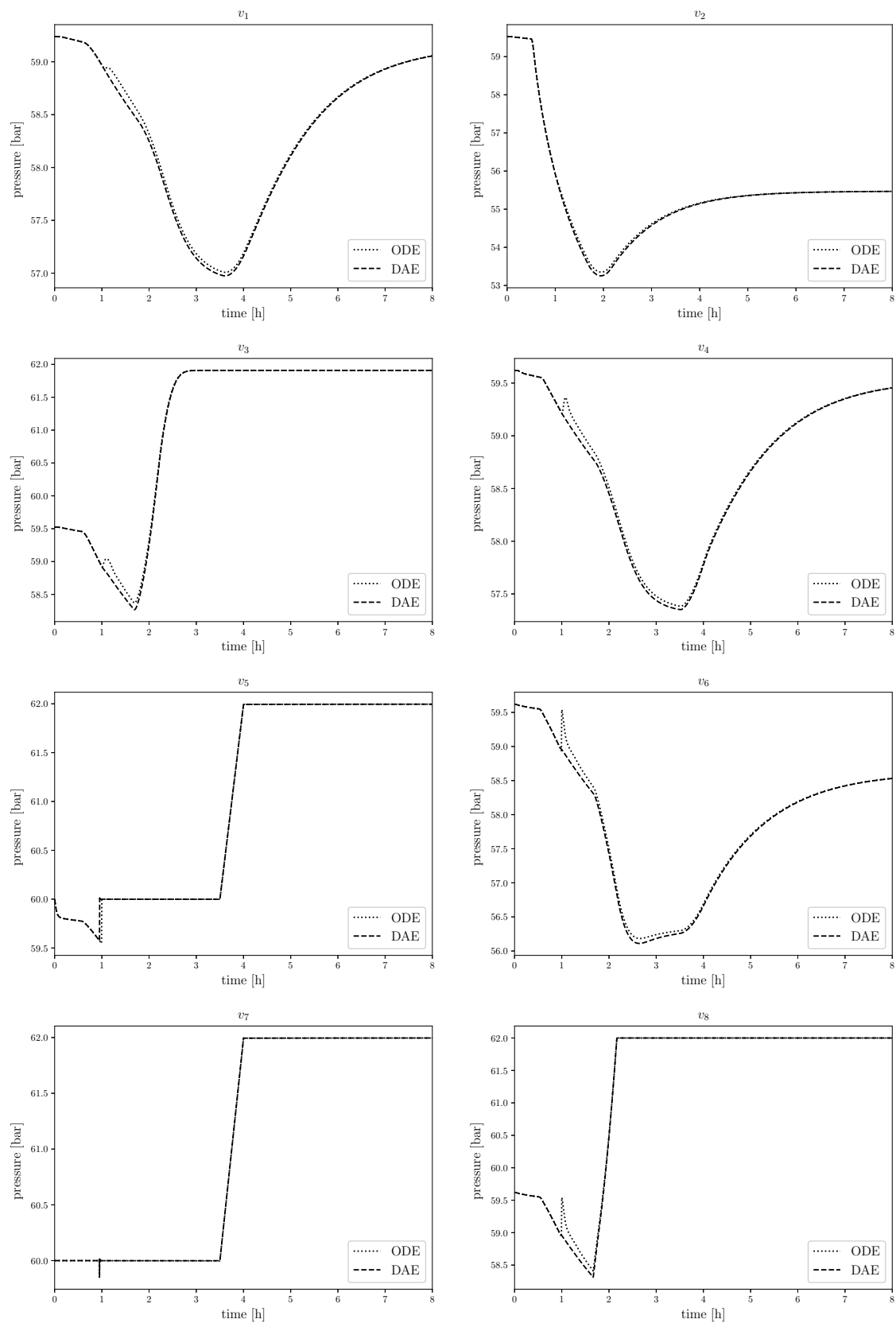


Figure 5.19: Pressure solution for the GasLib-11 (Figure 5.17).



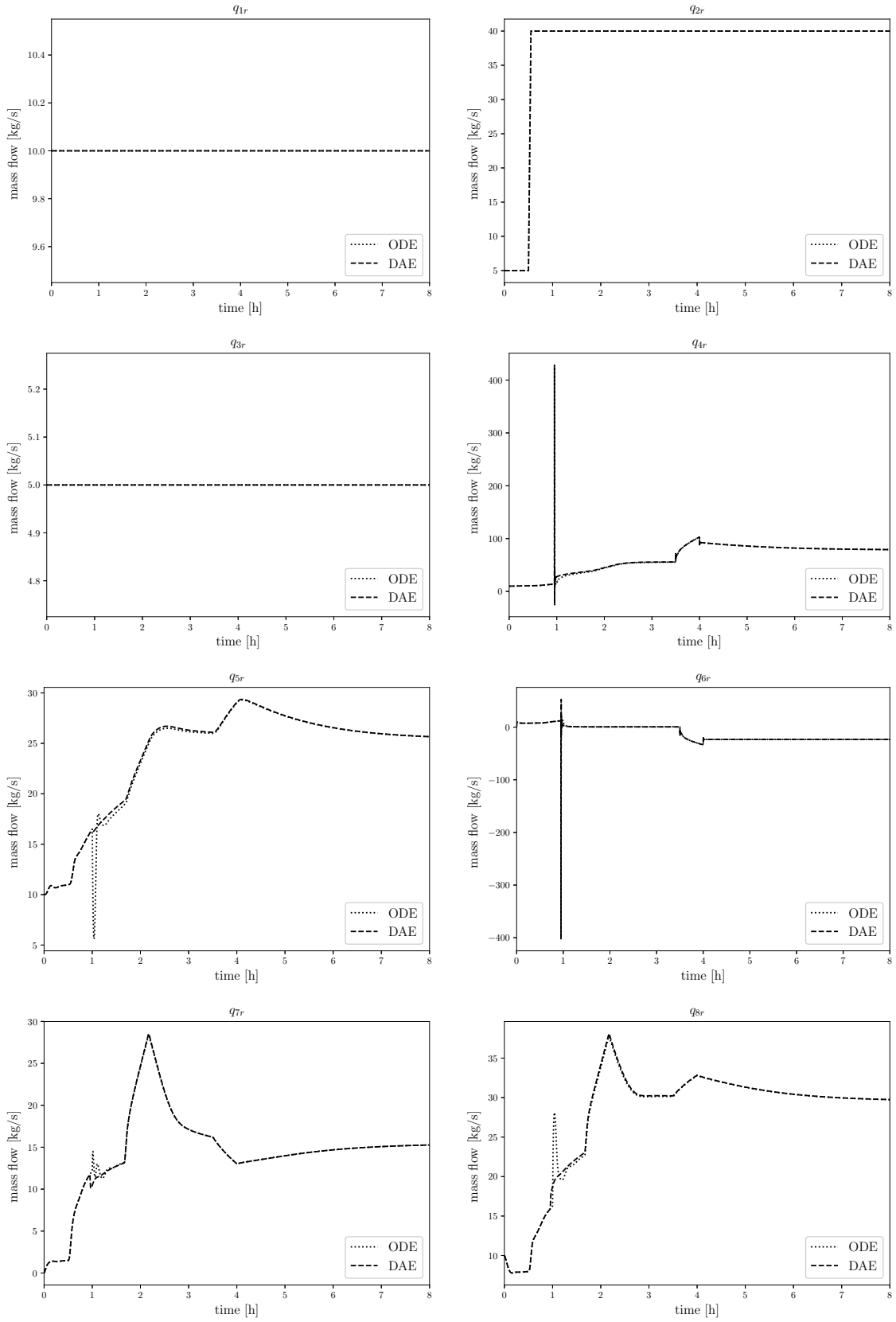


Figure 5.20: Right mass flow solution for the GasLib-11 (Figure 5.17).

The ODE and DAE solutions regarding the pressures at the sinks and the right mass flows of the pipes are depicted in Figures 5.19 and 5.20. They show that the solutions start to differ when the valve is switched open at  $t = 1$  h. We have demonstrated in Section 4.4, that the ODE of a gas network with valves changes when a valve is switched. Therefore, we had to split the computation of the ODE system in two parts. We first computed the numerical solution for the GasLib-11 with closed valve for  $t \in [0, 1]$  h. The ODE variables for that system are  $q_l$  and

$$p_{\mathcal{P}} = (p_{v_1} \quad \dots \quad p_{v_7} \quad p_{w_1})^{\top}.$$

After opening the valve, the dimension of the ODE is reduced by 1 and the differential variables of the new ODE system are  $q_l$  and

$$p_{\mathcal{P}} = (p_{v_1} \quad \dots \quad p_{v_4} \quad p_{v_6} \quad p_{v_7} \quad p_{w_1})^{\top}, \quad (5.7)$$

with  $p_{v_5}$  being equal to  $p_{v_7}$  which is incorporated within the ODE model. To continue the computation of the network with an open valve for  $t \in [1 \text{ h}, 8 \text{ h}]$ , we have used the solution of the previously computed closed-valve system. This, combined with the discontinuous behaviour of the valve, leads to differences in the solution, compared to the solution of the DAE (see Figures 5.19 and 5.20). For the DAE, the discontinuous change of state of the valve is smoothed in the valve modelling (see Section 2.2.4). However, the offset vanishes asymptotically.

**Pressure distribution** We consider the scenario in Figure 5.21 for the GasLib-11 (see Figure 5.17), where the pressure conditions at the nodes  $u_1, u_2, u_3 \in V_p$  are given in Figure 5.21a. The demand at  $v_1, v_2, v_3 \in V_q$  is given in Figure 5.21b and is zero for  $v_4, \dots, v_8, w_1, \dots, w_3$ . The operating modes of the active elements are depicted in Figure 5.21c.

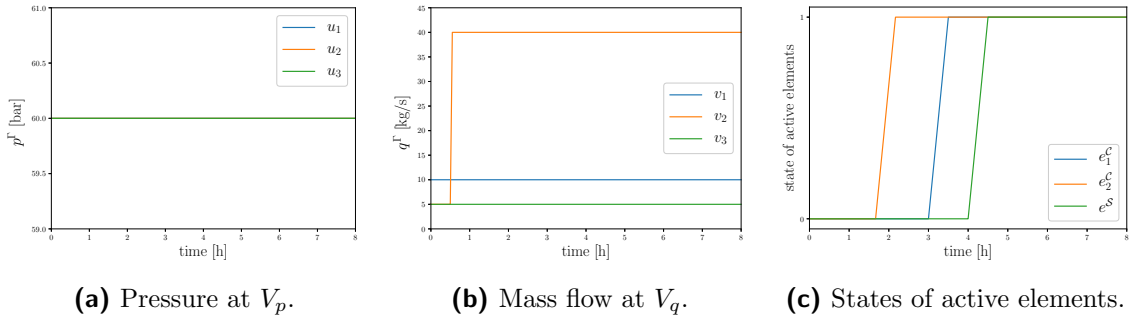


**Figure 5.21:** Scenario for the GasLib-11.

The pressure distribution over time in the GasLib-11 for the scenario described in Figure 5.21 is depicted in Figure 5.22, where a blue colouring indicates low and a green colouring indicates high pressure.

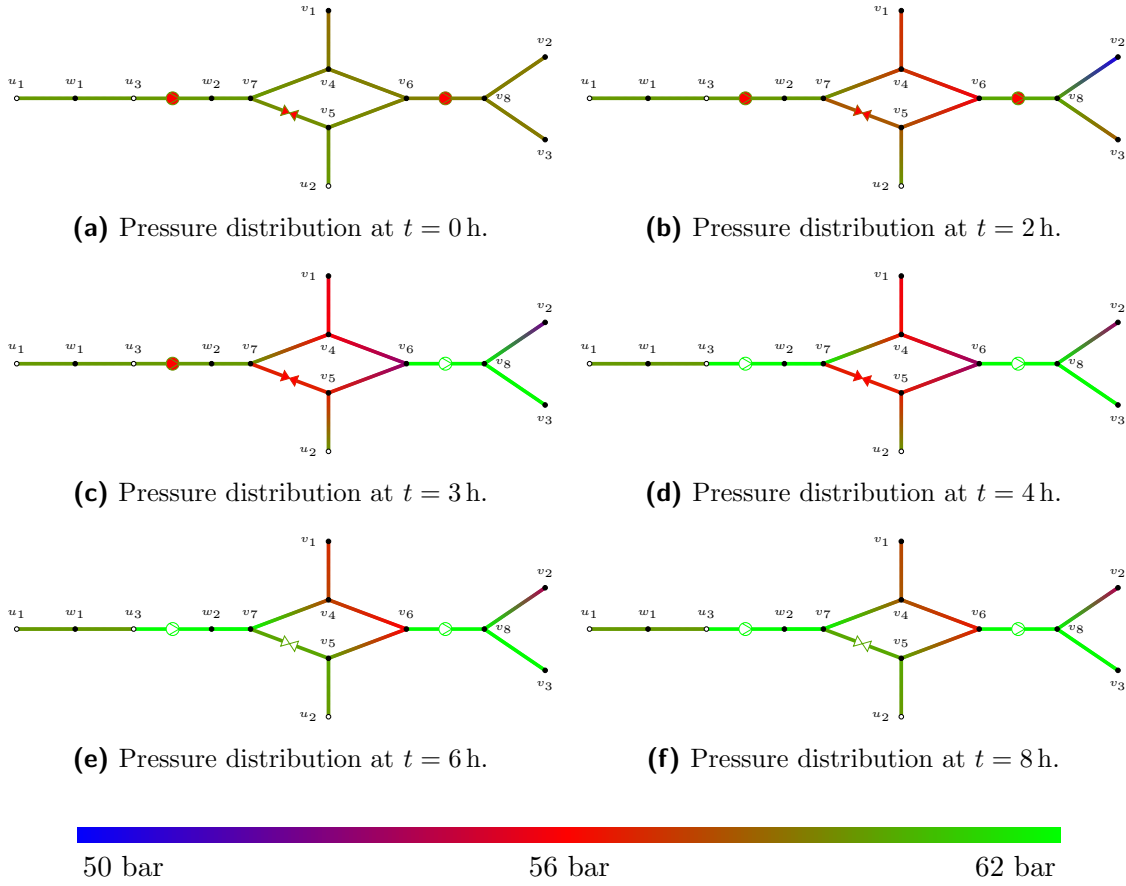


**Figure 5.22:** Pressure distribution over time for the GasLib-11.

Due to the rapid increase in demand of gas at  $v_2$ , the pressure in the network drops, especially in the right part of the network. After starting the compressor machine  $e_2^C$ , the pressure in the right part of the network increases over time. By starting compressor  $e_1^C$ , the pressure in the remaining part of network is elevated as well. The red colouring of the active elements e.g., in Figure 5.22a, indicates that they are operated in bypass mode (for compressors) or are closed (for valves).

### 5.4.2 GasLib-40

As before, where we have computed a pressure distribution over time for the GasLib-11 network, we now do the same for the GasLib-40 (see Figure 5.23). The topology data of the GasLib-40 does not fulfil Assumptions 4.11, since there exists a pipe  $e^P = (v_{33}, v_{38})$ , with  $v_{33}, v_{38} \in V_A$ . According to Section 4.4, we introduced an artificial node  $w_1$  and replaced the pipe by pipes  $(v_{33}, w_1)$  and  $(v_{38}, w_1)$  of length  $\frac{\ell_{e^P}}{2}$  each.

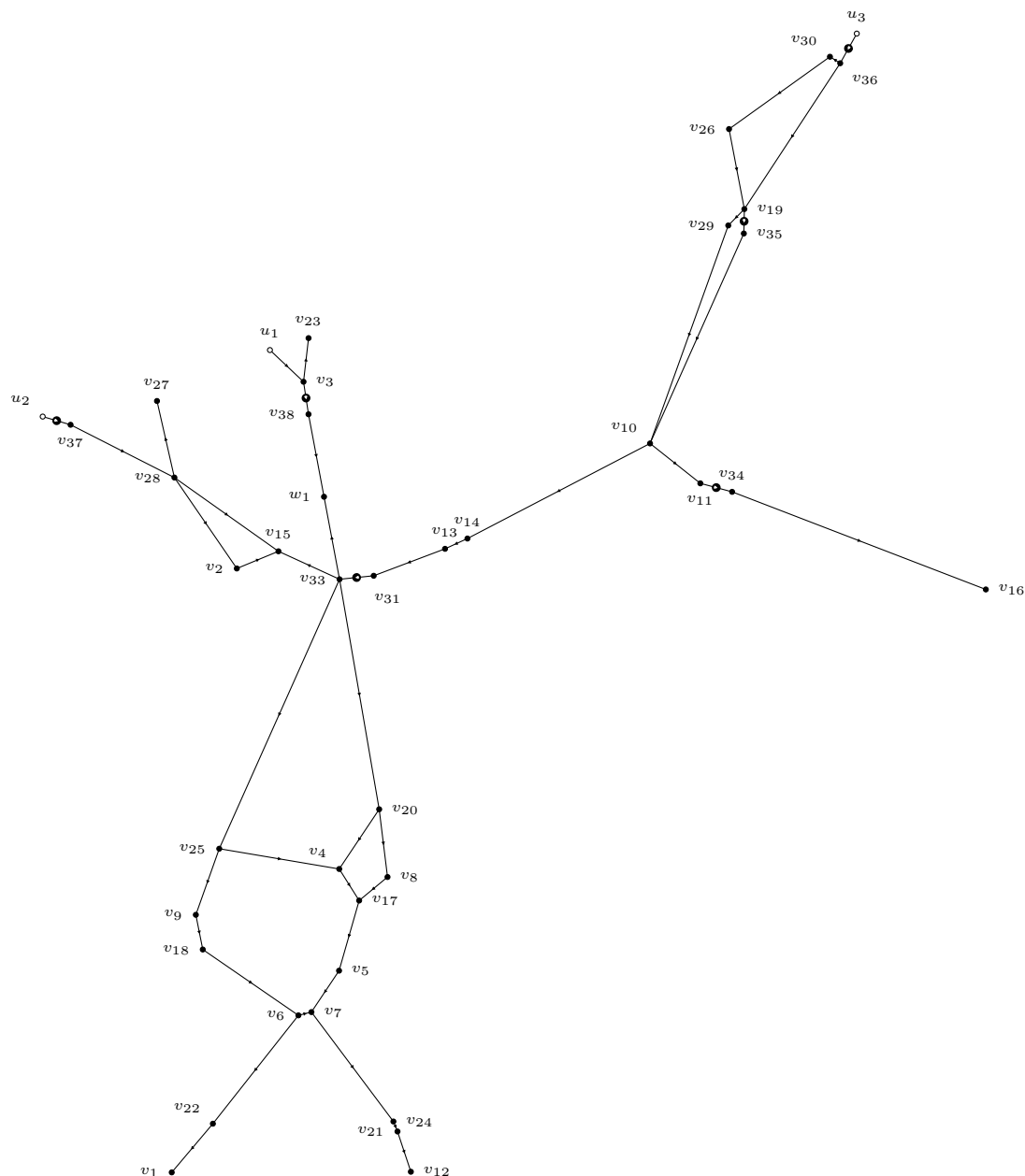


**Figure 5.23:** GasLib-40 network topology.

The node sets are

$$V_p = \{u_1, \dots, u_3\} \quad V_q = \{v_1, \dots, v_{32}, w_1\} \quad V_A = \{v_{33}, \dots, v_{38}\}.$$

Information regarding the compressors can be found in Table 5.3.

Compressor	Type	Compressor	Type
$e_1^C = (v_{31}, v_{33})$	Turbocompressor	$e_4^C = (u_3, v_{36})$	Turbocompressor
$e_2^C = (v_{11}, v_{34})$	Turbocompressor	$e_5^C = (u_4, v_{37})$	Turbocompressor
$e_3^C = (v_{19}, v_{35})$	Turbocompressor	$e_6^C = (v_3, v_{38})$	Turbocompressor

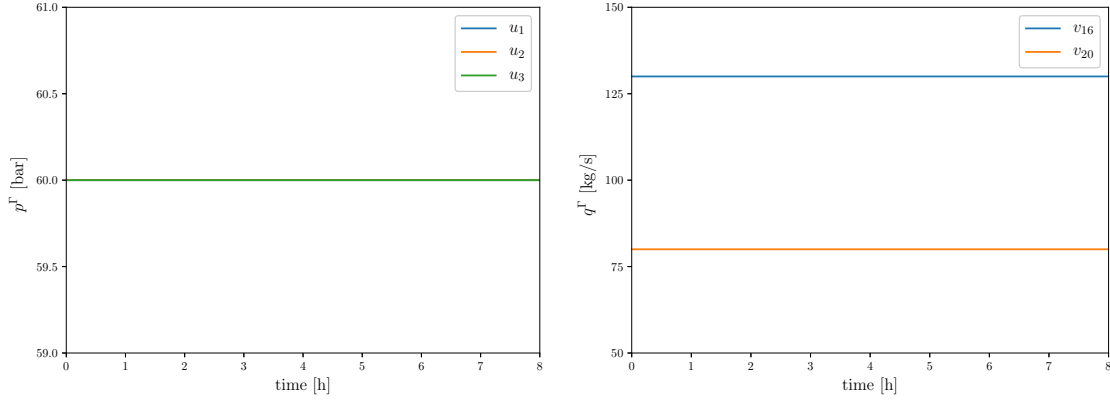
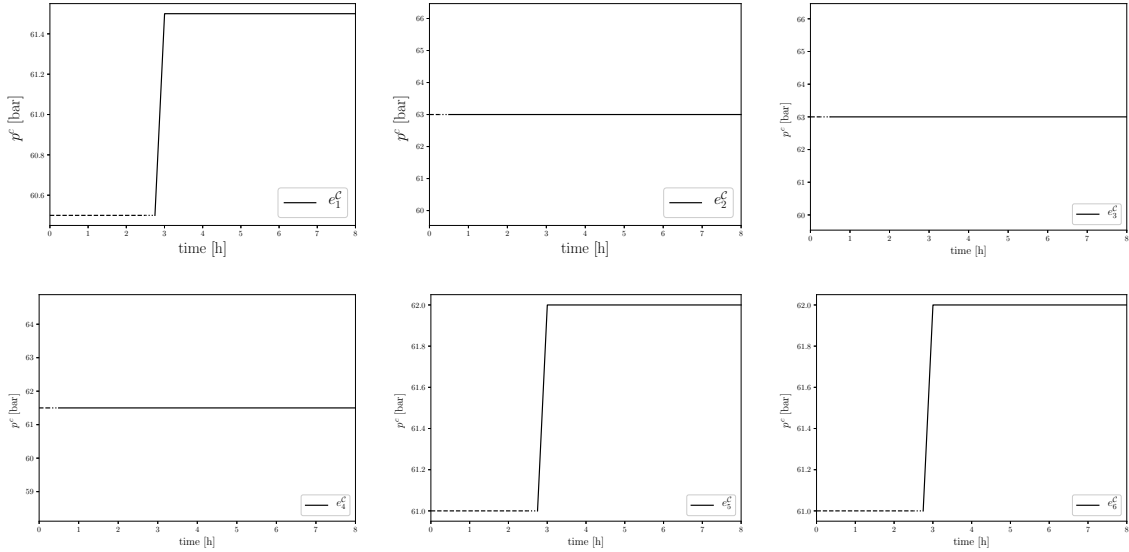
**Table 5.3:** Compressor machines of GasLib-40.**Figure 5.24:** Pressure-boundary (left) and mass flow boundary (right) for the GasLib-40 scenario.**Figure 5.25:** Compressor control for the GasLib-40. Dashed lines indicate bypass mode and dotted the start-up phase.

Figure 5.26 shows the pressure distribution in the GasLib-40 network over time. Due to a high demand at nodes  $v_{16}$  and  $v_{20}$  (see Figure 5.24), the pressure in the right and lower part of the network is in a low region (see Figure 5.26a). Over time, the compressor machines in the network are switched from bypass to compression mode (see Figure 5.25). This results in a higher pressure in the right and lower part of the network (see Figure 5.26d).

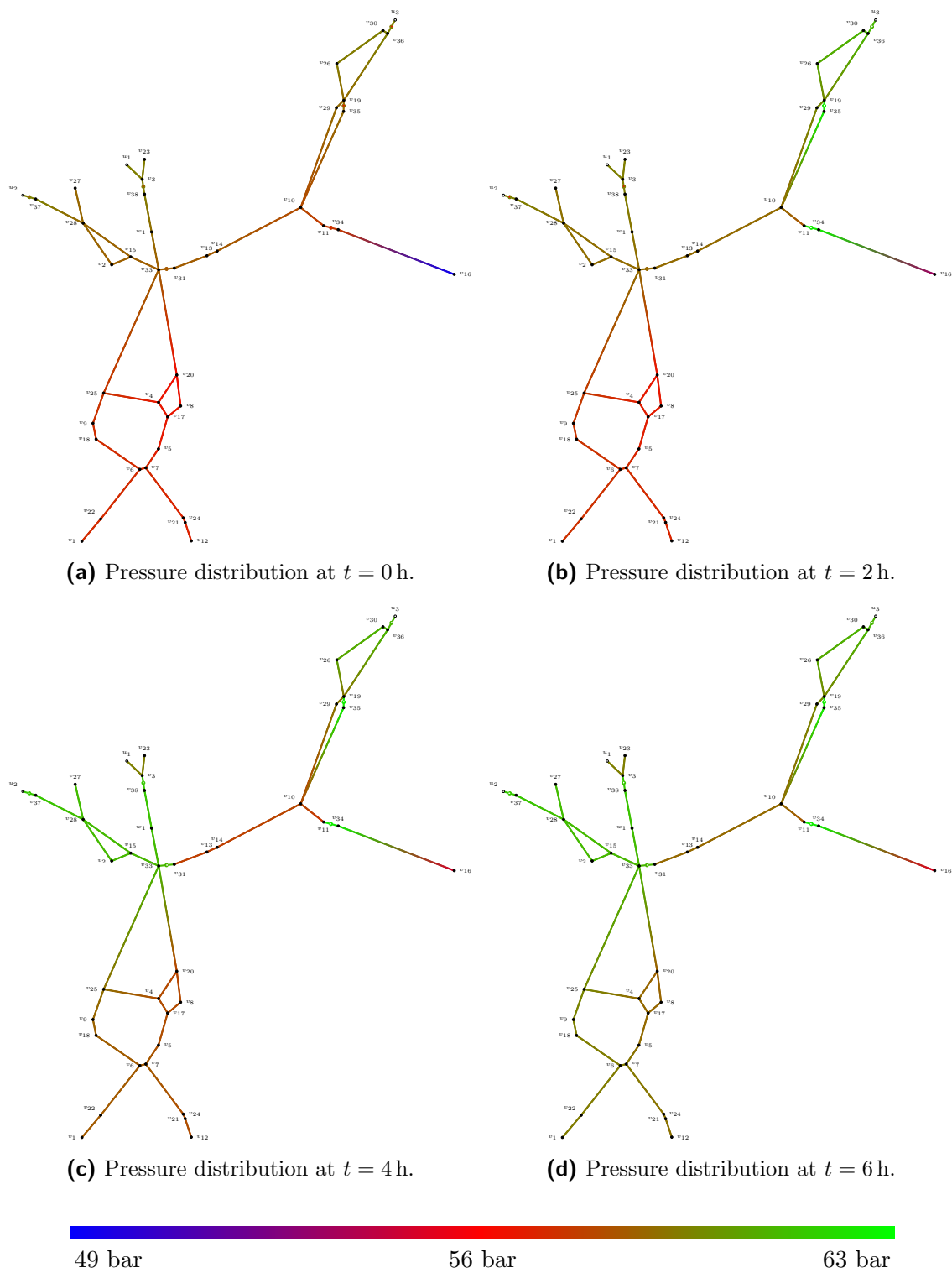


Figure 5.26: Pressure distribution over time for the GasLib-40.

### 5.4.3 GasLib-135

The GasLib-135 contains 135 nodes, six sources and 129 sinks, 144 pipes and 29 compressors. As for the GasLib-40, we had to make a slight modification to guarantee that Assumptions 4.11 are fulfilled.

1. The compressors  $e_{12}^C = (v_{100}, v_{102})$ ,  $e_{13}^C = (v_{101}, v_{102}) \in \mathcal{E}_C$  were replaced by  $e_{12}^C = (v_{100}, w_1)$  and  $e_{13}^C = (v_{101}, w_2)$  with additional pipes of short length  $(w_1, v_{102})$  and  $(w_2, v_{102})$  according to Section 4.4. This guarantees that there is at most one active element directed to any node in the network. For this purpose, we added the artificial nodes  $w_1$  and  $w_2$ .
2. The pipe  $e^P = (u_2, u_5)$  connecting two nodes in  $V_p$  was replaced by two pipes  $(u_2, w_3)$  and  $(u_5, w_3)$  of length  $\frac{\ell_{e^P}}{2}$ .

With the artificial nodes and additional pipes, the network contains 138 nodes, 147 pipes and 29 compressors. Figure 5.28 depicts the network topology. Figures 5.29 and 5.30 show the pressure distribution in the network at  $t = 0$  h and  $t = 12$  h. Due to a high demand in the lower part of the network, the pressure in that area was in a lower region (see Figure 5.29). By subsequently activating several compressors (see Figure 5.27), the pressure could be increased (see Figure 5.30). Table 5.4 contains the topology information regarding the active compressors.

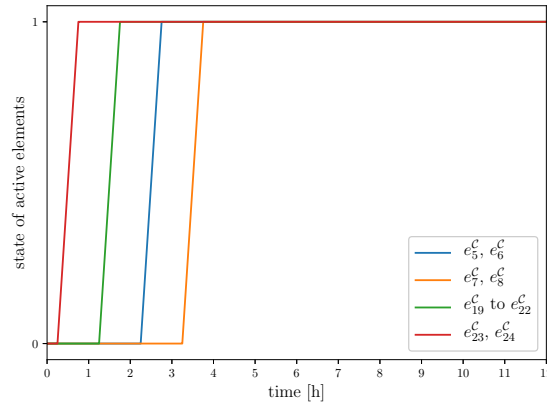


**Figure 5.27:** States of the compressors for the GasLib-135.

Compressor	Type	Compressor	Type
$e_5^C = (v_{58}, v_{108})$	Turbocompressor	$e_{20}^C = (v_{39}, v_{123})$	Turbocompressor
$e_6^C = (v_{58}, v_{109})$	Turbocompressor	$e_{21}^C = (v_{39}, v_{124})$	Turbocompressor
$e_7^C = (v_{29}, v_{110})$	Turbocompressor	$e_{22}^C = (v_{39}, v_{125})$	Turbocompressor
$e_8^C = (v_{29}, v_{111})$	Turbocompressor	$e_{23}^C = (v_{25}, v_{126})$	Turbocompressor
$e_{19}^C = (v_{39}, v_{122})$	Turbocompressor	$e_{24}^C = (v_{25}, v_{127})$	Turbocompressor

**Table 5.4:** Active compressor machines of the GasLib-135.

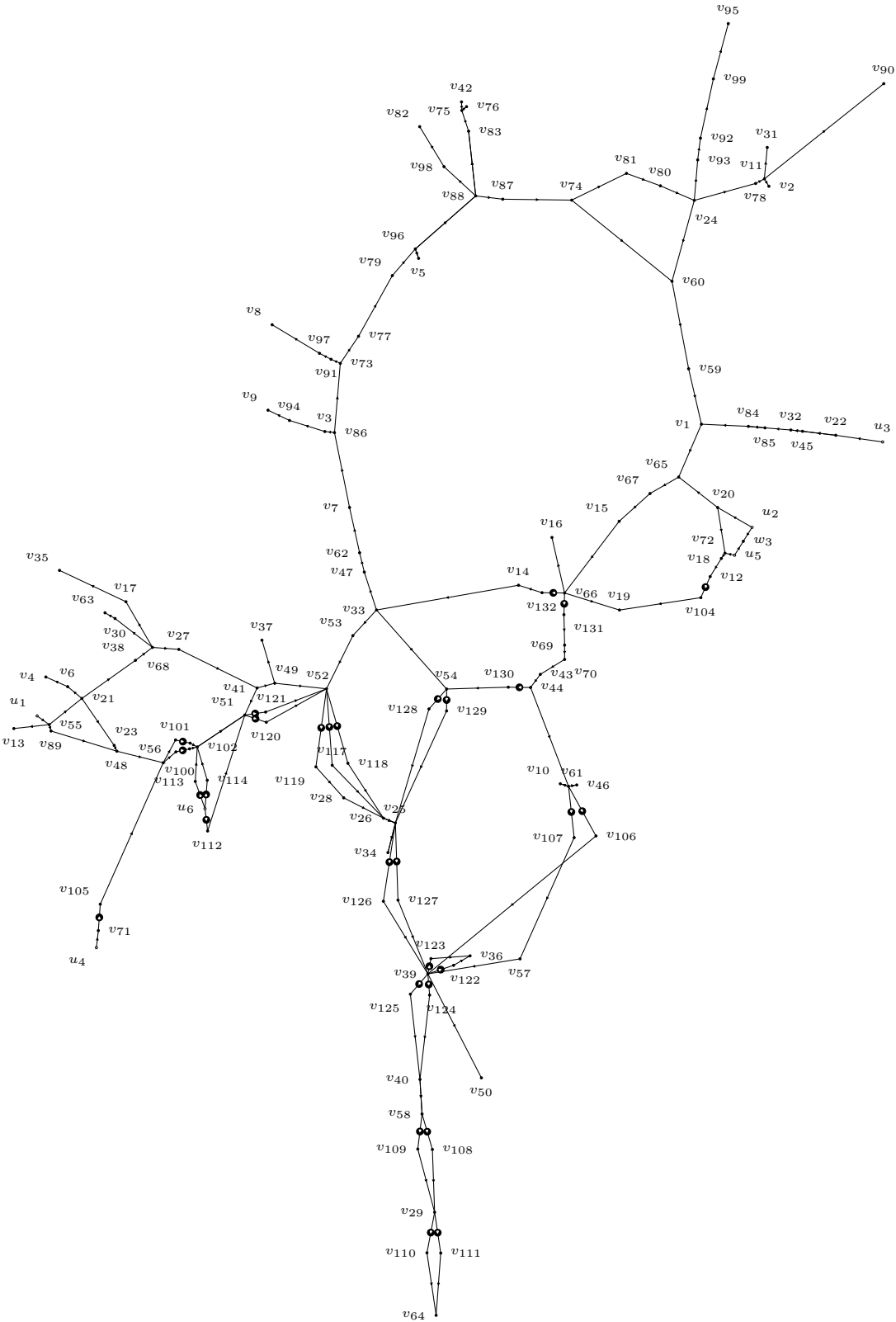
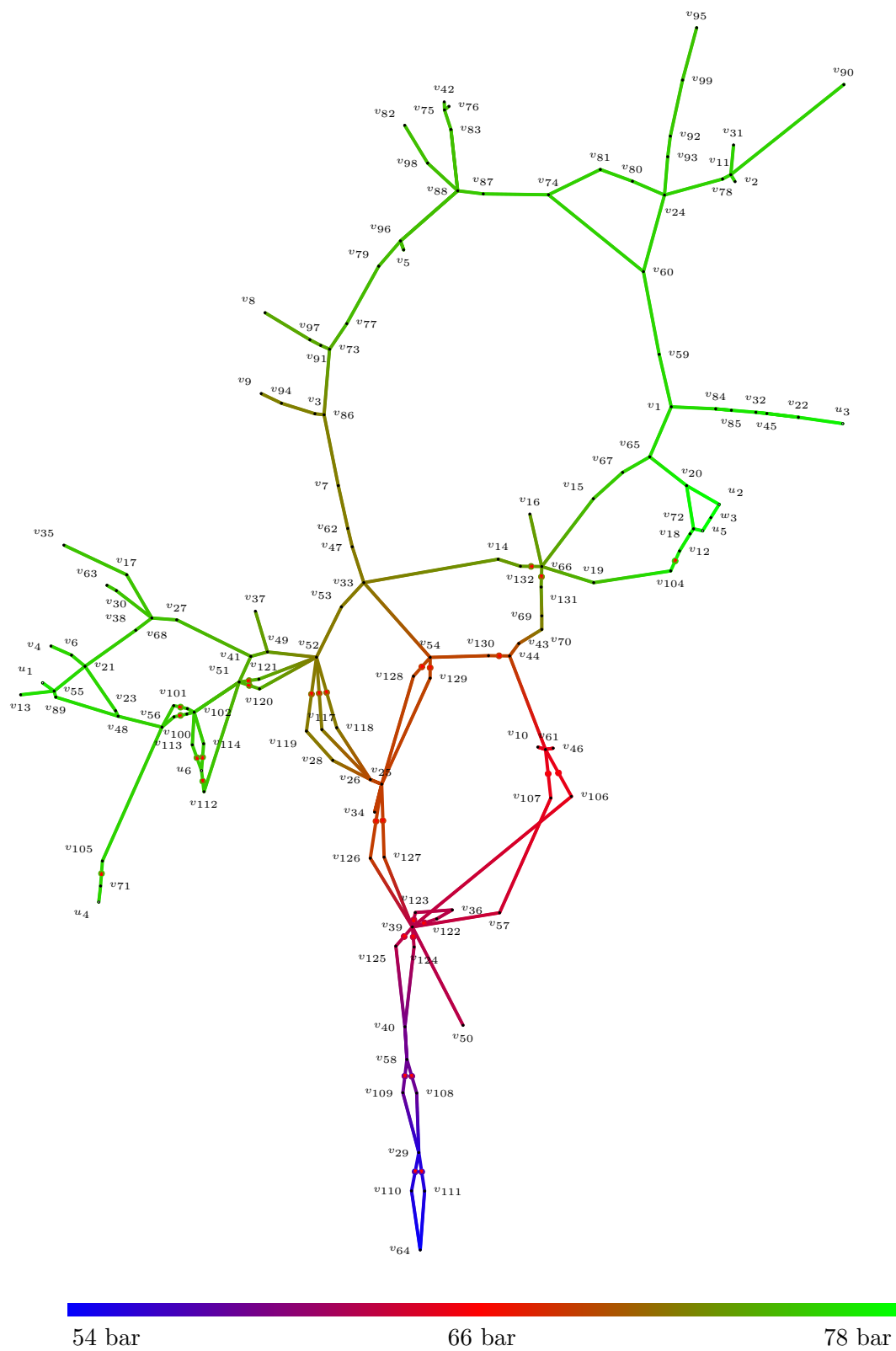


Figure 5.28: GasLib-135 network topology.





**Figure 5.29:** Pressure distribution over time for the GasLib-135 at  $t = 0$  h.

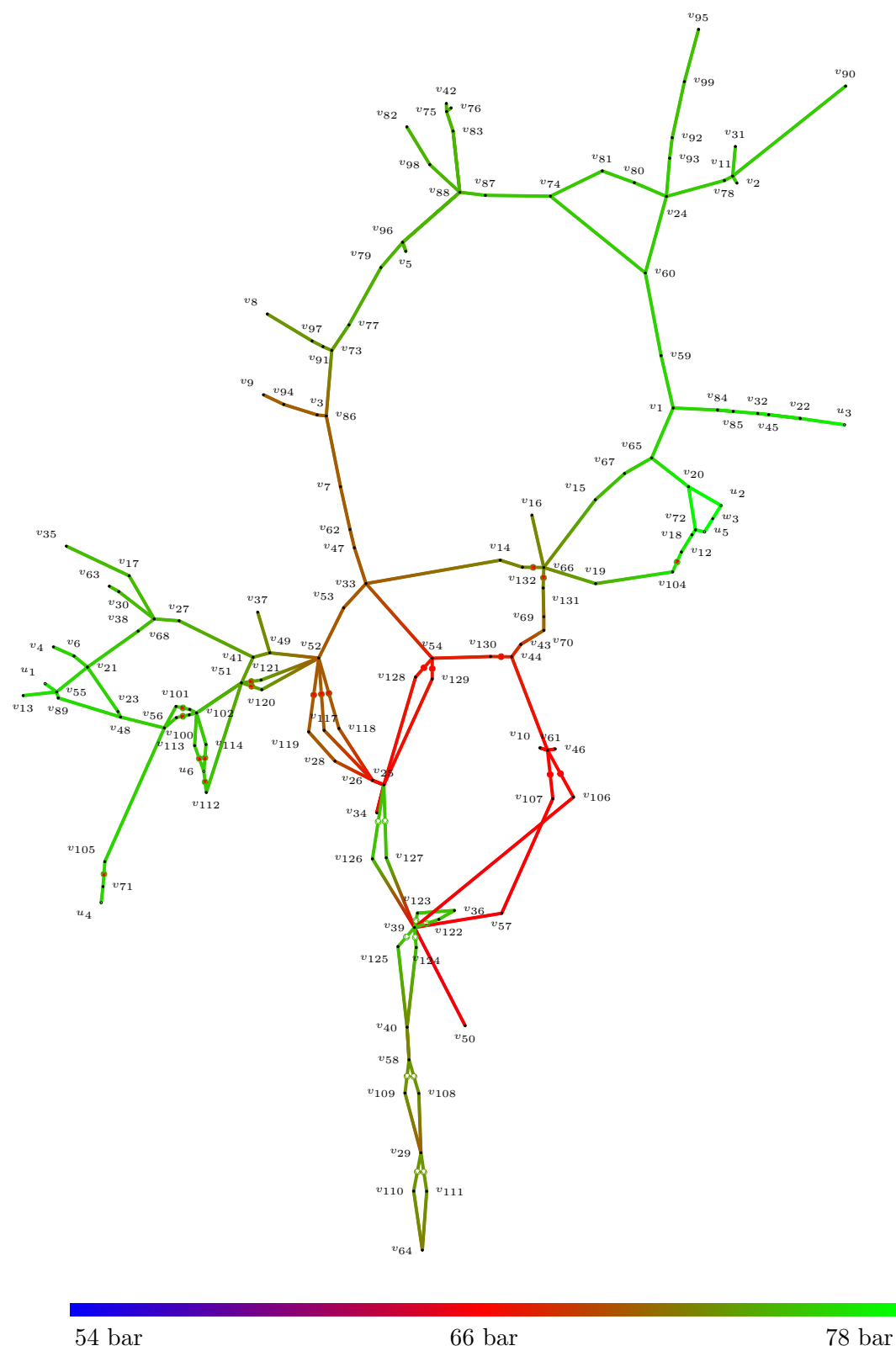


Figure 5.30: Pressure distribution over time for the GasLib-135 at  $t = 12$  h.

**Computational efficiency** We want to give some remarks regarding the numerical effort for solving the GasLib examples in this chapter, comparing the effort of solving the ODE system together with the decoupled algebraic equations, with the effort of solving the DAE system. Table 5.5 contains the respective dimensions of the systems, the simulation horizon and the Newton steps that were needed. For the comparison of the numerical effort, we have used a general linear method of up to order 3 with adaptive step size control. The relative error was set to  $10^{-4}$ .

GasLib-11 (Figure 5.13)				GasLib-11 (Figure 5.17)			
	Dimension	Interval	Newton		Dimension	Interval	Newton
ODE	17	[0, 8 h]	844	ODE	18/17	[0, 8 h]	3376
DAE	42	[0, 8 h]	873	DAE	44	[0, 8 h]	2312

GasLib-40				GasLib-135			
	Dimension	Interval	Newton		Dimension	Interval	Newton
ODE	72	[0, 8 h]	5057	ODE	247	[0, 12 h]	13848
DAE	151	[0, 8 h]	5126	DAE	571	[0, 12 h]	13752

**Table 5.5:** Comparison of numerical effort for solving the ODE and DAE system.

In all four examples, the dimension of the ODE system is significantly smaller than the dimension of the DAE system. Note that in Example 5.3, for solving the ODE, the simulation needed to be stopped at  $t = 1$  h and continued on a different ODE system after performing a pressure mapping (see Example 5.3). This introduced more oscillation into the system, which resulted in a higher computational effort. This also resulted in a 22% longer computational time compared to the time the DAE system needed to be solved.

For the other three examples, the needed Newton steps do not differ much. However, solving the ODE is more efficient in terms of computational time. Computing the numerical solution of the ODE system for the GasLib-11 (see Figure 5.13), combined with the time needed to compute the remaining algebraic variables, only required 84% of the computational time the DAE system needed. For the GasLib-40 and GasLib-135, solving the ODE needed 70% and 48% of the time compared to the DAE. The computational times for three scenarios stated in Table 5.5 can be found in Table 5.6.

	GasLib-11	GasLib-40	GasLib-135
ODE	6.46 s	85.58 s	633.92 s
DAE	7.73 s	121.48 s	1317.96 s

**Table 5.6:** Computational times for the GasLib-11 (Figure 5.13), GasLib-40 and GasLib-135.

The simulations were performed on a laptop computer with a 1.3 GHz Dual Core Intel Core M processor and 8 GB of RAM.

## 5.5 Conclusion

In this chapter, we have compared various numerical simulations of several instances from the GasLib and studied the impact of different spatial discretisations on the numerical solutions.

We compared the numerical solutions of three different DAEs resulting from different spatial discretisations: The topology-adapted discretisation we have introduced in Chapter 4, the implicit box scheme and a Galerkin discretisation. Furthermore, we demonstrated the advantages of the new, topology-adapted spatial discretisation, which yields good approximations, even at large spatial step sizes. In contrast to the topology-adapted DAE, the implicit box scheme and Galerkin discretisation are subject to the influence of derivatives of the boundary and coupling data. Thus, it required a finer spatial discretisation to achieve a valid approximation for these two methods. In addition, this behaviour indicates that the Galerkin discretisation proposed in [EKW17] yields a DAE of index 2. For a finer spatial discretisation, the topology-adapted discretisation and the Galerkin approach demonstrated a similar solution behaviour, whereas the implicit box schemes lead to solutions with a higher oscillation.

Furthermore, we compared numerical solutions of the DAE and the decoupled ODE we have introduced in Chapter 4 for two benchmarks based on the GasLib-11: One network only consisting of compressors and pipes and a second network that contains a valve. In the latter case, the ODE simulation needed to be stopped at the switching point and be continued on a slightly different ODE system to account for the change in topology due to the opening of the valve. This led to a difference in the solutions since in the DAE case the discontinuous opening is smoothed. In addition, this resulted in a higher computational effort for the ODE simulation, since the discontinuous behaviour of the valve introduced more oscillation into the network and more Newton steps were needed. Nevertheless, the offset in the solutions vanished asymptotically (see Figures 5.19 and 5.20).

In the last part of this chapter, we computed pressure distributions for the GasLib-11, GasLib-40 and GasLib-135 and compared the numerical effort needed for the computations. With exception of the example of the GasLib-11 that contained a valve, the ODE and DAE simulation needed a similar amount of Newton steps. However, the ODE system is of a significantly lower dimension in all examples, which resulted in a substantial gain in computational time of up to 52%. This could probably be improved further by using ODE specific solvers for the decoupled ODE system.

## 6 Conclusion and outlook

In this thesis, several aspects regarding mathematics in the context of gas networks were addressed. Our focus was on the modelling of gas networks as PDAEs and DAEs and the analysis of these systems.

We introduced the element models for the most common elements in gas networks like pipes, compressors and resistors. Even though the latter are merely artificial elements, they play an important role by substituting elements in front of and behind a compressor like preheaters and coolers. We also discussed the different types of nodes that appear in a network, and derived PDAE systems for gas pipe networks and gas networks that also include compressors and resistors. In addition, we put these two types of networks in an ADAE setting.

Furthermore, we studied properties of the ADAE describing gas pipe networks with special focus on the impact of perturbations. We explicitly allowed perturbations to affect all equations, in the differential part of the system but also in the algebraic part where boundary- and coupling conditions are modelled. The homogenisation we applied enabled us to derive a priori estimates for the solution of the perturbed and unperturbed PDAEs as well as for their first derivatives w.r.t. time. With these results, we were able to prove that only the perturbations themselves affect the solution of the perturbed PDAE but no derivatives of the perturbations. This estimate suggests a behaviour of the solution that is similar to perturbation index 1 as well as well-posedness. We only needed very general assumptions on the network topology to establish these results. In addition, we used the results to prove uniqueness of solutions.

The properties of the ADAE under the influence of perturbations motivated us to introduce a spatial discretisation that yields a DAE of index 1. This semi-discretisation is adapted to the network topology and depends on a proper orientation of the pipes in the network. In addition to the index 1 property, this discretisation enabled us to reformulate the DAE as a lower dimensional ODE system with a decoupled set of algebraic equations. Furthermore, the ODE system can be formulated from the topology and element information directly. We do not need to rely on certain projectors to derive the decoupled ODE, as it is often the case, e.g., [Gru<sup>+</sup>14] for gas networks, or in context of the tractability index in general. We mainly discussed networks under topology assumptions that are also fulfilled for some of the networks provided in the GasLib, but also illustrated possible extensions, that allow us to handle many GasLib-instances. Furthermore, the decoupled system can be used to compute consistent initial values for the DAE.

Finally, we demonstrated simulation results for the newly developed discretisation approach for several benchmark networks. Particularly, we compared the topology-adapted discretisation with well established, existing methods, that are used in the context of gas networks. We also compared the numerical solutions of the DAE and decoupled ODE

system for a network from the GasLib and computed pressure distribution for several benchmark networks. In general, solving the ODE system resulted in a significant gain regarding the computational time, compared to solving the DAE systems, at least for networks that do not contain valves.

Of course, there are directions for future research. The perturbation analysis from Chapter 3 could be extended to include non-linear algebraic equations modelling compressors and resistors. Due to the non-linearity, at least the homogenisation must be adapted somehow or one has to introduce another technique altogether, e.g., extending [AC16] to the Riemann system. Regarding the spatially discretised system, the inclusion of valves is an issue, since depending on the state of the valve, the decoupled ODE will change. Furthermore, it might also change the index of the DAE. Here, it might be fruitful to combine the semi-discretisation and the decoupling with a least-square collocation approach as in [Han<sup>+</sup>17], which works very well for linear DAEs of higher index.

## A Graph theory

Important properties and definitions from the theory of graphs that are needed for this thesis are summarized. For a more detailed overview, we refer to [Die10] or [Jun13].

**Definition A.1** (Graph). A *graph*  $\mathcal{G}$  is a tuple of finite sets  $\mathcal{G} = (V, \mathcal{E})$  so that  $\mathcal{E} \subseteq V \times V$  with  $|V|, |\mathcal{E}| < \infty$ . We call an element of the set  $V$  node and of the set  $\mathcal{E}$  edge, branch or arc.

**Definition A.2** (Digraph). A *directed graph*, or *digraph*, is a pair  $\mathcal{G} = (V, \mathcal{E})$ , where  $V$  is a (finite or countable) set and  $\mathcal{E}$  is a subset of  $V \times V$ . We refer to the elements of  $V$  and  $\mathcal{E}$  as nodes and edges, respectively. A digraph is said to be simple, if for any two elements  $u, v \in V$

(S1) at most one of the pairs  $e = (u, v)$ ,  $\bar{e} = (v, u)$  is an element of  $\mathcal{E}$  and

(S2) the pair  $(u, u)$  is not an element of  $\mathcal{E}$ .

Simple digraphs are called oriented graphs.

**Definition A.3** (Path). A set of  $n$  edges  $\{e_1, \dots, e_n\} \subseteq \mathcal{E}$  of a graph  $\mathcal{G}$  is called a *path* between nodes  $u$  and  $v$  if

(i) the edges  $e_i$  and  $e_{i+1}$  are incident,  $i \in \{1, \dots, n-1\}$ ,

(ii) each node is incident to at most two edges,

(iii) the nodes  $u$  and  $v$  belong to exactly one edge of the set.

**Definition A.4** (Connected graph). A graph is called a *connected graph* if there exists at least one path between any two nodes of the graph. Otherwise, we call the graph disconnected.

**Definition A.5** (Subgraph). A graph  $\mathcal{G}' := (V', \mathcal{E}')$  is called a *subgraph* of  $\mathcal{G}$  if  $V' \subseteq V$ ,  $\mathcal{E}' \subseteq \mathcal{E}$  and  $\mathcal{E}' \subseteq V' \times V'$ .

**Definition A.6** (Tree). A subgraph  $\mathcal{T}$  of a connected graph  $\mathcal{G}$  is called a *tree* if:

(i)  $\mathcal{T}$  is connected,

(ii)  $\mathcal{T}$  contains all nodes of  $\mathcal{G}$ ,

(iii)  $\mathcal{T}$  has no loops.

**Remark A.7** ([Die10, Propositions 1.5.6]). It is always possible to construct a tree for a connected graph.

**Definition A.8** (weighted Graph, [Mug14, Definition A.13]). A weighted digraph is a triple  $\mathcal{G} = (V, \mathcal{E}, \rho)$ , where  $(V, \mathcal{E})$  is a digraph and  $\rho: \mathcal{E} \rightarrow (0, \infty)$ . A weighted oriented graph is a weighted, simple digraph.

**Definition A.9** (Root). Let  $\mathcal{T} = (V, \mathcal{E})$  be a directed tree. Then we call the (unique) node  $u \in V$  with  $\delta^+(u) = \emptyset$  *root*.



## B DAE theory

This part of the appendix introduces basic definitions and results from the theory of differential algebraic equations. For a more detailed introduction, we refer the reader to [LMT13] or [KM06].

**Definition B.1** (DAE in standard form). Let  $(x, t) \in \mathcal{D} \times \mathcal{I}$  with  $\mathcal{D} \subset \mathbb{R}^n$  and  $\mathcal{I} \subset \mathbb{R}$ . We call the implicit system

$$f(x'(t), x(t), t) = 0 \quad (\text{B.1})$$

a DAE in standard form, if  $f \in \mathcal{C}(\mathbb{R}^n \times \mathcal{D} \times \mathcal{I}, \mathbb{R}^n)$ , the continuous partial derivatives  $f_x(y, x, t)$  and  $f_y(y, x, t)$  exist and, in addition, the partial derivative  $f_y(y, x, t)$  is singular with constant rank for all  $(y, x, t) \in \mathbb{R}^n \times \mathcal{D} \times \mathcal{I}$ .

**Definition B.2** (Properly stated leading term). Let the DAE

$$f(d(x(t), t)', x(t), t) = 0 \quad (\text{B.2})$$

satisfy the following assumptions:

- $f: \mathbb{R}^n \times \mathcal{D}_f \times \mathcal{I} \rightarrow \mathbb{R}^k$  is continuous on the open set  $\mathbb{R}^n \times \mathcal{D}_f \times \mathcal{I} \subseteq \mathbb{R}^n \times \mathbb{R}^m \times \mathbb{R}$  and has continuous partial derivatives  $f_y, f_x$  with respect to the first two variables  $y \in \mathbb{R}^n, x \in \mathcal{D}_f$ .
- The function  $d: \mathcal{D}_f \times \mathcal{I} \rightarrow \mathbb{R}^n$  is continuously differentiable.

Then the DAE has on  $\mathcal{D}_f \times \mathcal{I}$  a *properly involved derivative*, also called a *properly stated leading term*, if  $\text{im } d_x$  and  $\ker f_y$  are  $\mathcal{C}^1$ -subspaces in  $\mathbb{R}^n$ , and the transversality condition

$$\ker f_y(y, x, t) \oplus \text{im } d_x(x, t) = \mathbb{R}^n, \quad (y, x, t) \in \mathbb{R}^n \times \mathcal{D}_f \times \mathcal{I}$$

holds.

**Definition B.3** (Linear DAE with constant coefficients). Let the DAE in standard form (B.1) be given by

$$Ex'(t) + Fx(t) + q(t) = 0$$

with matrices  $E, F \in \mathbb{R}^{n \times n}$  and  $q \in \mathcal{C}(\mathcal{I}, \mathbb{R}^n)$ . We call such a DAE a *linear DAE with constant coefficients*.

**Definition B.4** (Quasi linear DAE with properly stated leading term). Let the DAE with properly stated leading term (B.2) be given by

$$f(y, x, t) = A(x, t)y + b(x, t), \quad d(x, t) = D(t)x.$$

Then the resulting DAE is a so called *quasi-linear DAE* with properly stated leading term of the form

$$A(x(t), t) (d(x(t), t))' + b(x(t), t) = 0. \quad (\text{B.3})$$

## C Functionanal analysis

We formulate the following inequalities which are used in functional analysis and can be found in [Eva10].

**Theorem C.1** (Gronwall's inequality (integral form)). Let  $\xi(t)$  be a non-negative, summable function on  $\mathcal{I}$  which satisfies for a.e.  $t$  the integral inequality

$$\xi(t) \leq C_1 + C_2 \int_{t_0}^t \xi(\tau) d\tau$$

for constants  $C_1, C_2 > 0$ . Then

$$\xi(t) \leq C_1(1 + C_2 t e^{C_2 t})$$

for a.e.  $t \in \mathcal{I}$ .

**Theorem C.2** (Cauchy's inequality). For  $a, b \in \mathbb{R}$  it holds that

$$ab \leq \frac{a^2}{2} + \frac{b^2}{2}.$$

**Theorem C.3** (Hölder's inequality). Assume  $1 \leq p, q \leq \infty$ ,  $\frac{1}{p} + \frac{1}{q} = 1$ . Then if  $f \in L_p(\Omega)$ ,  $g \in L_q(\Omega)$  we have

$$\int_{\Omega} |fg| dx \leq \|f\|_{L_p(\Omega)} \|g\|_{L_q(\Omega)}.$$



# Notation

## Abbreviations

a.e.	almost everywhere
ADAE	abstract differential-algebraic equation
AGA	American Gas Association
BVP	boundary value problem
DAE	differential-algebraic equation
e.g.	exempli gratia
f.a.a.	for almost all
i.e.	id est
IVP	initial value problem
MOL	method of lines
MOR	model order reduction
ODE	ordinary differential equation
PDAE	partial differential-algebraic equation
PDE	partial differential equation
w.r.t.	with respect to

## General

$\exists$	there exists
$\forall$	for all
$\mathcal{I}$	$= [t_0, T]$ time interval
$\mathbb{N}$	natural numbers
$\mathbb{R}$	real numbers
$\mathbb{R}^n$	real n-dimensional space
$I_n \in \mathbb{R}^{n \times n}$	identity matrix
$A \in \mathbb{R}^{n \times m}$	real matrix with $n$ rows and $m$ columns
$A^\top \in \mathbb{R}^{m \times n}$	transpose of $A$
$\text{diag}(a_1, \dots, a_n)$	diagonal matrix with entries $a_i, i = 1, \dots, n$
$\ker A$	kernel of $A$
$\text{im } A$	image of $A$
$S, U$	sets
$x \in S$	$x$ is an element of the set $S$
$x \notin S$	$x$ is not an element of $S$
$S \subset U$	$S$ is a subset of $U$
$S \cup U$	union of $S$ and $U$
$S \cap U$	intersection of $S$ and $U$
$ S $	number of elements in $S$
$f: S \rightarrow U$	map from $S$ to $U$

$f', \frac{d}{dt}f$	derivative of $f: \mathcal{I} \rightarrow U$
$\partial_x f(x, y), f_x(x, y)$	partial derivative of $f$ w.r.t. $x$
$\nabla f$	gradient of $f$
$\mathcal{C}(\mathcal{I}, \mathbb{R})$	space of continuous functions $f: \mathcal{I} \rightarrow \mathbb{R}$
$\mathcal{C}^k(\mathcal{I}, \mathbb{R})$	space of k-times continuously differentiable functions $f: \mathcal{I} \rightarrow \mathbb{R}$
$\mathcal{C}_0^\infty(\Omega)$	space of infinitely continuously differentiable functions $f: \Omega \rightarrow \mathbb{R}$ with compact support
$L_p(\Omega)$	space of p-integrable functions $f: \Omega \rightarrow \mathbb{R}$ ( $p \geq 1$ )
$L_{1,\text{loc}}(\Omega)$	space of locally integrable functions
$H^1(\Omega)$	Sobolev space of all functions $f \in L_2(\Omega)$ with weak derivatives in $L_2(\Omega)$
$V, W$	Banach spaces
$V^*$	dual space of $V$
$\ \cdot\ _V$	norm on $V$
$H$	Hilbert space
$(\cdot \cdot)_H$	scalar product on $H$
$\mathcal{C}(\mathcal{I}, V)$	space of continuous functions $f: \mathcal{I} \rightarrow V$
$\mathcal{C}^k(\mathcal{I}, V)$	space of k-times continuously differentiable functions $f: \mathcal{I} \rightarrow V$
$\mathfrak{G} = (V, \mathcal{E}, \ell)$	weighted graph with nodes $V$ , arcs $\mathcal{E}$ and weights $\ell \in \mathbb{R}^{ \mathcal{E} }$
$L_p(\mathfrak{G})$	Sobolev space of functions $f = (f_1, \dots, f_{ \mathcal{E} })$ with $f_i \in L_p([0, \ell_i])$
$H^1(\mathfrak{G})$	Sobolev space of functions $f = (f_1, \dots, f_{ \mathcal{E} })$ with $f_i \in H^1([0, \ell_i])$
$\ \cdot\ _{\mathfrak{G}} = \ \cdot\ _{L_2(\mathfrak{G})}$	norm on $L_2(\mathfrak{G})$
$(\cdot \cdot)_{\mathfrak{G}} = (\cdot \cdot)_{L_2(\mathfrak{G})}$	scalar product on $L_2(\mathfrak{G})$

### Gas networks

$V$	set of nodes
$\mathcal{E}$	set of branch elements
$\mathcal{G} = (V, \mathcal{E})$	graph with node set $V$ and arc set $\mathcal{E}$
$\mathcal{T} = (V_{\mathcal{T}}, \mathcal{E}_{\mathcal{T}})$	tree with node set $V_{\mathcal{T}}$ and arc set $\mathcal{E}_{\mathcal{T}}$
$V_p$	set of sources
$V_q$	set of sinks
$V_A$	set of nodes that have a resistor or compressor directed towards them
$V_{\mathcal{P}}$	$= V_q \setminus V_A$ , set of sinks that have no resistor or compressor directed towards them
$\mathcal{E}_{\mathcal{P}}$	set of pipes
$\mathcal{E}_A$	$= \mathcal{E} \setminus \mathcal{E}_{\mathcal{P}}$ , set of non-pipe branch elements
$\mathcal{E}_{\mathcal{C}}$	set of compressors
$\mathcal{E}_{\mathcal{R}}$	set of resistors
$\mathcal{E}_{\mathcal{S}}$	set of valves
$u, v$	nodes $u, v \in V$
$e$	arc, branch or edge of a network $e \in \mathcal{E}$
$e^{\mathcal{P}}$	pipe $e^{\mathcal{P}} \in \mathcal{E}_{\mathcal{P}}$
$e^{\mathcal{C}}$	compressor $e^{\mathcal{C}} \in \mathcal{E}_{\mathcal{C}}$
$e^{\mathcal{R}}$	resistor $e^{\mathcal{R}} \in \mathcal{E}_{\mathcal{R}}$
$e^{\mathcal{S}}$	valve $e^{\mathcal{S}} \in \mathcal{E}_{\mathcal{S}}$
$p$	pressure
$\rho$	density

---

$\nu$	velocity
$q$	mass flow
$p_u(t)$	pressure at node $u$
$p_p(t)$	vector of pressures at nodes $u \in V_p$
$p_{\mathcal{P}}(t)$	vector of pressures at nodes $u \in V_{\mathcal{P}}$
$p_{\mathcal{A}}(t)$	vector of pressures at nodes $u \in V_{\mathcal{A}}$
$q_{e^{\mathcal{P}}}(x, t)$	mass flow through pipe $e^{\mathcal{P}}$
$q_{e^{\mathcal{P}},r}(t) = q_{e^{\mathcal{P}}}(\ell, t)$	right pipe mass flow
$q_{e^{\mathcal{P}},l}(t) = q_{e^{\mathcal{P}}}(0, t)$	left pipe mass flow
$q_{e^c}(t)$	mass flow through compressor $e^c$
$H_{e^c}$	adiabatic enthalpy of a compressor
$Q_{e^c}$	volumetric flow rate along a compressor
$n_{e^c}$	speed of a compressor
$M_{e^c}$	torque shaft of a piston compressor
$\eta_{e^c}$	efficiency of a turbo compressor
$q_{e^{\mathcal{R}}}(t)$	mass flow through resistor $e^{\mathcal{R}}$
$q_{e^{\mathcal{S}}}(t)$	mass flow through valve $e^{\mathcal{S}}$
$q_r(t)$	vector of pipe mass flows at $x = \ell$
$q_l(t)$	vector of pipe mass flows at $x = 0$
$q_c(t)$	vector of compressor mass flows
$q_{\mathcal{R}}(t)$	vector of resistor mass flows
$q_{\mathcal{S}}(t)$	vector of valve mass flows
$q_{\mathcal{A}}$	vector of active elements mass flows
$\delta^+(u)$	set of ingoing arcs at node $u$ .
$\delta^-(u)$	set of outgoing arcs at node $u$ .
$A_r$	incidence matrix for the right pipe mass flows
$A_l$	incidence matrix for the left pipe mass flows
$A_c$	incidence matrix for the compressor mass flows
$A_{\mathcal{R}}$	incidence matrix for the resistor mass flows
$A_{\mathcal{S}}$	incidence matrix for the valve mass flows
$A_{\mathcal{A}}$	incidence matrix for the active element mass flows
$a$	cross-sectional area of a pipe
$D$	diameter of a pipe
$\lambda$	friction coefficient of a pipe
$k$	roughness of a pipe wall
$\kappa$	isentropic exponent
$R_s$	specific gas constant
$T_m$	gas temperature
$T_c$	critical gas temperature
$p_c$	critical gas pressure
$z$	compressibility factor
$Re$	Reynolds number
$c$	speed of sound
$g$	gravity constant
$h'$	elevation





## Bibliography

- [AC16] J. Alexandre dit Sandretto and A. Chapoutot. “Validated Simulation of Differential Algebraic Equations with Runge-Kutta Methods”. In: *Reliable Computing electronic edition* 22 (2016).
- [Alt15] R. Altmann. “Regularization and simulation of constrained partial differential equations”. PhD thesis. Technische Universität Berlin, 2015. DOI: 10.14279/depositonce-4491.
- [AR07] L. Angermann and J. Rang. “Perturbation index of linear partial differential-algebraic equations with a hyperbolic part”. In: *Central European Journal of Mathematics* 5.1 (2007), pp. 19–49. DOI: 10.2478/s11533-006-0035-4.
- [Arn98] M. Arnold. “A note on the uniform perturbation index”. In: *Rostock. Math. Kollo.* 52 (1998), pp. 33–46.
- [BCP95] K.E. Brenan, S.L. Campbell, and L.R. Petzold. *Numerical Solution of Initial-Value Problems in Differential-Algebraic Equations*. Society for Industrial and Applied Mathematics, 1995. DOI: 10.1137/1.9781611971224.
- [Ben<sup>+</sup>18] P. Benner, S. Grundel, C. Himpe, C. Huck, T. Streubel, and C. Tischendorf. “Gas Network Benchmark Models”. In: *to appear in DAE-Form* (2018).
- [BGH11] J. Brouwer, I. Gasser, and M. Herty. “Gas Pipeline Models Revisited: Model Hierarchies, Nonisothermal Models, and Simulations of Networks”. In: *Multiscale Modeling & Simulation* 9.2 (2011), pp. 601–623. DOI: 10.1137/100813580.
- [BKL09] P. Bales, O. Kolb, and J. Lang. “Hierarchical Modelling and Model Adaptivity for Gas Flow on Networks”. In: *Computational Science – ICCS 2009: 9th International Conference Baton Rouge, LA, USA, May 25-27, 2009 Proceedings, Part I*. Ed. by G. Allen, J. Nabrzyski, Seidel, G.D. van Albada, J. Dongarra, and P.M.A. Sloot. Berlin, Heidelberg: Springer Berlin Heidelberg, 2009, pp. 337–346. DOI: 10.1007/978-3-642-01970-8\_33.
- [Bod07] M. Bodestedt. “Perturbation Analysis of Refined Models in Circuit Simulation”. PhD thesis. Technische Universität Berlin, 2007. DOI: 10.14279/depositonce-1749.
- [Cam87] S.L. Campbell. “A General Form for Solvable Linear Time Varying Singular Systems of Differential Equations”. In: *SIAM Journal on Mathematical Analysis* 18.4 (1987), pp. 1101–1115. DOI: 10.1137/0518081.
- [CG95a] S.L. Campbell and C.W. Gear. “The index of general nonlinear DAEs”. In: *Numerische Mathematik* 72.2 (1995), pp. 173–196. DOI: 10.1007/s002110050165.
- [CG95b] S.L. Campbell and E. Griepentrog. “Solvability of General Differential Algebraic Equations”. In: *SIAM Journal on Scientific Computing* 16.2 (1995), pp. 257–270. DOI: 10.1137/0916017.

- [CM96] S.L. Campbell and W. Marszalek. “ODE/DAE integrators and MOL problems”. In: *Zeitschrift für Angewandte Mathematik und Mechanik* 76 (1996), pp. 251–254.
- [CM99] S.L. Campbell and W. Marszalek. “The Index of an Infinite Dimensional Implicit System”. In: *Mathematical and Computer Modelling of Dynamical Systems* 5.1 (1999), pp. 18–42. DOI: 10.1076/mcmd.5.1.18.3625.
- [Die10] R. Diestel. *Graph Theory (5th Edition)*. Graduate texts in mathematics. Springer, 2010.
- [DKL11] P. Domschke, O. Kolb, and J. Lang. “Adjoint-Based Control of Model and Discretization Errors for Gas and Water Supply Networks”. In: *Computational Optimization and Applications in Engineering and Industry*. Ed. by Xin-She Yang and Slawomir Koziel. Berlin, Heidelberg: Springer Berlin Heidelberg, 2011, pp. 1–17. DOI: 10.1007/978-3-642-20986-4\_1.
- [Dom<sup>+</sup>17] P. Domschke, B. Hiller, J. Lang, and C. Tischendorf. “Modellierung von Gasnetzwerken: Eine Übersicht”. 2017. URL: <https://opus4.kobv.de/opus4-trr154/frontdoor/index/index/docId/191>.
- [Egg16] H. Egger. “A mixed variational discretization for non-isothermal compressible flow in pipelines”. 2016. URL: <https://arxiv.org/abs/1611.03368v1>.
- [EK18] H. Egger and T. Kugler. “Damped wave systems on networks: exponential stability and uniform approximations”. In: *Numerische Mathematik* 138.4 (2018), pp. 839–867. DOI: 10.1007/s00211-017-0924-4.
- [EKW17] H. Egger, T. Kugler, and W. Wollner. “Numerical optimal control of stationary gas transport with control and state constraints”. 2017. URL: <https://opus4.kobv.de/opus4-trr154/frontdoor/index/index/docId/214>.
- [Eva10] L.C. Evans. *Partial Differential Equations*. Ed. by 2nd. American Mathematical Society, 2010.
- [Fei93] M. Feistauer. *Mathematical Methods in Fluid Dynamics*. Monographs and Surveys in Pure and Applied Mathematics. Taylor & Francis, 1993.
- [FF09] E.J. Finnemore and J.B. Franzini. *Fluid Mechanics with Engineering Applications*. 10th ed. Asia Higher Education Engineering/Computer Science Civil Engineering. McGraw-Hill Higher Education, 2009.
- [Gan70] F.R. Gantmacher. *Matrizenrechnung I+II*. VEB Deutscher Verlag der Wissenschaften, 1970.
- [Gea88] C.W. Gear. “Differential-Algebraic Equation Index Transformations”. In: *SIAM Journal on Scientific and Statistical Computing* 9.1 (1988), pp. 39–47. DOI: 10.1137/0909004.
- [GHM92] E. Griepentrog, M. Hanke, and R. März. “Toward a better understanding of differential algebraic equations (Introductory survey)”. In: (1992). Ed. by Eberhard Griepentrog, Michael Hanke, and Roswitha März. DOI: 10.18452/2513.
- [GHP81] C.W. Gear, H.H. Hsu, and L.R. Petzold. “Differential-Algebraic Equations Revisited”. In: *Proceedings from the meeting on Numerical Methods for Solving Stiff Initial Value Problems. Oberwolfach*. (1981).
- [GM86] E. Griepentrog and R. März. *Differential-algebraic equations and their numerical treatment*. Teubner-Texte zur Mathematik. BSB Teubner, 1986.

- [GP83] C.W. Gear and L.R. Petzold. “Differential/algebraic systems and matrix pencils”. In: *Matrix Pencils*. Ed. by Bo Kågström and Axel Ruhe. Vol. 973. Berlin, Heidelberg: Springer Berlin Heidelberg, 1983, pp. 75–89.
- [Gru<sup>+</sup>14] S. Grundel, L. Jansen, N. Hornung, T. Clees, C. Tischendorf, and P. Benner. “Model Order Reduction of Differential Algebraic Equations Arising from the Simulation of Gas Transport Networks”. In: *Progress in Differential-Algebraic Equations*. Differential-Algebraic Equations Forum. Springer, 2014, pp. 183–205. DOI: 10.1007/978-3-662-44926-4\_9.
- [GU17] M. Gugat and S. Ulbrich. “The isothermal Euler equations for ideal gas with source term: Product solutions, flow reversal and no blow up”. In: *Journal of Mathematical Analysis and Applications* 454.1 (2017), pp. 439–452. DOI: 10.1016/j.jmaa.2017.04.064.
- [Gün00] M. Günther. “Semidiscretization may act like a deregularization”. In: *Mathematics and Computers in Simulation* 53.4-6 (2000), pp. 293–301. DOI: 10.1016/S0378-4754(00)00216-0.
- [Han<sup>+</sup>17] M. Hanke, R. März, C. Tischendorf, E. Weinmüller, and S. Wurm. “Least-squares collocation for linear higher-index differential-algebraic equations”. In: *Journal of Computational and Applied Mathematics* 317 (2017), pp. 403–431. ISSN: 0377-0427. DOI: 10.1016/j.cam.2016.12.017.
- [Hei14] J. Heiland. “Decoupling and optimization of differential-algebraic equations with application in flow control”. PhD thesis. Technische Universität Berlin, 2014. DOI: 10.14279/depositonce-4069.
- [Her<sup>+</sup>09] A. Herrán-González, J.M. De La Cruz, B. De Andrés-Toro, and J.L. Risco-Martín. “Modeling and simulation of a gas distribution pipeline network”. In: *Applied Mathematical Modelling* 33.3 (2009), pp. 1584–1600. DOI: 10.1016/j.apm.2008.02.012.
- [Her07] M. Herty. “Modeling, Simulation and Optimization of Gas Networks with Compressors”. In: *Networks and Heterogenous Media* 2.1 (2007), pp. 81–97. DOI: 10.3934/nhm.2007.2.81.
- [Her08] M. Herty. “Coupling Conditions for Networked Systems of Euler Equations”. In: *SIAM Journal on Scientific Computing* 30.3 (2008), pp. 1596–1612. DOI: 10.1137/070688535.
- [HLR89] E. Hairer, C. Lubich, and M. Roche. *The Numerical Solution of Differential-Algebraic Systems by Runge-Kutta Methods*. Lecture Notes in Mathematics. Springer Berlin Heidelberg, 1989. ISBN: 978-3-540-51860-0. DOI: 10.1007/BFb0093947.
- [HSW16] B. Hiller, R. Saitenmacher, and T. Walther. “Analysis of Operating Modes of Complex Compressor Stations”. In: *Operations Research Proceedings 2016*. Springer International Publishing, 2016. DOI: 10.1007/978-3-319-55702-1\_34.
- [HT17] C. Huck and C. Tischendorf. “Transient Modeling and Simulation of Gas Pipe Networks with Characteristic Diagram Models for Compressors”. In: *PAMM*. Wiley-VCH Verlag, 2017, pp. 707–708. DOI: 10.1002/pamm.201710322.

- [Hum<sup>+</sup>17] J. Humpala, I. Joorman, N. Kanelakis, D. Oucherif, M. E. Pfetsch, L. Schewe, M. Schmidt, R. Schwarz, and M. Sirvent. *GasLib – A Library of Gas Network Instances*. Tech. rep. 2017. URL: [http://www.optimization-online.org/DB\\_HTML/2015/11/5216.html](http://www.optimization-online.org/DB_HTML/2015/11/5216.html).
- [HW17] B. Hiller and T. Walther. *Modelling compressor stations in gas networks*. Tech. rep. Zuse-Institut Berlin (ZIB), 2017.
- [Jac<sup>+</sup>08] D.P. Jacobs, C.M.S. Machado, E.C. Pereira, and V. Trevisan. “Computing the Inverse of a Tree’s Incidence Matrix”. In: 189 (2008), pp. 169–176.
- [Jan15] L. Jansen. “A Dissection concept for DAEs”. PhD thesis. Humboldt-Universität zu Berlin, Mathematisch-Naturwissenschaftliche Fakultät I, 2015. DOI: 10.18452/17166.
- [Jun13] D. Jungnickel. *Graphs, Networks and Algorithms*. 4th. Springer Publishing Company, Incorporated, 2013.
- [Kas05] H. Kastner. “AGA 8 gegen SGERG-88: Korrelative Energiemessung von abgereicherten (unnatürlichen) Erdgasen”. In: *Das Gas- und Wasserfach. Ausgabe Gas, Erdgas* 146.12 (2005), pp. 676–679.
- [KLB10] O. Kolb, J. Lang, and P. Bales. “An implicit box scheme for subsonic compressible flow with dissipative source term”. In: *Numerical Algorithms* 53.2 (2010), pp. 293–307. ISSN: 1572-9265. DOI: 10.1007/s11075-009-9287-y.
- [KM06] P. Kunkel and V. Mehrmann. *Differential-algebraic Equations: Analysis and Numerical Solution*. EMS textbooks in mathematics. European Mathematical Society, 2006.
- [Koc<sup>+</sup>15] T. Koch, B. Hiller, M. Pfetsch, and L. Schewe. *Evaluating Gas Network Capacities*. Ed. by Marc E. Pfetsch, Thorsten Koch, Lars Schewe, and Benjamin Hiller. Philadelphia, PA: Society for Industrial and Applied Mathematics, 2015. DOI: 10.1137/1.9781611973693.
- [Krö97] D. Kröner. *Numerical Schemes for Conservation Laws*. Advances in numerical mathematics. Wiley-VCH Verlag, 1997.
- [LeV02] Randall J. LeVeque. *Finite Volume Methods for Hyperbolic Problems*. Cambridge Texts in Applied Mathematics. Cambridge University Press, 2002. DOI: 10.1017/CB09780511791253.
- [LM18] J. Lang and P. Mindt. “Entropy-Preserving Coupling Conditions for One-dimensional Euler Systems at Junctions”. In: *Networks and Heterogenous Media* 13.1 (2018), pp. 177–190. DOI: 10.3934/nhm.2018008.
- [LMT05] R. Lamour, R. März, and C. Tischendorf. *PDAEs and Further Mixed Systems as Abstract Differential Algebraic Systems*. Humboldt-Universität zu Berlin, Mathematisch-Naturwissenschaftliche Fakultät II, Institut für Mathematik, 2005. DOI: 10.18452/2636.
- [LMT13] R. Lamour, R. März, and C. Tischendorf. *Differential-algebraic equations. A projector based analysis*. English. Berlin: Springer, 2013, pp. xxvii + 649.
- [LRS86] M.M. Lavrent’ev, V.G. Romanov, and S.P. Shishatskiĭ. *Ill-posed Problems of Mathematical Physics and Analysis*. Translations of Mathematical Monographs. American Mathematical Society, 1986.

- [LSE99] W. Lucht, K. Strehmel, and C. Eichler-Liebenow. “Indexes and Special Discretization Methods for Linear partial Differential Algebraic Equations”. In: *BIT Numerical Mathematics* 39.3 (1999), pp. 484–512. DOI: 10.1023/A:1022370703243.
- [Lur08] M.V. Lurie. *Modeling of Oil Product and Gas Pipeline Transportation*. Wiley-VCH Verlag GmbH Co. KGaA, 2008.
- [Mär15] R. März. “Differential-Algebraic Equations from a Functional-Analytic Viewpoint: A Survey”. In: *Surveys in Differential-Algebraic Equations II. Differential-Algebraic Equations Forum*. Ed. by A Ilchmann and T Reis. Springer, Cham, 2015. DOI: 10.1007/978-3-319-11050-9\_4.
- [Mat12] M. Matthes. *Numerical Analysis of Nonlinear Partial Differential-algebraic Equations: A Coupled and an Abstract Systems Approach*. Logos Verlag Berlin, 2012.
- [MB00] W.S. Martinson and P.I. Barton. “A Differentiation Index for Partial Differential-Algebraic Equations”. In: *SIAM Journal on Scientific Computing* 21.6 (2000), pp. 2295–2315. DOI: 10.1137/S1064827598332229.
- [Meh15] Volker Mehrmann. “Index Concepts for Differential-Algebraic Equations”. In: *Encyclopedia of Applied and Computational Mathematics*. Ed. by Björn Engquist. Berlin, Heidelberg: Springer Berlin Heidelberg, 2015, pp. 676–681. DOI: 10.1007/978-3-540-70529-1\_120.
- [MFH16] J. Mischner, H.G. Fasold, and J. Heymor. *gas2energy.net*. DIV, 2016.
- [Mug14] D. Mugnolo. *Semigroup methods for evolution equations on networks*. Springer, Cham, 2014.
- [OGE15] OGE. *Private communication*. 2015.
- [Osi96] Andrej J. Osiadacz. “Different Transient Flow Models - Limitations, Advantages, And Disadvantages”. In: *PSIG Annual Meeting*. San Francisco, California: Pipeline Simulation Interest Group, 1996.
- [Pan88] C. C. Pantelides. “The Consistent Initialization of Differential-Algebraic Systems”. In: *SIAM Journal on Scientific and Statistical Computing* 9.2 (1988), pp. 213–231. DOI: 10.1137/0909014.
- [Pet82] L.R. Petzold. “Differential/Algebraic Equations are not ODE’s”. In: *SIAM Journal on Scientific and Statistical Computing* 3.3 (1982), pp. 367–384. DOI: 10.1137/0903023.
- [Pry01] J. D. Pryce. “A Simple Structural Analysis Method for DAEs”. In: *BIT Numerical Mathematics* 41.2 (Mar. 2001), pp. 364–394. ISSN: 1572-9125. DOI: 10.1023/A:1021998624799.
- [Rei06] T. Reis. “System Theoretic Aspects of PDAEs and Applications to Electrical Circuits”. PhD thesis. Technische Universität Kaiserslautern, 2006.
- [Rei90] S. Reich. “On a geometrical interpretation of differential-algebraic equations”. In: *Circuits, Systems and Signal Processing* 9.4 (1990), pp. 367–382. DOI: 10.1007/BF01189332.
- [Rhe84] W. C. Rheinboldt. “Differential-Algebraic Systems as Differential Equations on Manifolds”. In: *Mathematics of Computation* 43.168 (1984), pp. 473–482.

- [Rhe91] W. C. Rheinboldt. “On the existence and uniqueness of solutions of nonlinear semi-implicit differential-algebraic equations”. In: *Nonlinear Analysis: Theory, Methods & Applications* 16.7 (1991), pp. 647–661. DOI: 10.1016/0362-546X(91)90172-W.
- [Ria08] R. Riaza. *Differential-algebraic systems*. World Scientific Publishing Co. Pte. Ltd., Hackensack, 2008. DOI: 10.1142/9789812791818.
- [Sal02] J.M. Saleh. *Fluid Flow Handbook*. McGraw-Hill Handbooks. McGraw-Hill Education: New York, 2002.
- [Sim00] B. Simeon. *Numerische Simulation gekoppelter Systeme von partiellen und differential-algebraischen Gleichungen in der Mehrkörperdynamik*. VDI-Verlag, 2000.
- [Sim98] B. Simeon. “DAEs and PDEs in elastic multibody systems”. In: *Numerical Algorithms* 19.1 (1998), pp. 235–246. DOI: 10.1023/A:1019118809892.
- [SS92] K. E. Starling and J. L. Savidge. *Compressibility factors of natural gas and other related hydrocarbon gases*. American Gas Association, Operating Section, 1992.
- [SSW15] M. Schmidt, M.C. Steinbach, and B.M. Willert. “High detail stationary optimization models for gas networks”. In: *Optimization and Engineering* 16.1 (2015), pp. 131–164. DOI: 10.1007/s11081-014-9246-x.
- [Tis04] C. Tischendorf. *Coupled Systems of Differential Algebraic and Partial Differential Equations in Circuit and Device Simulation*. Humboldt-Universität zu Berlin, Habilitation, 2004.
- [WHS18] T. Walther, B. Hiller, and R. Saitenmacher. “Polyhedral 3D Models for Compressors in Gas Networks”. In: *Operations Research Proceedings 2017*. Ed. by Natalia Kliever, Jan Fabian Ehmke, and Ralf Borndörfer. Cham: Springer International Publishing, 2018, pp. 517–523. DOI: 10.1007/978-3-319-89920-6\_69.

# Index

## B

Banach space.....	18
Basis functions .....	61
Bochner space.....	20

## C

Compressor.....	10
Piston .....	11
Turbo.....	10
Control valve .....	15

## D

DAE	
in standard form.....	45
linear with constant coefficients	119
properly stated leading term....	119
quasi-linear.....	120
standard form .....	119
Digraph .....	117

## E

Euler equations .....	6
isothermal .....	8

## F

Friction factor .....	7
Hagen-Poiseuille .....	8
Nikuradse .....	8
Prandtl and Colebrook .....	8

## G

Graph.....	117
connected.....	117
weighted .....	118

## H

Hilbert space .....	19
Homogenisation functions.....	27

## I

Index	
differentiation .....	45
Kronecker .....	45
perturbation for ADAEs.....	23
perturbation for DAEs .....	46
tractability .....	48
Inequality	
Cauchy's.....	121
Gronwall's.....	121
Hölder's.....	121
ISO2 model.....	8
ISO2' model .....	9

## L

Lebesgue space .....	20
----------------------	----

## P

Path .....	117
------------	-----

## R

Resistor .....	9
Reynolds number .....	7

## S

Short pipe.....	15
Sobolev space .....	19
Subgraph.....	117

## T

Tree .....	117
------------	-----

## U

Upwind method.....	50
--------------------	----

## V

Valve .....	15
-------------	----

## W

weak partial derivative .....	19
-------------------------------	----